CANADIAN THESES ON MICROFICHE

I.S.B.N.

THESES CANADIENNES SUR MICROFICHE

National Library of Canada
Collections Development Branch

Canadian Theses on
Microfiche Service

Ottawa, Canada
K1A 0N4

Bibliothèque nationale du Canada
Direction du développement des collections

Service des thèses canadiennes
sur microfiche

NOTICE

The quality of this microfiche is heavily dependent upon the quality of the original thesis submitted for microfilming. Every effort has been made to ensure the highest quality of reproduction possible.

If pages are missing, contact the university which granted the degree.

Some pages may have indistinct print especially if the original pages were typed with a poor typewriter ribbon or if the university sent us a poor photocopy.

Previously copyrighted materials (journal articles, published tests, etc.) are not filmed.

Reproduction in full or in part of this film is governed by the Canadian Copyright Act, R.S.C. 1970, c. C-30. Please read the authorization forms which accompany this thesis.

THIS DISSERTATION
HAS BEEN MICROFILMED
EXACTLY AS RECEIVED

AVIS

La qualité de cette microfiche dépend grandement de la qualité de la thèse soumise au microfilmage. Nous avons tout fait pour assurer une qualité supérieure de reproduction.

S'il manque des pages, veuillez communiquer avec l'université qui a conféré le grade.

La qualité d'impression de certaines pages peut laisser à désirer, surtout si les pages originales ont été dactylographiées à l'aide d'un ruban usé ou si l'université nous a fait parvenir une photocopie de mauvaise qualité.

Les documents qui font déjà l'objet d'un droit d'auteur (articles de revue, examens publiés, etc.) ne sont pas microfilmés.

La reproduction, même partielle, de ce microfilm est soumise à la Loi canadienne sur le droit d'auteur, SRC 1970, c. C-30. Veuillez prendre connaissance des formules d'autorisation qui accompagnent cette thèse.

LA THÈSE A ÉTÉ
MICROFILMÉE TELLE QUE
NOUS L'AVONS REÇUE

NL-339 (r. 82/08)

Canada

SIZE AND CONFIGURATIONAL FACTORS IN IONIC HYDRATION AND IONIZATION

by

Erol Ayranci

A thesis submitted in partial fulfillment of the requirements for the degree of Doctor of Philosophy in the Department of Chemistry, University of Ottawa, Ottawa, Canada.

April, 1982

B.E. Conway
Professor of Chemistry
Research Supervisor

E. Ayranci
Ph.D. Candidate

To my wife and son

PREFACE

For some time, the specificity of ion-solvent interaction behaviour, especially in the aqueous medium, has been emphasized and its role in various biophysical processes has been recognized. Evaluations of various individual ionic properties in solution have been made by extra-thermodynamic methods.

The availability now of a seemingly reliable scale of individual ionic volumes in solution at infinite dilution stimulates further investigation into the relationships between volumes of various types of ions in solution with respect to size, geometry and charge.

While the individual ionic hydration behaviour of monatomic cations and anions of the alkali halide salts has received much attention, relatively little understanding exists on the behaviour of oxyanions. Interpretation of ionic volume behaviour in aqueous electrolyte solutions and evaluations of the electrostriction volume involve unexpected difficulties owing to serious uncertainties in the intrinsic radii or corresponding volumes of oxyanions.

Much interest has also arisen in recent and earlier years in the shape, size and steric factors which are

involved in the ionization of organic compounds. Problems in this field were first quantitatively investigated about forty years ago and since then a large number of works have demonstrated the structural specificities of interaction of organic ions and molecules with water.

In this thesis, the volume and compressibility behaviour of various solutes in water is reported as these properties are known to provide important information on solute-solvent interactions. The compounds chosen for the work were a series of oxyanion salts and a series of organic bases. The members of each of these groups were selected so as to have clear structural relations to one another. In the case of the organic bases, the volume and compressibility changes associated with ionization as hydrochloride salts were also obtained.

Some of the work described here has been prepared for publication as indicated in the following list:

1. Size, Shape and Charge Effects in the Partial Molal Volume, Compressibility and Electrostriction Behaviour of S- and Cl-Oxyanions in Water, E. Ayranci and B.E. Conway, J. Chem. Soc., Faraday Trans. I, in course of publication.
2. A note on Concentration Dependence of Apparent Molal Volumes of Ions in Aqueous Solution:

Significance of Equations of Masson, and Redlich and Meyer, in Relation to Co-Sphere Overlap Effects, B.E. Conway and E. Ayranci, J. Solution Chemistry, in course of publication.

3. Structural Effects in the Partial Molal Volumes and Compressibilities of Organic Bases and their Conjugate Ions, B.E. Conway and E. Ayranci, J. Chem. Thermodynamics, in course of publication.

ACKNOWLEDGEMENTS

The author wishes to express his deepest and sincere thanks to Professor B.E. Conway for his direction and guidance throughout the course of this work. Professor Conway was always willing and able to give assistance and suggestions when difficulties arose, no matter how busy he was himself. The many stimulating discussions with Professor Conway that took place during the course of the research work as well as the preparation of the manuscript were invaluable to the author. It was a privilege and honour for the author to work with such a well-known, capable and understanding person.

Grateful acknowledgement is due to the Middle East Technical University, Gaziantep, Turkey, for giving the opportunity and the partial financial support to the author which enabled him to work at the Chemistry Department of the University of Ottawa.

The author is also grateful to his wife, both for her continual help and for taking on many responsibilities at home, although she was herself under the same conditions as the author, working for her Ph.D. in Chemistry. Appreciation also goes to the author's little boy, Çağri, for his great understanding, unexpected from his age, during the years.

TABLE OF CONTENTS

LIST OF FIGURES

LIST OF TABLES

ABSTRACT

Ionic size, shape and charge effects in the interaction of a series of Cl- and S-oxyanions with water have been investigated by means of apparent molal volume and adiabatic compressibility measurements. Electrostriction volumes have been calculated from the partial molal volumes of the ions at infinite dilution using intrinsic ionic volumes evaluated by four methods which are critically compared. A relation between electrostriction volumes and compressibilities of ions is demonstrated and compared with the results of earlier a priori calculations. Both the compressibilities and partial molal volumes of the series of oxyanions and simple halide ions are almost linearly related to the respective standard entropies of solution of these ions.

The treatment of concentration-dependence of apparent molal volume data according to Redlich and Meyer's equation and Masson's equation is critically examined. For a series of oxyanion salts, use of Masson's equation obscures some interesting inflections which are otherwise seen if ϕ_V is plotted according to Redlich and Meyer's equation, taking into account the Debye-Hückel limiting-law dependence on $c^{1/2}$. It is suggested that these inflections, which arise at substantially higher concentrations than would correspond to the onset of other deviations from Debye-Hückel limiting-

law behaviour, are due to Gurney co-sphere overlap effects. Elementary calculations support this proposal. Similar, though less striking, effects are observed in the compressibility behaviour.

The volume and compressibility behaviour of a series of organic N-bases and their conjugate acids in H_2O have also been examined. It was concluded that for the representation of partial molal volumes of organic bases, the concept of group contributions is not a correct viewpoint. Structural factors are found to play an important role in determining $\overline{V}^o$ and $\overline{K}_S^o$ values.

The volume and adiabatic compressibility changes associated with ionization of the organic bases have been determined and the relation between these two quantities, as well as between volume and entropy changes upon ionization (Hepler's relation), have been examined.

CHAPTER I

INTRODUCTION

1. Role of Ionic Hydration in Chemistry

The term hydration is employed for the special case of solvation in which the solvent is water. Since the majority of chemical and biochemical processes take place in water, the role of hydration of ions, or of solutes in a more general sense, is very important in these processes.

Hydration effects are primarily involved in redox reactions, solubility of salts, ionization of acids and bases, kinetics of reactions proceeding via ionic transition states, and the kinetics of ion discharge or ion formation reactions in electrode processes. Hydration also enters into the structure of the double-layer in relation to ion adsorption and solvent orientation at charged electrodes and colloid interfaces, and in many other processes.

In order to understand the hydration behaviour of ions and molecules, it is essential to examine first the structure of water itself. Then changes in the structure of water upon introduction of ions give information about specific hydration effects.

Until recently, there has existed no universal agreement with regard to the structure of water. The nature of structural theories is best illustrated by a variety of

models. These various models can be grouped into two main classes as "continuum" models and "mixture" models as treated in reviews by Conway[1], more recently by Kell[2], and by Davis[3]. The most important features of these approaches are as follows: continuum models consider the water structure to be characterized by a single distribution of oxygen-oxygen distances, oxygen-oxygen-oxygen angles and energies whereas, in the mixture models, water is considered as a solution of distinguishable species.

Although there is not good agreement on which model best represents the structure of water, the continuum model, which can also be called the distorted hydrogen bond model, seems to be in agreement with most of the experimental knowledge about the structure of water[4]. Also, recent work of Rahman and Stillinger[5] on the structure of water, using the so-called molecular dynamics technique which assumes only an electrostatic and a 6:12 potential, supports the continuum model. In their work, the properties of a sample of water consisting of 216 rigid molecules at a density of 1 g cm^{-3} have been simulated by means of computer calculations. The results of the studies on both static structural properties and kinetic behaviour, led them to conclude that the structure of liquid water is best represented as a highly strained, random hydrogen-bonded network.

However, regardless of the detailed structure of liquid water, changes of structure must certainly take place upon introduction of ions since it is known that large energies are associated with the interaction of ions with water molecules, and different experimental approaches characterize different aspects of these changes. Also, structure changes are directly observable by x-ray diffraction.

2. Methods for Studying Ionic Hydration

The methods by which information on ionic hydration can be obtained, directly or indirectly, can be summarized as follows:

1. Thermodynamic methods involve measurement of quantities such as free energies of solution and solvation, heats of solvation, entropies of solvation and partial molar entropies, apparent molar quantities, e.g., volumes, compressibilities, expansivities and heat capacities. The thermodynamic methods provide an overall basis for characterization of ionic solvation. The free energy of solvation, together with its heat and entropy components, is considered as the primary quantity characterizing ionic solvation, since it determines the "driving force" for the solvation process. Heat capacity changes upon solvation are of interest as they often reflect important structural interactions involving the solvent and the dissolved ions.

Apparent molar volumes of ions in solution give interesting information on (a) interaction of the ion with the solvent, especially the electrostriction, and (b) the structure of liquid solvent in relation to accommodation of ions within it and its reaction to the presence of ions. Similarly, compressibilities of ions give a sensitive indication of specific interactions involving solvent structure, as well as of electrostriction effects. The molar expansivity of electrolytes is of interest in relation to the temperature dependence of electrostriction or local compression in the solvent caused by the ions, as well as the structural free-volume of the solvent as a function of temperature.

2. Optical methods, e.g., infrared and Raman spectroscopy, reflect changes in the vibrational motions of the water molecules upon introduction of ions.

3. Magnetic spectroscopic methods, e.g., NMR shifts and relaxation times, provide information on changes in electron distribution around the nuclei of the solvent molecules and rotational freedom of solvent molecules.

4. X-ray diffraction methods yield mean ion-to-water distances and time-average coordination numbers of the solvated ions.

5. Mass spectrometric methods give information on solvation of ions in the gas-phase from the interaction of ions with vapor-phase solvent molecules.

6. Structural studies by means of diffraction: by means of X-ray and neutron diffraction studies, important advances of a more direct kind have been made with regard to elucidation of short-range structure in liquid and their solutions. Neutron diffraction reveals average positions of H atom in hydroxylic solvents. However, for the study of solutions, these methods are restricted to relatively high concentrations, > ca 1 M.

As pointed out in the previous section, all these methods characterize different aspects of ionic solvation. The work described in this thesis involves the study of ionic hydration mainly by measurements of apparent molar volumes and compressibilities.

3. Relation of the Volume and Compressibility of a System to the Free Energy

The equation for the volume of a system is derived from the important differential thermodynamic relation

$$dG = VdP - SdT \qquad \text{I-1}$$

for constant composition of a system. Under these conditions, since then G is a function of T and P, V is given by

$$V = \left(\frac{\partial G}{\partial P}\right)_T \qquad \text{I-2}$$

The partial molal volume, $\bar{V}$, is one of the very important thermodynamic quantities in the study of solutions. For a component A in a solution containing n_A moles of A and n_B moles of B, $\bar{V}$ is defined as

$$\bar{V}_A = \left(\frac{\partial V}{\partial n_A}\right)_{T,P,n_B} \qquad \text{I-3}$$

As with the volume of the system itself, this quantity $\bar{V}_A$ can be expressed in terms of partial molal free energy $\bar{G}_A$ as,

$$\bar{V}_A = \left(\frac{\partial \bar{G}_A}{\partial P}\right)_T \equiv \left(\frac{\partial \mu_A}{\partial P}\right)_T \qquad \text{I-4}$$

where μ_A is the chemical potential of A and is equivalent to partial molal free energy of A.

On the other hand, partial molal compressibility is defined by

$$\bar{K}_A = -\left(\frac{\partial \bar{V}_A}{\partial P}\right)_T \qquad \text{I-5}$$

or from I-4

$$\bar{K}_A = -\left[\frac{\partial}{\partial P}\left(\frac{\partial \mu_A}{\partial P}\right)_T\right]_T = -\left(\frac{\partial^2 \mu_A}{\partial P^2}\right)_T \qquad \text{I-6}$$

4. Dependence of Ionic Properties on Radii of Ions

As we have already seen for the partial molal volumes and compressibilities, which are the main subjects of this thesis, all other properties of a solution are also related to the chemical potential, e.g., the partial molal entropy and enthalpy

$$\bar{S}_A = - \left(\frac{\partial \mu_A}{\partial T}\right)_P \qquad \text{I-7}$$

$$\bar{H}_A = \mu_A - T\left(\frac{\partial \mu_A}{\partial T}\right)_P \qquad \text{I-8}$$

In the case where the component A is a salt, the chemical potential is the sum of the component ionic chemical potentials, i.e.,

$$\mu_{salt} = \nu_+ \mu_+ + \nu_- \mu_- \qquad \text{I-9}$$

for an electrolyte $M_{\nu_+} A_{\nu_-}$.

For the hydration of ions, even in its simplest treatment according to Born, the free energy is inversely proportional to the ionic radius. In a more complete treatment, this dependence is of course more complex and involves other terms such as the sum of the radius of the ion and that of the water molecule, so that all the ionic hydration properties are dependent on the radii of ions.

Although the chemical potential of the salt can be separated into ionic components according to Equation I-9, there is no experimental method to obtain individual ionic chemical potentials, the activity or activity coefficients. This well-known problem originates from the nature of electrolytic solutions that they contain both positive and negative ions in equivalent proportions to meet the requirement of electrical neutrality. The same reason makes direct evaluation of other individual ionic properties close to impossible.* Fortunately it is relatively easy to obtain, experimentally, the overall thermodynamic properties which include contributions from both types of ions. Then some non- or extra-thermodynamic method is employed to derive the individual ionic properties.

Most methods are based on using some extrapolation procedure which involves plotting a thermodynamic quantity as some function of the ionic radii, originating from the dependence of free energy of hydration on the ionic radius. The details of some of these methods, as well as the problem

* Mention should be made here about studies of ion-solvent interactions in the gas-phase, pioneered by Kebarle and his coworkers.[6] This is a promising method for the evaluation of thermodynamic functions such as energies, enthalpies and entropies of interaction of individual ions with solvent vapor molecules but the states of the resulting "solvated ion" are, of course, different from those of ions in the corresponding bulk solvent.

of the scale of ionic radii, will be discussed later in the section on individual ionic volumes and compressibilities.

5. Significance of Volumes of Ions in Solution

The determination of apparent (ϕ_V) and partial ($\overline{V}$) molal volumes of electrolyte solutions has proven to be a very useful for the examination of structural aspects of the interactions arising in ionic solution such as ion-ion and ion-solvent interactions. For example, the partial molal volumes of electrolytes at infinite dilution give information on ion-solvent interactions whereas the concentration dependence of $\overline{V}$ is determined mainly by the ion-ion interactions. Obviously, finding the individual ionic volumes from the salt values by an appropriate separation method using the additivity principle must be the first step.

The partial molal volume of an ion at infinite dilution, $\overline{V}_i^o$, is considered to be the sum of several components [7,8a]:

(a) the intrinsic volume V_i, including dead-space effects;

(b) the cavity volume V_c, viz. the volume available within the liquid which partially accommodates the ion; V_c is a negative contribution to $\overline{V}_i^o$;

(c) the solvent-structure reaction volume, V_r: this is the volume change in solvent which arises around the ion because of the presence of the ion, apart from

the electrostatic effects;

(d) the electrostriction volume, V_e.

Therefore the overall partial molal volume of an ion at infinite dilution can be written as

$$\overline{V}_i^o = V_i + V_c + V_r + V_e \qquad \text{I-10}$$

However, the boundaries between the components are difficult to define exactly due to some overlapping effects. For example, V_r cannot be considered as entirely independent of V_e, but usually the sum $V_e + V_r$ can be estimated. Also V_i and V_c involve problems since V_i depends to some extent on the immediate ion-solvent interactions and the dead-space.

(a) Intrinsic Volume; Free Space

This is the volume occupied by the ion itself in the solution. It cannot be measured directly. Usually it is based on the crystal ionic radius r_i assuming that the ions are perfect hard spheres. Therefore the intrinsic molal ionic volume is given by

$$V_i = \frac{4}{3} \pi r_i^3 \, N \, 10^{-21} \qquad \text{I-11}$$

where N is Avogadro constant and r_i is the crystal ionic radius in nm, or

$$V_i = 2520\ r_i^3 \qquad \text{I-12}$$

V_i is a positive contribution to $\bar{V}_i^o$. However, the effective intrinsic volume is somewhat larger than this. Since ions and solvent molecules have comparable sizes, there must be a free or dead-space around the ion associated with packing effects. In most treatments, this volume is included in the intrinsic volume by adding another term to V_i.

The semi-empirical relations obtained for the effective intrinsic volumes proposed by several workers have been summarized by Millero[7] in the following three equations:

$$V_i = 2520\ r_i^3 + (A-2520)r_i^3 = A\ r_i^3 \qquad \text{I-13}$$

$$V_i = 2520\ r_i^3 + A'r_i^2 \qquad \text{I-14}$$

$$V_i = 2520\ r_i^3 + [2520(r_i+a)^3 - 2520\ r_i^3] = 2520(r_i+a)^3 \qquad \text{I-15}$$

In the first equation, it is assumed that free space is proportional to ionic dimensions. In the second equation, it is assumed that the free space is proportional to the surface of the ion. Conway et al.[9] found A' to be 315 which is in good agreement with experimental results [91,92]. In the third equation, it is assumed that the radii of all ions increase by a constant amount "a" in solution.

It is not possible to say which of the three equations represents the intrinsic volume of the ion but each appears to provide a satisfactory "fit" of the experimental data.

Recently, Krumgalz[10] found that the last equation is the best for the volumes of ions in organic solvents. He showed that there is a perfect linear relationship between $(V_i)^{1/3}$ and r_i for an homologous series of tetraalkylammonium ions in various organic solvents. Hepler[11] calculated the partial molal volume of ions with an equation of the form

$$\bar{V}_i^o = Ar_i^3 - BZ^2/r_i \qquad \text{I-16}$$

where A and B are constants. He found that the relation of this form for the intrinsic volumes is different for cations and anions; thus A is 5300 for cations and 4600 for anions when r_i is in nm.

(b) The Electrostriction Effect

Electrostriction is defined as the volume change or compression (actually due to an internal tension) caused by an electric field, or especially an inhomogeneous electric field, such as that of an ion, which tends to concentrate electric dipoles in regions of highest field strength. There is a very high field near an ion in water; e.g., for Na^+, it is ca 1.32×10^8 V cm^{-1}. It is also very inhomogeneous. It falls off rapidly with distance because field strength is inversely proportional to the square of the distance between ion and the water dipole and also because the field strength is inversely proportional to the

dielectric constant, which itself increases rapidly with distance. Therefore, immediately beyond the periphery of the ion there is a region of very high field strength which can orient water dipoles and bring them as close as possible to the ion to minimize their energy. These effects result in a local collapse of the open structure of water and a consequent decrease of volume in the neighbourhood of the ion.

The "electrostriction volume" is a major contribution to the total ionic partial molal volume $\overline{V}_i^o$ and it has a negative value. Usually the difference $(\overline{V}_i^o - V_i)$ is negative which proves that the electrostriction is a leading component of the total volume measurable experimentally.

Electrostriction is also indicated by the observation of negative apparent molal compressibilities of ions since electrostricted water has lower compressibility than bulk water.

The simplest way of estimating the electrostriction volume (for a continuum dielectric model of the solution) is to differentiate the Born equation for the electrostatic part of the free energy of hydration with respect to pressure since $(\partial G/\partial P)_T = V$ (Equation I-2). Drude and Nernst[12] made a related electrostatic calculation and obtained

$$V_e = - \frac{z^2 e^2}{2r\varepsilon} \left(\frac{\partial \ln \varepsilon}{\partial P}\right)_T \qquad \text{I-17}$$

where ε is the dielectric constant and other terms have their usual meanings. However, this method assumes the solvent to be a continuous dielectric medium having a field- and pressure-independent dielectric constant.

A more satisfactory treatment should consider also the dielectric saturation effects [14,41]. The basic equation required for more accurately calculating electrostriction is the one derived by Frank [13]. It gives the change in volume of a fluid when subjected to an electrostatic field E while its chemical potential μ and temperature are held constant:

$$\frac{1}{V}\left(\frac{\partial V}{\partial E}\right)_{\mu,T} = -\frac{E}{4\pi}\left(\frac{\partial \varepsilon}{\partial P}\right)_{E,T} \qquad \text{I-18}$$

Here V is the molar volume of the solvent. Starting with this equation, and taking into account additional factors such as pressure-dependence of the compressibility, the dielectric constant and the solvent refractive index, Desnoyers, Verrall and Conway[14] derived the following expression for the effect of electrostriction:

$$\log \frac{V_o}{V} = 0.1469 \log(1.1023\ 10^{-11}\ E^2 + 1) \qquad \text{I-19}$$

where V and V_o are the volumes with and without the electrostriction, respectively. From this relation, the volume

change, ΔV, of one mole of water as a function of field can be calculated. Then the electrostriction volume, V_e, is given by

$$V_e = X_1 \Delta V_1 + X_2 \Delta V_2 \qquad I\text{-}20$$

where X_1 and X_2 are the number of water molecules in the first and second hydration shells, respectively, and ΔV_1 and ΔV_2 are the changes in volume of one mole of water in the field in the first and second hydration shells, respectively.

A test of the method was made by applying these equations to the data for Na^+F^-. Considering that electrostriction is important only in the first hydration shell and assuming there are 4 water molecules in this shell, i.e., X_1 is 4 for both Na^+ and F^-, they arrived at a result which was in good agreement with the experimental data.

Recently, Zana and Yeager [15], using Desnoyers, Verrall and Conway's[14] method of calculating electrostriction per water molecule, found that electrostriction is significant in the first hydration layer and practically negligible in the second hydration layer for alkali metal and halide ions. For divalent ions, again more than 90% of the electrostriction occurs in the first hydration layer. It is only for trivalent ions that the second hydration layer is significantly (> 25% of the total electrostriction) electrostricted.

(c) The Volume of Water Molecules

It was mentioned that electrostriction is a result of the collapse of the open water structure caused by the ions. Normally, liquid water has a volume of 18.07 cm^3 mol^{-1} at 298 K. On the other hand, water molecules at very high pressures would have a volume of ca 12 cm^3 mol^{-1} [120]. These figures show that the maximum electrostriction will be ca 6 cm^3 (mol H_2O)$^{-1}$. Per ion, it will be larger because several (4 ~ 6) water molecules are influenced by each ion.

The density of close-packed water has been given[44] as 1.84 which corresponds to a molar volume of 9.7 cm^3 mol^{-1}. This is probably the smallest practical volume attained by water under the most strongly electrostricting conditions, giving a maximum electrostriction of 8.37 cm^3 (mol H_2O)$^{-1}$.

From space-filling models[8g], the actual volume of a static water molecule would be substantially smaller, viz. 7.5 cm^3 mol^{-1}, taking into account the known Pauling-Brockway covalent bond distances and Van der Waals radii of H and O, based on Courtauld or Fisher-Hirshfelder models. The spherical rotational envelope of such an individual molecule would have a larger volume of ca 22.5 cm^3 mol^{-1}.

(d) Dependence of Electrostriction on the Nature of the Solvent

The collapse of the open water structure is an endoenergetic process which involves bending or breaking of H-bonds. Therefore, it is expected that larger electrostriction or more compression arises with unassociated polar solvents in which H-bonding is absent, e.g., CH_3CN, propylene carbonate, etc. Thus, the compressibilities of these solvents themselves are much greater than that of water. It is expected that introduction of ions into such solvents causes larger electrostrictions as compared to that caused by the same ion in water.

The property which gives information about the dependence of electrostriction on solvent is primarily the intrinsic compressibility, β, and its dependence on pressure. Also, the dielectric constant and its pressure and field derivatives are important [13]. This can be seen from the simple Drude and Nernst equation (Equation I-17); thus electrostriction depends on dielectric constant and its change with pressure. Hamann and Lim[16] found a linear relation between ionic molal volumes and the compressibilities of solvents, with a negative slope.

(e) Structure Rearrangement in the Solvent Around the Ion

The terms V_c and V_r in Equation I-10 can be discussed in the same context as the structural contribution, V_s, to the total partial molal volume. The first component, V_c, is the volume due to inclusion of the ion in a cavity which already exists for thermal and/or structural reasons within the solvent structure itself (negative volume contribution). The second component, V_r, is the volume change due to (a) any reaction which the inserted ion has upon the solvent structure to produce an increase in "ice-like" character[95] (so-called "structure-making" effect; positive volume contribution) locally about the ion, or (b) any breakdown of the H-bonded structure of the solvent (so-called "structure-breaking" effect[98]) due to the field of the ion and misfit of the ion into the original solvent's structure. These concepts were introduced first by Frank and Evans[95] in relation to entropies of electrolyte solutions and have been critically examined by Holtzer and Emerson[96] and treated by Nemethy and Scheraga.[98]

The "structure-making" effects play an important role in the hydration of tetraalkylammonium ions. The charge on these ions is shielded by the alkyl groups. Therefore, the electrostriction component is not very important so that the partial molal volume can be expressed by

$$\bar{V}_i^o = V_i + V_s \qquad \text{I-21}$$

It is believed[8b] that tetraalkylammonium ions increase the "local structure" of the water (positive contribution for V_s). It is also expected that they can usually be accommodated in their solvent cages with an overall economy of space (negative contribution for V_s). Therefore, due to the compensation between these two contributions, V_s is probably small compared to V_i, and the $\bar{V}_i^o$'s are close to the intrinsic volumes of these ions.

(f) Relation to Hydration Numbers

Hydration numbers are related to, and can be evaluated from, apparent molal volumes using a method developed by Conway and Bockris[17] following the early work of Darmois[93]. The volume of an ionic solution can be written as

$$V = n_1 V_{H_2O} + n_2 V_2 \qquad \text{I-22}$$

where n_1 and n_2 are the numbers of moles of water and solute, respectively, and V_{H_2O} is the normal volume of liquid water. The volume V_2 of the hydrated ion is given by

$$V_2 = n(\bar{V}_{H_2O} - V_{H_2O}) + V_i \qquad \text{I-23}$$

where $\bar{V}_{H_2O}$ is the effective volume of water molecules which are affected by the presence of ions, V_i is the total

intrinsic volume of the ions resulting from dissolution of one mole of solute and n is the hydration number. Then, by combining these two equations and solving for n, one obtains

$$n = \frac{V - n_1 V_{H_2O} - n_2 V_i}{n_2 (\bar{V}_{H_2O} - V_{H_2O})} \qquad \text{I-24}$$

By definition, the apparent molal volume of a solute is given by

$$\phi_v = \frac{V - n_1 V_{H_2O}}{n_2} \qquad \text{I-25}$$

so that

$$n = \frac{\phi_v - V_i}{\bar{V}_{H_2O} - V_{H_2O}} \qquad \text{I-26}$$

It can be seen that this final equation gives n as the total electrostriction divided by the electrostriction per mole of water. It is to be noted that n is the total hydration number for the ions present in one molecule of solute. ϕ_v can be determined experimentally and V_i can be calculated by choosing a suitable scale for ionic radii; however, evaluation of $\bar{V}_{H_2O} - V_{H_2O}$ presents some problem because it will depend on charge density of the ion, ion-solvent packing and structural volume change outside the primary hydration shell.

In a general way, the ionic solvation number n_i can be written as[18]

$$n_i = \frac{V_e}{\text{electrostriction per mol of water}} \qquad \text{I-27}$$

Of course, the evaluation of the denominator involves the same problems as those mentioned above.

6. Relation Between $\bar{V}_i^o$ and Entropy $\bar{S}_i^o$

It is possible to correlate the volumes and entropies of ions. Following the early work of Latimer and Kasper[94], Conway, Verrall and Desnoyers[19] examined the relation between entropy of hydration and the electrostriction. Linear relations have been found between electrostriction volume and entropy of hydration for groups of monatomic ions, namely monovalent cations, monovalent anions and divalent cations[8c]. However, the direction of the relation for divalent cations was rather anomalous.

Hepler[20] found empirically that there is a linear dependence of changes in entropy on volume of ionization of 53 acids. The slope was found to be 1.05 cal deg^{-1} cm^{-3}. This has become known as "Hepler's Relation".

It was pointed out that[20] entropies of ionization are chiefly determined by the effects of various solute species on the "orderliness" of arrangement of nearby water

molecules and volumes of ionization are determined by the related space occupied by the water-molecules near the various ionic species. The value of the slope was explained in terms of a high-pressure value of $(\partial P/\partial T)_V$ for water. The high-pressure involved here is that corresponding to the effective electrostrictive tension near ions or polar solute molecules in water.

Correlations similar to Hepler's[20] were examined for a series of alkylammonium ions by Verrall and Conway[21] and for some 39 organic acids by Cabani et al [22]. However, for these cases, it was found that there is no simple correlation between these two thermodynamic functions.

In general, the relation between the entropy and the volume of ions is not exactly understood. This is probably because the structural factors that determine, in part, the hydration entropy, operate differently in determining volumes of ions.

7. Organic Ions and Steric Effects in Ionic Volumes

Steric effects play an important role in determining ionic volumes. This is especially true for organic ions. The most direct steric effects can be observed with ions containing a positively charged nitrogen center. These ions include primary, secondary, tertiary and quaternary ammonium types, as well as those derived from heterocyclic

N-compounds (such as pyridine, piperidine, pyrazine, imidazole, etc.) ionized at the N-center. Steric effects arise from the substitution of alkyl groups on "N". As the number of substitutions, as well as the size of substituent, increase (e.g., from NH_4^+ to R_4N^+) (a) the accessibility of water molecules to the N^+ center decreases and (b) the effect of charge on the surrounding water molecules decreases since the charge is shielded by alkyl groups. The ionic volumes increase with substitution both because of addition of the alkyl groups which are much larger than H and because of the decrease in electrostriction. Therefore, the direct steric effect on ionic volumes is positive (since the contribution of V_e to $\overline{V}_i^o$ is negative).

Verrall and Conway[21] studied the volumes of alkylammonium ions in the series R_3NH^+, $R_2NH_2^+$, RNH_3^+ and NH_4^+, R being Me, Et and n-Pr. They found that the volumes decrease from R_3NH^+ to NH_4^+ more than could be accounted for by the replacement of R by H for each homologue. Laliberté and Conway[23,24] made similar studies on the volumes of pyridinium ($PyrH^+$) and piperidinium ($PipH^+$) ions and their Me-substituted analogues. Again they found that the volumes increase from $PyrH^+$ to $Pyr.Me^+$ and from $PipH_2^+$ to $Pip.MeH^+$ and $Pip\ Me_2^+$ more than would be expected just from the volume difference arising by replacement of H by Me. This effect was attributed to the diminution of electrostriction. They also

observed a decrease in electrostriction when the substitution of Me was on the ortho position to "N". However, this decrease was not as much as in the N-substituted molecules because, in this case, the steric effect was rather indirect.

Steric effects can also be observed in substituted carboxylic acids [29]. However, since the substitution cannot, in this case, be directly on the ionized centre (R-C 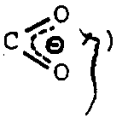), the effect is indirect and relatively small.

Another kind of steric effect can be expected when different "conformations" of a molecule of fixed "configuration"[8d] can exist. Examples of this type of steric effect which have relevence to the work described in this thesis, are morpholine and 1,4 dioxane. Both compounds can exist in chair or boat forms. The boat forms having the greater dipole moment are stabilized in an ionic field. The volumes of the two forms are also expected to be somewhat different.

8. Volumes of Oxyanions

The volumes of oxyanions can be obtained in the usual way by measuring the densities of their salt solutions and then subtracting the cationic volume contribution. However, problems arise in the interpretation of the experimental data in terms of the different contributions

according to Equation I-10. Thus, the oxyanions cannot be considered as simple spheres as in the case of monatomic ions.

The problem of defining a suitable effective radius for oxyanions was discussed by Couture and Laidler [25]. They extended their treatment of the determination of partial molal volumes of monatomic ions[26] to the case of more complex oxyanions by representing the partial molal volume of the latter as

$$\bar{V}_i^o = 58.8 + 890\ r_{eff}^3 - 26\ |z_-| \qquad \text{I-28}$$

where $\bar{V}_i^o$ for H^+ was taken as $-6.0\ cm^3\ mol^{-1}$ or as

$$\bar{V}_i^o\ (\text{conventional}) = 58.8 + 890\ r_{eff}^3 - 32\ |z_-| \qquad \text{I-29}$$

where $\bar{V}_i^o$ for H^+ was taken as zero as in the case of most conventional thermodynamic ionic quantities. In both equations r_{eff} is in nm. The important term for the oxyanions is the effective radius, r_{eff}, which was defined as $0.25\ \ell r$ where ℓ is the number of charge-bearing ligands ("O" for oxyanions) and r is the sum of interatomic distance (from the centre of the central atom to the centre of the oxygen atom) and the Van der Waals radius of the oxygen atom. The constant 0.25 comes from the consideration that ions with four charge-bearing ligands are taken as a reference standard. Therefore, the radius of the reference standard

is simply r, (0.25 x 4 = 1). They[25] reported a mean deviation in volume of 3.5 cm^3 mol^{-1} from the volumes that are predicted by Equation I-28 for a large number of oxyanions.

Mukerjee[27] criticized Couture and Laidler's method of calculation of ionic volumes as being physically implausible. They objected to the presence of a large constant in the equation which does not contain "r" or "z". Mukerjee[27] developed a method similar to Hepler's[11] (Section I-5-a) for monatomic ions and pointed out the difficulties involved with polyatomic ions (e.g., oxyanions). However, he applied the same model and general ideas used for monatomic ions to the polyatomic ions, indicating that no new approach is necessary.

The basic equation used was

$$\bar{V}_i^o = V_i - V_e \qquad \text{I-30}$$

where $\bar{V}_i^o$ is the partial molal volume at infinite dilution, V_i is the intrinsic volume and V_e is the electrostriction volume. The treatment for symmetrical MO_4^{z-} type anions was as follows. The intrinsic volume V_i was calculated as $(2520\ r^3)K'$ where the 2520 factor arises according to Equation I-11, r is the sum of the M-O bond distance and the Van der Waals radius of oxygen (0.140 nm). The cavity produced by these ions was assumed to be a constant fraction

K' of 2520 $\pm^3$. A mean value of 0.88 was used for K'.

Furthermore, V_e's were assumed to be the same as those found for monatomic ions (0.8/r for monovalent, 32.5 for divalent and 58.5 $cm^3\ mol^{-1}$ for trivalent anions). $\overline{V}_i^o$ values calculated for 8 oxyanions of MO_4^{z-} type by this method showed a mean deviation of 1.7 $cm^3\ mol^{-1}$ from the experimental values when AsO_4^{3-} was excluded.

Mukerjee's[27] treatment included only MO_4^{z-} and some HMO_4^{z-} type of ions. The agreement between the experimental $\overline{V}_i^o$ and calculated $\overline{V}_i^o$'s for HMO_4^{z-} type ions was rather poor. The experimental volumes were quite low compared to those calculated by the above method. This was explained by the presence of partial positive charge on H. This increases the negative charge on $-MO_4^{z-}$ by the same fraction. Therefore, the electrostriction is expected to be larger than that simply predicted from the charge "z-".

Other types of oxyanions which can be generalized by a formula $M_xO_y^{z-}$ where x and y are integers having values 1 to 4 and 1 to 12, respectively, were not treated by Mukerjee [27]. However, in a very recent and comprehensive work by Akitt[28] some oxyanions were also included.

It was found[28] that for a series of ions of similar size but having different charges, the electrostriction is a linear function of z as proposed previously by Couture and Laidler [25,26]. Volumes of the following groups of ions

having similar size were plotted against the absolute value of charge: (a) ClO_4^-, BF_4^-, CrO_4^{2-}, SO_4^{2-}, AsO_4^{3-}; (b) NO_3^-, CO_3^{2-}; (c) Ag^+, Sr^{2+}, La^{3+}, Th^{4+}; (d) K^+, Ba^{2+}. The relation for each group was linear and had a similar slope but different intercept. The average slope was 25.4 which is close to Couture and Laidler's[25] value of 26. The intercepts give directly the intrinsic volumes, V_i, of the ions. Therefore, the equation for $\overline{V}_i^o$ was given as

$$\overline{V}_i^o = V_i - 25.4\,|z| \qquad \text{I-31}$$

or the intrinsic volume of an ion can be calculated by

$$V_i = \overline{V}_i^o + 25.4\,|z| \qquad \text{I-32}$$

which was applied to a large number of ions.

An interesting relation is found when the intrinsic volumes are expressed in terms of equivalent water molar volume V_w (V_w = 18.07 $cm^3\ mol^{-1}$). For the above series of ions, it was found[28] that (a) $V_i(MO_4^{z-}) = 4.11\ V_w$, (b) $V_i(MO_3^{z-}) = 3.4\ V_w$, (c) $V_i(M^{z+}) = 1.00\ V_w$, and (d) $V_i(M^{z+}) = 1.69\ V_w$. These values were taken as a strong indication that tetrahedral MO_4^{z-} displaces a tetrahedron of 4 water molecules, planar MO_3^{z-} a group of 3 water molecules and the smaller M^{z+} a single water molecule in the water structure. Oxyanions were further examined by plotting V_i against the number of oxygen atoms in the ion, N_O. A linear relationship

was found with a slope of 17.73 $cm^3\ mol^{-1}\ N_O^{-1}$, which is close to the water molar volume, 18.07 $cm^3\ mol^{-1}$. The ion $S_2O_3^{2-}$ was found to fit at $N_O = 5$ on this line. This was explained by considering $S_2O_3^{2-}$ in effect as SO_4^{2-} with one oxygen replaced by sulfur. Since S^{2-} is large, it displaces an extra water molecule.

Similar relations were found[28] between volumes of alkylammonium ions and the number of carbon atoms and between volumes of complex cyanide ions and number of CN^- ligands. The general indication was that an increment in size corresponding to addition of one carbon atom, one oxygen atom or one CN^- ligand results in a volume increment equivalent to the displacement of one water molecule. The main conclusion of Akitt[28] was that the intrinsic volume of an ion or of any solute is determined primarily by the structure of the solvent and the way this forms cavities to accept a solute and only secondarily by the parameters of the ion itself. This seems an unexpected conclusion, not altogether consistent with the known individuality of the volumetric properties of ions.

9. Volume of Ionization of Bases and Acids

The thermodynamics of ionization of aqueous acids and bases are closely related to the hydration of the species involved. Free energies, enthalpies, entropies and heat

capacities of ionization for a number of organic and inorganic acids have been studied; the observed trends were interpreted in terms of specific structural effects by Everett and Wynne-Jones [29].

The volume change, $\Delta\overline{V}_i^o$, associated with the ionization of an acid HA

$$HA = H^+ + A^- \qquad \text{I-33}$$

at infinite dilution is given by

$$\Delta\overline{V}_i^o = \overline{V}^o(H^+) + \overline{V}^o(A^-) - \overline{V}^o(HA) \qquad \text{I-34}$$

$\Delta\overline{V}_i^o$ for this type of ionization is normally expected to be negative because of the electrostriction produced by the ions H^+ and A^-. However, for ionizations of the type

$$BH^+ = B + H^+ \qquad \text{I-35}$$

for which

$$\Delta\overline{V}_i^o = \overline{V}^o(B) + \overline{V}^o(H^+) - \overline{V}^o(BH^+) \qquad \text{I-36}$$

where B is a base and BH^+ is its conjugate acid, prediction of $\Delta\overline{V}_i^o$ is not so simple since there is no change of charge in the process.

Hamann and Lim[16] evaluated volume changes which accompany the ionization of weak electrolytes from measurement of

partial molal volumes of strong and weak electrolytes, including some alkylammoniumhydroxides and carboxylic acids. However, no simple relation was found between the $\Delta\overline{V}_i^o$ values and the structure of the electrolytes.

Examination of solvent effects on $\Delta\overline{V}_i^o$ showed that the latter decreases appreciably from water to methanol. As was discussed earlier (Section I-6), a linear relationship was found between $\Delta\overline{V}_i^o$ and $\Delta\overline{S}_i^o$ for 53 acids by Hepler [20]. A similar relationship was examined by Cabani et al.[22] for some 39 organic acids. Verrall and Conway[21] studied the volumes of ionization of alkylamines such as CH_3NH_2, $(CH_3)_2NH$, $(CH_3)_3N$ and $(C_2H_5)_3N$. They found that the values of $\Delta\overline{V}_i^o$ do not vary greatly with the different protonated bases. It was very difficult to draw any final conclusion from $\Delta\overline{V}_i^o$ values as they were surprisingly independent of coordination at the N^+ centre by CH_3 groups and the consequent blocking of hydration. Conway and Laliberté[24] examined the relations between $\Delta\overline{V}_i^o$, $\Delta\overline{K}_{S,i}^o$ (compressibility of ionization) and other thermodynamic functions such as $\Delta\overline{H}_i^o$, $\Delta\overline{G}_i^o$ and $\Delta\overline{S}_i^o$ for substituted pyridines. Systematic relations were found only in the case of $\Delta\overline{G}_i^o$.

Lown, Thirsk and Wynne-Jones[30] studied the effect of pressure on ionic equilibria in water. They proposed a graphical method for the evaluation of standard partial molal volume ($\Delta\overline{V}_1^o$) and compressibility ($\Delta\overline{K}_1^o$) changes

(subscript 1 stands for 1 atm.) on ionization at atmospheric pressure through the relation

$$\frac{RT}{P-1} \ln \frac{K_P}{K_1} = - \Delta\bar{V}_1^\circ + \frac{1}{2} \Delta\bar{K}_1^\circ \ (P-1) \qquad \text{I-37}$$

where K_1 and K_P are the equilibrium constants at 1 and P atm., respectively. Hence, a plot of $\frac{RT}{P-1} \ln \frac{K_P}{K_1}$ against (P-1) will have an intercept of $-\Delta\bar{V}_1^\circ$ and a slope of $\frac{1}{2} \Delta\bar{K}_1^\circ$. In the derivation of the above equation, they assumed[30] $\Delta\bar{K}_1^\circ$ to be independent of pressure over the first few 1000 bars. It was suggested that activation volumes and compressibilities could be evaluated from similar plots of the log of the rate constant against pressure. Furthermore, an approximately linear relation was found between $\Delta\bar{V}_1^\circ$ and $\Delta\bar{K}_1^\circ$ values for a wide range of acid-base equilibria. Such a relation can be used for predicting the effect of pressure on ionization equilibria for which $\Delta\bar{V}_1^\circ$ but not $\Delta\bar{K}_1^\circ$ data are available.

Another correlation of volumes of ionization was made by Rochester and Rossall[31] with pK values. A good linear relation was found between these two quantities ($\Delta\bar{V}_i^\circ$ vs pK) for substituted phenols in methanol. As was found by Hamann and Lim [16], the volumes of ionization were smaller (more negative) in methanol than in water due to the larger electrostrictions of the ionic species in methanol than in water.

Other works on volumes of ionization were reviewed by Millero [18]. Very recently, Cabani et al.[32] studied the volume changes (ΔV_{zw}) in the formation of zwitterions for several amino acids and polypeptides. ΔV_{zw} corresponds to the volume change in the following process :

$$NH_2RCOOH = H_3N^+RCOO^- \qquad \text{I-38}$$

It is experimentally impossible to obtain ΔV_{zw} as the equilibrium lies completely in the zwitterionic state. They therefore calculated the volume of neutral amino acids from group contributions using various methods. The results were compared with the volume changes associated with the reaction of proton exchange between primary amines and carboxylic acids. A mean ΔV_{zw} value of -14.7 ± 0.8 cm^3 mol^{-1} was obtained for α-amino acids and was attributed to the ΔV of reaction when the $-NH_3^+$ and $-COO^-$ centres are separated by only one carbon atom. However, when charged centres are moved away by interposing methylene groups, a more negative mean ΔV_{zw} value of -18.5 ± 0.4 cm^3 mol^{-1} is reached after 4 or more CH_2 groups have been inserted. This value was found to be very close to the mean volume change $\Delta V = -18.9 \pm 1.7$ cm^3 mol^{-1} for the proton-exchange reaction between primary aliphatic amines and aliphatic monocarboxylic acids.

10. Ionic Volumes and Activation Volumes in Kinetics of Chemical and Electrochemical Reactions

The volume of activation, $\Delta V^{\ddagger}$, for a chemical or electrochemical reaction is the difference between the volume of the activated complex, $V^{\ddagger}$, and the volume of reactants, V_R. $\Delta V^{\ddagger}$ can be obtained through the relation

$$\left(\frac{\partial \ln k}{\partial P}\right)_T = -\frac{\Delta V^{\ddagger}}{RT} \qquad \text{I-39}$$

where k is the rate constant of the reaction. The slope of a plot of lnk against pressure P at any P is $-\Delta V^{\ddagger}/RT$. However, if it is assumed that $\Delta V^{\ddagger}$ is independent of pressure the integration of the above relation gives

$$\ln k = \ln k_o - \left(\frac{\Delta V^{\ddagger}}{RT}\right) P \qquad \text{I-40}$$

where k_o is the rate constant at zero pressure. Thus, a plot of $\ln\frac{k}{k_o}$ against P will be a straight line through the origin. If such a linear plot is obtained, it can be concluded that $\Delta V^{\ddagger}$ is independent of pressure.

Transition states which are more polar than the initial reactants, as in the case of solvolysis of t-butyl chloride, will tend to have smaller volumes and lower entropies in solution than the reactants, owing to electrostriction effects. Therefore both the volume and entropy of activation are negative. According to the above equations, such

reactions will proceed faster at high pressures. Negative volume and entropy of activation are strong indications of formation of a polar or ionic transition state from relatively non-polar reactants. A reverse trend arises when the transition state is less polar than the reactants, in other words, when the electric field is weakened by the formation of the activated complex.

As in the case of volume and entropy of ionization [20], a linear relation is found between volumes and entropies of activation [33]. However, the volumes of activation were found[34] to be more reliable than the entropies of activation in suggesting the type of reaction that is taking place. This was attributed to the entropies of activation being very sensitive to factors such as the loosening or strengthening of chemical bonds, whereas volumes of activation depend to a much greater extent on electrostriction than on any other effects.

11. Ionic Compressibilities

(a) Significance of Compressibilities

The partial molal volume $\overline{V}^{o}$ at infinite dilution is a useful function by which solute-solvent interactions can be characterized and several aspects of this approach have been discussed above. However, any interpretation of $\overline{V}^{o}$ must rely on some semi-empirical estimate of the ionic

intrinsic volume. In this respect, study of partial molal compressibilities at infinite dilution which do not invdlve the intrinsic volume provide useful complementary information on solute-solvent interactions. If the ions are considered as incompressible spheres (which may not be the case with organic or polyatomic ions), then partial molal compressibility at infinite dilution depends only on ion-solvent interactions.

The most direct compressibility function is the isothermal quantity given by

$$\overline{K}_i = - \left(\frac{\partial \overline{V}_i}{\partial P}\right)_T \qquad \text{I-41}$$

where $\overline{K}_i$ and $\overline{V}_i$ are respectively partial molal compressibility and volume of the ion and P is the pressure. A specific compressibility coefficient (mostly referred to as compressibility), designated by β, is defined by

$$\beta = - \frac{1}{V} \left(\frac{\partial V}{\partial P}\right)_T \qquad \text{I-42}$$

or, in words, it is the relative fractional change in volume with pressure at constant temperature.

Isothermal compressibilities must normally be determined by means of P-V measurements on liquids or liquid solutions. However, this method presents a problem. The pressure dependence of β is such that β decreases most

rapidly at low pressures, where it is most difficult to obtain experimental results of high accuracy.

An alternative method to obtain isothermal compressibility is through the adiabatic compressibility which can be evaluated quite accurately from density and sound velocity measurements in solutions.

The adiabatic partial molal compressibility, $\bar{K}_S$, is the derivative of partial molal volume, $\bar{V}$, with respect to pressure at constant entropy, S:

$$\bar{K}_S = - \left(\frac{\partial \bar{V}}{\partial P}\right)_S \qquad \text{I-43}$$

and the adiabatic specific compressibility coefficient β_S is given by

$$\beta_S = - \frac{1}{\bar{V}} \left(\frac{\partial \bar{V}}{\partial P}\right)_S \qquad \text{I-44}$$

The relation between β and β_S is given by

$$\beta_S = \frac{C_V}{C_P} \beta \qquad \text{I-45}$$

where C_P and C_V are the heat capacities at constant pressure and volume, respectively. However, data on C_p and C_V for ionic solutions are often unavailable so that adiabatic compressibilities are often directly used in discussions of compressibility of aqueous ionic solutions.

Recently, Desnoyers and Philip[35] derived equations for the difference between apparent molal isothermal and adiabatic compressibilities and for the difference between infinite dilution values of the same quantities. The latter equation* is quite simple and requires data only on apparent molal expansivity, ϕ_E^o, and heat capacity, ϕ_C^o, at infinite dilution in aqueous solutions. It was found that this difference for NaCl and KCl amounts to less than 10% [8e]. Furthermore, Millero[36] showed that, for NaCl, the difference between apparent molal adiabatic and isothermal compressibilities is not strongly dependent on concentration. He took this as an indication that the relative partial molal compressibilities of electrolytes can be estimated from adiabatic partial molal compressibilities without serious errors. The same differences at infinite dilution for some tetraalkylammonium ions are much more than 10% [35]. It was also found[35] that the main contribution to this difference was from the apparent molal expansivity at infinite dilution.

---

* $$\phi_K^o - \phi_{KS}^o = \delta_o \left(\frac{2\phi_E^o}{\alpha_o} - \frac{\phi_C^o}{\sigma_o}\right) \qquad \text{I-46}$$

where $\delta_o = \beta^o - \beta_S^o$ (superscript "o" stands for pure solvent), α_o is the coefficient of thermal expansion of solvent and σ_o is volumetric specific heat of the solvent. These quantities are well known for water.

The qualitative features of compressibility behaviour of solutes can be summarized as follows [37]. (a) The electrostricted water gives a negative compressibility because it is least compressible compared to the bulk water. (b) The "structure-broken" water, which is the water between electrostricted and bulk water, has probably a negative compressibility because it is closer packed than bulk water. (c) Water affected by H-bonding to the solute gives a negative compressibility change because H-bonded networks tend to collapse upon increase of pressure.

(b) Relation to Electrostriction

It was already stated in Section I-5-b that electrostriction is indicated by a negative apparent molal compressibility since electrostricted water would have lower compressibility than that of bulk water. Therefore, a relation between electrostriction and compressibility is expected. Of course, this relation must originate from the definition of compressibility [$\equiv \frac{1}{V} \left(\frac{\partial V}{\partial P}\right)_T$]. If the partial molal volume at infinite dilution of an ion is written simply as the sum of intrinsic and electrostriction volumes,

$$\overline{V}_i^o = V_i + V_e \qquad \text{I-47}$$

then the partial molal compressibility at infinite dilution of the ions is given by

$$\bar{K}_i^o = K_i + K_e \qquad \text{I-48}$$

where K_i is the intrinsic partial molal compressibility [$\equiv -(\frac{\partial V_i}{\partial P})_T$], K_e is the electrostriction partial molal compressibility [$\equiv -(\frac{\partial V_e}{\partial P})_T$] and $\bar{K}_i^o$ is the partial molal compressibility at infinite dilution of the ion.

Since the effect of pressure on the volume of crystals is small, K_i is expected to be close to zero. Therefore, $\bar{K}_i^o$ is determined mainly by K_e. The relation between K_e and V_e was examined by Millero et al.[38] by using continuum and hydration models for ion-water interactions. In the continuum model, the electrostriction volume is simply given by Drude and Nernst's equation (Equation I-17), but probably inaccurately. The derivative of it with respect to pressure is the electrostriction compressibility contribution, i.e.,

$$K_e = \{(\frac{\partial^2 \ln\varepsilon}{\partial P^2})_T - (\frac{\partial \ln\varepsilon}{\partial P})_T^2\} \frac{e^2 z^2}{2\varepsilon r} \qquad \text{I-49}$$

or

$$K_e' = \{(\frac{\partial^2 \ln\varepsilon}{\partial P^2})_T - (\frac{\partial \ln\varepsilon}{\partial P})_T^2\} \frac{V_e}{(\frac{\partial \ln\varepsilon}{\partial P})_T} \qquad \text{I-50}$$

In the hydration model, the electrostriction volume is given by

$$V_e = n(\bar{V}_{H_2O} - V_{H_2O}) \qquad \text{I-51}$$

where $\bar{V}_{H_2O}$ and V_{H_2O} are the molar volumes of electrostricted and bulk water molecules. If $\bar{V}_{H_2O}$ is assumed to be independent of pressure, the K_e is given by

$$K_e = - n\left(\frac{\partial V_{H_2O}}{\partial P}\right)_T \qquad \text{I-52}$$

or, since compressibility of bulk water is $\beta_{H_2O} = - \frac{1}{V_{H_2O}} \left(\frac{\partial V_{H_2O}}{\partial P}\right)_T$ and n is $V_e/(\bar{V}_{H_2O} - V_{H_2O})$ (i.e., Equation I-27),

$$K_e = \frac{\beta_{H_2O} V_{H_2O}}{\bar{V}_{H_2O} - V_{H_2O}} \cdot V_e \qquad \text{I-53}$$

Both methods show that the relation between K_e and V_e (Equations I-50 and I-53) can be represented by

$$K_e = k V_e \qquad \text{I-54}$$

where k is given by

$$k = \frac{\left(\frac{\partial^2 \ln\varepsilon}{\partial P^2}\right)_T - \left(\frac{\partial \ln\varepsilon}{\partial P}\right)_T^2}{\left(\frac{\partial \ln\varepsilon}{\partial P}\right)_T} \qquad \text{I-55}$$

for the continuum model and by

$$k = \frac{\beta_{H_2O} V_{H_2O}}{\bar{V}_{H_2O} - V_{H_2O}} \qquad \text{I-56}$$

for the hydration model. Of course, if it is assumed that the intrinsic volume of the ion is independent of pressure, the relation $K_e = kV_e$ automatically becomes $\bar{K}_i^o = kV_e$. However, such an assumption is hard to visualize, especially if the void space which is included in the intrinsic volume (as discussed earlier in Section I-5-a) is considered.

Mathieson and Conway[39] developed a method for the assignment of the individual ionic compressibilities in which they also considered the pressure-dependence of the intrinsic volume. This method will be discussed later in Section I-12-b.

(c) Compressibility Changes in Ionization Processes

As in the case of the volume of ionization, the compressibility of ionization, $\Delta\bar{K}_i^o$, can be defined as the change in compressibility for the process

$$HA = H^+ + A^- \qquad \text{I-33}$$

or

$$BH^+ = B + H^+ \qquad \text{I-35}$$

which is given by

$$\Delta\overline{K}_i^o = \overline{K}^o(H^+) + \overline{K}^o(A^-) - \overline{K}^o(HA) \qquad \text{I-57}$$

or

$$\Delta\overline{K}_i^o = \overline{K}^o(H^+) + \overline{K}^o(B) - \overline{K}^o(BH^+) \qquad \text{I-58}$$

for the two processes, respectively. Again, it should be noted that, in the second process (I-35), there is no loss or gain of charge. $\Delta\overline{K}_i^o$ is mostly negative.

The use of $\Delta\overline{K}_i^o$ together with $\Delta\overline{V}_i^o$ leads to estimations of effects of pressure on ionization constants. This has been investigated e.g., by Owen and Brinkley [40]. The variation of the thermodynamic equilibrium constant with pressure is given by[40]

$$RT\left(\frac{\partial \ln K}{\partial P}\right)_{T,m} = -\Delta\overline{V} \qquad \text{I-59}$$

where $\Delta\overline{V}$ is the algebraic difference between the partial molal volumes of products and reactants in the equilibrum. In order to integrate this equation, $\Delta\overline{V}$ must be expressed in terms of pressure. This was done by Owen and Brinkley[40] through the definition of compressibility [$K = -\left(\frac{\partial V}{\partial P}\right)_{T,m}$]. By assuming K to be independent of pressure over a moderate pressure range, they derived a relation by which the equilibrium constant can be calculated at any pressure from $\Delta\overline{V}$ and $\Delta\overline{K}$ data. They used this relation to estimate the effect of pressure upon ionization (including the

ionization of water) and solubility constant. For water, it was found that the ionization constant increases with pressure and the relative increase is the greater, the lower the temperature.

As was already mentioned in Section I-9, a similar but simpler equation was used by Lown, Thirsk and Wynne-Jones [30]. However, they used the equation to obtain volumes and compressibilities of ionization from the pressure-dependence of ionization constants. It will be recalled that they found[30] a linear relation between $\Delta\overline{V}_i^o$ and $\Delta\overline{K}_i^o$. Verrall and Conway[21] obtained compressibilities of ionization for primary, secondary and tertiary methylammonium chlorides from separate measurements of compressibilities of the species involved in the ionization process. They found positive $\Delta\overline{K}_i^o$ values in all cases and attributed them to a stronger structure-promoting effect of the alkyl groups in the aminium cations relative to that caused by H_3O^+ ion.

(d) Relation to Hydration Numbers

The relation of hydration number to the compressibility was first considered by Passynski[77] and can easily be found by combination of the equation for hydration number in terms of volume, Equation I-26, and the definition of compressibility. Equation I-26 can be written as

$$\phi_V = V_i + n(\overline{V}_{H_2O} - V_{H_2O}) \qquad \text{I-60}$$

If the intrinsic volume, V_i, the hydration number, n, and the volume of electrostricted water, $\bar{V}_{H_2O}$, are assumed to be independent of pressure, differentiation of Equation I-60 with respect to pressure at constant temperature gives

$$\left(\frac{\partial \phi_V}{\partial P}\right)_T = n\left(-\frac{\partial V_{H_2O}}{\partial P}\right)_T \qquad \text{I-61}$$

or

$$\phi_K = -n\beta_{H_2O}V_{H_2O} \qquad \text{I-62}$$

i.e.

$$n = -\frac{\phi_K}{\beta_{H_2O}V_{H_2O}} \qquad \text{I-63}$$

Here ϕ_K is the isothermal apparent molal compressibility of the solution, β_{H_2O} the isothermal compressibility of water and V_{H_2O} is the molar volume of water. This equation was used by Padova[41] and by Desnoyers and Jolicoeur [42].

This method again gives, as usual, the <u>total</u> hydration number for the salts. A suitable method has then to be found to evaluate the individual ionic hydration numbers. This can be done by assuming the hydration number of an ion having small charge-to-size ratio (e.g., I^-) to be zero.

12. Individual Ionic Volumes and Compressibilities

The problem of obtaining individual ionic properties has already been mentioned in Section I-4. In this section, the methods used to determine the individual ionic volumes and compressibilities will be discussed. The excellent reviews on this subject by Conway[43,8f] and by Millero[7,18] must be noted.

(a) Individual Ionic Volumes

Most of the earlier methods for obtaining individual ionic volumes involve some relation to the ionic radii. Bernal and Fowler[44] set up a scale for ionic volumes by dividing the volume of CsCl in proportion to volumes of the two types of ions in the solid, considering the similar sizes of Cs^+ and Cl^-. Thus, the partial molal volumes of Cs^+ and Cl^- ($\overline{V}^o_{Cs^+}$ and $\overline{V}^o_{Cl^-}$) were found from the two equations

$$\overline{V}^o_{Cl^-} + \overline{V}^o_{Cs^+} = \overline{V}^o_{CsCl} \qquad \text{I-64}$$

and

$$\frac{\overline{V}^o_{Cs^+}}{\overline{V}^o_{Cl^-}} = \frac{r^3_{Cs^+}}{r^3_{Cl^-}} \qquad \text{I-65}$$

where r_{Cs^+} and r_{Cl^-} are the crystal ionic radii of Cs^+ and Cl^- in solid CsCl.

Noyes[45] used an extrapolation procedure to find the partial molal volume of the hydrogen ion. He used the equations

$$V_i - \bar{V}^o_{conv.} = \bar{V}^o_{H^+} + \frac{0.4175}{r} + \frac{C_2}{r^2} \qquad \text{I-66}$$

for cations and

$$V_i - \bar{V}^o_{conv.} = \bar{V}^o_{H^+} - \frac{0.4175}{r} + \frac{A_2}{r^2} \qquad \text{I-67}$$

for anions, where V_i is the intrinsic partial molal volume and $\bar{V}^o_{conv.}$ is the conventional partial molal volume obtained by assuming $\bar{V}^o_{H^+} = 0$. C_2 and A_2 are constants. $\bar{V}^o_{H^+}$, C_2 and A_2 were obtained by the method of least-squares "best" fit for values of the left hand sides of the above equations plotted against 1/r. Some void space effects were taken into account in V_i.

Glueckauf[46] also used a method involving ionic radii. He assumed that the intrinsic volume is given by (Equation I-15)

$$V_i = 2520(r_i + a)^3 \qquad \text{I-68}$$

where "a" is a packing factor, taken as 5.5 nm. The volume data were fitted for alkali metal chlorides (from Na^+ to Cs^+)

according to the relation

$$\overline{V}^{o} - 2520(r_i + 5.5)^3 = \overline{V}^{o}_{Cl^-} - \frac{A}{\overline{r}} \qquad \text{I-69}$$

where $\overline{V}^{o}$ is the partial molal volume of the alkali metal chloride, r_i is the radius of the alkali metal ion concerned and $\overline{r}$ is the sum of the radii of the alkali metal ion and the water molecule. $\overline{V}^{o}_{Cl^-}$ was obtained by extrapolating the linear plot of the left-hand-side of Equation I-69 against $1/\overline{r}$ to zero $1/\overline{r}$.

All these methods involve ionic radii. However, "true"* ionic radii are not known. There are several scales for crystal ionic radii such as Pauling's, Goldschmidt's and Gourary and Adrian's. Depending on the set of radii used, different values for the individual ionic volumes will be obtained. This is especially true if Gourary and Adrian's scale is selected, because it is significantly different from the others. Therefore, choice of a proper scale is as critical as the choice of a method for obtaining individual ionic volumes. Of course, the use of a method that is independent of ionic radii is a better alternative.

Conway, Verrall and Desnoyers[47] developed such a method for the assignment of individual ionic volumes which does not involve ionic radii. They found that the partial molal volumes at infinite dilution for the series of homologous

* They depend on the environment of the ions.

tetra-n-alkylammonium bromides are excellently linear in molecular weight of the cation. By extrapolating this linear relation to zero R_4N^+ cation molecular weight, the volume of the co-anion was obtained. This excellent linear relationship was supposed to be due to a compensation between any small electrostriction that these ions might cause and any positive volume effect due to the known structure enhancement which these ions promote in water. The point for NH_4^+ in the plot was below the line due to larger electrostriction for NH_4^+, as expected.

Recently, Krumgalz[10] reviewed various methods for separating partial molal volumes into ionic contributions and pointed out that in the last few years, Conway, Verrall and Desnoyers'[47] method has been used most frequently. He applied this method successfully to all existing data for non-aqueous electrolyte solutions over a wide temperature range.

Another interesting method, proposed by Kay [48], makes use of the well known complexation[49,97] between cations and crown ethers. The volume change, ΔV for the process;

$$\text{Polyether} + M^+ \rightleftharpoons \text{Polyether Complex} \qquad \text{I-70}$$

is given by

$$\Delta V = \overline{V}^{o}_{\text{Polyether Complex}} - \overline{V}^{o}_{\text{Polyether}} - \overline{V}^{o}_{M^+} \qquad \text{I-71}$$

If it is assumed that the partial molal volumes of the polyether complex and of the polyether are equal, then the partial molal volume of cation can be obtained from the pressure derivative of the stability constant of the complex. This assumption can be expected to be valid especially for complexation by polycyclic ligands[50] since they can sequester the ions almost completely.

One final and important method for individual ionic volumes is due to Zana and Yeager [51]. It is important because it gives the absolute individual ionic volumes experimentally. From ultrasonic vibration potential measurements, they were able to obtain the difference in partial molal volumes of cation and anion of a salt. Since the density measurements lead to the sum of the same quantities, the two equations can be solved for the individual ionic volumes. The results obtained, e.g., for $\overline{V}^{o}_{H^+}$ or $\overline{V}^{o}_{Cl^-}$ are in good agreement with those derived by the R_4N^+ extrapolation procedure.

(b) Individual Ionic Compressibilities

Glueckauf[52] derived an equation yielding ionic volumes, taking account of dielectric saturation effects. By considering the relative contributions to the decrease of compressibility of water due to the ionic field, from second- and third-, as well as first-layer water molecules, Glueckauf calculated isothermal ionic compressibilities.

Noyes[45] applied a method to find individual ionic compressibilities similar to the one used for volumes (previous section). However, structural contributions to the intrinsic compressibility were not allowed for. He used the same intrinsic compressibility term, Ar_i^3, where A is a constant and r_i is the ionic radius, for both anions and cations.

Laliberté and Conway[23] suggested a scale for ionic compressibilities based on extrapolation to zero cation molecular weight of $\overline{K}_S^o$ (adiabatic partial molal compressibility at infinite dilution) for a series of tetraalkylammonium and pyridinium halides. This method was analogous to that of Conway, Verrall and Desnoyers [47] for ionic volumes. However, they recognized that $\overline{K}_S^o$ is not so simple an additive property in molecular weight (or number of atoms in the molecule) as is the volume.

Mathieson and Conway[39] developed a method for individual ionic compressibilities. This method starts with Hepler's[11] equation for ionic volumes (Equation I-16),

$$\overline{V}_i^o = Ar_i^3 - \frac{Bz^2}{r_i} \qquad \text{I-16}$$

Assuming r_i is independent of pressure, $\overline{V}_i^o$ can be differentiated with respect to pressure,

$$\overline{K}_{S,i}^o = -\left(\frac{\partial \overline{V}_i^o}{\partial P}\right)_S = A'r_i^3 - B'z^2/r_i \qquad \text{I-17}$$

where A' and B' are the derivatives of A and B with respect to pressure. For an electrolyte of M_aX_b, $\bar{K}_S^o$ can be written as

$$\bar{K}_S^o(M_aX_b) = a\, r_+^3 A'_+ + b\, r_-^3 A'_- - \frac{az_+^2}{r_+} B'_+ - \frac{bz_-^2}{r_-} B'_- \qquad \text{I-73}$$

where subscripts + and - stand for cation and anion, respectively. Considering this as an equation with four unknowns, namely A'_+, A'_-, B'_+ and B'_-, they used a computer program for four-variable linear regression analysis to estimate the values of these parameters. Pauling's radii and compressibility data for the halides of K^+, Rb^+ and Cs^+ were used in these calculations.

Almost all the methods to find individual ionic compressibilities depend on data for ionic radii ; thus, the discussion about the choice of ionic radii, given in the previous section, also applies to compressibilities as well.

13. Previous Work on the Specific Topics Examined in the Present Research

Studies of partial molal volumes and compressibilities have been carried out on a considerable number of electrolytes and non-electrolytes, and some thorough reviews are available, e.g., Millero [7,18,36], Conway [1,8,43], Akitt [28] and Krumgalz [10]. Some recently published works which are closely related to the present subject will be summarized in this section.

(a) Partial Molal Volumes

The work of Couture and Laidler[25] on partial molal volumes of oxyanions has already been discussed (Section I-8). Recently, Desnoyers' and Hepler's group in a joint paper [53], and Hepler's group [54], reported apparent molal volumes of a set of salts of oxyanions including $NaClO_3$, $NaClO_4$, Na_2SO_4 and $Na_2S_2O_3$ which were also studied in the present work. They determined the apparent molal volumes at infinite dilution by the usual extrapolation procedure to zero concentration. They also listed conventional individual ionic volumes for the ions they studied.

Wen, Takeguchi and Wilson[55] reported viscosity and apparent molal volumes of aqueous triethylenediamine and its protonated form. They concluded that the hydrochloride is a weak water structure-breaker while the free base interacts with water and enhances the structure markedly. Kiyahora, Perron and Desnoyers[56] studied volumes and heat capacities of some cyclic ethers and amines in water. They found all the ethers and amines they studied (tetrahydropyran, p-dioxane, piperazine, morpholine and piperidine) to be hydrophobic. The overall structural influence was very small with dioxane and large with piperidine. They also estimated group contributions from $-CH_2-$, -NH-, and -O- to the thermodynamic functions studied. Enea, Jolicoeur

and Hepler[57] reported apparent molal volumes and heat capacities of some unsaturated heterocyclic solutes in aqueous solution. These compounds include pyrazine, pyridazine, imidazole and pyrazole in common with the compounds used in part of the present work.* They tabulated the infinite dilution values of volumes and heat capacities, and treated the data in terms of group and atomic additivity relationships. Conway and Laliberté[24] and Laliberté and Conway[23] studied the volume and compressibility behaviour of pyridine and piperidine, and their derivatives as well as their hydrochlorides. The results obtained for pyridine, piperidine and their protonated forms will be used together with the present results for interpretation since they were obtained in the same lab with the same method (except compressibility). Cabani and his co-workers[58,22] reported their work on volumetric properties of saturated cyclic amines, ethers and their proton ionization. They tried to correlate the volumes of ionization with some other thermodynamic properties as was discussed earlier (Section I-6).

(b) Partial Molal Compressibilities

In general, the works on compressibility reported in the literature are not so extensive as those on volume. This is probably due to the relatively greater difficulties involved

* The present work on these compounds was in progress at the time the work of Enea, Jolicoeur and Hepler[57] (1980) was published.

in experimental determination of compressibilities. It is only recently that experimental methods have been developed[59,60] for accurate measurement of compressibilities down to sufficiently low concentrations that limiting-law behaviour is approached. The compressibilities of simple salts such as NaCl and Na_2SO_4 studied in the present research as standards have been reported previously by several authors[38,39,60,61,62,63,64]. However, little work has been described on compressibilities of the salts of other oxyanions such as $NaClO_2$, $NaClO_3$, $Na_2S_2O_6$, $Na_2S_2O_3$, etc. On the other hand, studies on the compressibilities of organic molecules and ions investigated in the present research are also limited in the literature. Conway and Laliberté[24] and Laliberté and Conway[23] studied the compressibilities of pyridine, piperidine and their derivatives (methyl substituted on the ring or on "N") and the hydrohalides of these molecules. As in the case of volumes, their results for pyridine, piperidine and their protonated forms will be used together with the present results for interpretations. Conway, Mathieson and Dhar[65] examined the volumes and compressibilities of neutral pyrazine and pyridine in relation to their orientation behaviour when adsorbed at the mercury-water interface. Kaulgud and Patil[66] investigated volume and compressibility behaviour of aqueous solutions of amines including

ethylenediamine, pyrrolidine, piperidine and morpholine (neutral compounds only). Lawrence and Conway[67] studied the compressibility and its change upon ionization for ethylenediamine and some other polyethylenimines in relation to polyion hydration. Some of these early works and their results will be discussed and compared with the present observations in later chapters.

14. General Aims of the New Work

The general aim of the present research was to investigate the effects of size and configurational factors in ionic hydration and ionization of a selection of structurally related organic bases and a series of salts with polyatomic anions. The work involves the study of interactions of ions of various sizes, geometries and configurations with water.

The methods used were (a) evaluation of apparent molal volumes; and (b) evaluation of apparent molal compressibilities. Both these approaches have been shown previously[68,69] to be sensitive to steric, size and configurational factors in ion-solvent interactions.

The types of ions studied were some inorganic oxyanions and ions of some organic heterocyclic compounds ionized at the nitrogen centre. For the oxyanions, the problem of separation of ionic volumes into intrinsic and electro-

striction volume contributions will be discussed. A relation between the volume and the compressibility as well as the entropy will be sought. The results will be discussed in terms of size and charge effects, and number of oxygen ligands. From measurements of volumes and compressibilities of organic bases and their ions, the changes in these functions upon ionization were determined. The relation between volume and compressibility of ionization, as well as between these functions and some other functions, for example entropy of ionization was investigated. The results will be discussed in terms of configurational and conformational effects.

The organic compounds were chosen in a systematic way in order to be able to investigate the effect of (a) the number of cyclic ring systems; (b) $>$NH, $>$O replacement in the ring; (c) the number of "N" centres in the ring; (d) aromaticity; (e) position of "N"s in the ring and (f) the number of $-CH_2-$ groups in the ring, on the hydration and ionization properties of several series of structurally related substances.

CHAPTER II

GENERAL FORMULATION OF PARTIAL MOLAL VOLUMES AND COMPRESSIBILITIES

1. Partial Molal Volumes

The partial molal volume of a solute may be visualized by considering a large reservoir of solution, so large that the addition of one mole of solute will not alter the concentration. The change in volume of the solution upon the addition of one mole of solute to this large reservoir of volume is the partial molal volume of the solute at the indicated concentration at constant temperature, pressure and moles of other components. Mathematically, this can be represented by the partial derivative of the total volume, V, with respect to concentration at constant temperature T, pressure P and numbers of moles of other components, n_1 ...., i.e.,

$$\bar{V}_i = \left(\frac{\partial V}{\partial n_i}\right)_{T,P,n_{j\neq i}} \qquad \text{II-1}$$

For a binary solution, where component 1 is water and component 2 is a solute, II-1 is written as

$$\bar{V}_2 = \left(\frac{\partial V}{\partial n_2}\right)_{T,P,n_1} \qquad \text{II-2}$$

where $\bar{V}_2$ is the partial molal volume of the solute, n_2 is the number of moles of solute and n_1 is the number of moles of water. The total volume of the solution, V, is related to the partial molal volumes of the components by

$$V = n_1\bar{V}_1 + n_2\bar{V}_2 \qquad \text{II-3}$$

where $\bar{V}_1$ is the partial molal volume of water.

The partial molal volumes can be determined from density or volume data by employing a very useful quantity known as the apparent molal volume, first introduced by Marignac[70]. When n_2 moles of solute are added to a large volume of water and the partial molal volume of water is taken as its infinite dilution value, $\bar{V}_1^o$, then the apparent molal volume of the solute ϕ_v is defined by

$$\phi_v = (V-V_{H_2O})/n_2 = (V-n_1\bar{V}_1^o)/n_2 \qquad \text{II-4}$$

where $V_{H_2O} = n_1\bar{V}_1^o$ is the volume of water in the solution.

For a molal solution (n_2=m), V and V_{H_2O} are given by

$$V = (1000 + mM_2)/d \qquad \text{II-5}$$

$$V_{H_2O} = 1000/d_o \qquad \text{II-6}$$

where m is the molality (moles per kilogram of water), M_2 the molecular weight of the solute and d and d_o are the densities of solution and water, respectively. Substituting

Equations II-5 and II-6 into II-4 yields

$$\phi_v = \frac{1000(d_o - d)}{mdd_o} + \frac{M_2}{d} \qquad \text{II-7}$$

When molar concentrations are used (n_2=c), V and V_{H_2O} are given by

$$V = 1000\ cm^3 \qquad \text{II-8}$$

and

$$V_{H_2O} = (1000d - cM_2)/d_o \qquad \text{II-9}$$

Substituting Equations II-8 and II-9 into II-4 yields

$$\phi_v = \frac{1000(d_o - d)}{cd_o} + \frac{M_2}{d_o} \qquad \text{II-10}$$

The partial molal volume of a solute in terms of its apparent molal volume can be obtained by differentiating Equation II-4 with respect to n_2; thus

$$\bar{V}_2 = \phi_v + n_2\left(\frac{\partial \phi_v}{\partial n_2}\right)_{T,P,n_1} \qquad \text{II-11}$$

This shows that, at infinite dilution, i.e., $n_2 \to 0$, the partial molal volume becomes identical with the apparent molal volume ($\bar{V}_2^o \equiv \phi_v^o$), a well known result.

In order to determine ϕ_v^o or $\bar{V}_2^o$, the extrapolation of the apparent molal volumes of solute to infinite dilution

is necessary. For nonelectrolytes this extrapolation can simply be done according to

$$\phi_v = \phi_v^o + b_v' m \qquad \text{II-12}$$

where b_v' is an adjustable parameter. For electrolytes, on the other hand, the Redlich-Meyer[71] equation can satisfactorily be applied. It is given by

$$\phi_v = \phi_v^o + S_v \sqrt{c} + b_v c \qquad \text{II-13}$$

where S_v is the theoretical Debye-Hückel limiting slope. The value of S_v is well characterized and this is one of the reasons for the satisfactory applicability of Equation II-13. S_v depends only on the charge type but not on the nature of the electrolyte. For 1:1 and 1:2 type electrolytes its values are 1.868 and 9.706 $cm^3\ mol^{-3/2}\ L^{1/2}$, respectively [7]. b_v is again an experimentally observed parameter.

2. Partial Molal Compressibilities

The partial molal compressibility of a solute is defined by

$$-\bar{K} = \left(\frac{\partial V}{\partial P}\right)_T \qquad \text{II-14}$$

The apparent molal compressibility is similarly

$$-\phi_K = \left(\frac{\partial \phi_v}{\partial P}\right)_T \qquad \text{II-15}$$

So, differentiation of Equation II-4 with respect to pressure gives

$$-\phi_K = \frac{\left(\frac{\partial V}{\partial P}\right)_T - n_1 \left(\frac{\partial \bar{V}_1^o}{\partial P}\right)_T}{n_2} \qquad \text{II-16}$$

By introducing the compressibility, β, defined by Equation I-41, the relation

$$-\phi_K = (-\beta V + n_1 \bar{V}_1^o \beta_o)/n_2 \qquad \text{II-17}$$

is obtained where β_o is the compressibility of water.

For a molal solution, combination of Equations II-5, II-6, II-7 and II-17 yields

$$\phi_K = \frac{1000}{m d_o} (\beta - \beta_o) + \beta \phi_v \qquad \text{II-18}$$

Similarly, for a molar solution, Equations II-8, II-9, II-10 and II-17 yield

$$\phi_K = \frac{1000}{c} (\beta - \beta_o) + \beta_o \phi_v \qquad \text{II-19}$$

The partial molal compressibility of a solute in terms of apparent molal compressibility can be obtained as

$$\bar{K} = \phi_K + n_2 \left(\frac{\partial \phi_K}{\partial n_2}\right)_T \qquad \text{II-20}$$

which follows from Equations II-14 and II-16. Here $\bar{K}$ and ϕ_K are the partial and apparent molal compressibilities of a solute, respectively. Again, Equation II-20 shows that, at infinite dilution, i.e., as $n_2 \to 0$, the partial and apparent molal compressibilities become identical, i.e., $\bar{K}^o \equiv \phi_K^o$.

As already mentioned in the introduction, evaluation of the isothermal compressibility from P-V measurements is difficult. An alternative method involves the measurement of the adiabatic compressibility by determining the velocity of propagation of sound waves through a solution. An acoustic or pressure wave travelling through a solution produces a rapid compression which, unlike a static compression, does not allow sufficient time for any heat flow to or from the system. Therefore, the compression process is adiabatic. The adiabatic compressibility, β_S, is related to the velocity of sound, u, by

$$\beta_S = \frac{100}{u^2 d} \qquad \text{II-21}$$

When the density of solution, d, is in g cm^{-3}, and the velocity of sound is in m s^{-1}, β_S is obtained in bar^{-1} through Equation II-21. The apparent molal adiabatic compressibility, ϕ_{KS} is given by

$$\phi_{KS} = \frac{1000(\beta_S - \beta_S^o)}{md_o} + \beta_S \phi_v \qquad \text{II-22}$$

or

$$\phi_{KS} = \frac{1000(\beta_S - \beta_S^o)}{c} + \beta_S^o \phi_v \qquad \text{II-23}$$

where β_S^o is the adiabatic compressibility of water. The relation between adiabatic and isothermal compressibilities is given by Equation I-45, i.e., $\beta_S = (C_V/C_P)\beta$. Because the C_V and C_P data were not available for these solutions, the adiabatic compressibilities have been used directly in the present work.

The concentration dependence of apparent molal adiabatic compressibility of a non-electrolyte can be expressed in terms of the equation

$$\phi_{KS} = \phi_{KS}^o + b_{KS} m \qquad \text{II-24}$$

where ϕ_{KS}^o is the apparent molal adiabatic compressibility at infinite dilution and b_{KS} is an empirical parameter. For an electrolyte, on the other hand, an equation analogous to II-13 can be written. However, the theoretical limiting slope (slope with respect to $\sqrt{c}$) is not known for compressibilities. Therefore, a simpler limiting law equation

$$\phi_{KS} = \phi_{KS}^o + S_{KS}^* \sqrt{m} \qquad \text{II-25}$$

can be used. Mathieson and Conway[39] pointed out that an extrapolation procedure according to an equation analogous to II-13, (a) requires that the theoretical limiting slope be known; (b) has no advantages over the ϕ_{KS} versus $m^{1/2}$ plot (Equation II-25) if the data are obtainable in the region where the limiting law applies experimentally.

CHAPTER III

EXPERIMENTAL

1. Methods of Measurement

(a) Partial Molal Volumes

Determinations of partial molal volumes are usually made from the corresponding apparent molal volumes. In practice, the apparent molal volume data are obtained from density measurements on the solution, d, and the solvent (water), d_o. Since differences of d and d_o determine the apparent molal volume (Equation II-7), they must be very accurately known.

Various methods are available for the measurement of densities of solutions, e.g., the Archimedian balance procedure, the magnetic float method, regular pyknometry (less accurate), dilution dilatometry and flow densitometry [8g]. Certain factors such as the concentration range under study, the volatility of the solvent, the temperature and the reactivity of the solvent or solute toward O_2 or CO_2 determine the choice of a suitable method for measuring the density. Among the above methods, dilution dilatometry gives very accurate density data at high dilutions. However, it requires that the density of the starting solution be known. Then the densities at higher dilutions may be obtained

relatively by means of further dilution using this method. Therefore, it can only be used together with one of the other methods.

The hydrostatic balance method of Kohlrausch [72], based on the Archimedian principle, was shown by Wirth [73] to give results of a high degree of accuracy when used differentially. This method has been successfully used in this laboratory for measurements of partial molal volumes in studies on steric, size and configurational factors in ion-solvent interactions [21,23,24,47,74]. It was therefore also used in the present work. This method allows a more direct comparison of the density of the sample and reference solution and provides partial cancellation of errors. Furthermore, it has the advantage that changes of the concentration of the sample solution can easily be made by addition of solute without changing the whole solution for measurements at increasing concentrations.

i. Apparatus

The principal parts of the apparatus used in density measurements are shown schematically in Figure 1. The system is essentially the same as that used by Verrall [68] and Laliberté [69].

The balance was an Oertling model HO3, modified for under-pan weighing on both the front and back pans. The

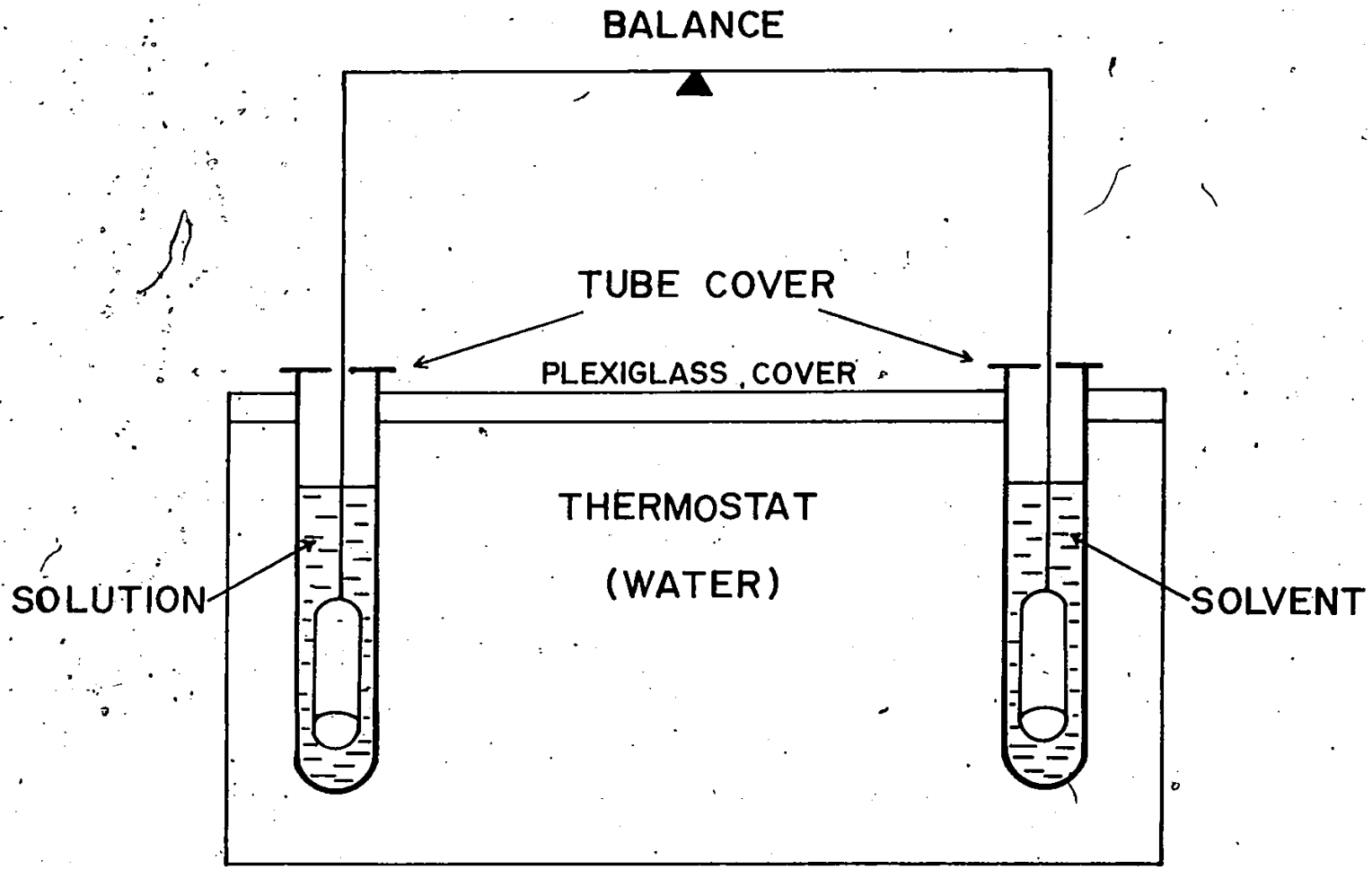

Figure 1 - A schematic diagram of the differential buoyancy balance.

vessels, in which the solvent and solution were placed, were made of Pyrex tubing, 48 mm i.d., and were mounted beneath the balance in plexiglass holders in a thermostat. These holders were fixed in two separate polystyrene mounts supported by aluminum plates in such a way that they keep the vessels in a vertical position in the thermostat. Polystyrene mounts were also useful as a cover for the thermostat. The vessels were provided with plexiglass covers having small holes for the support wires joined to the balance pans (Figure 1).

The floats, blown of Pyrex tubing of 40 mm o.d. were cylindrically shaped with a conical base and a spherical top. The floats had a volume of about 120 cm^3 and were loaded with mercury to have an apparent density of about 1.12 g cm^{-3}. They were suspended in the vessels by means of 0.05 mm diameter tungsten wires. The upper parts of the suspension were fine gold plated chains connected to the pans of the balance.

All measurements were made in a 150 dm^3, well lagged water thermostat provided with an annular window and heated by means of a partially immersed electric bulb. The temperature was controlled by a large hand-made mercury thermo-regulator (approximately 100 cm^3 of mercury). A high speed stirrer situated at a slight angle and immersed deeply in the bath, provided good circulation.

ii. Accuracy and Calibrations

The overall accuracy of the apparatus was sufficient to allow densities to be measured to six decimal places. For this purpose, the temperature of the bath had to be maintained at 25.000 ± 0.005°C as monitored on a Beckmann thermometer which was calibrated with a thermometer having a 5.5 cm scale for 1°C (each division on its scale was 0.002°C). Temperature differences across the thermostat were undetectable. The floats were examined in each measurement for adhering small air bubbles which were removed if present and for any "sticking" to the walls of the vessels. The length of the suspension wire submerged during a run with any particular solute was always kept the same in both the solvent and solution vessels.

The main sources of errors in the determination of apparent molal volumes are expected to be densities and concentrations of solutions. Thus, differentiation of Equation II-10 with respect to c at constant d and with respect to d at constant c yields

$$\text{Probable error in } \phi_v = \left(\frac{M_2}{d_o} - \phi_v\right) \frac{(\delta c)}{c} \qquad \text{III-1}$$

and

$$\text{Probable error in } \phi_v = \left(\frac{-1000}{c}\right) \frac{(\delta d)}{d_o} \qquad \text{III-2}$$

respectively. Equations III-1 and III-2 show that in dilute solutions, ϕ_v is not seriously influenced by errors in c; however, errors in d do, of course, cause corresponding uncertainties in ϕ_v.

The density measurements with the apparatus used in this work were reproducible to 2 in the sixth decimal place. This leads to an uncertainty of ± 0.2 cm^3 mol^{-1} in ϕ_v at c=0.01 M while the uncertainty decreases to ± 0.02 cm^3 mol^{-1} at c=0.1 M. The reliability of the measurements was determined with test runs on KCl solutions. The values obtained agreed to within 0.1% of the published data [75].

iii. Procedure Used in Density Determinations

Two slightly different procedures were used. In the work with most of the solutes, the procedure was as follows. Approximately 150 cm^3 water, prethermostatted at 298 K, were weighed accurately into the test vessel and the vessel was placed in the thermostat. The float, which had an accurately known volume, previously determined at the same temperature was suspended in this vessel from the front pan of the balance. Then, approximately the same amount of water, again prethermostated at 298 K, was placed in the solvent vessel. The level of water in this vessel was such that after the suspension of the second float from the rear pan of the balance, the length of the suspension wire

submerged was the same as that in the test vessel. It was not necessary to know the weight or volume of water in the "solvent" vessel. After making sure that both floats are not adhering to the walls of the vessels, the vessels were covered with plexiglass covers and allowed to reach thermal equilibrium with the thermostat fluid for about one hour. A stable reading on the balance for at least a minute indicated that this equilibrium has been attained. For every measurement this test was repeated.

The reading from the balance, with both vessels containing water, was recorded as w_o. Then an accurately weighed amount of solute was added to the test vessel and dissolved by moving the float slightly up and down. The solution was again allowed to attain thermal equilibrium after covering it with the plexiglass cover, but this time for only about ten minutes. A reading from the balance was recorded as w. The difference in density, Δd, between the water and solution is then given by

$$\Delta d = d_o - d = (w - w_o)/V_B \qquad \text{III-3}$$

where d_o and d are the densities of water and solution, respectively, and V_B is the volume of the float in the test vessel. Addition of solute to the solution was repeated 8-13 times (for some salts up to 23 times, e.g., NaCl) and the density was determined each time. The density of water

was taken from reference 76 as* 0.997075 g cm^{-3} at 298 K.

In cases where the solute is a liquid, the addition to the test vessel was made by means of a calibrated micrometer syringe which delivered a volume of 1 x 10^{-4} cm^3 per division on its scale.

For some of the solutes, e.g., ethylenediamine monohydrochloride, imidazole hydrochloride, pyrazine, pyrazole hydrochloride and pyrrolidine hydrochloride, a slightly different procedure was applied. The solutions were first made up volumetrically in volumetric flasks and measurements were carried out by changing the solution in the test vessel each time. The same precautions as in the former procedure were taken for each measurement, e.g., thermal equilibration, ensuring that the same length of suspension wire was submerged in each of the two vessels, lack of adherence of the float to the walls of the vessels or of air bubbles to the float. The flasks containing the solutions were also kept in an auxiliary thermostat at 298 K prior to measurements on the solutions contained therein.

(b) Partial Molal Compressibilities

The difficulties which arise in determination of isothermal compressibilities by means of P-V measurements were already discussed in Sections I-11-a and II-2. It was pointed out that an alternative method involves the

* This value is based on the definition of the "old" ml. The new value should be taken as 0.997047 g cm^{-3} but this does not significantly affect the calculations of ϕ_V and β_S here.

measurement of adiabatic compressibility by determining the velocity of propagation of sound waves through solutions [Section II-2] which can be done with impressive accuracy.

Early methods used for determining the velocity of sound in solutions are: (i) Ultrasonic interferometry, developed by Passynski [77], (ii) differential interferometry, a method first described by Carstenson[78] and used successfully in the early work in our laboratory [68,69]. However, an improved method has recently become available. It is based on measurement of the delay time in transmission of a pulsed ultrasonic signal between a transmitter and a receiver transducer, through a double-reflection path. The technique is called the "sing-around" method [60]. It is suitable for small solution samples (about 80 cm^3) and works well down to moderate dilutions just in the Debye-Hückel limiting law range. A commercially produced instrument is available [79]. This method was recently employed for accurate adiabatic compressibility measurements by Mathieson and Conway[59,37] and Garnsey et al [60]. It was also used in the present work. The details of the apparatus and the experimental procedure will be described next.

i. Apparatus

The apparatus used was the Model 6105 "Velocimeter" of NUS Corporation; the principal components are as shown in

Figure 2.

The system employs two transducers and two reflecting surfaces in the liquid. A pulse of ultrasonic radiation is sent from a transducer, marked A in Figure 2a, and reflected twice through the liquid being examined, back to a receiving transducer B. The transducers and reflectors are mounted in a corrosion resistant, stainless steel probe. After transmission of a given pulse, a transmission time t_s is involved before the reception of the reflected signal at the receiver. This delay time is determined by the velocity of sound in the solution. A further calibrated delay time t_d is also involved between the reception of the reflected pulse signal and generation of a new pulse from the transmitter transducer. Pulse repetition rate is determined by the total time $t_s + t_d$ and the measurement consists of counting the number of pulses received in a given time. A Philips decade scalar and timer, and a counter were used to record the counts. The number of counts per second is the pulse frequency f, typically ca. 10^5 s^{-1}. If ℓ is the length of the sound path at 0^oC and α is the coefficient of expansion of the stainless steel probe, then the sound velocity u in m s^{-1} is given by the following empirical equation

$$u = \frac{\ell f(1 + \alpha T)}{7 - t_d f} \qquad \text{III-4}$$

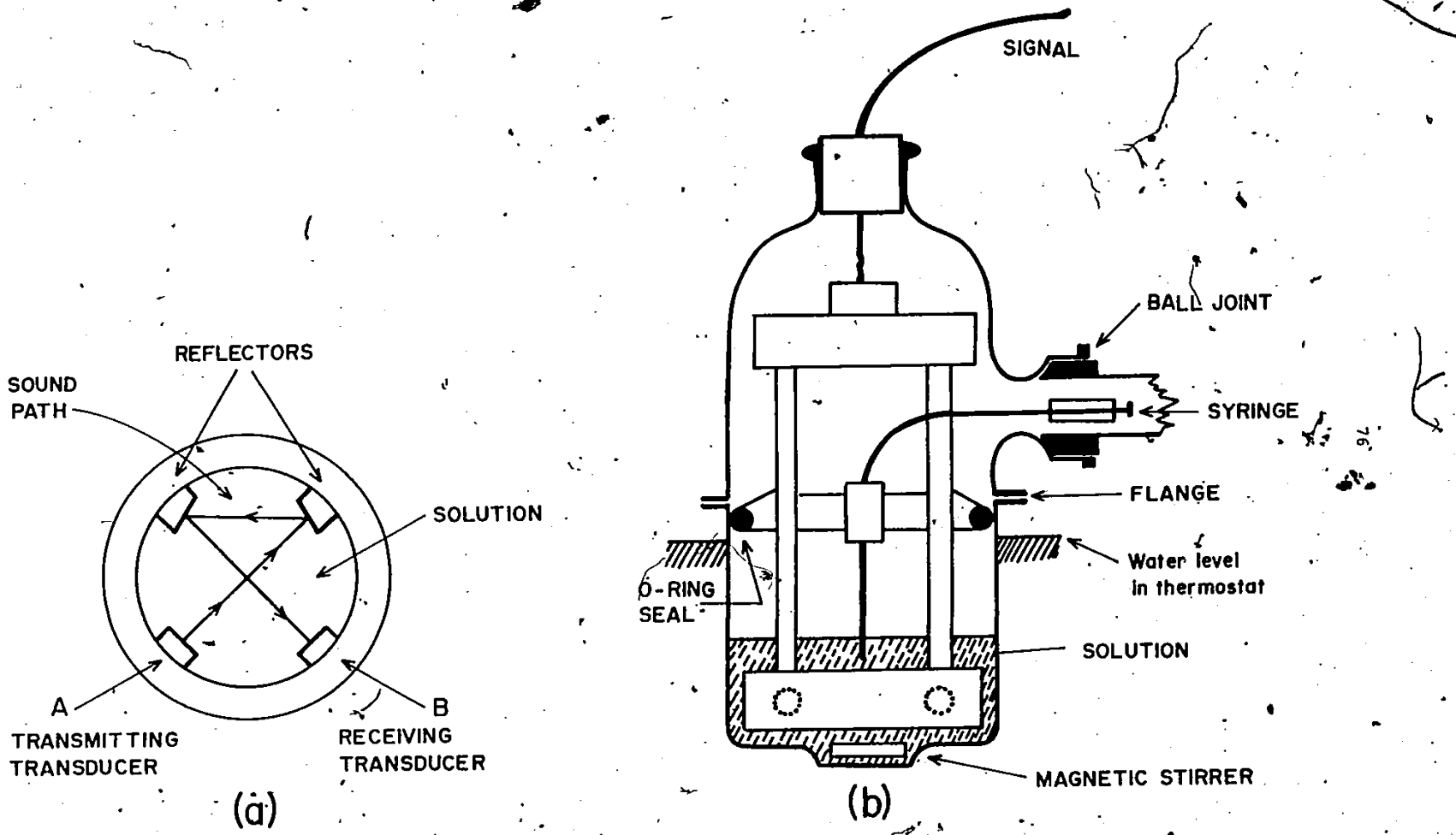

Figure 2 - Reflection arrangements and the cell for measurements of ultrasonic velocities in solutions.

as provided by the manufacturer [80], where T is the temperature expressed in °C. Calibration values of ℓ and t_d were supplied again by the manufacturer and were used directly in this work since they were verified previously [59].

The probe was fitted with a plexiglass platform (Figure 2.b) into the glass cell by means of an O-ring seal. The plexiglass platform had a hole in the middle through which additions of solute to change the concentration of solution under study could be made. This hole was kept closed with a plexiglass stopper except during the solute addition. The assembly was partly immersed in a large water thermostat, details of which are given in the following section. The solutions under investigation were stirred magnetically by a teflon-coated bar which followed a submerged rotating magnet driven by a motor through a flexible cable beneath the glass cell.

ii. Temperature Controlled Bath

A large rectangular (70 x 30 x 40 cm) bath made of copper and insulated by polystyrene foam on all sides except the top was used.

Temperature control of the bath was made by means of a mercury-toluene regulator constructed as follows. About 13 m of 1.27 cm diameter copper tubing was wound on a frame about the inside walls of the bath. This tubing was filled

with sulphur-free toluene (about 1.5 L) and attached to the regulator head. The attachment was made by means of a Cajon fitting having O-rings on both sides, made of viton, to prevent any leakage of toluene. A schematic diagram of mercury-tuluene regulator head is shown in Figure 3. A thread of mercury was maintained through the teflon taps as toluene alone was found to leak through the tap. The regulator head was connected to a light bulb, partly immersed into the thermostat to provide heating, through an electronic relay. A platinum wire was used to contact mercury along the capillary. The Pt wire could be moved up or down by means of a screw, to make fine temperature adjustments. The platinum wire and the surface of Hg were kept in a N_2 atmosphere to avoid bad contact by oxidation of the Hg. The thermostat was operated at 298 K.

The temperature throughout the thermostat was maintained at a uniform value by means of a powerful stirrer. No other source of heat than the light bulb was necessary. However, during the summer, water, cooled to about 295 K in an auxiliary bath, had to be circulated in the main bath through a copper coil, since occasionally the room temperature was above 298 K. The temperature was monitored with a Beckmann thermometer calibrated with a very accurate thermometer.

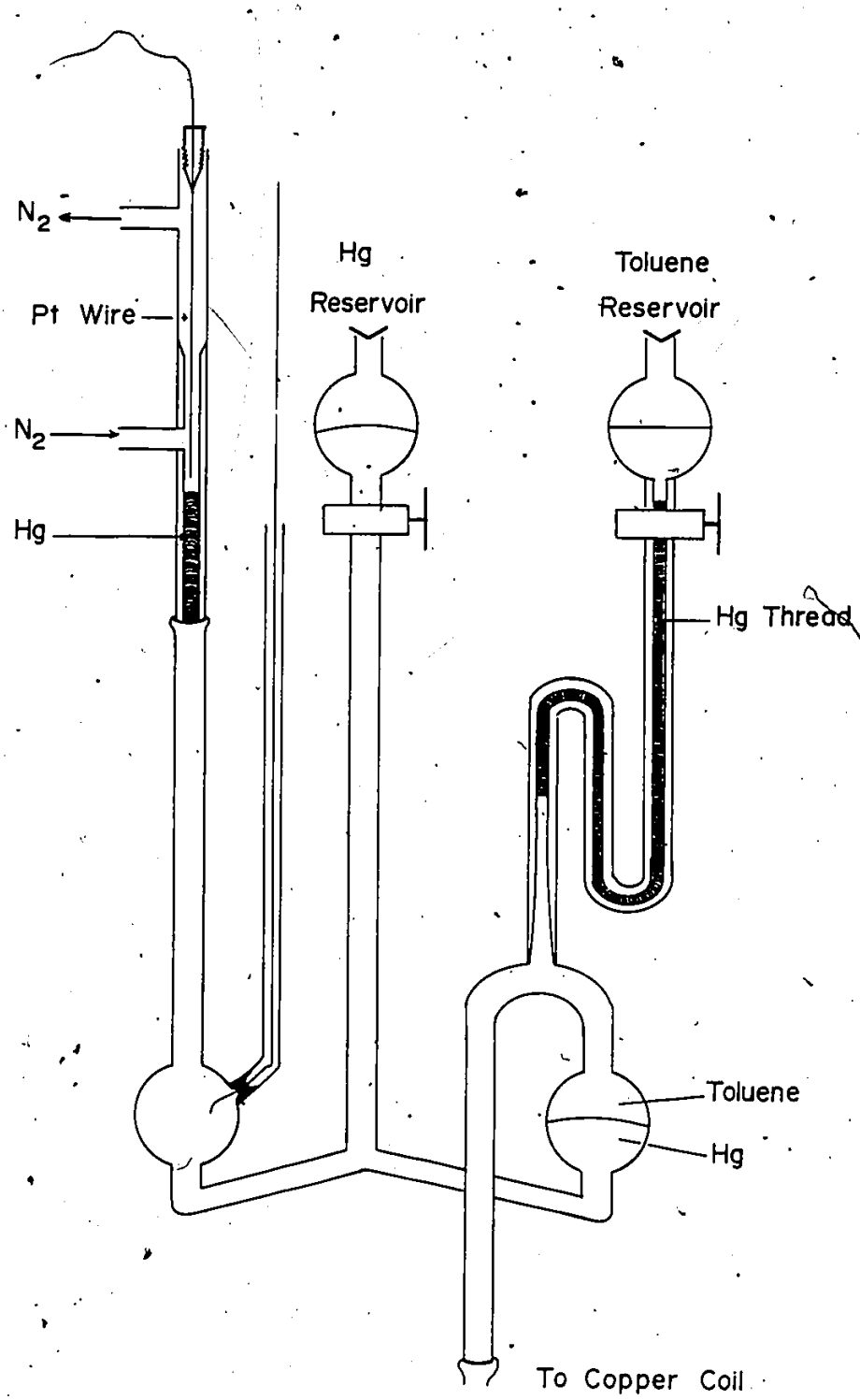

Figure 3 - Mercury-toluene regulator head for temperature controlled bath.

iii. Procedure Used in Sound Velocity Determinations

About 95 to 100 cm^3 of water were accurately weighed into the solution vessel, and a thermal equilibration period of about one hour was allowed before velocity determinations were made. When using a solid solute, additions were made by removing the plexiglass stopper momentarily and transferring accurately weighed amounts of the solute into the vessel from a small ladle made from a 1 cm^3 beaker attached to a 10 cm glass rod. When the solute was liquid, the calibrated micrometer syringe, mentioned in Section III.1.a.iii, was used for additions. After each addition, a period of 10 to 15 min. was allowed for thermal equilibration. The dissolution of solute and the equilibration was helped by stirring the solution as described in Section III.1.b.i. For the solutes for which the solutions were prepared in volumetric flasks, the measurements were carried out by changing the solution in the vessel each time, instead of by successive additions of solute.

Forty-second count measurements were taken (4×10^6 counts) until five successive determinations agreed to ±5 counts, i.e., about ±1 in 10^6. The average of these five readings, divided by 40 was the pulse frequency, f. Using Equation III-4, the velocity for each solution was calculated.

iv. Accuracy and Calibrations

The temperature control of the thermostat was better than $\pm 0.0005^{\circ}C$ as monitored by a Beckmann thermometer and differences in temperature across the thermostat were undetectable. Since the temperature coefficient of sound velocity in water[81] is 2.4 m s^{-1} $^{\circ}C^{-1}$, $\pm 5 \times 10^{-4}$ $^{\circ}C$ uncertainty in temperature would produce $\pm 1.2 \times 10^{-3}$ m s^{-1} uncertainty in velocity. On the other hand, the uncertainty in frequency, f, is ± 0.1 s^{-1} for a typical frequency of 10^5 s^{-1} as discussed in the previous section. This leads to an uncertainty of $\pm 1.5 \times 10^{-3}$ m s^{-1} in sound velocity as estimated by differentiation of Equation III-4 with respect to f. Thus the total uncertainty in sound velocity is $\pm 3 \times 10^{-3}$ m s^{-1}.

In order to find the corresponding error or uncertainty in apparent molal compressibility, ϕ_{KS}, Equation II-23 has to be differentiated with respect to u at constant d and with respect to d at constant u, if errors in concentration are neglected. Doing that and using the uncertainties $\pm 3 \times 10^{-3}$ m s^{-1} and $\pm 2 \times 10^{-6}$ g cm^{-3} for the velocity and the density, respectively, the total uncertainty in apparent molal compressibility was estimated as $\pm 0.4 \times 10^{-4}$ cm^3 mol^{-1} bar^{-1} at 0.01 M concentration.

The degree of absolute accuracy was tested by comparison of the apparent molal compressibility at infinite dilution of -50.52×10^{-4} cm^3 mol^{-1} bar^{-1} obtained for NaCl in the present work with the literature values of -50.5×10^{-4}, -50.63×10^{-4}, -50.45×10^{-4} cm^3 mol^{-1} bar^{-1}, from references 39, 64 and 36, respectively. The agreement is within 0.12%.

2. Preparation and Purification of Solutes Used

(a) Inorganic Salts

NaCl, $NaClO_3$, $NaClO_4$, Na_2SO_3, Na_2SO_4, $Na_2S_2O_3$ and $Na_2S_2O_6$ solutes were all reagent or analytical grade salts and were recrystallized from double distilled water at least once. $NaClO_2$ was obtained from Alfa Chemicals and it was the commercially available 80% pure product. The purification to a reagent grade level was carried out according to the method described in Reference 82.

All the salts were dried in vacuo at about 323 K and kept in a desiccator until the time of use. When there was a possibility of obtaining the hydrated salt after recrystallization, the salts were dried to a constant weight above the temperature at which they lose their water of hydration.

(b) Organic Compounds

Triethylenediamine, piperazine, ethylenediamine, pyrazine, pyridazine, pyrazole, imidazole, 1,2,4 triazole, pyrrolidine, quinuclidine and morpholine were obtained from Aldrich Chemicals and 1,4 dioxane was from Fisher Chemicals.

The neutral compounds were at least 99% pure except triethylenediamine (97%), pyrazole (98%) and pyridazine (97%). The apparent molal volume results obtained for triethylenediamine before and after recrystallization were in agreement to within 0.1%. Pyridazine was distilled twice under vacuum. The other compounds were used without further purification. The solid solutes, triethylenediamine, piperazine, pyrazine, pyrazole, imidazole, 1,2,4 triazole and quinuclidine, were dried in vacuo below their respective melting points and kept in a desiccator. Since some of these compounds are very hygroscopic, they were taken out of the desiccator only during the addition to solution under study and kept in the desiccator until the next addition was required. The liquid solutes were also kept in the desiccator. The apparent molal volume results obtained for 1,4 dioxane, when used directly and after drying over a desiccant, were in agreement to within 0.1%.

(c) Hydrochlorides of the Organic Bases

Mono and dihydrochlorides of triethylenediamine and piperazine and the monohydrochloride of pyridazine, were prepared by dissolving the neutral compounds in methanol and adding a stoichiometric amount of standard hydrochloric acid. The hydrochlorides were crystallized and dried *in vacuo*.

Hydrochlorides of pyrazine, 1,2,4 triazole and morpholine were prepared in a different way. The neutral compounds were dissolved in acetone. The hydrochloride salts were formed directly as crystals when HCl gas, prepared by dropping concentrated sulphuric acid onto a slurry of analytical grade NH_4Cl and concentrated HCl, was passed into the acetone solution.

All hydrochlorides were at least 99% pure based on the Cl^- analyses carried out according to Volhard's method [83].

Quinuclidine hydrochloride and ethylenediamine dihydrochloride were obtained from Aldrich Chemicals and used without further purification.

Ethylenediamine monohydrochloride was prepared in solution by mixing stoichiometric amounts of ethylenediamine and ethylenediamine dihydrochloride. The monohydrochloride could not be satisfactorily crystallized but instead, measurements were carried out directly using the resulting

solutions. Similarly, imidazole hydrochloride, pyrazole hydrochloride and pyrolidine hydrochloride were prepared in solution from stoichiometric amounts of the neutral compounds and standard hydrochloric acid.

The method used for preparation of the hydrochlorides was determined according to their solubility and specific difficulties in crystallization.

(d) Water

All water used to make up solutions and rinse the test vessels, was doubly distilled, the second distillation being from alkaline permanganate.

CHAPTER IV

RESULTS

1. General

In this chapter, the apparent molal volume and compressibility results obtained for the various systems studied will be presented in tabular and graphical forms. A complete tabulation of the experimental data can be found in the appendices following the last chapter. First, how the experimental density and sound velocity data were treated, to obtain apparent molal volumes and compressibilities, will be discussed.

2. Treatment of Data

(a). Partial Molal Volumes

First, the apparent molal volumes, ϕ_v, were determined using the experimentally measured densities in Equation II-7 or II-10, depending on the scale of concentrations. Then, for the non-electrolytes, the apparent molal volumes were plotted against concentration according to Equation II-12. For the salts, $\phi_v - S_v \sqrt{c}$ data were plotted against concentration, c, according to Equation II-13. The value for S_v, the theoretical Debye-Hückel limiting slope, was taken as 1.868 $cm^3\ mol^{-3/2}\ L^{1/2}$ for 1:1 and 9.706 $cm^3\ mol^{-3/2}\ L^{1/2}$ for 1:2 type electrolytes[7]. When

necessary, the interconversion between molarity and molality was made according to the equation

$$m = 1000\ c/(1000\ d - cM) \qquad \text{IV-1}$$

where c and m are molarity and molality, respectively, d is the density of the solution and M is the molecular weight of the solute.

On the basis of these graphs [ϕ_v vs c or m and $(\phi_v - S_v)\sqrt{c}$ vs c], a subjective decision was made whether to ignore the one or two experimental points for the lowest concentrations which, in some cases, appeared definitely out of line. Upper limits of concentration were set where the functions could be considered linear. The data were then fitted by a linear least-squares plot and the values of ϕ_v^o, the apparent molal volume at infinite dilution ($\equiv \overline{V}^o$, partial molal volume at infinite dilution), and the parameter b_v were determined.

(b) Partial Molal Compressibilities

The experimentally measured velocities of sound, u, in solutions were used in Equation II-21 to calculate the adiabatic compressibilities, β_S. The densities required for this calculation were obtained from the measurements which were made for the determination of apparent molal volumes by the differential buoyancy balance method.

In some experiments, the same solution was used for both the density and the sound velocity measurements in the case where the solution was prepared in a volumetric flask. Thus, for these solutions, the density obtained from the differential buoyancy balance was directly used in the calculation of β_S. However, for solutions which were prepared by successive additions of solute to an initially weighed amount of water, the concentrations employed in density measurements may not be exactly the same as the concentrations used for the sound velocity measurements. The densities corresponding to concentrations for the sound velocity measurements were determined by interpolations in the known density vs concentration relations. For the salts of oxyanions, the interpolation was made by assuming a straight-line relation between the appropriate two consecutive concentrations. On the other hand, for the organic compounds, a polynomial regression method was employed to relate the measured density data to the respective concentrations. Then the density at any concentration was calculated from the polynomial expression which represented the best fit for the measured data.

The adiabatic compressibilities and densities obtained in this way were used to calculate the apparent molal compressibilities, ϕ_{KS}, according to Equation II-22 or II-23. For non-electrolytes, the ϕ_{KS} data were plotted

against concentration according to Equation II-24. For the salts, the ϕ_{KS} data were plotted against square-root of concentration according to Equation II-25.

On the basis of these graphs, the apparent molal adiabatic compressibilities at infinite dilution ϕ_{KS}^{o} ($\equiv \overline{K}_S^o$, partial molal adiabatic compressibility at infinite dilution) and the parameters b_{KS} and S_{KS}^{*} of Equations II-24 and II-25, respectively, were determined by the method described in the previous section (i.e., using least-squares fitting).

(c) Corrections for Hydrolysis and Acidic Dissociation

In the case of some of the un-ionized bases studied, an appreciable degree of hydrolysis may occur leading to some ionization according to the equation

$$B + H_2O \rightleftharpoons BH^{+} + OH^{-} \qquad \text{IV-2}$$

where B is the un-ionized basic compound and BH^{+} is its conjugate acid cation. For the determination of apparent molal quantities (volume or compressibility) of the base itself, the process IV-2 is obviously undesired. Therefore, it must either be prevented or a correction must unavoidably be made to the data obtained by allowing the hydrolysis to take place. Prevention or supression of hydrolysis can be achieved by carrying out the measurements in alkaline medium. This method was chosen in the present

work. The required degree of alkalinity of the supporting solution can be estimated from the known hydrolysis constants, K_h, which can be expressed for process IV-2 as

$$K_h = [BH^+][OH^-]/[B] \qquad \text{IV-3}$$

Therefore, in order that hydrolysis be < 1%, i.e., for $[BH^+]/[B]$ to be less than 0.01, $[OH^-]$ must be $10^2 K_h$ or more.

Based on the above method of calculation, the measurements were carried out in 0.01 N NaOH for triethylenediamine, piperazine, ethylenediamine, imidazole and morpholine and in 1N NaOH for quinuclidine and pyrrolidine. The hydrolysis constants were calculated from the pK_a values for acidic dissociation compiled by Perrin[84].

In the case of some of the hydrochloride salts, the acidic dissociation, corresponding to the hydrolysis of the cation BH^+ of the base B, viz

$$BHCl + H_2O \overset{K_a}{\rightleftharpoons} B + H_3O^+ + Cl^- \qquad \text{IV-4}$$

may also be important, depending on the K_a value and the corresponding degree of dissociation, α, at a given concentration. However, a correction may be made to the observed apparent molal quantity, ϕ, to take into account the effects of the dissociation process. The observed ϕ is then given by:

$$\phi(\text{observed}) = \alpha\phi(B) + \alpha\phi(HCl) + (1-\alpha)\phi(BHCl) \qquad \text{IV-5}$$

from which the true ϕ for the salt BHCl can be obtained as

$$\phi(BHCl) = \frac{\phi(\text{observed}) - \alpha[\phi(B) + \phi(HCl)]}{1-\alpha} \qquad \text{IV-6}$$

In the present work, ϕ(observed) and ϕ(B) were determined experimentally, ϕ(HCl) was evaluated from the reported parameters for Equations II-13 and II-25[7,39] and α was calculated from

$$K_a = \alpha^2 c/(1-\alpha) \qquad \text{IV-7}$$

where c is the concentration of the salt and K_a the acid dissociation constant[84]. The extents of the corrections will later be shown by plotting both corrected and uncorrected ϕ values against concentration for some typical salts. In a number of cases, the corrections are quite significant when the pK_a values are lower than 4. It should also be noted that the concentration has also to be corrected to c-αc or m-αm, depending on the scale. It is evident that in the study of the solution properties of protonated basis of the kinds investigated here, the hydrolysis corrections are of substantial importance for the proper evaluation of $\bar{V}^o$ and $\bar{K}_S^o$ values and the consequent interpretations of the results, especially down to low concentrations.

3. Sodium Salts of Oxyanions Having Cl as Central Atom

(a) Apparent Molal Volumes

Apparent molal volume, ϕ_v, data obtained for sodium chloride, NaCl, sodium chlorite, $NaClO_2$, sodium chlorate, $NaClO_3$, and sodium perchlorate, $NaClO_4$ were plotted according to Equation II-13 as shown in Figure 4. The infinite dilution values, ϕ_v^o, and the respective parameters, b_v, evaluated according to the method described in the previous section (IV.2.a), are recorded in Table 1.

The infinite dilution values are in very good agreement with the available literature data. For example, the ϕ_v^o value 16.6_3 cm^3 mol^{-1} for the common salt, NaCl, obtained in this work is in excellent agreement with the value of 16.6 cm^3 mol^{-1} reported by several workers[7]. There is no published work on the volume or compressibility of $NaClO_2$. ϕ_v^o values reported[53] recently during the course of the present work are 35.5 cm^3 mol^{-1} for $NaClO_3$ and 43.0 cm^3 mol^{-1} for $NaClO_4$. These data also agree well with the present results, to within the error limits given in both works.

The plots in Figure 4 show two distinct linear regions for the dependence of apparent molal volumes plotted according to Equation II-13 on concentration for these salts. The transition between the two regions occurs at

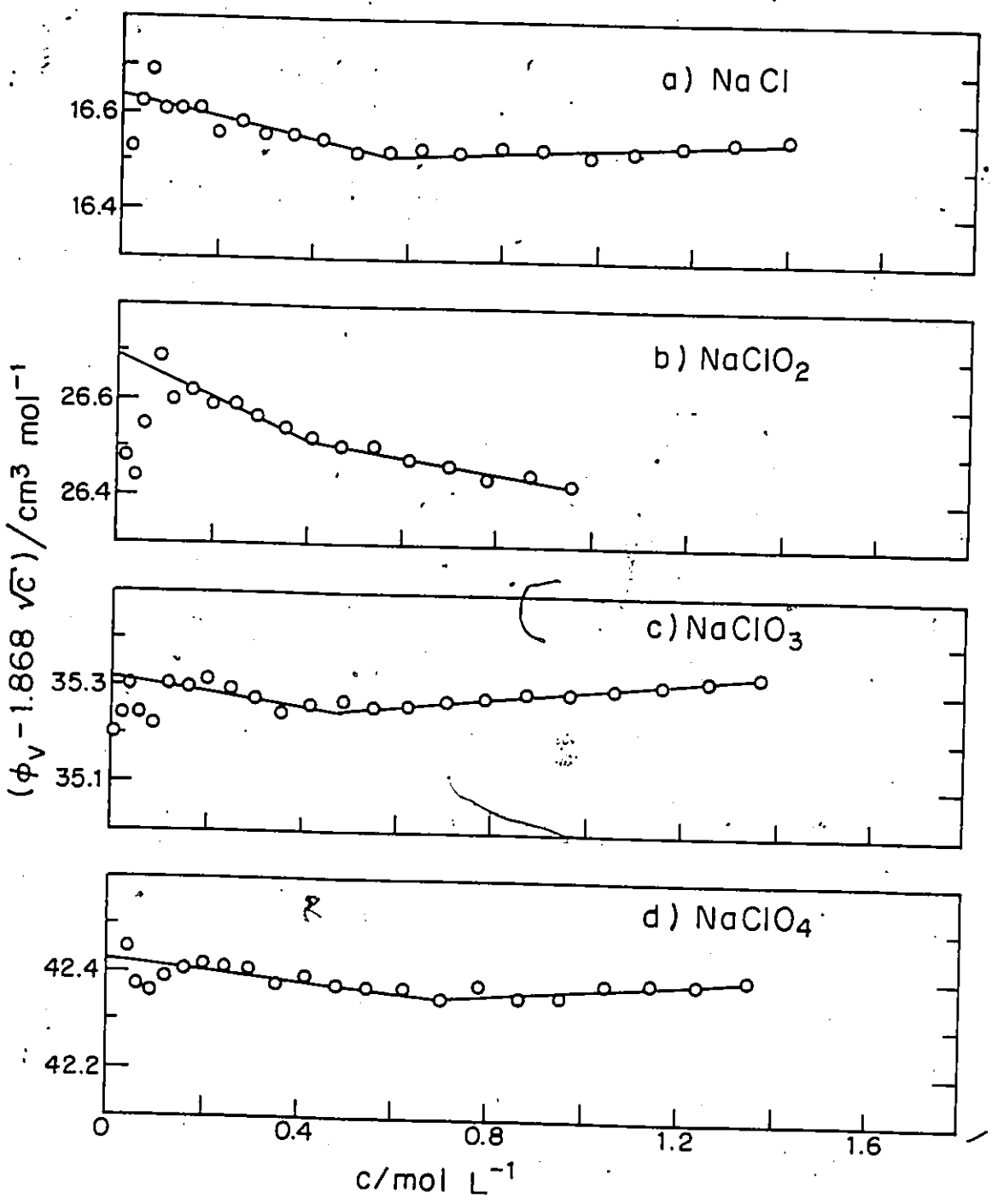

Figure 4 - Plots of $\phi_v - 1.868\ c^{1/2}$ against c for (a) NaCl; (b) $NaClO_2$; (c) $NaClO_3$ and (d) $NaClO_4$.

about 0.6 M for NaCl, 0.4 M for $NaClO_2$, 0.5 M for $NaClO_3$ and 0.7 M for $NaClO_4$. Similar trends had been observed by Vaslow[75,85] for LiCl, NaCl, KCl and RbCl and the change in slope was attributed to "some kind of physical transition" in the behaviour of these solutions. The graph in his paper[75] shows that for NaCl, the transition starts at about 0.6 M which is comparable to the transition concentration observed in the present work (Figure 4).

It should be noted that, in the present work, when ϕ_v data were plotted against square-root of concentration, i.e., according to Masson's equation[7] ($\phi_v = \phi_v^o + S_v^* \sqrt{c}$ where S_v^* is an adjustable parameter), excellent <u>single</u> linear lines were obtained in all cases. However, it appears preferable to plot the basic ϕ_v data in terms of the Redlich-Meyer equation (Equation II-13, see Section II.1), which takes into account any residual linear term in c associated with any remaining electrostatic effects together with non-electrostatic or hydration factors, after the limiting-law electrostatic interaction term in $\sqrt{c}$ has been subtracted out; then any effects not taken into account in the $\sqrt{c}$ term become more easily apparent, e.g., the existence of two linear regions, in some cases, with different slopes. The Redlich-Meyer equation also, it is believed, gives a better basis for extrapolation of ϕ_v to obtain ϕ_v^o.

In Table 1, the b_v values shown are the slopes of the first linear regions (at low concentrations) in Figure 4.

The agreement between the b_v values reported here and in the literature is not as good as in the case of ϕ_v^o values. For example, for NaCl, the published b_v value[7] is -0.03 cm^3 mol^{-2} L. For $NaClO_3$ and $NaClO_4$, the b_v values obtained by Roux et al.[53] were 0.1 and 0.06 cm^3 mol^{-2} kg, respectively.

(b) Apparent Molal Adiabatic Compressibilities

Apparent molal adiabatic compressibility, ϕ_{KS}, data obtained for NaCl, $NaClO_2$, $NaClO_3$ and $NaClO_4$ were plotted according to Equation II-25 and are shown in Figures 5 and 6. The infinite dilution values, ϕ_{KS}^o ($\equiv \overline{K}_S^o$; partial molal adiabatic compressibility at infinite dilution) and the slopes, S_{KS}^*, are recorded in Table 2.

As far as could be ascertained from a literature search, there appear to be no data on compressibilities of these salts in the literature for comparison, except for NaCl. The agreement of the present results with the published ones for that salt has already been shown in Section III.1.b.iv to be excellent.

It should be noted that the two linear regions with different slopes, seen in each of the plots of $\phi_v - 1.868\sqrt{c}$ against concentration (Figure 4) for these salts, are not always observed in the concentration dependence of apparent molal adiabatic compressibilities, e.g., in the case of $NaClO_2$ (Figure 6a).

Table 1

VALUES OF ϕ_V^o ($\equiv\overline{V}^o$) AND b_V IN EQUATION II-13 (298 K)

Salt	$\phi_V^o \pm 0.05$ $cm^3\ mol^{-1}$	$b_V \pm 0.08$ $cm^3\ mol^{-2}\ L$
NaCl	16.6_3	-0.2_1
$NaClO_2$	26.6_9	-0.4_4
$NaClO_3$	35.3_2	-0.1_5
$NaClO_4$	42.4_3	-0.1_2

Table 2

VALUES OF ϕ_{KS}^o ($\equiv\overline{K}_S^o$) AND S_{KS}^* IN EQUATION II-25 (298 K)

Salt	$(\phi_{KS}^o \pm 0.1)10^4$ $cm^3\ mol^{-1}\ bar^{-1}$	$(S_{KS}^* \pm 0.3)10^4$ $cm^3\ mol^{-3/2}\ kg^{1/2}\ bar^{-1}$
NaCl	-50.5	6.2
$NaClO_2$	-49.2	8.2
$NaClO_3$	-42.0	6.5
$NaClO_4$	-31.9	2.7

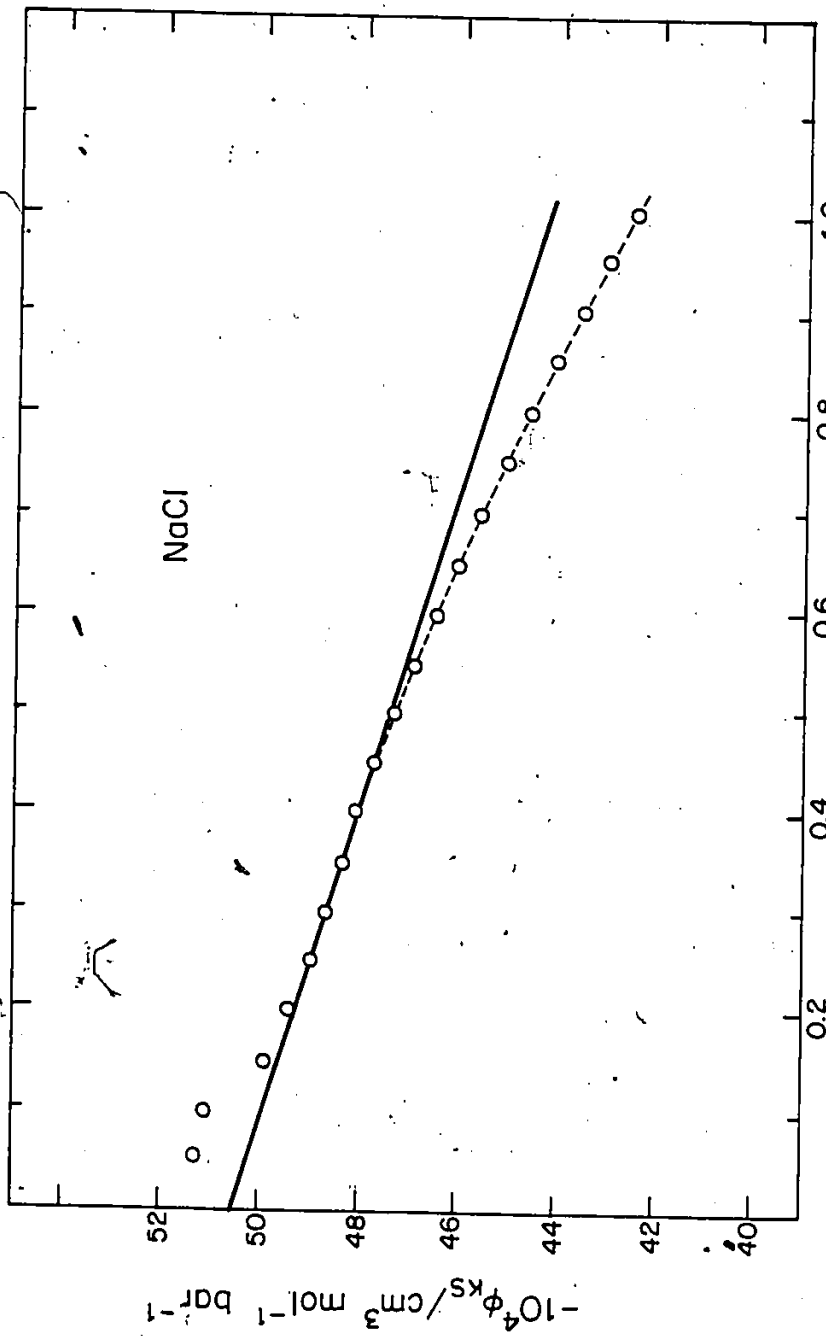

Figure 5 - A plot of ϕ_{KS} against $m^{1/2}$ for NaCl.

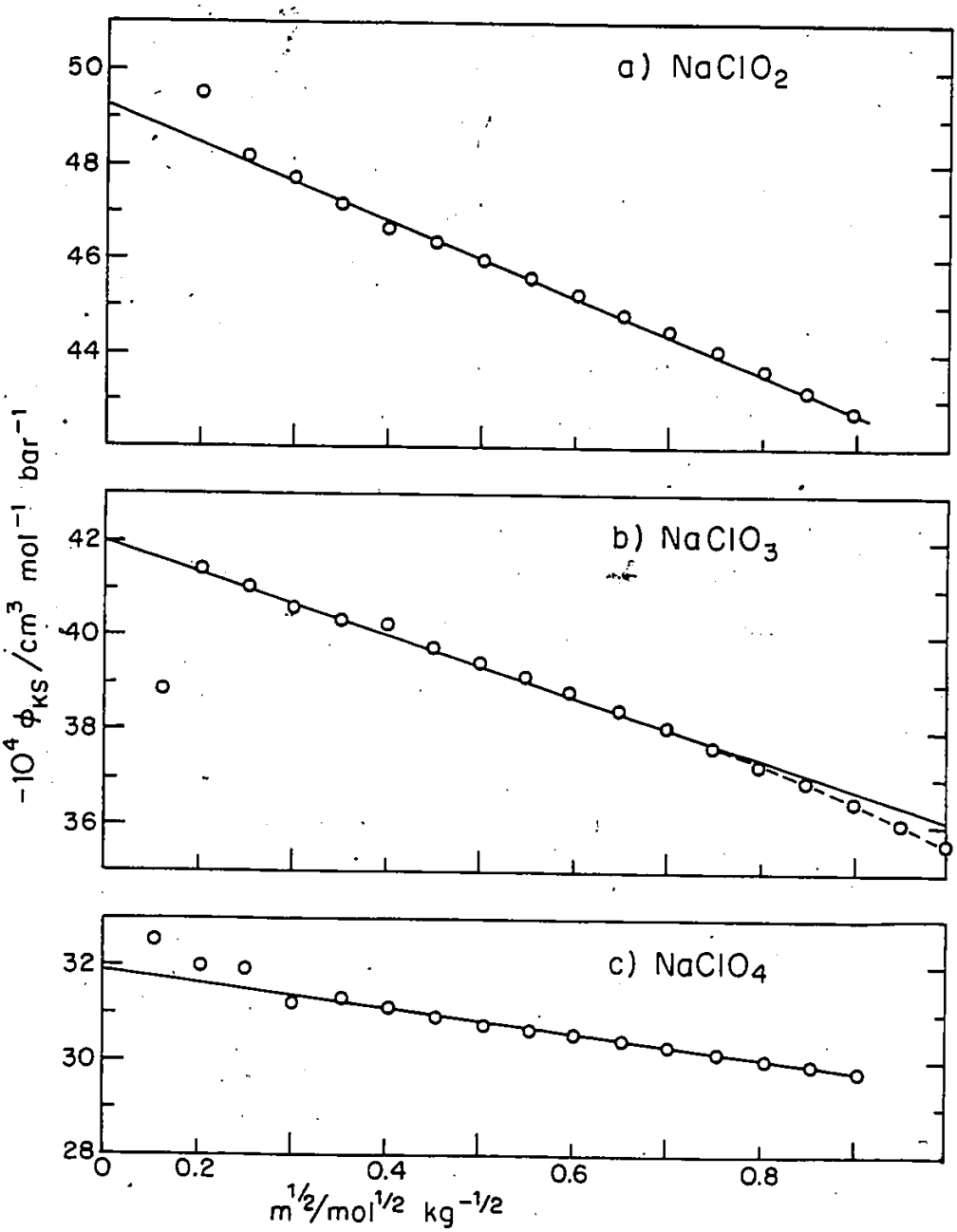

Figure 6 - Plots of ϕ_{KS} against $m^{1/2}$ for (a) $NaClO_2$; (b) $NaClO_3$ and (c) $NaClO_4$.

4. Sodium Salts of Sulphur Containing Oxyanions

(a) Apparent Molal Volumes

Apparent molal volumes for sodium salts of some sulphur-containing oxyanions were investigated. These salts were sodium sulphite, Na_2SO_3, sodium sulphate, Na_2SO_4, sodium thiosulphate, $Na_2S_2O_3$, and sodium dithionate, $Na_2S_2O_6$. The data were plotted again according to Equation II-13 using 9.706 cm^3 $mol^{-3/2}$ $L^{1/2}$ for S_v since these salts are of the 1:2 type. The plots are shown in Figures 7 and 8. The ϕ_v^o ($\equiv\overline{V}^o$) and b_v values obtained from these plots are given in Table 3.

Figures 7 and 8 show that for the salts Na_2SO_3, Na_2SO_4 and $Na_2S_2O_3$, there is a linear region below 0.15 M with a higher slope compared to the slope characterizing the rest of the data at higher concentrations. It should be noted again, however, that when the data on ϕ_v are plotted directly against square-root of concentration, excellent single linear lines are obtained (see comments in Section IV.3.a). The linear regions of higher slope seen in Figures 7a, b and 8a at low concentrations do not seem to be due to hydrolysis of the sulphur oxyanions. This conclusion was reached from the result, e.g., of an experiment in which similar behaviour was observed for Na_2SO_3 in 0.01 N NaOH. Also, for the Na_2SO_4 case where hydrolysis is less significant, similar behaviour is seen (Figure 8a).

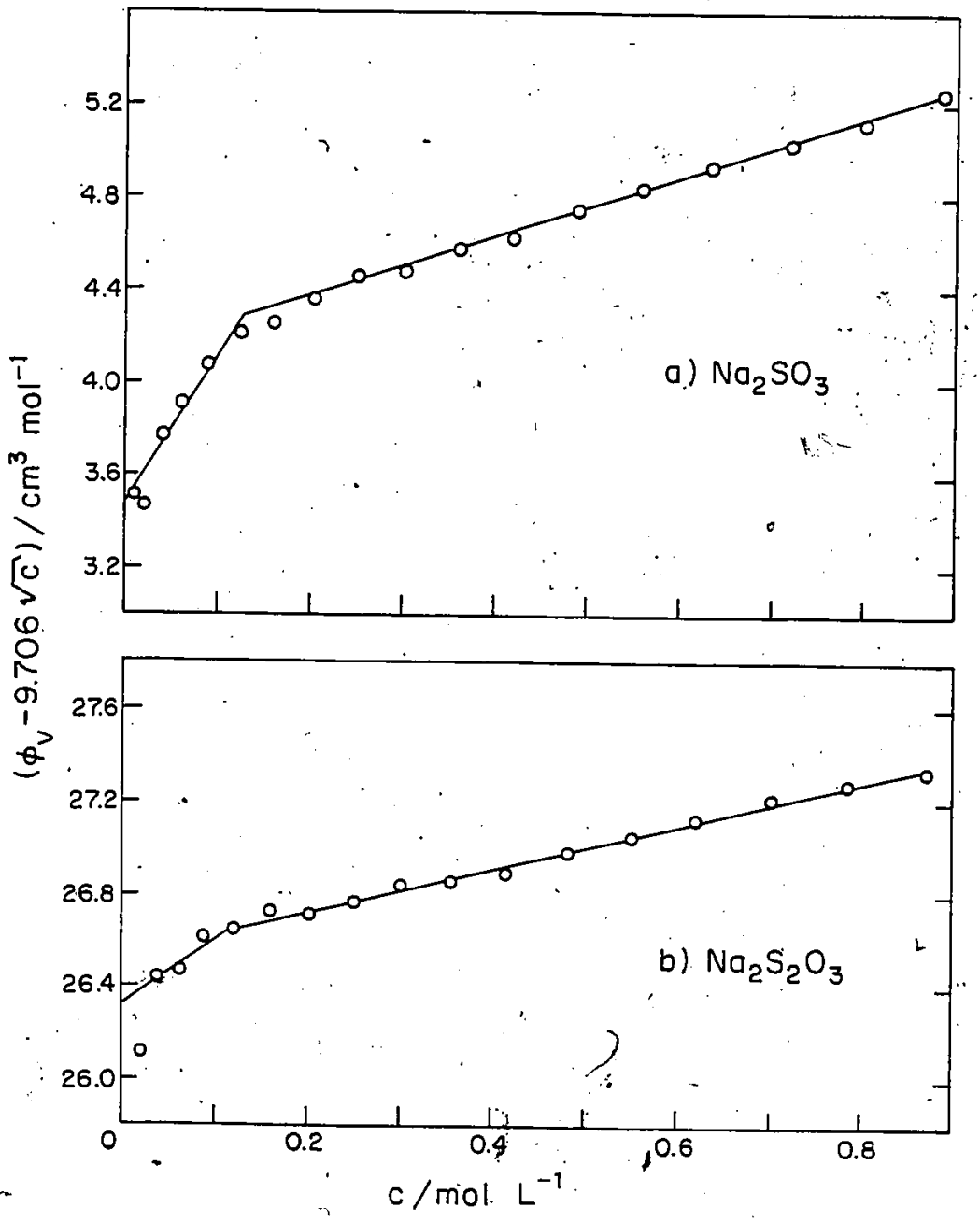

Figure 7 - Plots of $\phi_v - 9.706\, c^{1/2}$ against c for (a) Na_2SO_3 and (b) $Na_2S_2O_3$.

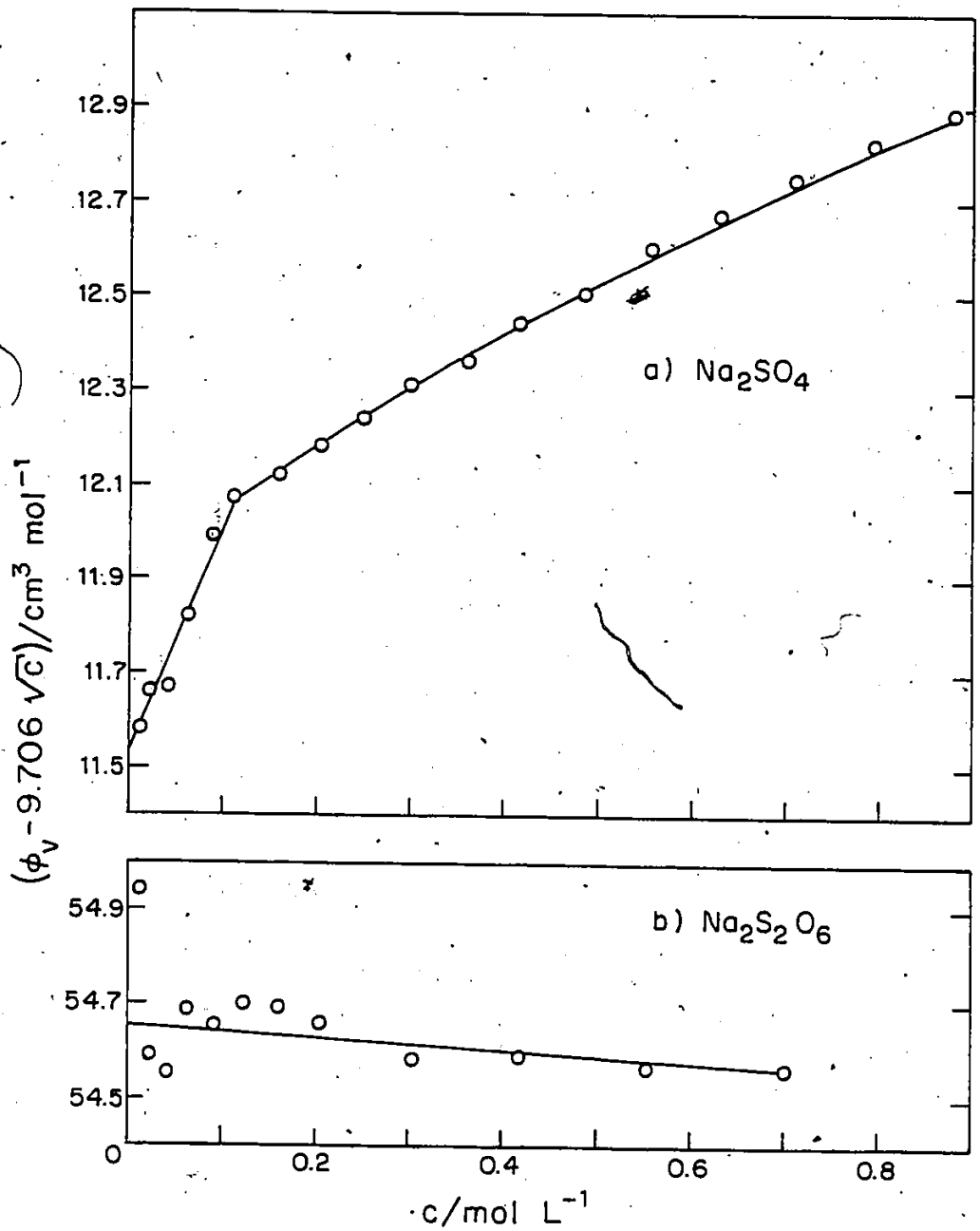

Figure 8 - Plots of $\phi_v - 9.706\ c^{1/2}$ against c for (a) Na_2SO_4 and (b) $Na_2S_2O_6$.

Table 3

VALUES OF ϕ_V^o ($\equiv\overline{V}^o$) AND b_V IN EQUATION II-13 (298 K)

Salt	$\phi_V^o \pm 0.05$ $cm^3\ mol^{-1}$	$b_V \pm 0.10$ $cm^3\ mol^{-2}\ L$
Na_2SO_3	3.5_0	6.0_8
Na_2SO_4	11.5_4	4.5_6
$Na_2S_2O_3$	26.3_2	2.7_4
$Na_2S_2O_6$	54.6_5	-0.1_3

Table 4

VALUES OF ϕ_{KS}^o ($\equiv\overline{K}_S^o$) AND S_{KS}^* IN EQUATION II-25 (298 K)

	$(\phi_{KS}^o \pm 0.3)10^4$ $cm^3\ mol^{-1}\ bar^{-1}$	$(S_{KS}^* \pm 1.0)10^4$ $cm^3\ mol^{-3/2}\ kg^{1/2}\ bar^{-1}$
Na_2SO_3	-163.6	55.2
Na_2SO_4	-159.0	49.0
$Na_2S_2O_3$	-148.8	46.2
$Na_2S_2O_6$	-121.2	41.4

A comparison of the present results with the published data show good agreement. For example, ϕ_v^o values of 11.52, 11.62, 11.4 and 11.56 $cm^3\ mol^{-1}$ for Na_2SO_4 from references 86, 87, 54 and 36, respectively, compare very well with that of $11.5_4\ cm^3\ mol^{-1}$ found in the present work. However, the reported b_v values, 2.96 $cm^3\ mol^{-2}$ L and 0.8 $cm^3\ mol^{-2}$ kg for this salt from references 82 and 54, respectively, do not agree very well with the present value of $4.5_6\ cm^3\ mol^{-2}$ L. Both the ϕ_v^o, 26.3 $cm^3\ mol^{-1}$ and b_v, 3.0 $cm^3\ mol^{-2}$ kg reported by Olofsson et al.[54] for $Na_2S_2O_3$ are in very good agreement with the present values of $26.3_2\ cm^3\ mol^{-1}$ and $2.7_4\ cm^3\ mol^{-2}$ L, respectively.

(b) Apparent Molal Adiabatic Compressibilities

Apparent molal adiabatic compressibility, ϕ_{KS}, data obtained for Na_2SO_3, Na_2SO_4, $Na_2S_2O_3$ and $Na_2S_2O_6$ were plotted according to Equation II-25 and are shown in Figures 9 and 10. The partial molal adiabatic compressibilities at infinite dilution, $\overline{K}_S^o$ ($\equiv\phi_{KS}^o$), and the slopes, S_{KS}^*, obtained from these plots are recorded in Table 4.

Among the above salts, the only data reported in the literature for the adiabatic compressibility are those for Na_2SO_4. For example, the ϕ_{KS}^o values of $-157.7 \times 10^{-4}\ cm^3\ mol^{-1}\ bar^{-1}$ reported by Millero[36] for Na_2SO_4 is within 0.8% of the present value of $-159.0 \times 10^{-4}\ cm^3\ mol^{-1}\ bar^{-1}$. The two distinct linear regions observed in the plots of

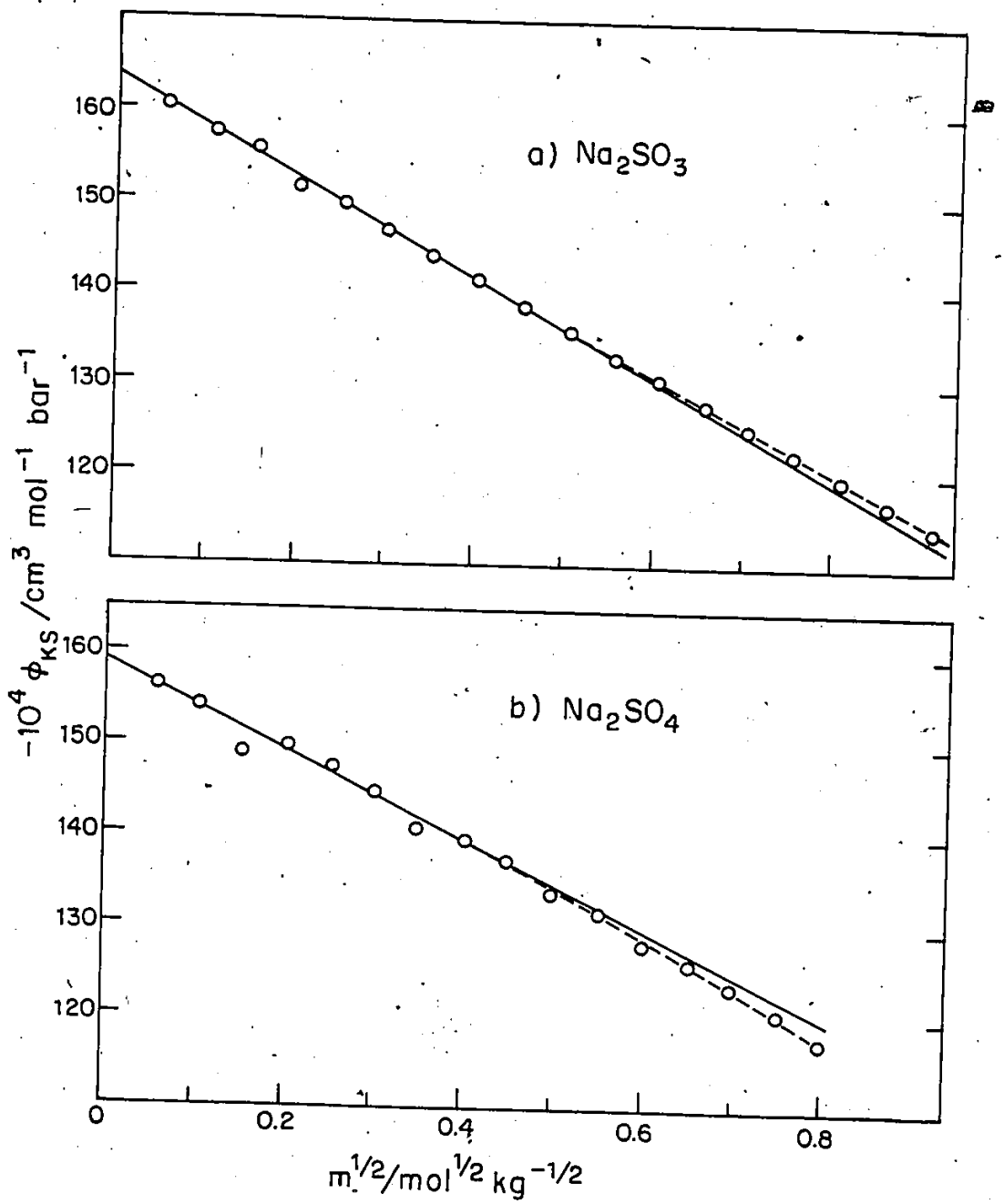

Figure 9 - Plots of ϕ_{KS} against $m^{1/2}$ for (a) Na_2SO_3 and (b) Na_2SO_4.

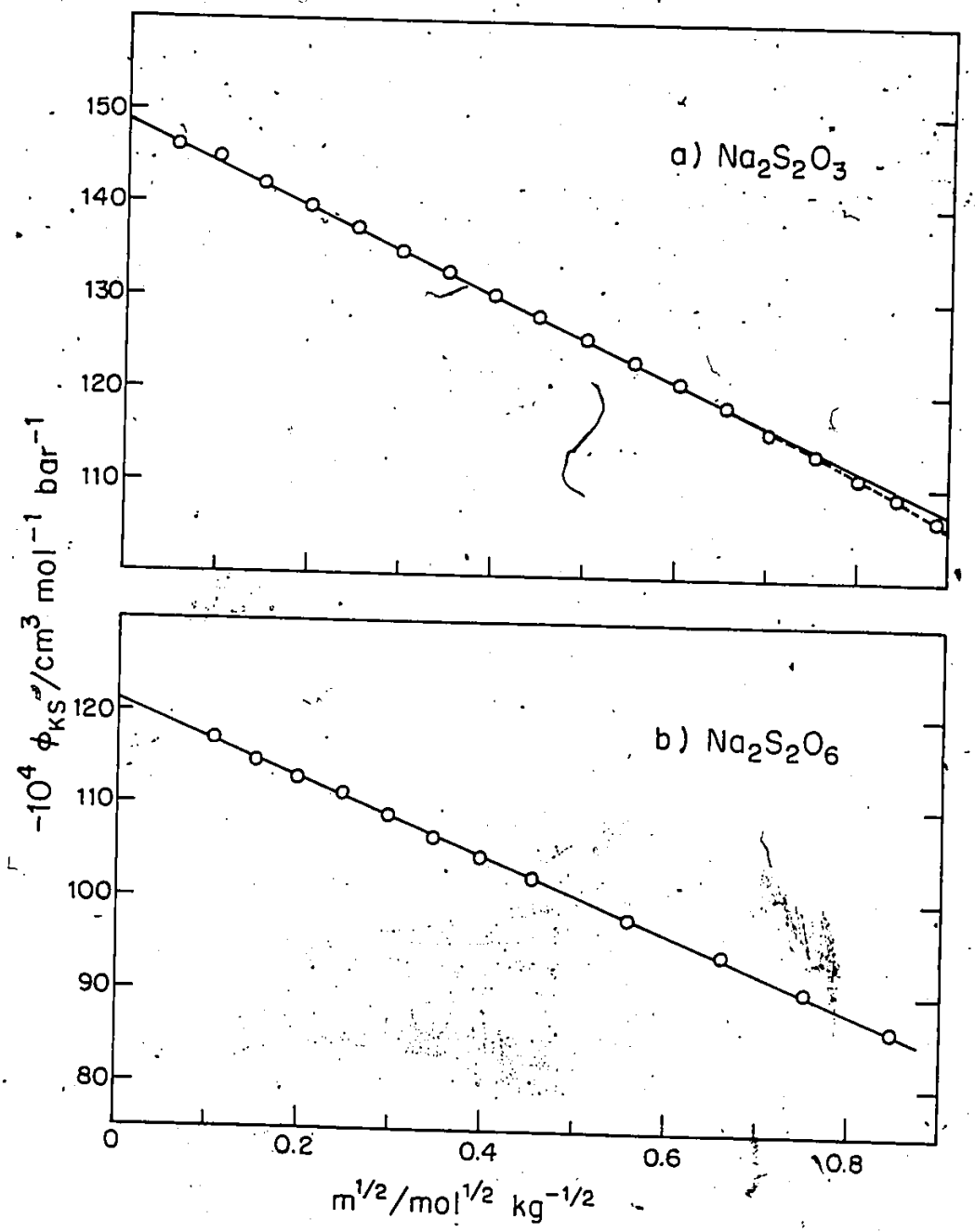

Figure 10 - Plots of ϕ_{KS} against $m^{1/2}$ for (a) $Na_2S_2O_3$ and (b) $Na_2S_2O_6$.

$\phi_v - 9.706\sqrt{c}$ against c for Na_2SO_3, Na_2SO_4 and $Na_2S_2O_3$ were again (cf. Section IV.3.b) not always so clearly observed in the concentration dependence of the apparent molal adiabatic compressibilities.

The systematic series of oxyanions studied in the present work would be more complete if anions such as ClO^- in the Cl-oxyanion series and S^{2-}, $S_2O_4^{2-}$, $S_2O_5^{2-}$, $S_2O_7^{2-}$ and $S_2O_8^{2-}$ in S-oxyanion series could also have been studied. However, owing to problems such as hydrolysis and decomposition of some of these ions in aqueous solution and unavailability of the salts of others, these anions could not be included in the study. Although at least $S_2O_8^{2-}$ ion of $Na_2S_2O_8$ might be expected to be stable, a qualitative test with $BaCl_2$ showed that a considerable amount of SO_4^{2-} exists in solution (BaS_2O_8 is known to be readily soluble in water) arising from unavoidable decomposition of $S_2O_8^{2-}$, as noted in the early inorganic chemistry literature[109,110]. Therefore, this part of the work was restricted to anions in the series Cl^-, ClO_2^-, ClO_3^-, ClO_4^-; SO_3^{2-}, SO_4^{2-}, $S_2O_3^{2-}$ and $S_2O_6^{2-}$.

5. Un-ionized Organic Compounds

(a) General

For this work, organic compounds were chosen among nitrogen and/or oxygen containing heterocyclics, that were ionizable at an N-centre (except 1,4 dioxane). Ethylene-diamine (non-cyclic) was also included for comparison. A list of compounds studied and their pK_a values are given in Table 5. In addition, pyridine and piperidine, studied previously in this laboratory, will be included in the discussion and the results will be referred to in the sections which follow.

The measurements on some of these compounds were carried out in slightly alkaline medium in order to suppress the hydrolysis as was discussed in Section IV.2.c. The alkaline solution (NaOH), used as the solvent, was prepared in a sufficient amount to carry out both the series of density and sound velocity measurements. In this way, the density data could also be conveniently used in the compressibility calculations. The concentration of NaOH required for suppression of ionization of pyrrolidine and quinuclidine had to be quite high (~ 1N). The reason for this was to make sure that hydrolysis had been suppressed since these two bases have high pK_a values. Furthermore, in Reference 84, the comment on the reliability of pK_a

Table 5

THE ORGANIC COMPOUNDS STUDIED AND THEIR pK_a VALUES*

Compound	Structure	pK_a(1)	pK_a(2)
1,4 Diazabicyclo [2.2.2] octane (triethylenediamine)	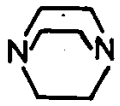	8.8	2.95
Piperazine	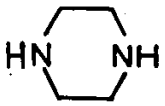	9.82	5.55
Ethylenediamine	$H_2NCH_2CH_2NH_2$	9.93	6.85
Pyrazine	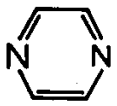	0.65	-5.78
Pyridazine	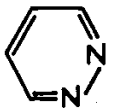	2.24	-
Pyrazole	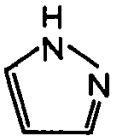	2.48	-
Imidazole	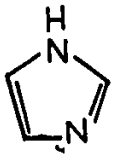	6.95	-
1,2,4 Triazole	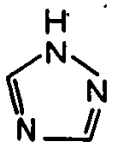	2.30	-

Table 5 cont'd.

Compound	Structure	pK_a(1)	pK_a(2)
Pyrrolidine	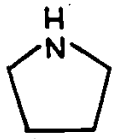	11.27	-
Quinuclidine	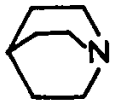	10.95	-
1,4 Dioxane	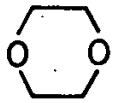	-4.3	-
Morpholine	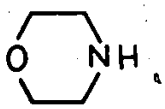	8.33	-
Piperidine	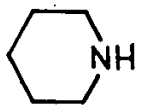	11.12	-
Pyridine	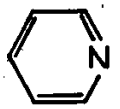	5.21	-

* pK_a values were taken from Reference 84
(1) First ionization
(2) Second ionization

data was given as "uncertain" for these two compounds.

1,4 Dioxane was also studied both in H_2O and in 1M $MgCl_2$ to investigate the possibility of a conformational effect, due to interaction with Mg^{2+}, on ϕ_v^o and ϕ_{KS}^o.

(b) Apparent Molal Volumes

ϕ_v data obtained for the organic compounds listed in Table 5 were plotted against molality according to Equation II-12 and are shown in Figures 11 to 16. The corresponding ϕ_v^o results, determined by extrapolation, and the parameter b_v', determined from the slope are listed for these compounds in Table 6. The available literature values for the same parameters are also included in the table for comparison. As mentioned earlier (Section IV.5.a), the data for piperidine and pyridine were obtained previously[69] in this laboratory.

For those compounds for which previously determined data exist, the results obtained in the present work are generally in very good agreement with those reported in the literature. Again, the agreement is much better for the ϕ_v^o than for the b_v' values. Several different reasons can account for the discrepancies: for example, the compounds for which hydrolysis is significant were studied in alkaline medium. However, Cabani et al.[22,58] preferred to make measurements in water but apply corrections for hydrolysis

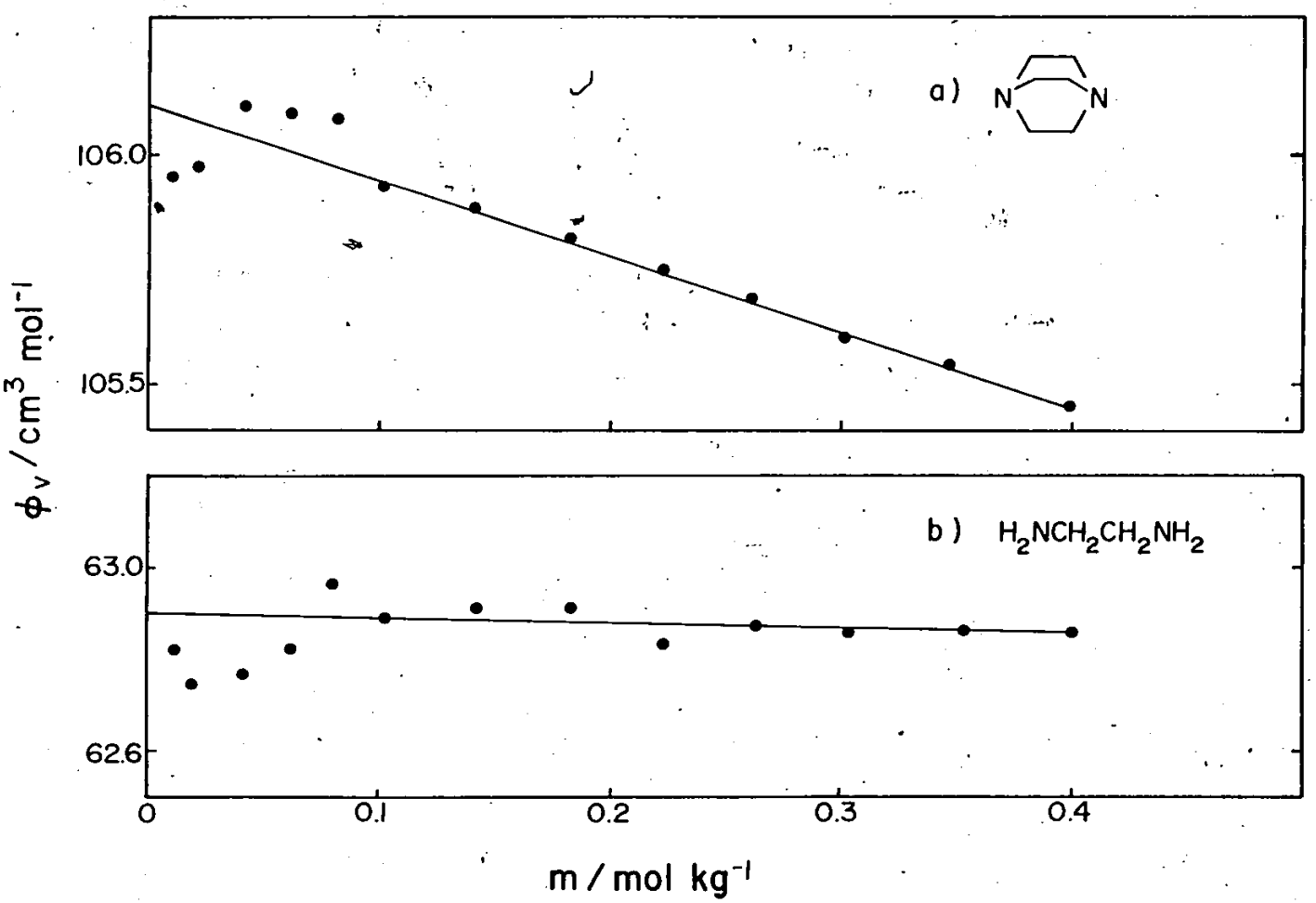

Figure 11 - Plots of ϕ_v against m for (a) triethylenediamine in 0.01 N NaOH and (b) ethylenediamine in 0.01 N NaOH.

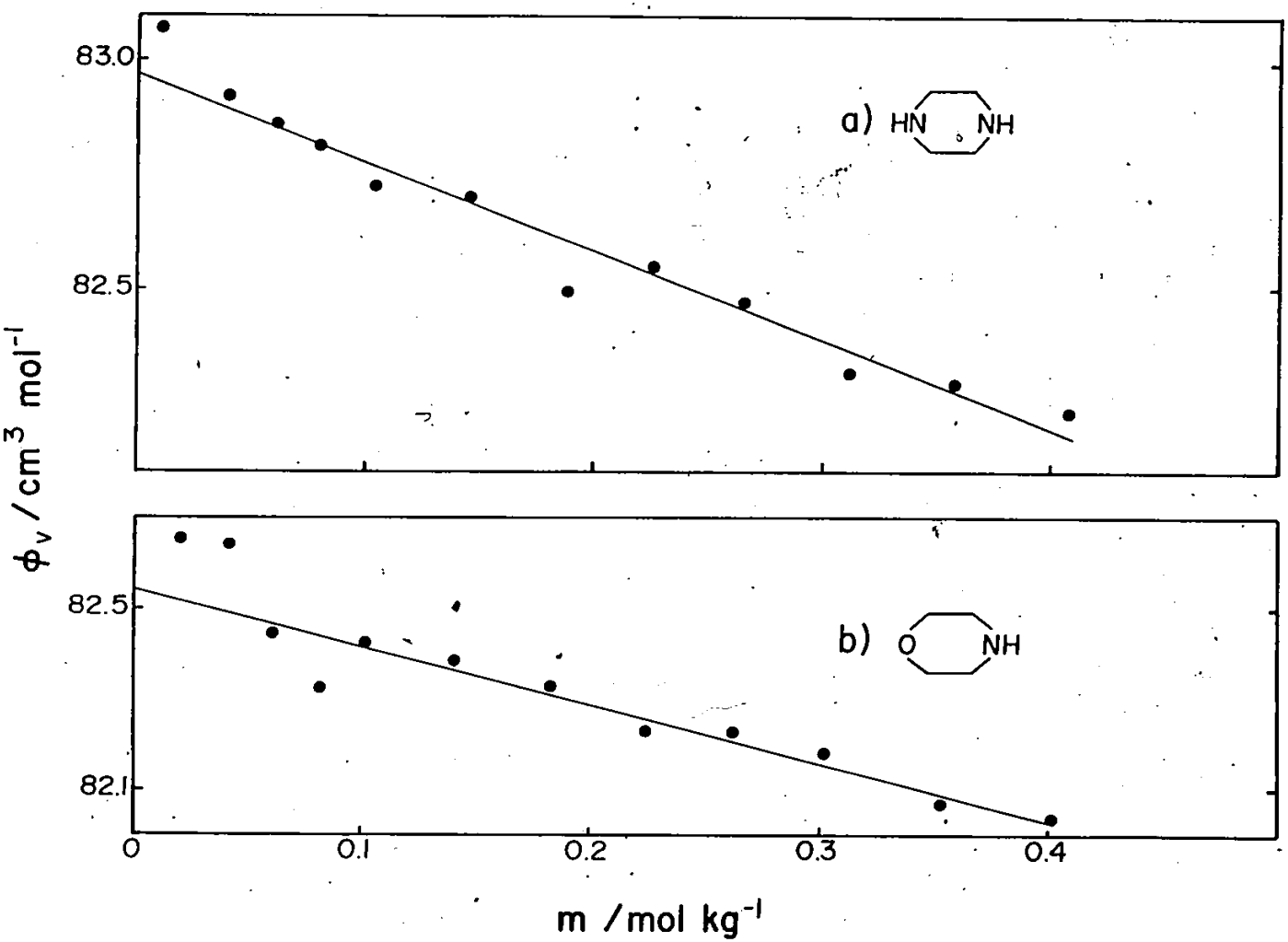

Figure 12 - Plots of ϕ_v against m for (a) piperazine in 0.01 N NaOH and (b) morpholine in 0.01 N NaOH.

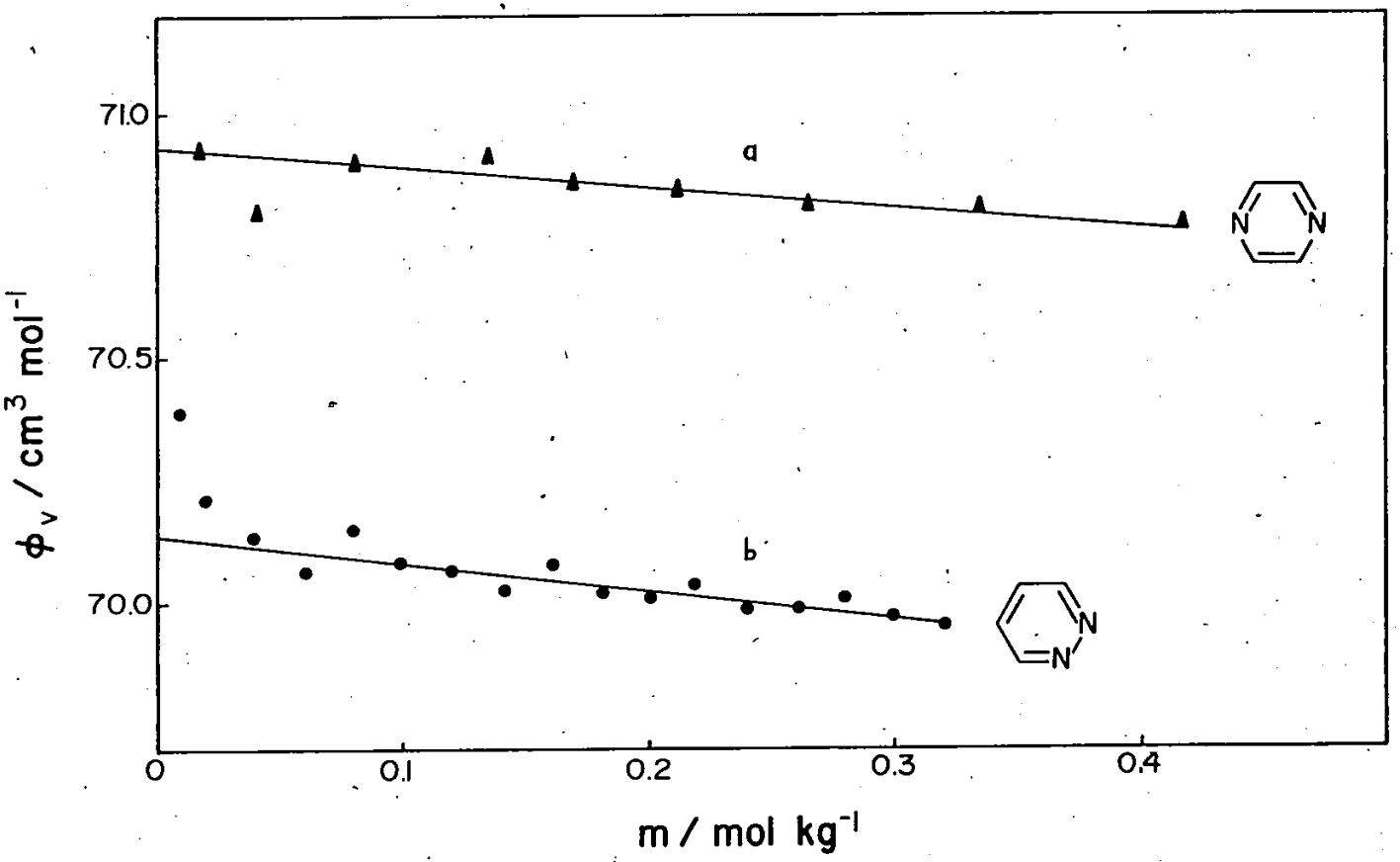

Figure 13 - Plots of ϕ_v against m for (a) pyrazine in H_2O and (b) pyridazine in H_2O.

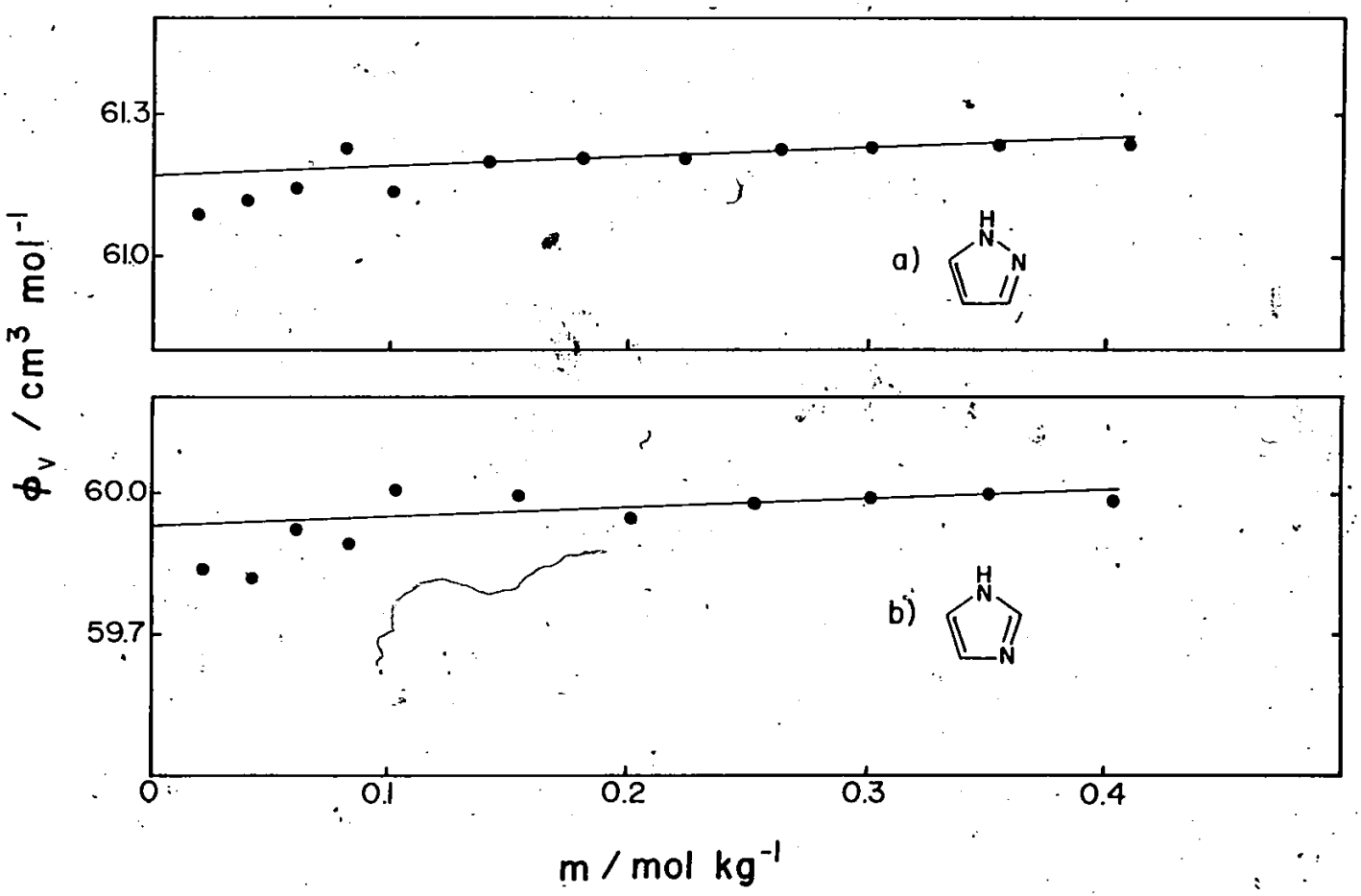

Figure 14 - Plots of ϕ_v against m for (a) pyrazole in H_2O and (b) imidazole in 0.01 N NaOH.

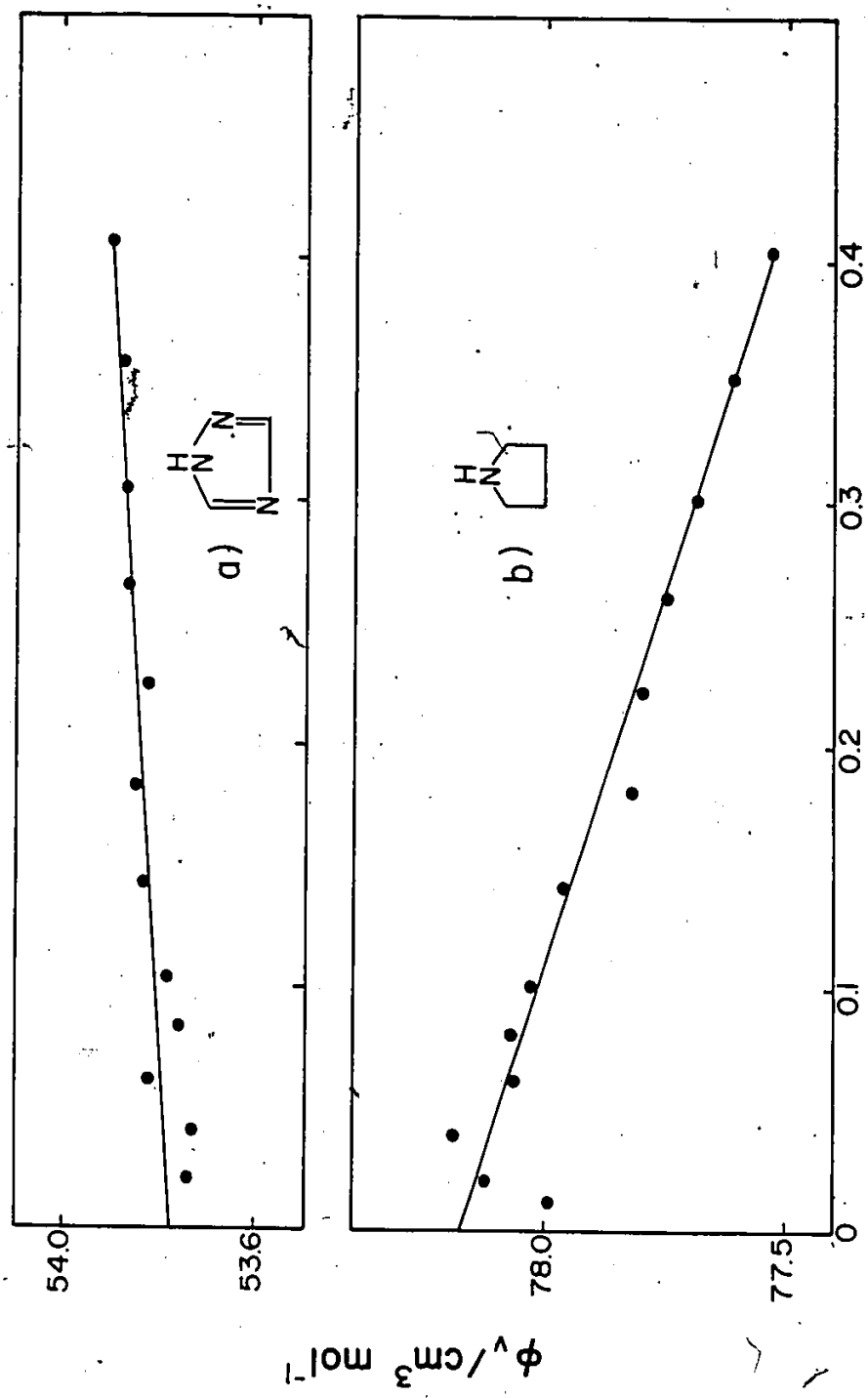

Figure 15 - Plots of ϕ_v against m for (a) 1,2,4, triazole in H_2O and (b) pyrrolidine in 1N NaCl.

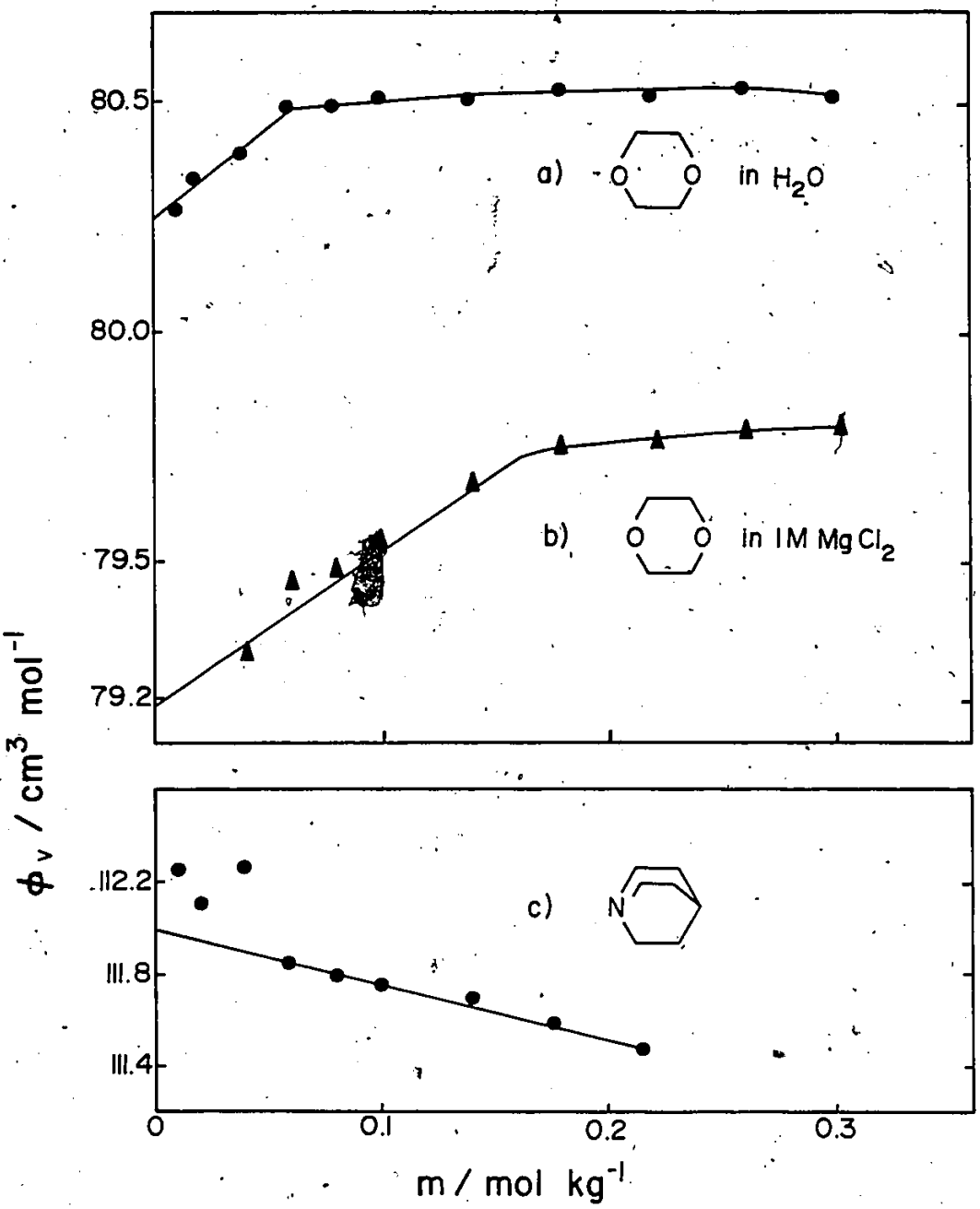

Figure 16 - Plots of ϕ_v against m for (a) 1,4 dioxane in H_2O; (b) 1,4 dioxane in 1M $MgCl_2$ and (c) quinuclidine in 1N NaOH.

Table 6

VALUES OF ϕ_V^o ($\equiv\bar{V}^o$) AND b_V' IN
EQUATION II-12 AT 298K FOR VARIOUS ORGANIC BASES

Base	($\phi_V^o \pm 0.05$[a]) $cm^3\ mol^{-1}$	($b_V' \pm 0.2$[a]) $cm^3\ mol^{-2}\ kg$[b]	Reference
Triethylenediamine	106.1$_1$	-1.7	This work
	105.9	-1.8*	22
	105.7	-1.5*	55
Piperazine	82.9$_7$	-1.9	This work
	83.5	-0.9*	22
	83.3	-1.0	56
Ethylenediamine	62.9$_0$	-0.1	This work
	62.9	-0.1*	22
	63.1	-	88
Pyrazine	70.9$_3$	-1.1	This work
	70.8	-0.1	57
Pyridazine	70.1$_4$	-0.6	This work
	70.4	0.2	57
Pyrazole	61.1$_7$	0.2	This work
	62.2	0.1	57
Imidazole	59.9$_3$	0.2	This work
	59.9	0.1	57
1,2,4 Triazole	53.7$_8$	0.3	This work
Pyrrolidine	78.1$_8$	-1.6	This work
	77.8	-1.2*	58
	77.0	-	66
Quinuclidine	112.0$_0$	-2.4	This work
1,4 Dioxane in H_2O	80.2$_5$	4.1	This work
	81.0	-0.2*	58
in 1M $MgCl_2$	79.1$_8$	3.8	This work

Table 6 cont'd.

Base	$(\phi_v^o \pm 0.05^{(a)})$ $cm^3\ mol^{-1}$	$(b_v' \pm 0.2^{(a)})$ $cm^3\ mol^{-2}\ kg^{(b)}$	Reference
Morpholine	82.5_4	-1.3	This work
	82.6	-0.5*	22
	82.5	-0.5	56
	82.7	-	66
Piperidine[c]	91.1_0	0.0*	69
Pyridine[c]	77.7_0	-10.5*	69

(a) Maximum error limit for results of the present work

(b) Units for the values with asterisks are $cm^3\ mol^{-2} L$

(c) From previous work in this laboratory

afterwards. Kaulgud and Patil[66] made the extrapolation to ϕ_v^o from relatively high concentrations (> 1.5 m). Therefore, the medium and the concentration range studied are two important factors which can lead to some differences in the results. For 1,4 dioxane, Figure 16(a) shows that ϕ_v first increases rapidly with concentration up to ca. 0.06 m, and then attains a limiting value. This was not observed by Cabani et al.[58] because their measurements commenced above 0.05 M concentration. The present observations were reproducible. On the other hand, in 1M $MgCl_2$, ϕ_v values for the same compound decreased by about 1 cm^3 mol^{-1} and also the first steep region continued up to 0.16 m and then reached the limiting value (Figure 16b). The measurements in 1M $MgCl_2$ were made to examine if the conformation of 1,4 dioxane in water, i.e., the populations in the boat or chair forms (Section I.6), were influenced by local interaction with Mg^{2+}. The results concerned with this point will be discussed in the next chapter.

(c) Apparent Molal Adiabatic Compressibilities

The dependence of apparent molal adiabatic compressibility on concentration is shown in Figures 17 to 21 for the organic compounds studied, using Equation II-24. ϕ_{KS}^o and b_{KS} parameters are collected in Table 7 together with the few available literature data.

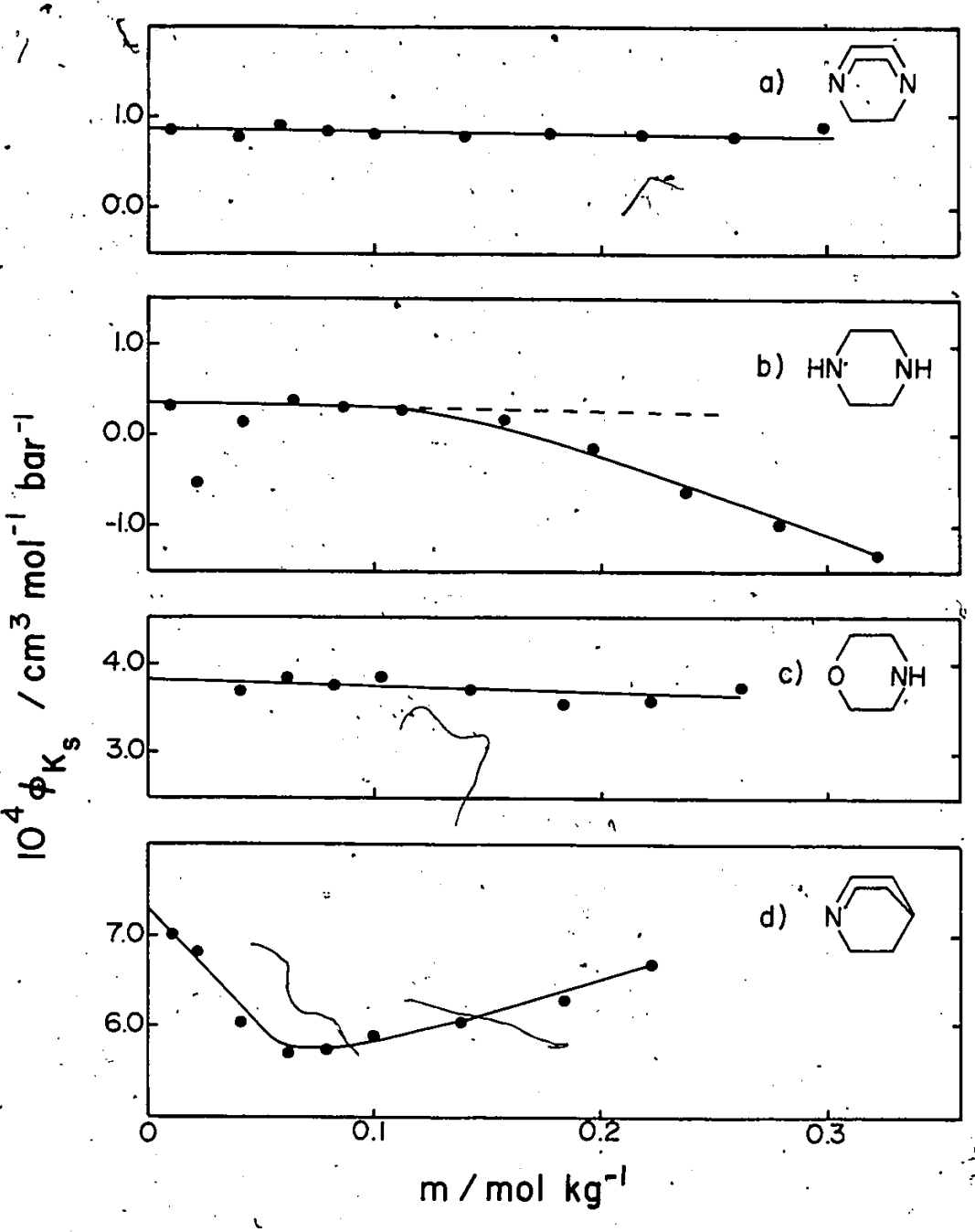

Figure 17 - Plots of ϕ_{KS} against m for (a) triethylenediamine in 0.01 N NaOH; (b) piperazine in 0.01 N NaOH; (c) morpholine in 0.01 N NaOH and (d) quinuclidine in 1N NaOH.

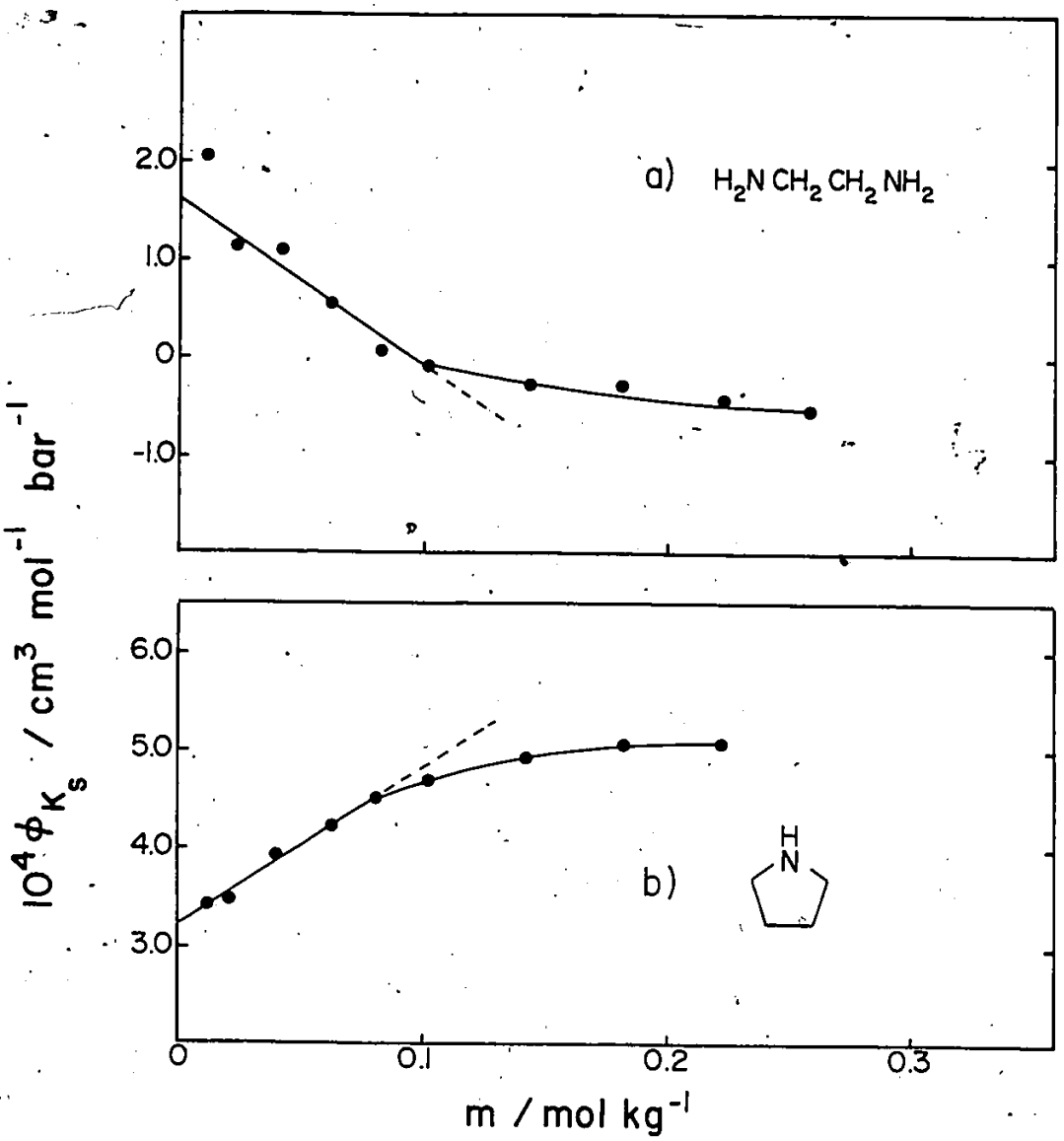

Figure 18 - Plots of ϕ_{KS}, against m for (a) ethylenediamine in 0.01 N NaOH and (b) pyrrolidine in 1N NaOH.

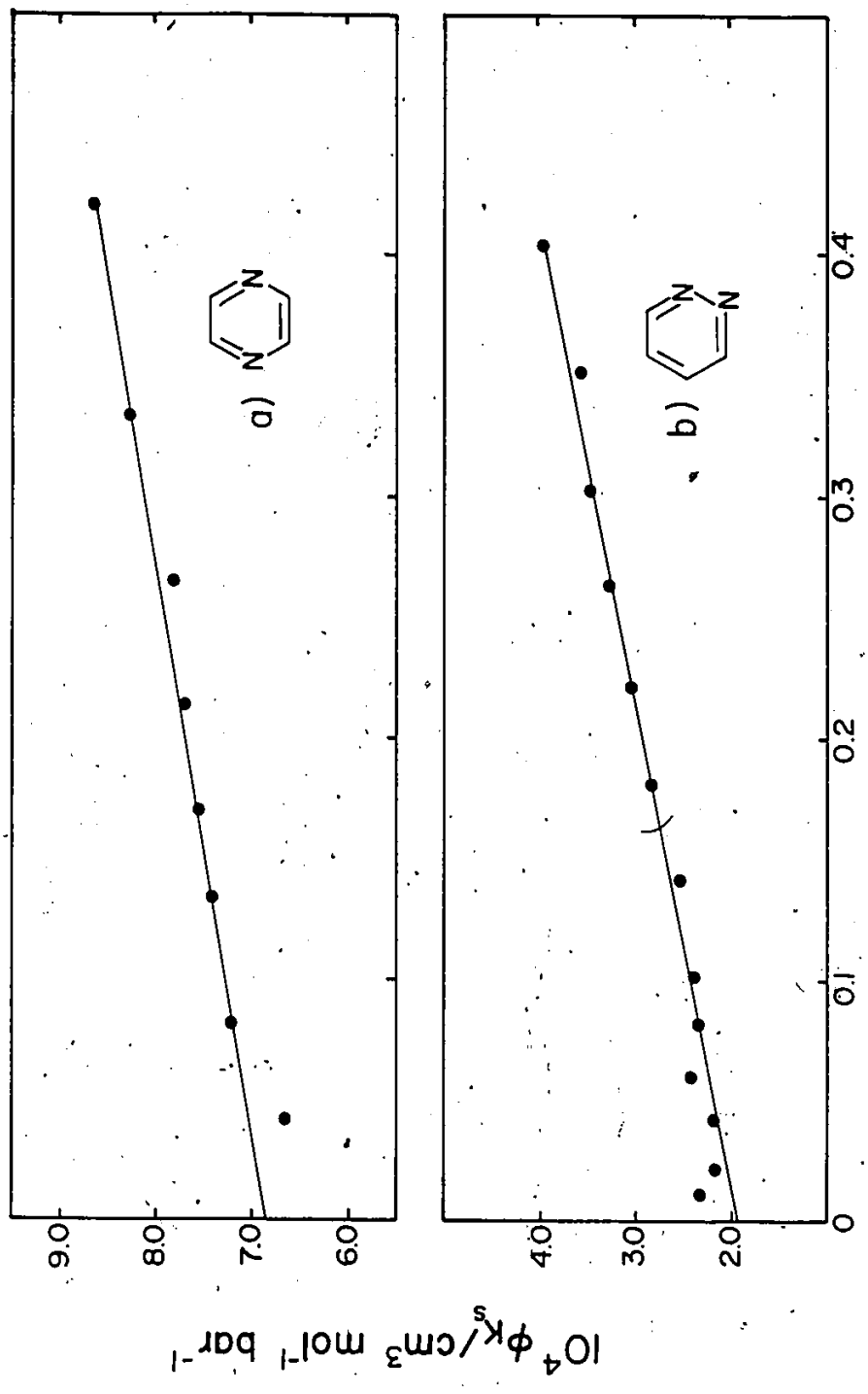

Figure 19 - Plots of ϕ_{KS} against m for (a) pyrazine in H_2O and (b) pyridazine in H_2O.

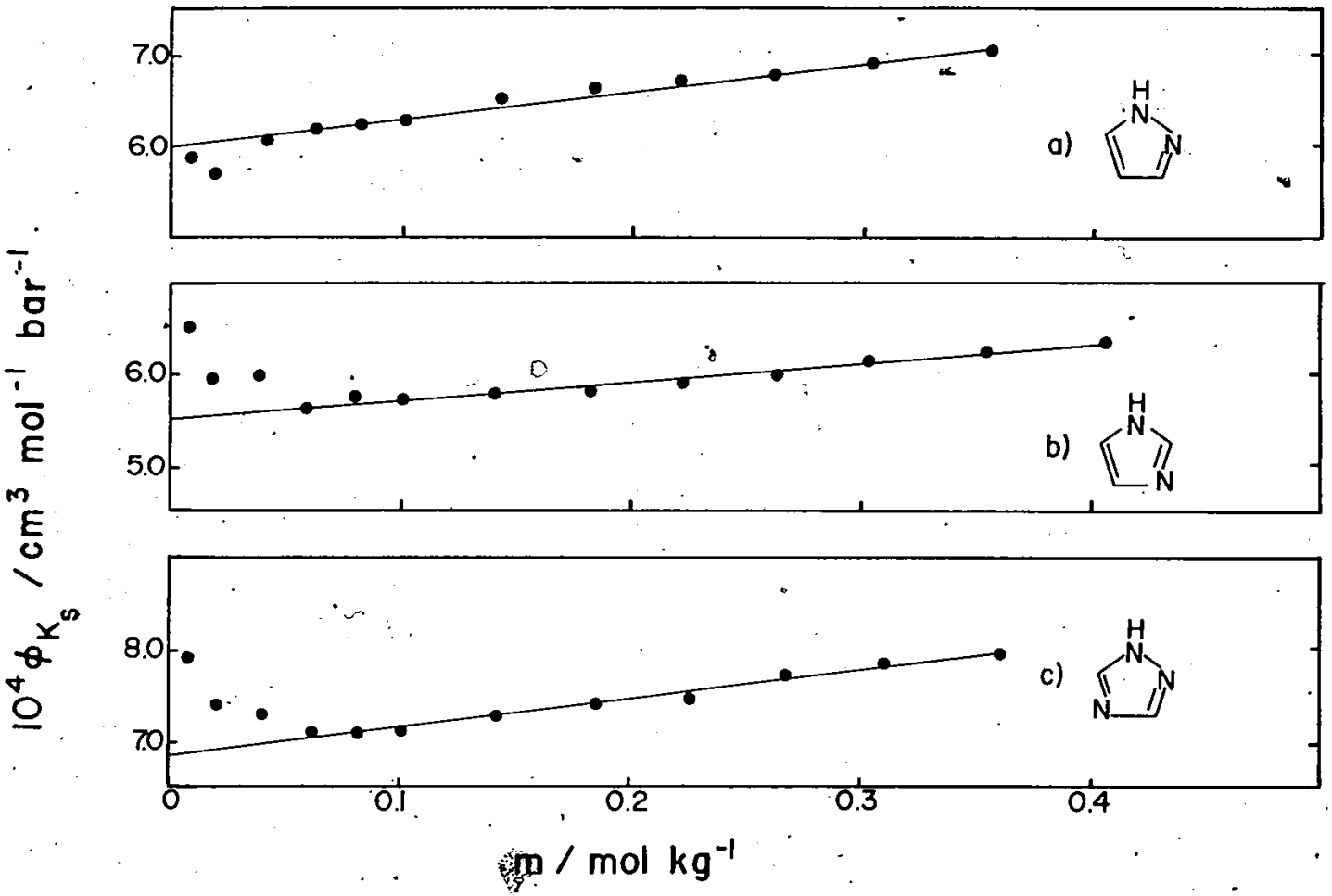

Figure 20 - Plots of ϕ_{KS} against m for (a) pyrazole in H_2O; (b) imidazole in 0.01 N NaOH and (c) 1,2,4 triazole in H_2O.

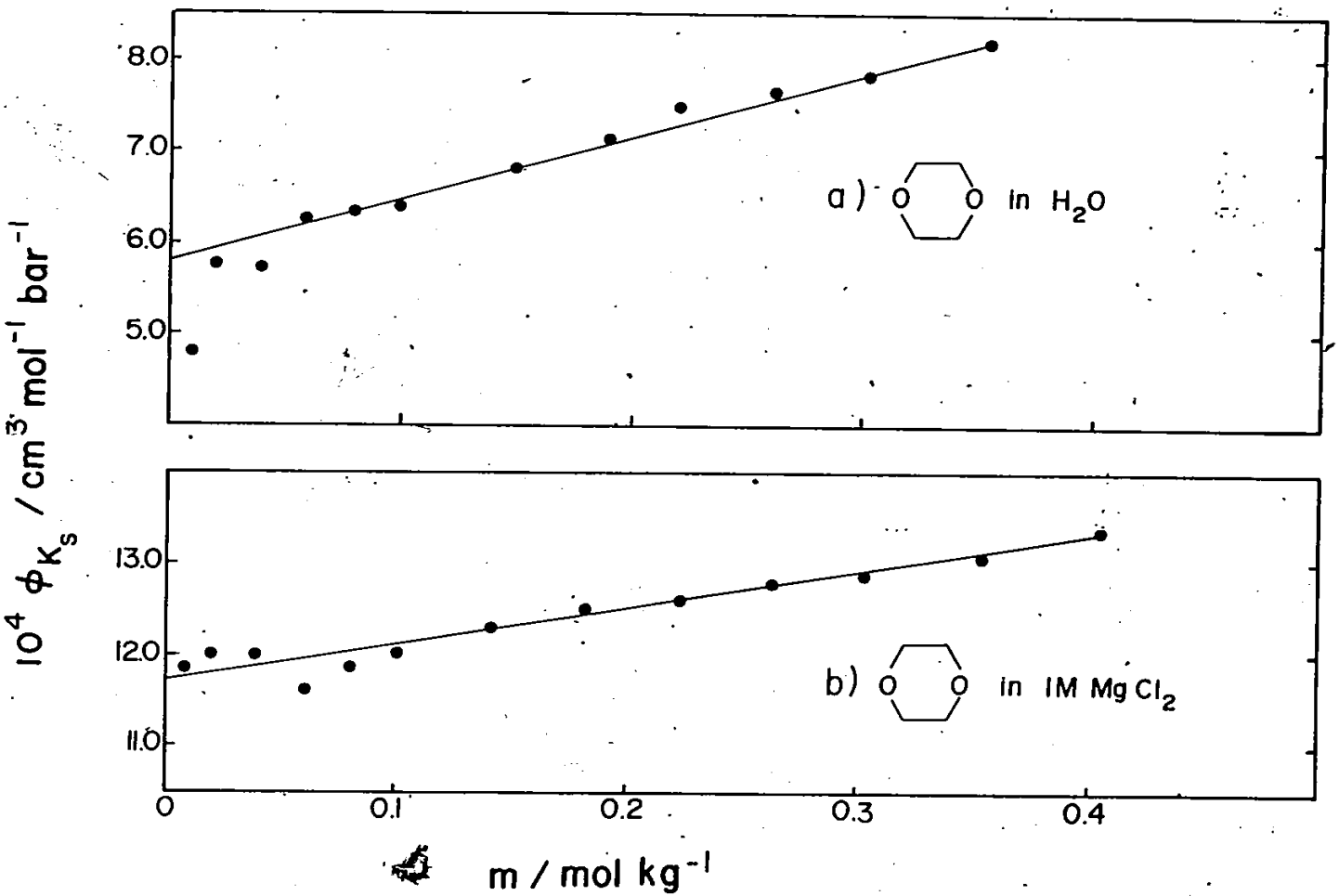

Figure 21 - Plots of ϕ_{KS} against m for (a) 1,4 dioxane in H_2O and (b) 1,4 dioxane in 1M $MgCl_2$.

Table 7

VALUES OF ϕ^{o}_{KS} ($\equiv \bar{K}^{o}_{S}$) AND b_{KS} IN EQUATION II-24 AT 298K FOR ORGANIC BASES

Base	$10^4(\phi^{o}_{KS} \pm 0.1^{(a)})$ $cm^3\ mol^{-1}\ bar^{-1}$	$10^4(b_{KS} \pm 0.3^{(a)})$ $cm^3\ mol^{-2}\ bar^{-1}\ kg^{(b)}$	Reference
Triethylenediamine	0.9	- 0.3	This work
Piperazine	0.4	- 0.5	This work
Ethylenediamine	1.6	-16.9	This work
	-6.5[c]	-	66
	0.4	0.8*	67
Pyrazine	6.9	4.3	This work
	6.3	4.8*	65
Pyridazine	2.0	5.0	This work
Pyrazole	6.0	3.0	This work
Imidazole	5.6	1.9	This work
1,2,4 Triazole	6.9	3.2	This work
Pyrrolidine	3.2	16.0	This work
	-3.5	-	66
Quinuclidine	7.3	-26.4	This work
1,4 Dioxane in H_2O	5.8	6.8	This work
	9.3	-	89
in 1M $MgCl_2$	11.7	4.0	This work
Morpholine	3.8	- 0.6	This work
	4.0	-	66
Piperidine[d]	-0.4	0.0*	69
Pyridine[d]	2.2	10.5*	69

(a) Maximum error limit for the results of the present work except for b_{KS} of ethylenediamine, pyrrolidine and quinuclidine. For these bases the error limits on b_{KS} are as much as ± 2.0 $cm^3\ mol^{-2}\ bar^{-1}\ kg$
(b) Units for the values with asterisks are $cm^3\ mol^{-2}\ bar^{-1}\ L$
(c) At 293 K
(d) From previous work in this laboratory

The discrepancies between the present results and those of Kaulgud and Patil[66] are again due to extrapolation from rather high concentration (> 1.5 m) by Kaulgud and Patil. The present ϕ_{KS}^{o} value for 1,4 dioxane in water is within the error limit of the value given by Franks et al[89]

As can be seen from Figures 17 to 21, the dependence of ϕ_{KS} on concentration is not simply linear for some of the compounds, e.g., the data for piperazine, quinuclidine, ethylenediamine and pyrrolidine show large deviations from an initially linear relation observed at low concentrations.

6. Monohydrochloride Salts of Organic Bases

(a). Apparent Molal Volumes

Apparent molal volume data obtained for the monohydrochloride salts of the organic bases listed in Table 5 were plotted according to Equation II-13 and are shown in Figures 22 to 27. For the salts pyrazine hydrochloride, pyridazine hydrochloride, pyrazole hydrochloride and 1,2,4 triazole hydrochloride, relatively large corrections for acid dissociation (Section IV.2.c) had to be made especially at very low concentrations. In order to show the extents of these corrections, both the corrected and uncorrected data have been plotted comparatively for these salts in Figures 23, 24, 25(a) and 26. For the other salts,

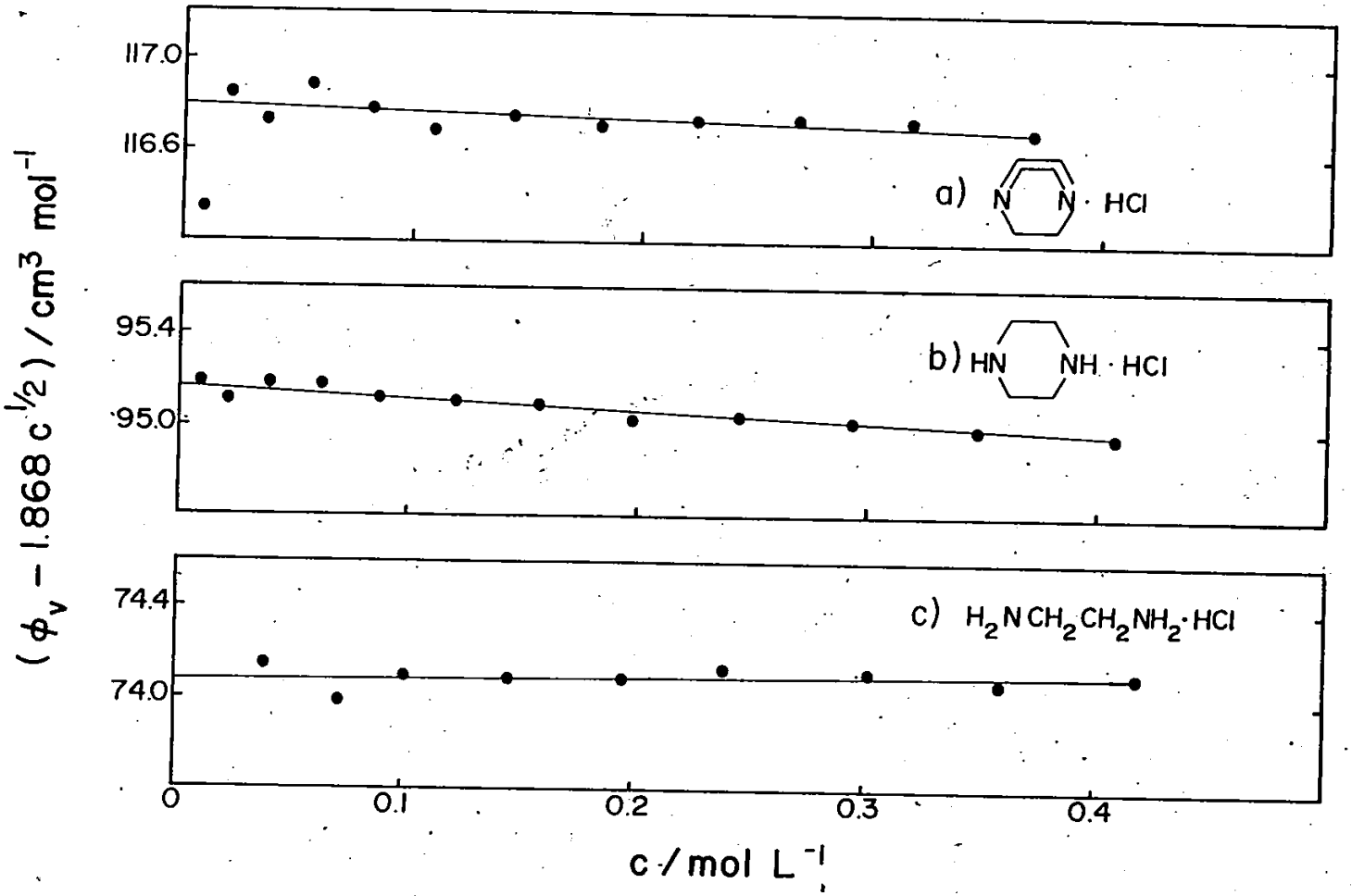

Figure 22 - Plots of $\phi_v - 1.868\ c^{1/2}$ against c for (a) triethylenediamine monohydrochloride; (b) piperazine monohydrochloride and (c) ethylenediamine monohydrochloride.

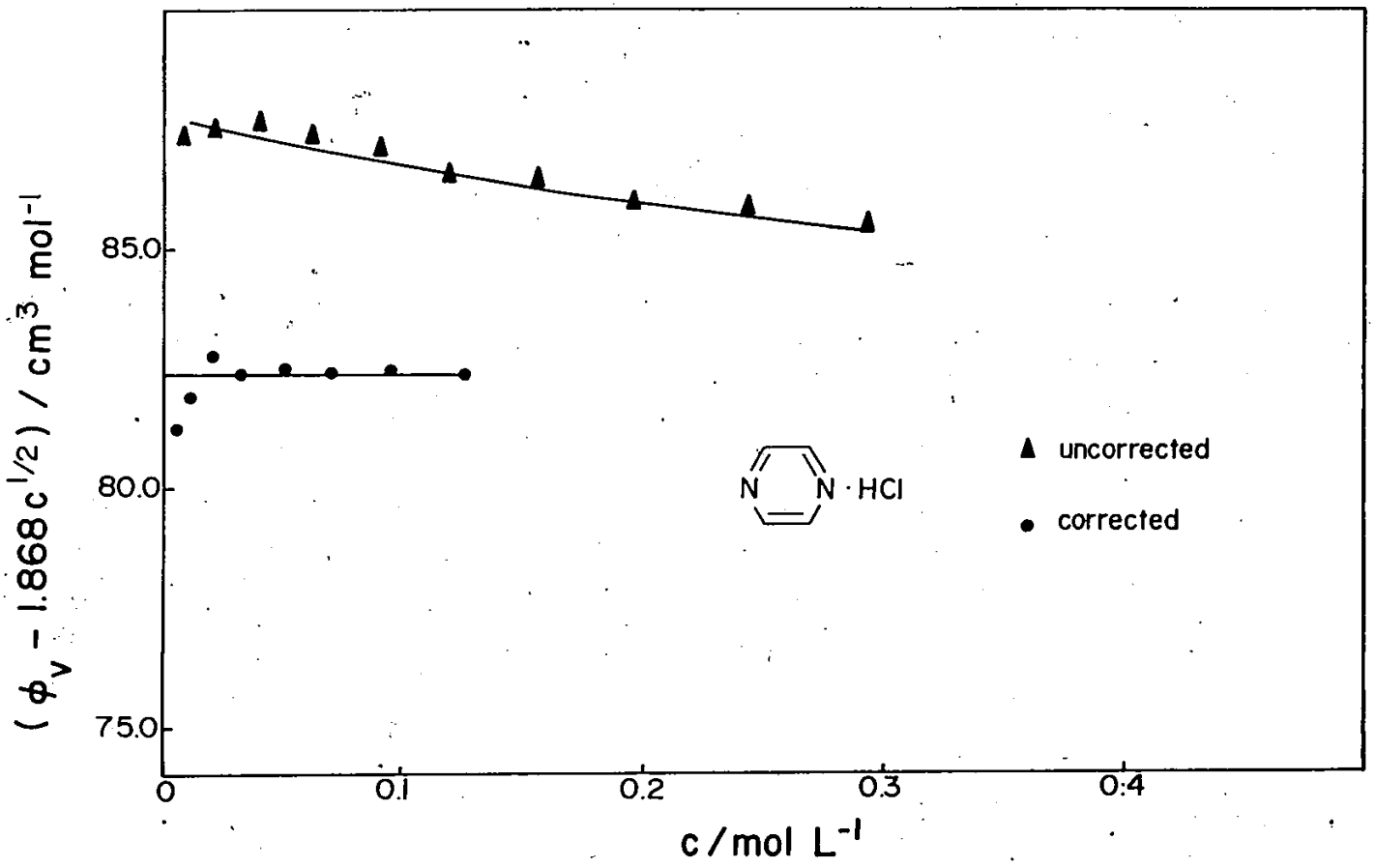

Figure 23 - Plots of ϕ_v - 1.868 $c^{1/2}$ against c for pyrazine hydrochloride both with data uncorrected and corrected for acid dissociation.

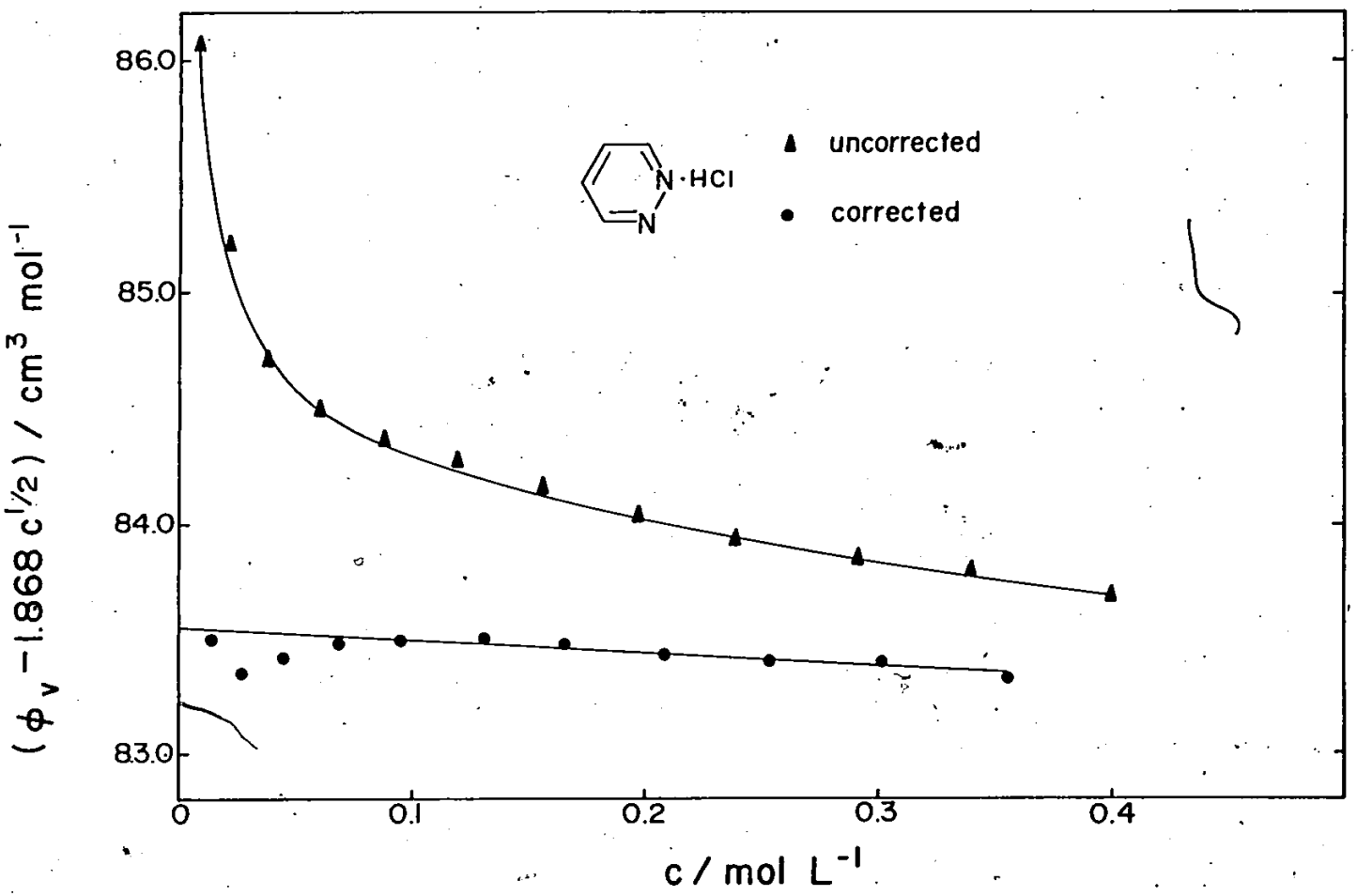

Figure 24 - Plots of $\phi_v - 1.868\ c^{1/2}$ against c for pyridazine hydrochloride both with data uncorrected and corrected for acid dissociation.

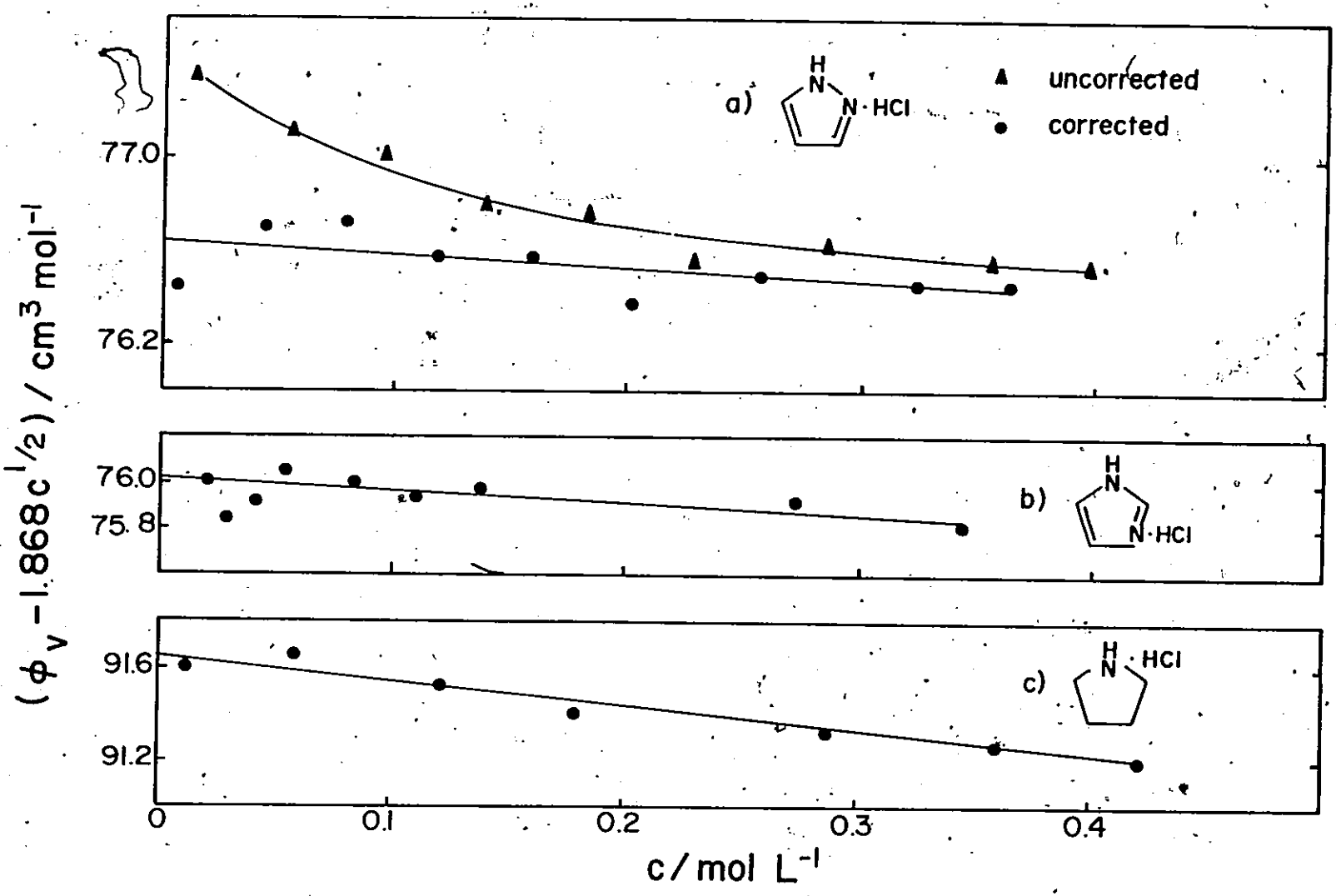

Figure 25 - Plots of $\phi_v - 1.868\ c^{1/2}$ against c for (a) pyrazole hydrochloride both with data uncorrected and corrected for acid dissociation; (b) imidazole hydrochloride and (c) pyrrolidine hydrochloride.

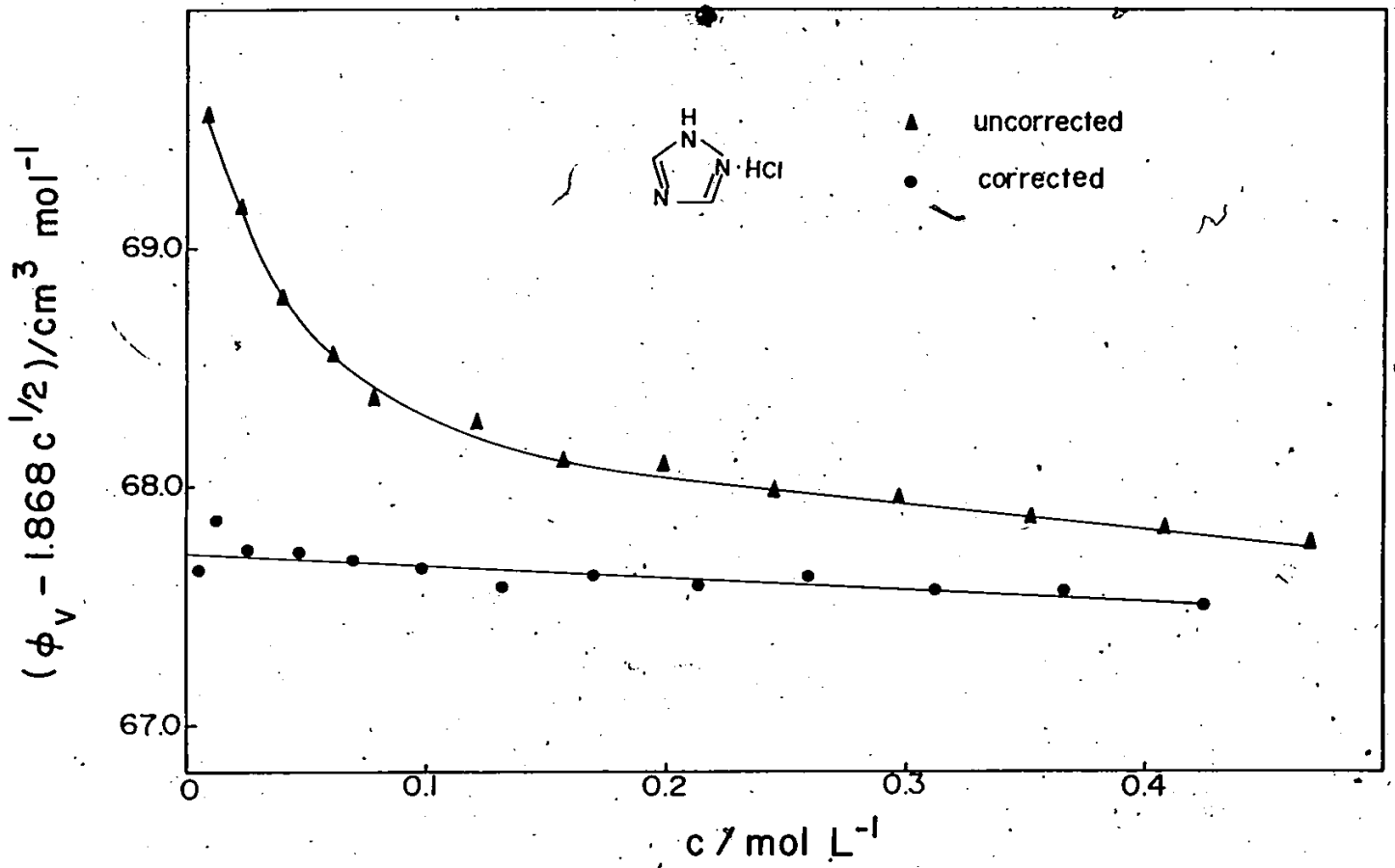

Figure 26 - Plots of $\phi_v - 1.868\, c^{1/2}$ against c for 1,2,4 triazole hydrochloride both with data uncorrected and corrected for acid dissociation.

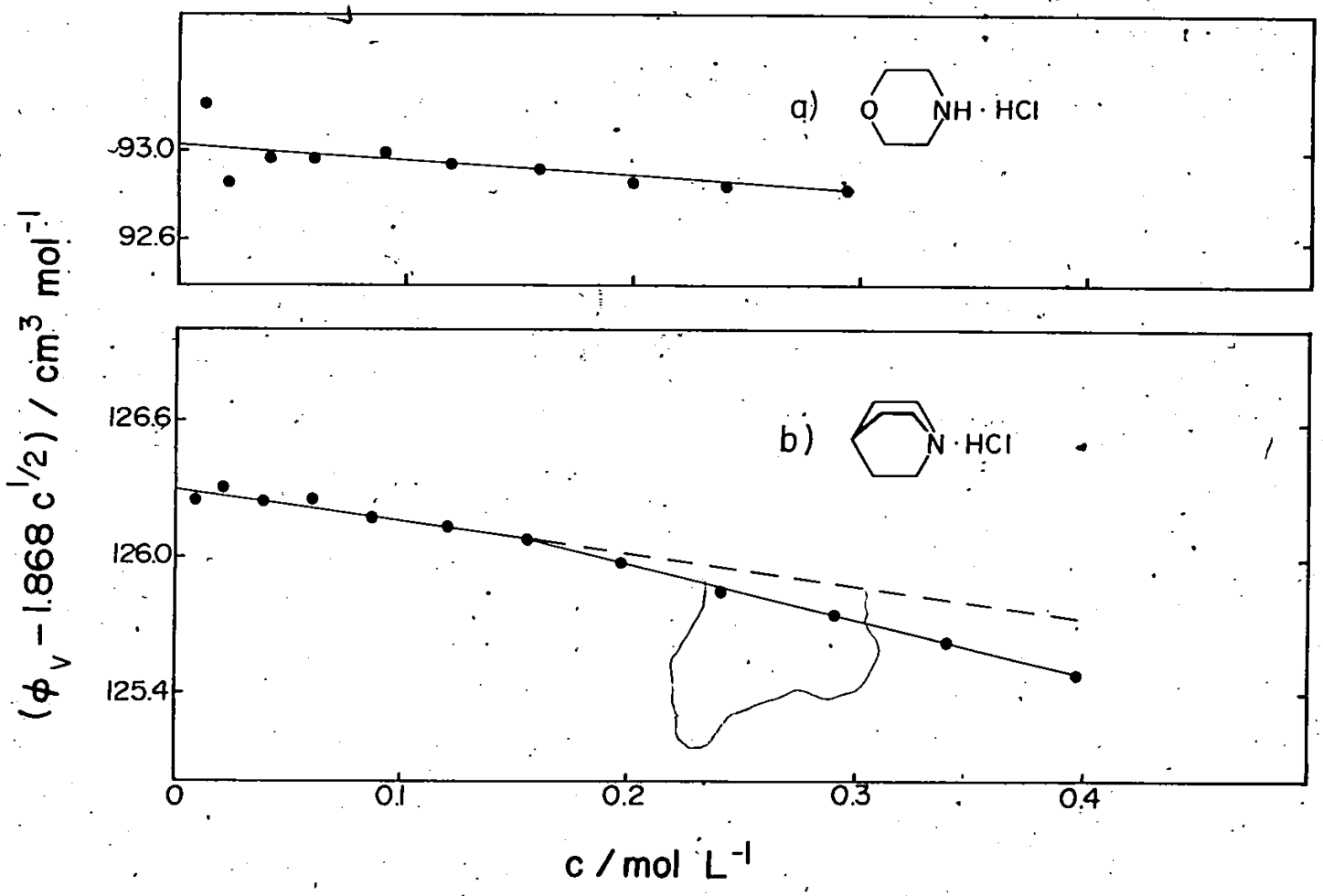

Figure 27 - Plots of ϕ_v - 1.868 $c^{1/2}$ against c for (a) morpholine hydrochloride and (b) quinuclidine hydrochloride.

triethylenediamine monohydrochloride, piperazine monohydrochloride, ethylenediamine monohydrochloride, imidazole hydrochloride, pyrrolidine hydrochloride, morpholine hydrochloride and quinuclidine hydrochloride, the corrections were found to be negligible, i.e., less than 0.01 cm^3 mol^{-1} in ϕ_v at the lowest concentration measurements made.

All the salts except quinuclidine hydrochloride exhibit a linear relation when $\phi_v - 1.868\sqrt{c}$ is plotted vs c in the concentration range studied. For quinuclidine hydrochloride (Figure 27b), a deviation was observed from the initial linearity beyond a concentration of ca. 0.15 M. The parameters ϕ_v^o and b_v in Equation II-13 for these salts, and piperidine and pyridine hydrochlorides, are given in Table 8 where the few previously known data are also included. The agreement of the present results with the known data is very good, especially for ϕ_v^o values.

(b) Apparent Molal Adiabatic Compressibilities

ϕ_{KS} data obtained for the monohydrochloride salts of organic compounds were plotted against square-root of molality according to Equation II-25 and are shown in Figures 28 to 32. The corrections due to acid dissociation were made whenever they were not negligible, and both corrected and uncorrected data were plotted. The corrections

Table 8

VALUES OF ϕ_V^o ($\equiv\bar{V}^o$) AND b_V IN EQUATION II-13 AT 298K FOR MONOHYDROCHLORIDE SALTS OF ORGANIC BASES

Salt	$\phi_V^o \pm 0.05$[a] $cm^3\ mol^{-1}$	$b_V \pm 0.2$[a] $cm^3\ mol^{-1}\ L$	Reference
Triethylenediamine	116.8$_1$	-0.3	This work
monohydrochloride	117.0	-0.9	22
	117.0	-0.9	55
Piperazine monohydrochloride	95.1$_7$	-0.5	This work
	95.1	-0.3	22
Ethylenediamine	74.0$_9$	0.1	This work
monohydrochloride	74.1	0.3	22
Pyrazine hydrochloride	82.4$_3$	-0.1	This work
Pyridazine hydrochloride	83.5$_5$	-0.5	This work
Pyrazole hydrochloride	76.6$_4$	-0.5	This work
Imidazole hydrochloride	76.0$_2$	-0.5	This work
1,2,4 Triazole hydrochloride	67.7$_2$	-0.5	This work
Pyrrolidine hydrochloride	91.6$_5$	-1.1	This work
	71.7	-1.1	58
Morpholine hydrochloride	93.0$_2$	-0.7	This work
	93.0	-0.2	22
Quinuclidine hydrochloride	126.3$_0$	-1.4	This work
Piperidine hydrochloride[b]	106.6$_7$	0.0	69
Pyridine hydrochloride[b]	90.9$_6$	-1.7	69

(a) Maximum error limit for results of the present work
(b) From previous work in this laboratory

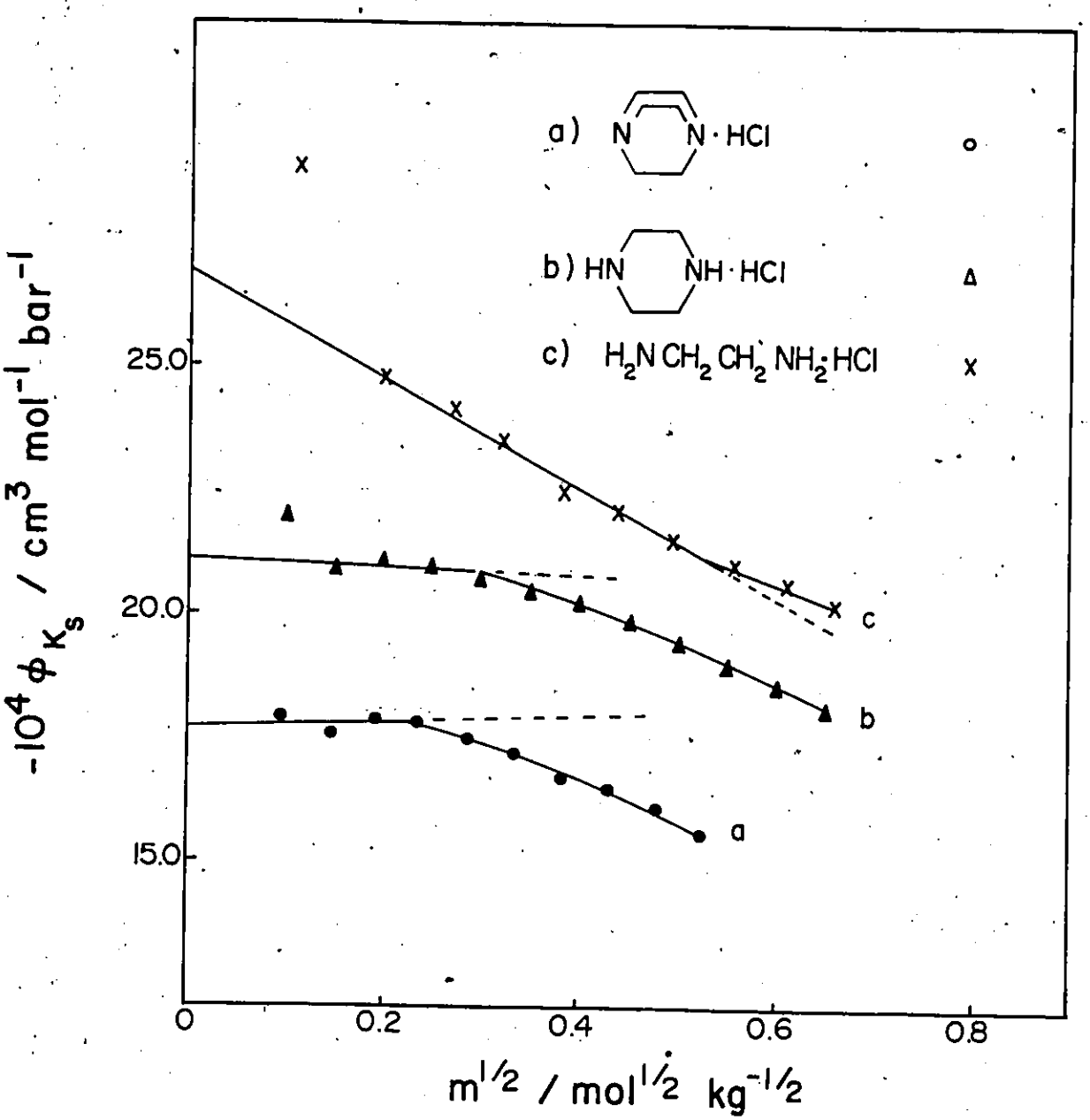

Figure 28 - Plots of ϕ_{KS} against $m^{1/2}$ for (a) triethylenediamine monohydrochloride; (b) piperazine monohydrochloride and (c) ethylenediamine monohydrochloride.

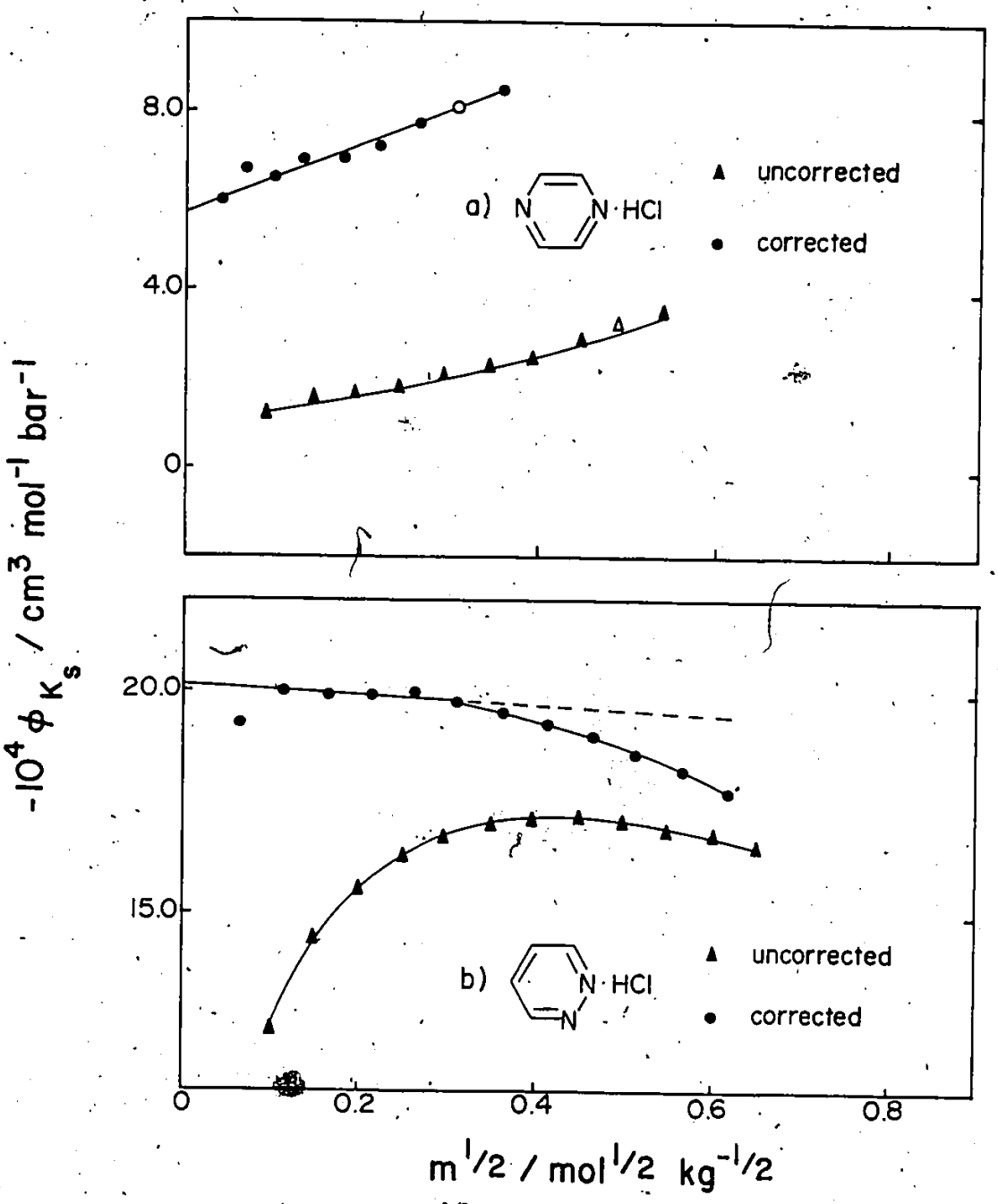

Figure 29 - Plots of ϕ_{KS} against $m^{1/2}$ for (a) pyrazine hydrochloride and (b) pyridazine hydrochloride both with data uncorrected and corrected for acid dissociation.

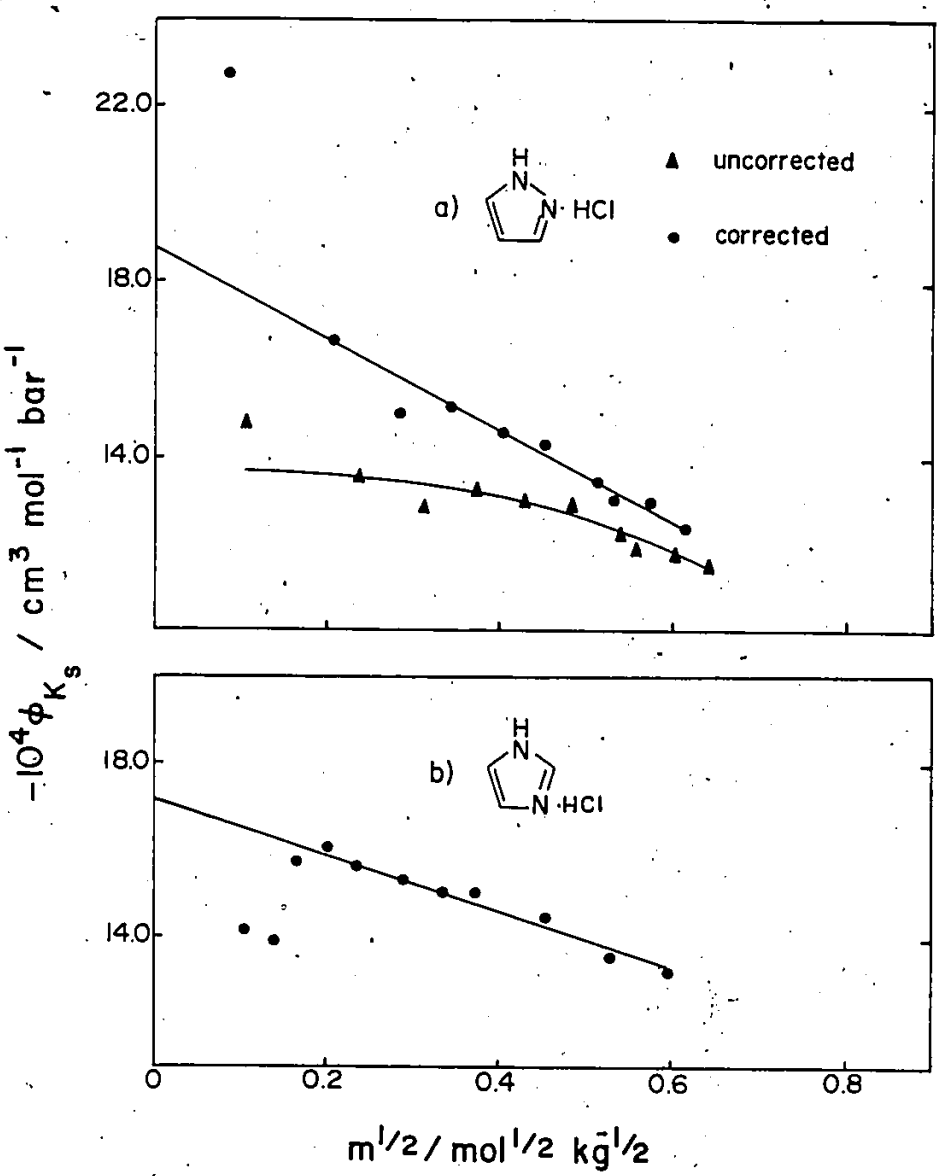

Figure 30 - Plots of ϕ_{KS} against $m^{1/2}$ for (a) pyrazole hydrochloride both with data uncorrected and corrected for acid dissociation; and (b) imidazole hydrochloride.

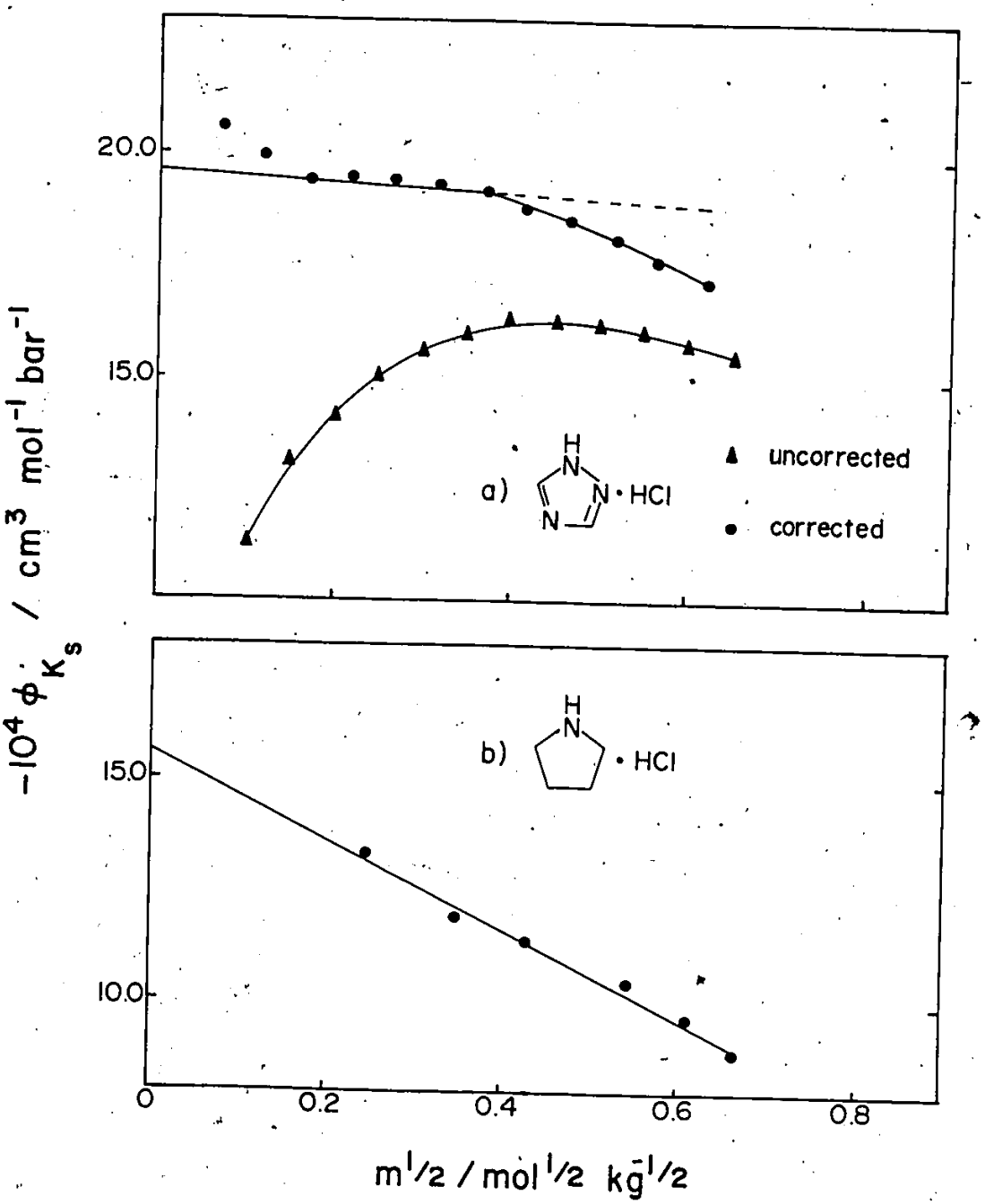

Figure 31 - Plots of ϕ_{KS} against $m^{1/2}$ for (a) 1,2,4 triazole hydrochloride both with data uncorrected and corrected for acid dissociation; and (b) pyrrolidine hydrochloride.

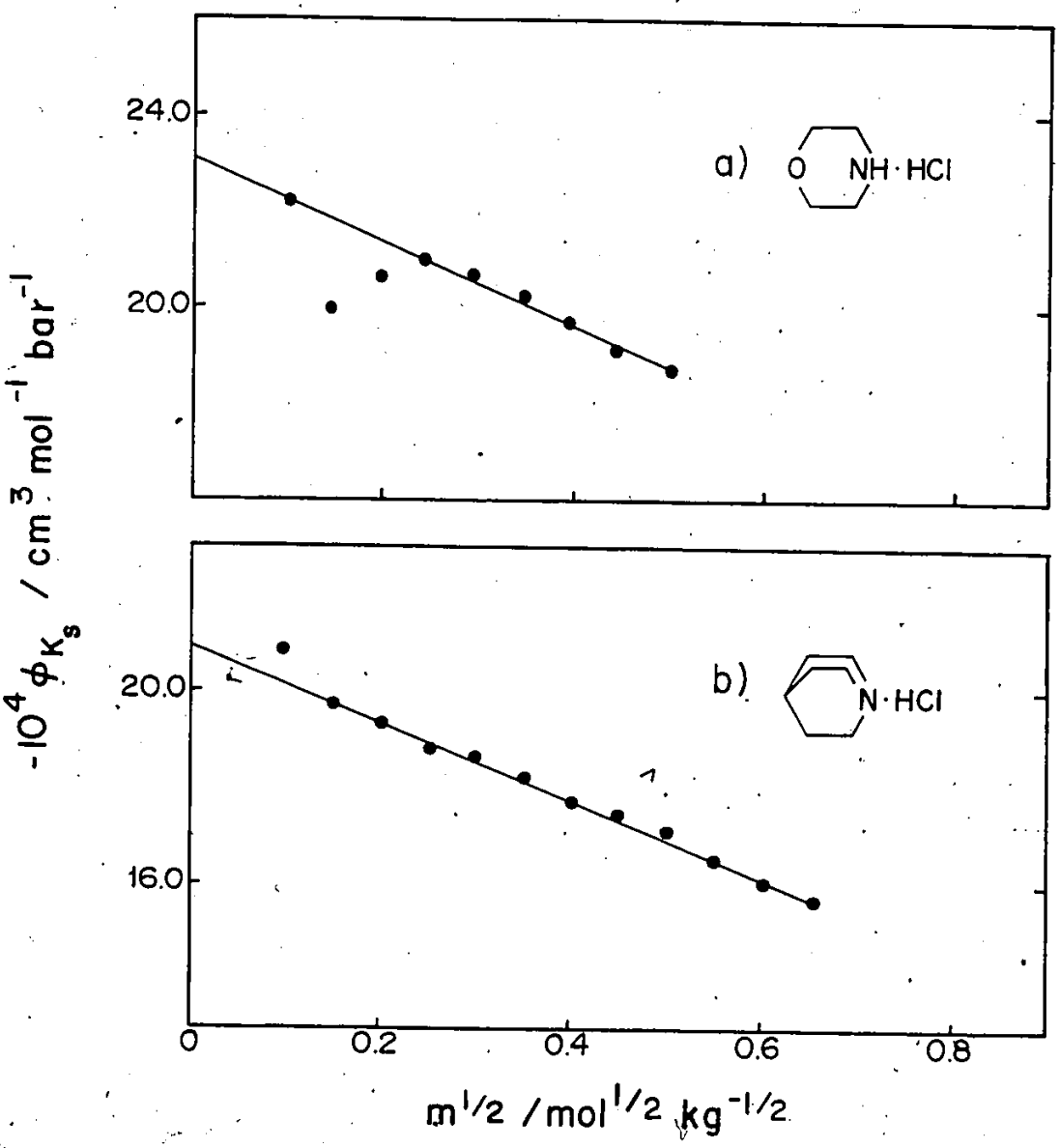

Figure 32 - Plots of ϕ_{KS} against $m^{1/2}$ for (a) morpholine hydrochloride and (b) quinuclidine hydrochloride.

were found to be smaller at higher concentrations, as expected, except in the case of pyrazine hydrochloride for which the two data (corrected and uncorrected) showed a nearly parallel trend in the concentration range studied. This is due to a large degree of dissociation, α, which was 0.96 at the lowest and 0.57 at the highest concentration studied. It was also dependent on the values of ϕ^{o}_{KS} and b_{KS} of pyrazine itself. The point shown by the open circle in Figure 29a is the datum of an independent measurement which shows the reproducibility of the results.

The parameters, ϕ^{o}_{KS} and S^{*}_{KS} of Equation II-25 for these salts obtained from the plots are given in Table 9. There are no literature data on compressibilities of these salts, as far as could be found.

7. Dihydrochloride Salts of Some Organic Diacidic Bases

The weak basic character of the second nitrogen centre in molecules of this kind makes the formation, thus the preparation of dihydrochloride salts of all the organic bases investigated in this section of the work very difficult. As can be seen in Table 5, the pK_a values for the second ionization of triethylenediamine, piperazine and ethylenediamine, all being non-aromatic, are comparable to the pK_a values for the first ionization of some of the aromatic heterocyclic compounds. For the other compounds

Table 9

VALUES OF ϕ^{o}_{KS} ($\equiv \bar{K}^{o}_{S}$) AND S^{*}_{KS} IN EQUATION II-25 FOR MONOHYDROCHLORIDE SALTS OF ORGANIC BASES AT 298K

Salt	$10^4(\phi^{o}_{KS} \pm 0.2^{(a)})$ $cm^3\ mol^{-1}\ bar^{-1}$	$10^4(S^{*}_{KS} \pm 1.0^{(a)})$ $cm^3\ mol^{-3/2}\ kg^{1/2}\ bar^{-1}$
Triethylenediamine monohydrochloride	-17.7	-0.6
Piperazine monohydrochloride	-21.1	-0.9
Ethylenediamine monohydrochloride	-26.9	10.9
Pyrazine hydrochloride	- 5.7	-7.6
Pyridazine hydrochloride	-20.1	1.1
Pyrazole hydrochloride	-18.8	10.5
Imidazole hydrochloride	-17.1	6.4
1,2,4 Triazole hydrochloride	-19.6	1.0
Pyrrolidine hydrochloride	-15.6	10.0
Morpholine hydrochloride	-23.1	8.8
Quinuclidine hydrochloride	-21.0	8.0
Piperidine hydrochloride[b]	-22.0	8.6
Pyridine hydrochloride[b]	-18.6	4.6

(a) Maximum error limit for the results of the present work
(b) From previous work in this laboratory[69]

(with the exception of the above three), the $pK_a(2)$ values are expected to be very low (mostly negative) since their $pK_a(1)$ values for the first ionization are already low. Therefore, it was possible to study only triethylenediamine dihydrochloride, piperazine dihydrochloride and ethylenediamine dihydrochloride as 2:1 salts of the organic bases.

The apparent molal volume and compressibility of these three salts were plotted in the usual way according to Equations II-13 and II-25, respectively. The graphs are shown in Figures 33 to 36. Significant corrections had to be made to the experimental data obtained for triethylenediamine dihydrochloride to allow for the second acid dissociation process. Both corrected and uncorrected data have been plotted. For piperazine dihydrochloride, the corrections were important but not as large as for triethylenediamine dihydrochloride. The corrections for ethylenediamine dihydrochloride were almost negligible due to the relatively high $pK_a(2)$ value for ethylenediamine. These corrections were made and only the corrected values were plotted in Figures 34(b) and 36. However, both corrected and uncorrected data are given in appendices.

From the plots, the parameters ϕ_V^o and b_V, and ϕ_{KS}^o and S_{KS}^* in Equations II-13 and II-25 were obtained and are recorded in Tables 10 and 11. Previously published data for volumes were also included in the tables for comparative

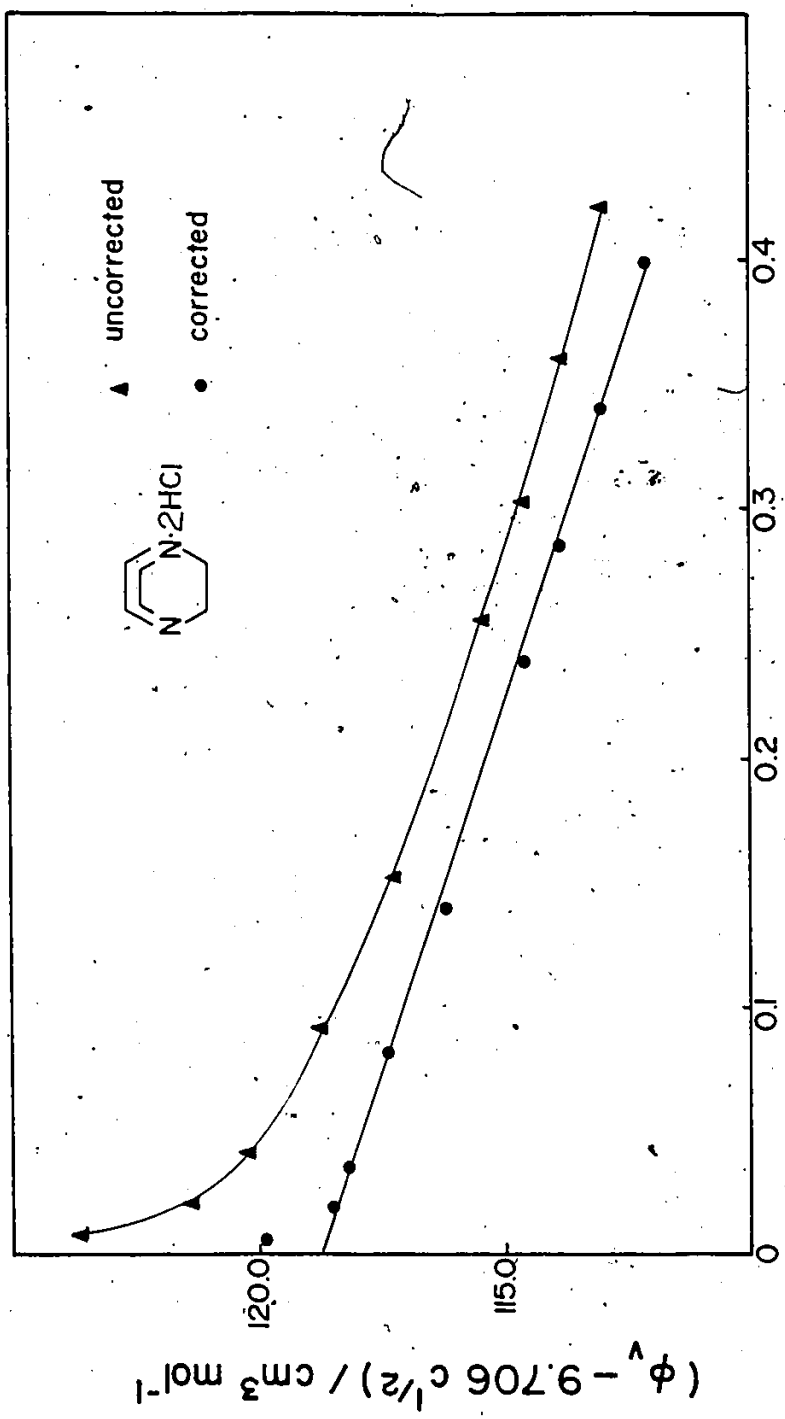

Figure 33 - Plots of $\phi_v - 9.706\ c^{1/2}$ against c for triethylenediamine dihydrochloride both with data uncorrected and corrected for second acid dissociation.

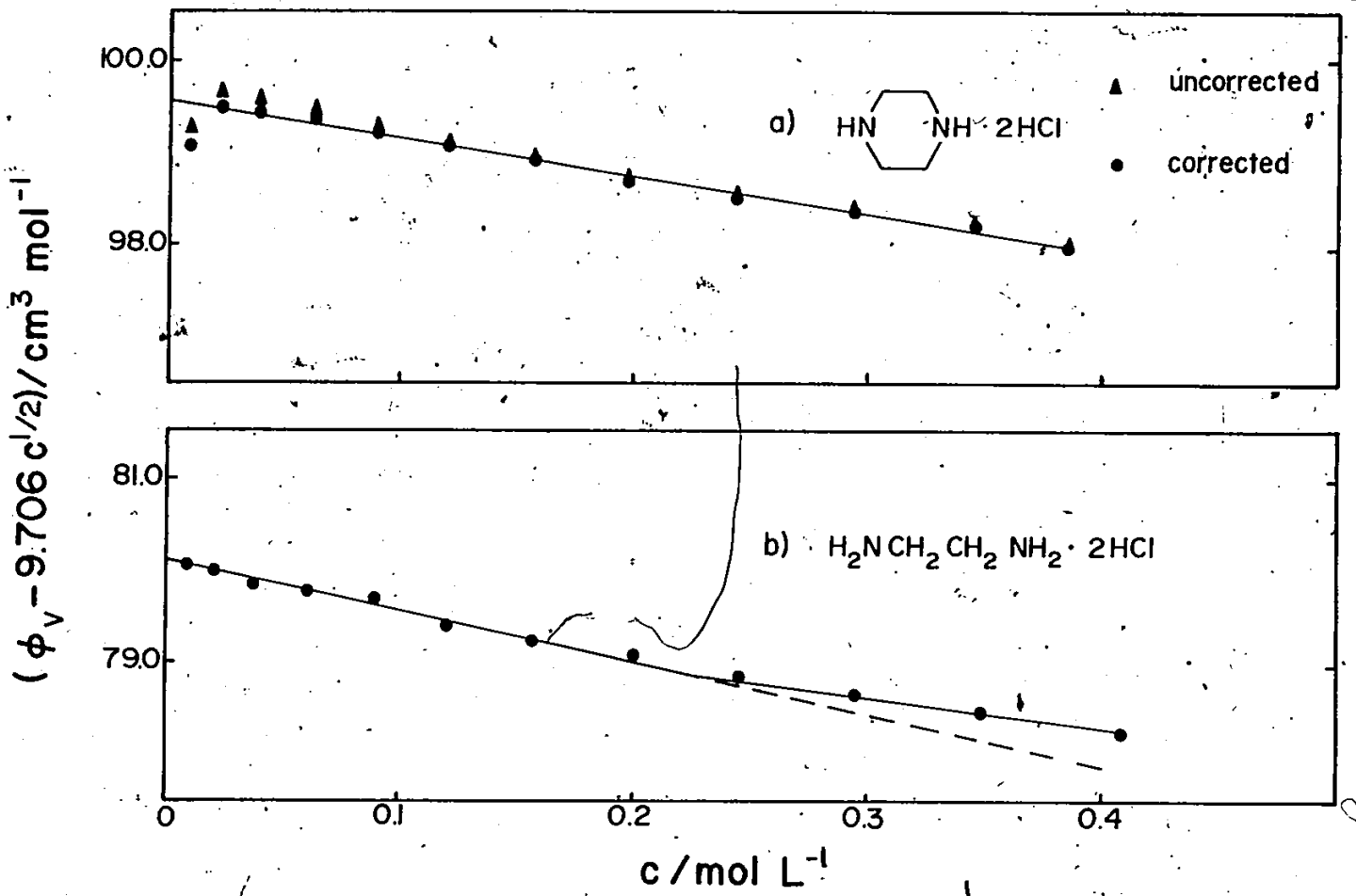

Figure 34 - Plots of $\phi_v - 9.706\ c^{1/2}$ against c for (a) piperazine dihydrochloride both with data uncorrected and corrected for second acid dissociation; and (b) ethylenediamine dihydrochloride with data corrected for second acid dissociation.

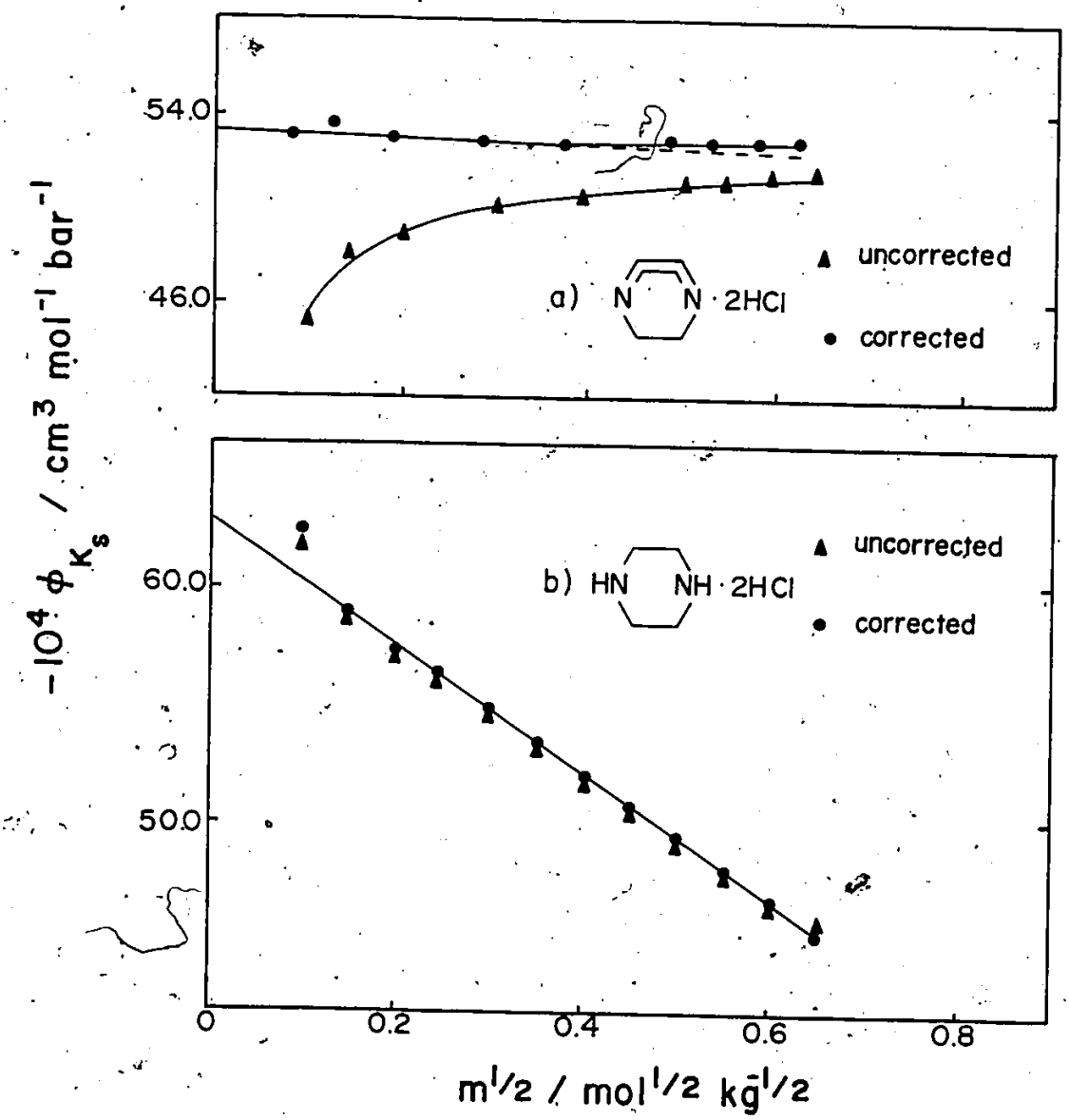

Figure 35 - Plots of ϕ_{KS} against $m^{1/2}$ for (a) triethylenediamine dihydrochloride and (b) piperazine dihydrochloride both with data uncorrected and corrected for second acid dissociation.

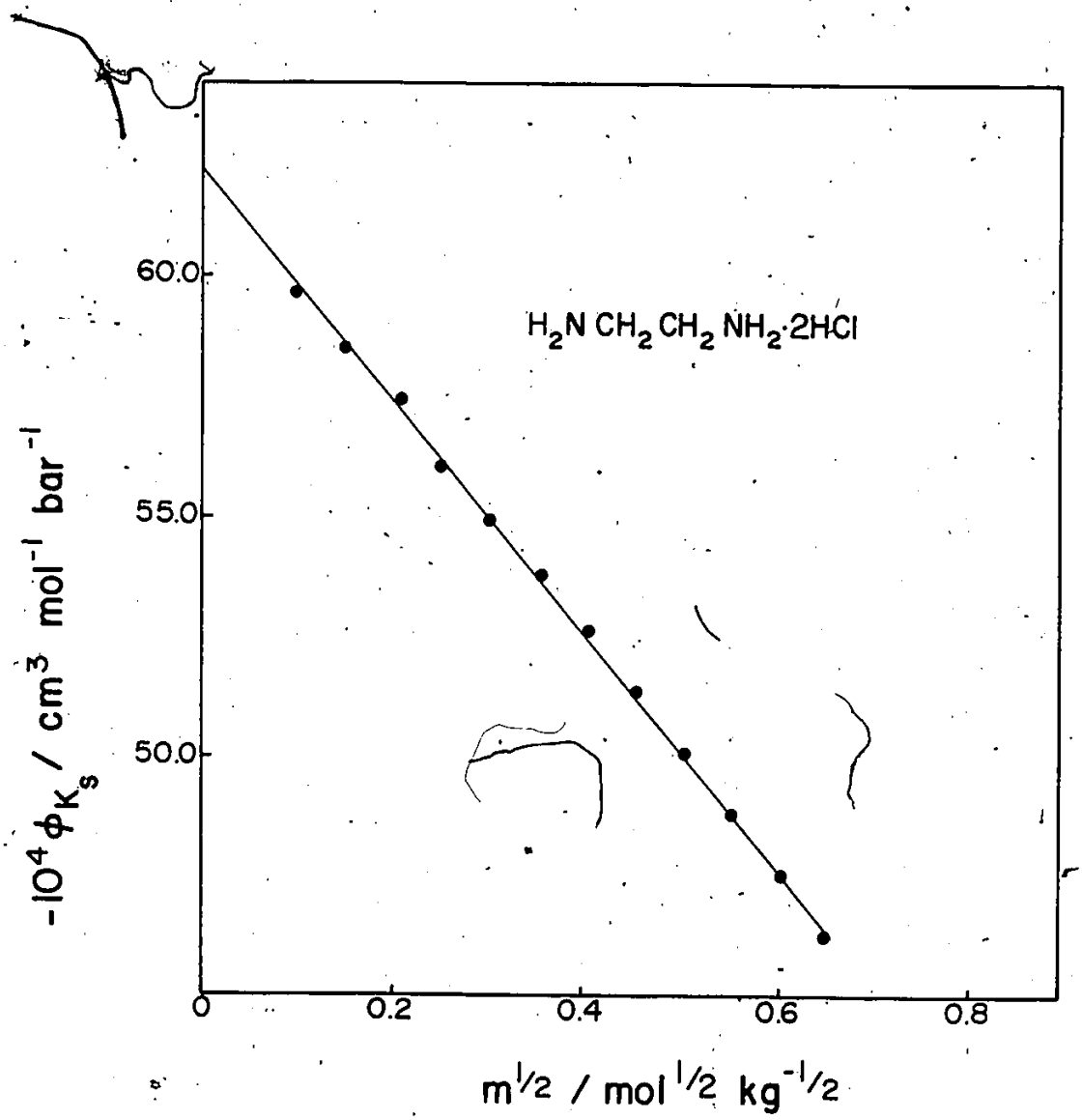

Figure 36 - A plot of ϕ_{KS} against $m^{1/2}$ for ethylenediamine dihydrochloride.

Table 10

VALUES OF ϕ_V^o ($\equiv\bar{V}^o$) AND b_V IN EQUATION II-13
AT 298K FOR DIHYDROCHLORIDE SALTS OF ORGANIC BASES

Salt	($\phi_V^o \pm 0.1$[a]) $cm^3\ mol^{-1}$	($b_V \pm 1.0$[a]) $cm^3\ mol^{-2}\ L$	Reference
Triethylenediamine	118.7	-16.8	This work
dihydrochloride	118.6	- 4.0	22
Piperazine	99.6	- 4.0	This work
dihydrochloride	99.3	- 4.1	22
Ethylenediamine	80.1	- 5.6	This work
dihydrochloride	79.8	- 5.0	22
	80.1	- 5.5	90

(a) Maximum error limit for results of the present work

Table 11

VALUES OF ϕ_{KS}^o ($\equiv\bar{K}_S^o$) AND S_{KS}^* IN EQUATION II-25
AT 298K FOR DIHYDROCHLORIDE SALTS OF ORGANIC BASES

Salt	10^4($\phi_{KS}^o \pm 0.1$[a]) $cm^3\ mol^{-1}\ bar^{-1}$	10^4($S_{KS}^* \pm 1.0$[a]) $cm^3\ mol^{-3/2}\ kg^{1/2}\ bar^{-1}$
Triethylenediamine dihydrochloride	-53.4	1.4
Piperazine dihydrochloride	-62.9	26.9
Ethylenediamine dihydrochloride	-62.2	24.1

(a) Maximum error limit for results of the present work

purposes, while there were no available data on compressibilities of these three salts. The agreement is again very good, especially for ϕ_V^o.

CHAPTER V

DISCUSSION

A. Basis of Interpretation of Volume and Compressibility Measurements

1. Introductory Remark

Since both volume and compressibility measurements form much of the body of the present work, it is desirable to explain the basis of interpretation of such measurements and how they are related.

2. Significance of Compressibility of Water

Compressibility measures the relative change, $-\delta V/V$, of the volume V of a phase for an increase of pressure, δP. In the case of liquids, most of the compressed volume near ordinary pressures and temperatures is associated with diminution of the free volume in the liquid. Only at very high pressures is this free volume almost completely collapsed so that, for further increase of pressure, the molecules themselves are forced into a closer contact situation where increasing overlap of their van der Waals electronic envelopes must occur. Then the compressibility becomes much lower. The free volume of water is almost completely collapsed when a pressure of ca. 10,000 bars is attained[120]. It is this volume change that is associated

with the electrostriction caused by small ions in water; the compressibility is correspondingly diminished.

In water, the structural free volume is quite large (ca. 6 cm^3 mol^{-1}) so that the low-pressure compressibility is mainly determined by the effect of pressure in diminishing this "intermolecular" volume by changing the H-bonded structure of the liquid. Since this is relatively rigid, as in ice, due to the strong directional character of O — H --- O H-bonds, the compressibility of water, like that of ice, is rather low compared with the values for other liquids such as CH_3OH, CCl_4, C_6H_6, etc. (Table 12). In fact, ice, which has a larger structural free volume than water at the same temperature, 273 K, is substantially less compressible than water[121,122] as shown in Table 12.

With regard to compression of the free volume of water, we must identify the physical molecular process as a rearrangement of the tetrahedral geometry of H-bonded water molecules to one eventually of hexagonal close packing at sufficiently high pressures (ca. 10,000 bar). Therefore, the compressibility will be determined mainly at low pressures near 1 bar by bending of H-bonds to allow smaller free volume. Hence the compressibility will be determined at first by the derivative of the free energy of the lattice with respect to average intermolecular distance, the latter being determined by average angular displacement of

Table 12

COMPRESSIBILITIES, β, OF ICE, WATER AND SOME OTHER LIQUIDS AT 273 K

	Ice(258K)	Ice(273K)	H_2O(273K)	H_2O(298K)
$10^6\beta/bar^{-1}$	12	33	50.98	45.24

	C_6H_6	CCl_4	CH_3OH	$n\text{-}C_6H_{14}$
$10^6\beta/bar^{-1}$	97	107.7	125.6	160.6

Notes on Table 12

i) Comparison of compressibilities of various liquids should probably best be made at "corresponding temperatures", e.g., at some defined fraction of the temperature difference between the b.p. and m.p. or at the m.p. itself.

ii) β in SI units, m^2N^{-1}, is 10% of the figures listed here.

O — H --- O H-bonds from their optimum average orientation at a given temperature. It may therefore be supposed that the low-pressure compressibility is determined by the energy associated with H-bond bending. Formally, since $V = (\partial G/\partial P)_T$, it is seen that β is, in fact, determined by the second derivative of the free energy with pressure, $-\frac{1}{V}\left(\frac{\partial^2 G}{\partial P^2}\right)_T$. Also it can be shown that [123]

$$\left(\frac{\partial^2 E}{\partial V^2}\right)_T = \frac{1}{\beta V}\left[1 + T\left(\frac{\partial \ln\beta}{\partial T}\right)_V\right] \equiv \frac{1}{\beta V}\left[1 + \left(\frac{\partial \ln\beta}{\partial \ln T}\right)_V\right] \qquad V.1$$

which is approximately

$$\left(\partial^2 E/\partial V^2\right)_T = 1/\beta V \qquad V.2$$

A molecular model calculation requires a relation in terms of the intermolecular potential energy function, $u(r)$, where u is the energy as a function of intermolecular distance r. It may be obtained as follows: let r^3 be the volume occupied by one molecule and u its energy in the liquid lattice. Then for Avagadro's number N of molecules

$$V = Nr^3 \text{ and } E = Nu.$$

dE/dV is written

$$dE/dV = (dE/dr)(dr/dV) = \frac{1}{3Nr^2}(dE/dr) \qquad V.3$$

and

$$d^2E/dV^2 = \frac{1}{3Nr^2}\frac{d}{dr}\left[\frac{1}{3r^2}\frac{du}{dr}\right] \qquad V.4$$

$$= \frac{1}{3Nr^2}\left[\frac{1}{3r^2}\left(\frac{d^2u}{dr^2}\right) - \frac{1}{6r}\left(\frac{du}{dr}\right)\right] \qquad V.5$$

$$= \frac{1}{\beta V} \equiv \frac{1}{\beta Nr^3} \qquad V.6$$

the derivatives being taken at constant temperature of the liquid lattice.

It is seen that evaluation of β requires differentiation of the intermolecular potential energy function u(r) once and twice. u(r) will be determined in a probably complex way in water by changes both in average intermolecular separation (the O ---- O distances) and in orientation of O — H ---O H-bonds as compression occurs. The energy of such a system of molecules could be calculated by means of Pople's point-charge model[124] of the H-bonding in water as was done[125], for example, for the angular motions of H_2O dipoles in dielectric relaxation behaviour. A simpler approach would be to use the potential function employed by Rahman and Stilinger[5] in their molecular dynamics calculation on the properties of water. This potential function was a combination of two terms: one for 4-point coulombic interactions between water quadrupoles and the second a "6:12" Lennard-Jones type function for the "non-coulombic" interactions.

3. Electrostriction and Compressibility

Passynski[77] first introduced the idea that compressibility measurements on ions in solution would give information on hydration numbers for ions through the extents of electrostrictive compression that ions cause in

water. Applying Frank's theory[13] of the thermodynamics of electrostriction, Desnoyers, Verrall and Conway[14] derived limiting cases for electrostriction of water in ionic fields and a general numerical solution for any condition. Using the same approach they also evaluated the compressibilities β of water as a function of field.

The approach based on the electrostatic tension generated by an ion's inhomogeneous field will always give a decrease of compressibility of a polar fluid with increasing field, related to electrostriction volume, as was shown in Reference 14.

However, using a series of alkylammonium salts $R_nN^+H_{4-n}\ X^-$ with a common anion X^-, Verrall and Conway[21] showed experimentally that the partial molal adiabatic compressibility became more negative in the direction $Me_4N^+ \rightarrow NH_4^+$, i.e., in the way expected with diminishing ion size and accessibility of the N^+ center to water dipoles, paralleling the electrostriction, but also more negative in the direction Me → Bu in the tetra-alkylammonium series $R_4N^+X^-$. In this case, there is only small or virtually zero electrostriction of the cation yet the compressibility $\bar{K}^o_{S,i}$ becomes increasingly negative. This effect was interpreted[21] as due to the strong structure-making effect of R_4N^+ ions in water, due to their hydrophobic interactions with water, giving rise to a compressibility decrease

corresponding (cf. Frank and Evans[95]) to the known smaller compressibility of ice[121,122] than that of liquid water which arises notwithstanding a 10% greater molar volume of H_2O in ice at 273 K than of liquid water at the same temperature. Hence a greater bond rigidity of the H-bonded liquid lattice of water can give rise to a decrease of compressibility but simultaneously an increase of volume relative to an initially more disordered liquid lattice.

This kind of compressibility decrease of water in the presence of hydrophobic solutes is paralleled by observation of increase of partial molal heat capacity, lengthening of the proton nmr spin-lattice relaxation time and lowering of the "structural-temperature" of water[126].

It must be concluded that both these types of effect must be taken into consideration in interpretation of compressibility changes in aqueous solutions due to the presence of ions or neutral organic solutes, depending on the balance of the types of interaction which obtain in a given solute solution.

B. Oxyanions and their Salts

1. Partial Molal Volumes and Compressibilities of Oxyanions at Infinite Dilution

The volumetric and compressibility properties of ionic solutions can usefully be considered in terms of (a) infinite dilution conditions where only ion-solvent interactions and intrinsic properties of the ions determine the behaviour of the ions in the solution and (b) finite concentration conditions where ion-ion interactions coupled with certain aspects of the ion-solvent interactions determine the experimentally observable properties. In this section, we shall examine the results for condition (a).

The additivity principle (e.g., for M^+A^-: $\phi^o(M^+A^-) = \phi^o(M^+) + \phi^o(A^-)$, where ϕ^o is the apparent molal property at infinite dilution) allows, in principle, the determination of ionic partial molal volumes, $\overline{V}_i^o$, and adiabatic compressibilities, $\overline{K}_{S,i}^o$, at infinite dilution. All the salts studied were chosen to have the same cation in order to investigate the hydration effects at a series of oxyanions. Therefore, if $\overline{V}_i^o$ and $\overline{K}_{S,i}^o$ values for the common cation, Na^+, are known, then $\overline{V}_i^o$ and $\overline{K}_{S,i}^o$ for all the oxyanions can be determined.

Recently, Conway[43] critically examined the methods for evaluation of properties of individual ions in solution.

He tabulated the "best" extra-thermodynamic data for some simple monovalent ions based on the reliability of the data and the method of evaluation. In that table $\overline{V}_i^o$ of Na^+ was given as -5.9 ± 1.1 cm^3 mol^{-1}. $\overline{K}_{S,i}^o$ values were not included in that table. However, it is believed that the best available $\overline{K}_{S,i}^o$ value for Na^+ is $(-33.5 \pm 2.0)\ 10^{-4}$ cm^3 mol^{-1} bar^{-1} obtained by Mathieson and Conway[39].

$\overline{V}_i^o$ and $\overline{K}_{S,i}^o$ values for the oxyanions studied were calculated using the above figures for Na^+ and are given in Table 13.

2. The Dependence of $\overline{V}_i^o$ and $\overline{K}_{S,i}^o$ on the Number of Oxygen Ligands

It is interesting to see the dependence of ionic volumes and compressibilities on the number of charge-bearing oxygen ligands. In Figure 37, ionic volumes and compressibilities were plotted as a function of the number of oxygen atoms. It can be seen that both $\overline{V}_i^o$ and $\overline{K}_{S,i}^o$ increase with increasing number of oxygen atoms in a series of oxyanions having the same central atom or atoms. However, the increase in $\overline{V}_i^o$ and $\overline{K}_{S,i}^o$ is not constant for each successive increase in the number of oxygen ligands for a given net charge.

The change in ionic partial molal volume at infinite dilution upon increase in the number of oxygen atoms by

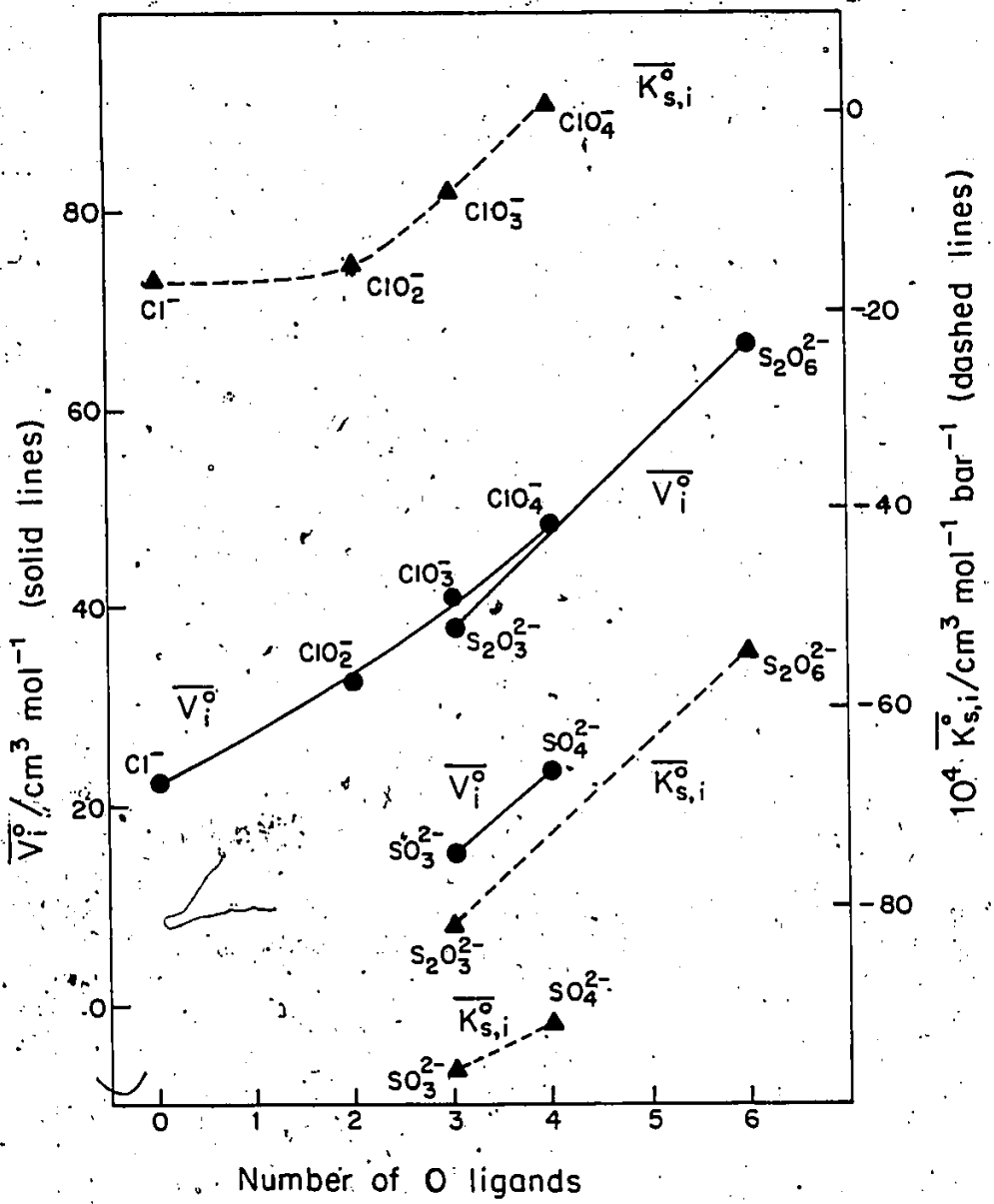

Figure 37 - Ionic volumes and adiabatic compressibilities as a function of number of oxygen atoms for oxyanions; broken lines are for $\overline{K}_{s,i}^o$ and solid lines are for $\overline{V}_i^o$ data.

Table 13

$\bar{V}_i^o$ AND $\bar{K}_{S,i}^o$ FOR OXYANIONS

Oxyanion	$\bar{V}_i^o$/cm^3 mol^{-1}	10^4 $\bar{K}_{S,i}^o$/cm^3 mol^{-1} bar^{-1}
Cl^-	22.5	-17.0
ClO_2^-	32.6	-15.7
ClO_3^-	41.2	- 8.5
ClO_4^-	48.3	+ 1.6
SO_3^{2-}	15.3	-96.6
SO_4^{2-}	23.3	-92.0
$S_2O_3^{2-}$	38.1	-81.8
$S_2O_6^{2-}$	66.5	-54.2

one is expected to be caused by the following factors: (1) increase in intrinsic volume of the ion associated with the extra oxygen ligand; (2) decrease in electrostriction due to spreading of charge over a large number of electronegative atoms thus reducing the effectiveness of the charge in electrostricting water; (3) increase of H-bonding between water molecules and the O-ligands[105] and (4) a possible steric effect influencing the degree of ~~clo~~sest approach of an H_2O dipole to the central atom of the ion. Factors (1), (2) and (4) operate in the direction of increasing the volume. This is consistent with what is observed in Figure 37.

Interpretations of partial molal ionic compressibilities are usually based on the assumption[77] that the ions themselves are incompressible. This is justified by the known compressibilities of solid alkali halide salts which have β values about 10% of that for liquid water. Values for larger polyatomic anions may be somewhat greater than for the alkali halides but will probably still give only a small contribution to the overall ϕ^{o}_{KS} which is mainly determined by the solute ion's compressive effect on neighbouring water structure having, as it does, a large free volume. There seems to be no basis for supposing that the intrinsic compressibility increases with increasing number of oxygen ligands, as would the intrinsic volume.

Because it is usually assumed[77] that the ions themselves are incompressible, the change in compressibility of an ion with increasing number of O-ligands can mainly be attributed to decrease in electrostriction. Since the smaller is the degree of electrostriction of water the greater is its compressibility[13,14], the ϕ_{KS}^{o} of oxyanions is expected to increase with increasing number of oxygen ligands as confirmed by the relations shown in Figure 37 which illustrate how $\overline{K}_{S,i}^{o}$ depends on the number of O-ligands, and hence on the size of the ion, for the series of Cl- and S-oxyanions. The directions of variation of $\overline{K}_{S,i}^{o}$ in this figure are consistent with electrostatic effects of compression[13,14]. These results appear to indicate that the electrostriction, as manifested in a decrease of compressibility of water, is not merely a function of charge, independent of ion size or geometry, as recently concluded from convincing $\overline{V}_{i}^{o}$ plots by Akitt[28]. On the other hand, while $\overline{V}_{i}^{o}$ varies systematically in the ion series Cl^- to ClO_4^- (Figure 37) if the estimated intrinsic volumes (see next section and Table 14) are subtracted and the dead space correction is applied, then the electrostriction at these ions is found to change from Cl^- to ClO_4^- (by ca. 10 cm^3 mol^{-1}) but not in the direction expected according to electrostatic

theory. Thus, the present and other earlier works (e.g., ref. 43) show that factors such as radius of the ion and the number of ligands are significant in determining the electrostriction.

3. The Separation of Volumes of Oxyanions into Intrinsic and Electrostriction Volume Contributions

Although the question of how $\overline{V}_i^o$ is made up of several components was discussed earlier (Section I.5), the determination of each component separately is actually very difficult owing to some overlap effects. In most treatments of the significance of $\overline{V}^o$ quantities, the intrinsic and the electrostriction volumes are considered to be the principal components of $\overline{V}_i^o$. The separation of ionic volumes into these components is important. The electrostriction volume can be obtained by subtracting a correctly calculated (or known) intrinsic volume from the partial molal volume of the ion at infinite dilution. The electrostriction volume is the major part of the change in volume of the solvent due to the presence of ions, i.e., due to ion-solvent interactions.

However, to evaluate the intrinsic volumes of ions is not so easy even in the case of simple spherical ions. The radii of ions in solution are not exactly known. Mostly, they are assumed to be the same as in crystal structures. Further difficulty arises due to the dead-

volume, V_f, associated with packing of solvent molecules around the ion[100]. This can be seen in the following diagram.

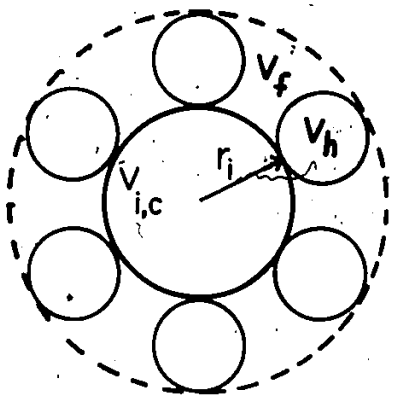

r_i crystal radius

$V_{i,c}$ "crystallographic volume" for ion in solution

V_f dead-volume

V_h effective volume of water

The calculation of V_f is complicated owing to the dependence of the effective local volume of water, V_h, on the ion with which it is associated and to unknown hydration numbers.

In the case of polyatomic ions, even the crystallographic volume, $V_{i,c}$, becomes difficult to obtain, because the shapes of these ions are not simple spheres, as with monatomic ions. For ClO_4^- or SO_4^{2-} they can be assumed to be quasi-spherical having a radius equal to the sum of the interatomic distance (S-O or Cl-O) and the van der Waals radius of oxygen. In this representation, there is a large dead-volume allowed around the ion which might be accessible to water molecules. A better assumption for shapes of these ions would be that they are represented by a tetrahedron which is spherical at the corners but calculation of volume

of such a shape presents difficulties. The problem is, of course, more difficult for the ions ClO_2^-, ClO_3^-, SO_3^{2-}, $S_2O_3^{2-}$ and $S_2O_6^{2-}$.

Intrinsic volumes, V_i, of oxyanions studied in the present work were calculated using several different methods the results of which are given in Table 14. The methods used can be summarized as follows:

a) Using Pauling's and Kapustinskii's "Thermochemical" Radii

Pauling radii (r_p) have been commonly used* for volume calculations ($V_i = 4\pi N\, r_p^3/3$) but are available only for monatomic ions. "Thermochemical" radii[102] (r_T) are available only for ClO_4^-, ClO_3^- and SO_4^{2-} among the anions involved in the present work. Corrections were made to the V_i's calculated from r_p or r_T by means of the formula[9]

$$V_i = 2520\, r_i^3 + 315\, r_i^2 \quad cm^3\ mol^{-1} \qquad V.7$$

where $r_i \equiv r_p$ or r_T in nm, in order to take into account the dead volume which depends[102] on the relative ion size r_i/r_{H_2O}.

* In recent years the compilation of "electron-density" radii of Gourary and Adrian[101] has also been used for a number of lattice and solvation energy calculations.

b) Using Couture and Laidler's[103] Effective Radii, r_{eff}

Couture and Laidler proposed that r_{eff} for oxyanions = 0.25 ℓr where ℓ is the number of O ligands on the ion, and r is the interatomic Cl-to-O or S-to-O distance plus the Van der Waals radius of the O. V_i, and dead-space corrected V_i values, calculated by this method are given in Table 14.

c) Using Padova's Method

Padova[41] showed that

$$V_i = \phi_v^o - \phi_K^o S_v^*/S_K^* \qquad V.8$$

where ϕ_v^o and ϕ_K^o are the apparent molal volume and (isothermal) compressibility at infinite dilution, and S_v^* and S_K^* are the empirical $\sqrt{c}$-dependencies of ϕ_v and ϕ_K, respectively. The present work provides all the data required for calculation of V_i's by Padova's equation for the oxyanions studied.

Padova's equation gives the total V_i for the cations and anions of the salt. He assumed $V_{i,H^+} = 0$ and then with data for aq. HCl[7,39], the V_i for Cl^- can be obtained. Then, with the results of the present work on NaCl, V_i for Na^+ and each of the co-oxyanions can be derived (Table 14), together with corresponding V_e values. The V_i's thus derived do not require[41] the assumption of any solvation model nor a dead-space correction.

d) Using Atomic Models

As a final method, the intrinsic volumes were evaluated from Fisher-Hirschfelder-Taylor space-filling scale models. The molecular models were made up and wrapped by parafilm; their volumes were then determined by water displacement.

Since the models were for only "neutral" molecules, the estimated volumes had to be converted into "ionic" volumes by the following procedure: First, for the following four sets of ions and respective isoelectronic noble gas atoms, volumes were calculated using the Pauling radii: (i) Te^{2-}, I^-, Xe^o; (ii) Se^{2-}, Br^-, Kr^o; (iii) S^{2-}, Cl^-, Ar^o; and (iv) O^{2-}, F^-, Ne^o. These volumes were then plotted against ionic charge. From this plot, the slopes of the lines I^- to Xe^o, Br^- to Kr^o, Cl^- to Ar^o and F^- to Ne^o were calculated and plotted against the volume of the respective neutral atom of the pair. A slightly curved line was obtained.

The slopes corresponding to the volumes of ClO_2, ClO_3 and ClO_4 as neutral molecules, measured as described in the first paragraph, were then determined by inter- or extrapolation on that curve. A similar procedure for the divalent oxyanions using data for Te^{2-} to Xe^o, Se^{2-} to Kr^o, S^{2-} to Ar^o and O^{2-} to Ne^o was employed. From the slopes thus obtained and the volumes of the neutral oxy-Cl and

Table 14

INTRINSIC AND ELECTROSTRICTION VOLUMES IN $cm^3\ mol^{-1}$ OBTAINED BY SEVERAL DIFFERENT METHODS

Method		Cl^-	ClO_2^-	ClO_3^-	ClO_4^-	SO_3^{2-}	SO_4^{2-}	$S_2O_3^{2-}$	$S_2O_6^{2-}$
Experimental*	$\bar{V}_i^o$	22.5	32.6	41.2	48.3	15.3	23.3	38.1	66.5
(a) (i) Pauling and thermochemical radii	V_i	15.0		20.2	33.2		30.7		
	V_e	7.5		21.0	15.1		- 7.4		
(ii) When V_i's in (i) are corrected for dead-space[9]	V_i	25.3		32.8	50.7		47.3		
	V_e	- 2.8		8.4	- 2.4		-24.0		
(b) (i) Couture and Laidler's effective radii	V_i		7.9	25.4	62.8	23.1	61.5		
	V_e		24.7	15.8	-14.5	- 7.8	-38.2		
(ii) When V_i's in (i) are corrected for dead-space[9]	V_i		14.6	40.1	89.6	36.9	88.0		
	V_e		18.0	1.1	-41.3	-21.6	-64.7		
(c) Padova's equation	V_i	21.5	26.5	38.0	54.1	18.8	28.8	41.5	63.2
	V_e	1.0	6.1	3.2	- 5.8	- 3.5	- 5.5	- 3.4	3.5
(d) (i) Atomic models after conversion to equivalent ionic volumes	V_i	15.0	26.6	32.7	40.7	35.7	44.9	51.3	72.4
	V_e	7.5	6.0	8.5	7.6	-20.4	-21.6	-13.2	- 5.7
(ii) When V_i's in (i) are corrected for dead-space[9]	V_i	25.3	41.8	50.1	60.8	54.1	66.4	74.8	82.0
	V_e	- 2.8	- 9.2	- 8.9	-12.5	-38.8	-43.1	-36.7	-15.3

* Based on the individual $\bar{V}_i^o$ value for Na^+ in water at 298 K taken as $-5.9 \pm 1.1\ cm^3\ mol^{-1}$, referred to $\bar{V}^o_{H^+} = -4.7 \pm 1.1\ cm^3\ mol^{-1}$ (Reference 43).

oxy-S species, the intrinsic volumes of the corresponding oxyanions were determined.

V_i and thus V_e values obtained in this way are recorded in Table 14. While the method described in this section for converting molecular volumes into ionic volumes can be questioned, the main idea was to find an approach which would enable the change of volume in going from a neutral species to a corresponding singly or doubly negative charged ion to be evaluated.

For Cl^-, the values obtained by direct use of the Pauling radius [method (a)] were taken.

The V_i's obtained by the above procedure from measurements on the atomic models were also corrected for the dead-space effect[9] according to Equation V.7 (in the case of $S_2O_6^{2-}$ an equation similar to V.7, derived for cylindrical ions in Reference 9, was used to correct for the dead-space effect) and a second set of V_e data were calculated (Table 14). It is interesting that only by method (d), with this procedure, do negative values of V_e arise for the Cl-oxy-anions, and large negative values, corresponding to ca. 6 fully electrostricted water moles, for the S-oxyanions.

Comparatively, methods (a), (b) and (c) seem to give unreliable and inconsistent results for V_i, and hence V_e, while method (d) seems to give the most satisfactory values, minimizing anomalies in V_e as a function of

oxyanion size and charge, and with respect to the sign of V_e. For the S-oxyanions (Table 14), the V_e are all negative and large (-38.8 through -43.1 to -15.3 $cm^3\ mol^{-1}$), and appear to be both reasonable and correct in sign. Allowing ca. -6 $cm^3\ mol^{-1}$ for maximum electrostriction[14] at these 6-fold nearest neighbour coordinated divalent ions would give $V_e \approx -36\ cm^3\ mol^{-1}$, close to the large negative values in Table 14 for the S-oxyanions.

4. Comparison of V_i and V_e Data

Table 14 clearly indicates that each method gives an appreciably different value of V_i or V_e for the same ion, even for Cl^-. Thus, no single method for estimating r_i's and corresponding V_i's of oxyanions is *a priori* reliable. This means that interpretations of data in various papers, where one or another method only has been used, are doubtful. Only by a comparative approach can the true situation be perceived: it is evidently far from satisfactory.

It is interesting that methods (a), (b) and (c) give principally positive values for V_e (unexpected[13,14,41]) which decrease in the order ClO_2^- > ClO_3^- > ClO_4^-, and SO_3^{2-} > SO_4^{2-}. This unexpected result implies that the normally anticipated volume contraction[13,41] of the solvent which is greater with smaller ions (e.g., in the series $Cs^+ \rightarrow Li^+$) does not take place in the series of oxyanions. Even

taking the results for calculations (d, ii) (Table 14) which give more rational negative values for V_e, the result for ClO_4^- is still found to be numerically more than that for the other three Cl-oxyanions of the series. Such behaviour may arise because of the known[105] H-bonding of H_2O molecules to ClO_4^- shown by spectroscopic experiments[105].

The problem of interpretation of the results for the Cl-oxyanions is that the $\overline{K}^o_{S,i}$ values go in the opposite direction to that for the V_e values, assuming both $\overline{K}^o_{S,i}$ and V_e are mainly determined by electrostatic field effects. Thus the trend of $\overline{K}^o_{S,i}$ values for both the Cl- and S-oxyanion series does go in the expected direction with increasingly negative values from ClO_4^- to Cl^- and $S_2O_6^{2-}$ to SO_3^{2-} (Table 13).

The difficulty with the Cl-oxyanion series may arise because, with these ions, the local field in the hydration shell is barely sufficient to cause significant electrostriction so that other factors may become the predominant influence in determining the volume behaviour, e.g., H-bonding[105] between O ligands and surrounding H_2O molecules. Thus a calculation for ClO_4^-, assuming as a minimum a value of the local dielectric constant of ca. 6 at 0.430 nm from the centre of the ion (Cl-O distance of 0.152 nm + Van der Waals radius of 0.140 nm per O + radius

of an H_2O molecule, 0.138 nm), gives a value of V_e at the field corresponding to this distance of only 13% of the maximum V_e attainable at high fields according to the calculations of Reference 14. On the other hand, the H-bond energy of H_2O to ClO_4^- would be about 4 x the ion-dipole interaction energy at that field (at 0.430 nm from the ClO_4^- ion) so that structural factors other than just the electrostatic field at these ions of intermediate size could determine the volume behaviour.

5. Relation Between Volumes and Compressibilities of Oxyanions

For the Cl- and S-oxyanions studied, the relation between $\overline{V}_i^o$ and $\overline{K}_{S,i}^o$ is shown in Figure 38. Two smooth curves represent the results. For comparison, data for F^-, Br^- and I^- [6,24] are also shown. When $\overline{V}_i^o$ is plotted against "specific compressibility", $\overline{K}_{S,i}^o/\overline{V}_i^o$, (Figure 39), an excellent linear relation is found for Cl-oxyanions and a smooth curve for the S-oxyanions.

Theoretically[14], V_e should be related to the decrease of compressibility of water at ions, due to electrostriction. Figure 40 shows that V_e, obtained in methods (d, i) and (d, ii), plotted against $\overline{K}_{S,i}^o$, gives common smooth curves [one curve for the data obtained in (d, i) and one curve for those in (d, ii)] for all the mono- and divalent oxyanion series in a rational sequence, thus supporting

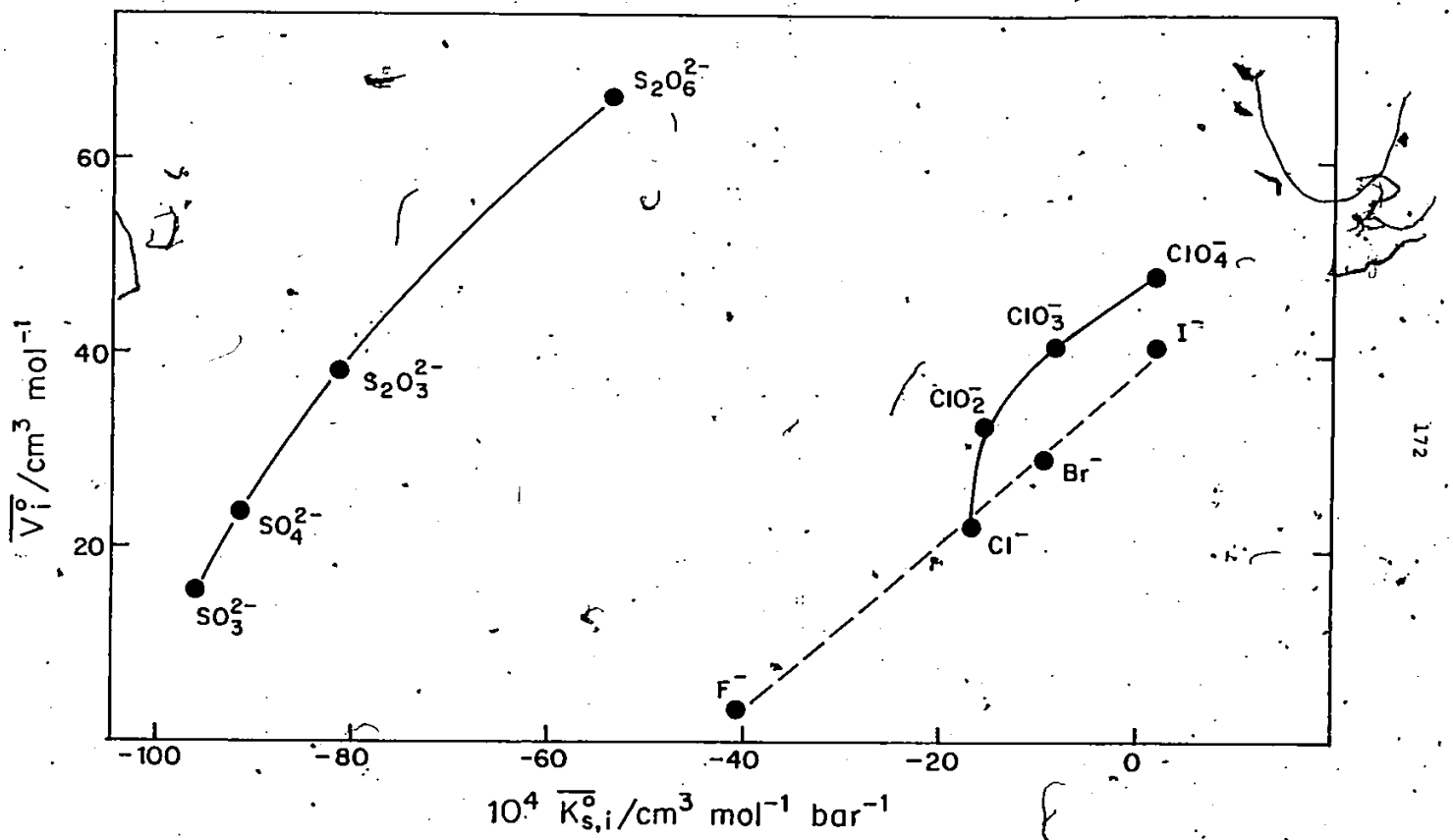

Figure 38 - A plot of $\overline{V}_i^o$ against $\overline{K}_{s,i}^o$ for oxyanions.

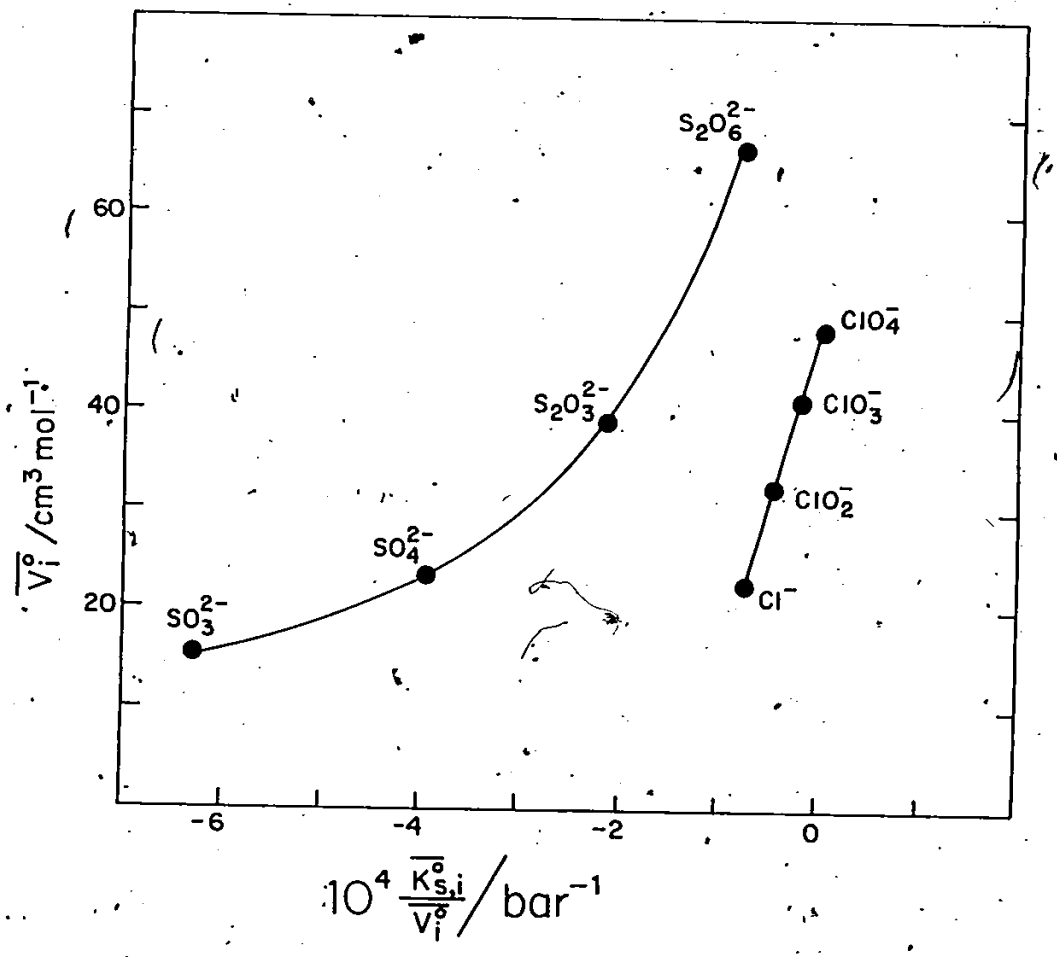

Figure 39 - A plot of ionic volumes $\overline{V}_i^o$ against integral specific compressibility $\overline{K}_{S,i}^o/\overline{V}_i^o$ for oxyanions.

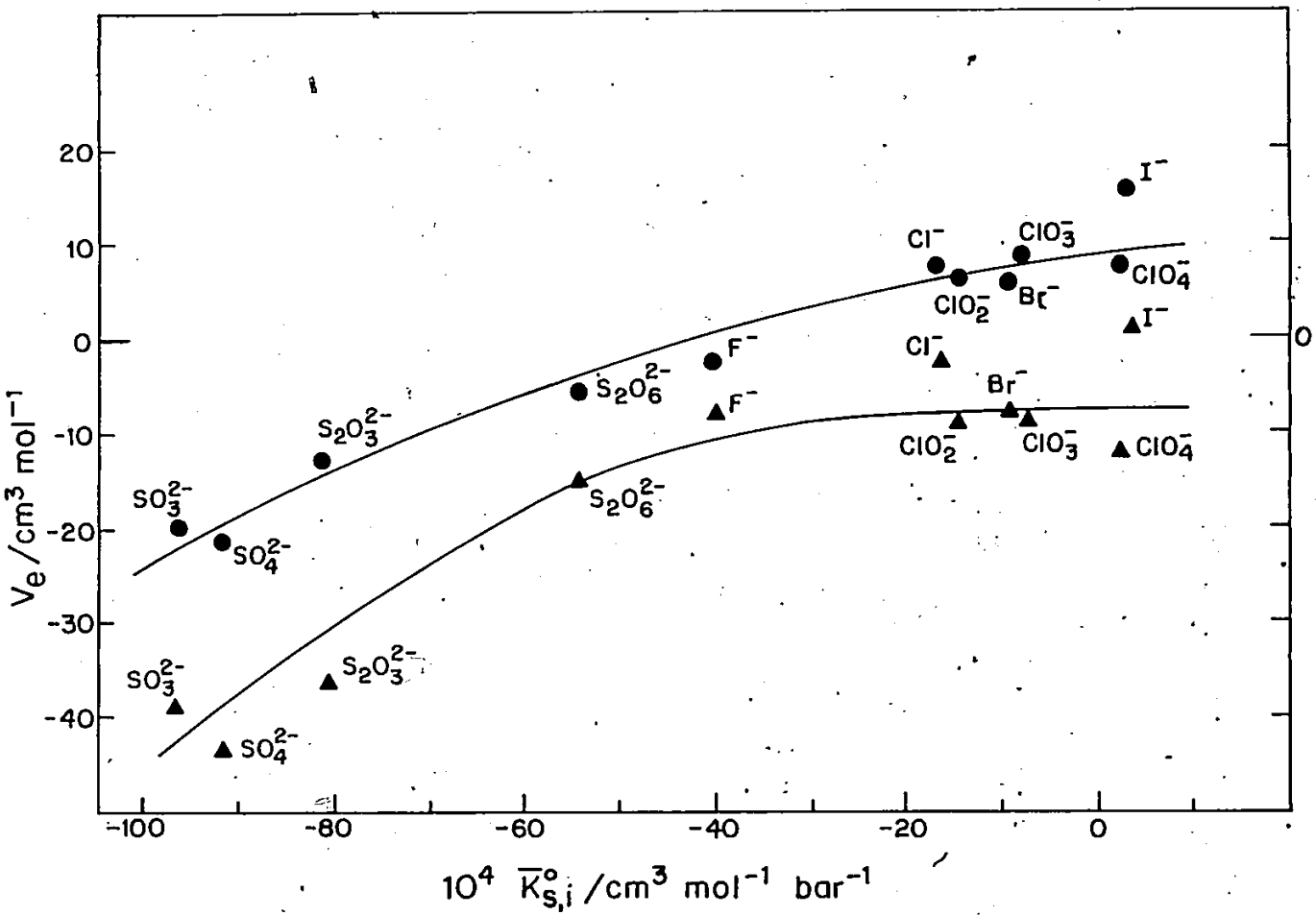

Figure 40 - Plots of V_e evaluated from method (d, i): ● and method (d, ii): ▲, against $\bar{K}^o_{S,i}$ for oxyanions.

the validity of method (d) for evaluation of V_i.

It is of interest to compare Figure 40 with a plot (Figure 41) that can be made of the electrostriction volume change, ΔV_e, against the specific compressibility, β (bar^{-1}), each being dependent on field according to Reference 14. Figure 41 has the correct form (cf. Figure 40) but a direct comparison with the experimentally based plot of Figure 40 is difficult because the latter curve depends on some number n of water molecules in the hydration shells that are changed in effective volume and in compressibility. For $S_2O_3^{2-}$ and SO_4^{2-}, for example, the observed V_e (Figure 40) corresponds, as we noted above, to 6 ~ 7 fully electrostricted moles of H_2O; for this range of V_e, the change of β in Figure 41 would be ca. $-42 \sim -44 \times 10^{-6}$ bar^{-1} relative to β for field-free water.

It should be possible to relate this change of β to an "experimental" specific compressibility change $\overline{K}^{o}_{S,i}/\overline{V}^{o}_{i}$ (Figure 39). For $S_2O_3^{2-}$ and SO_4^{2-}, the values are -2.2×10^{-4} and -3.9×10^{-4} bar^{-1}, respectively. For 6-fold inner-sphere coordination, the total change of compressibility expressed as $\overline{K}^{o}_{S,i}/\overline{V}^{o}_{i}$ would be $-6 \times 42 \times 10^{-6}$ and $-6 \times 44 \times 10^{-6}$ bar^{-1}, respectively; these results are in fair agreement with the respective "experimental" $\overline{K}^{o}_{S,i}/\overline{V}^{o}_{i}$ values of Figure 39. It is seen (cf. Reference 14) that the compressibility behaviour of the divalent ions corresponds

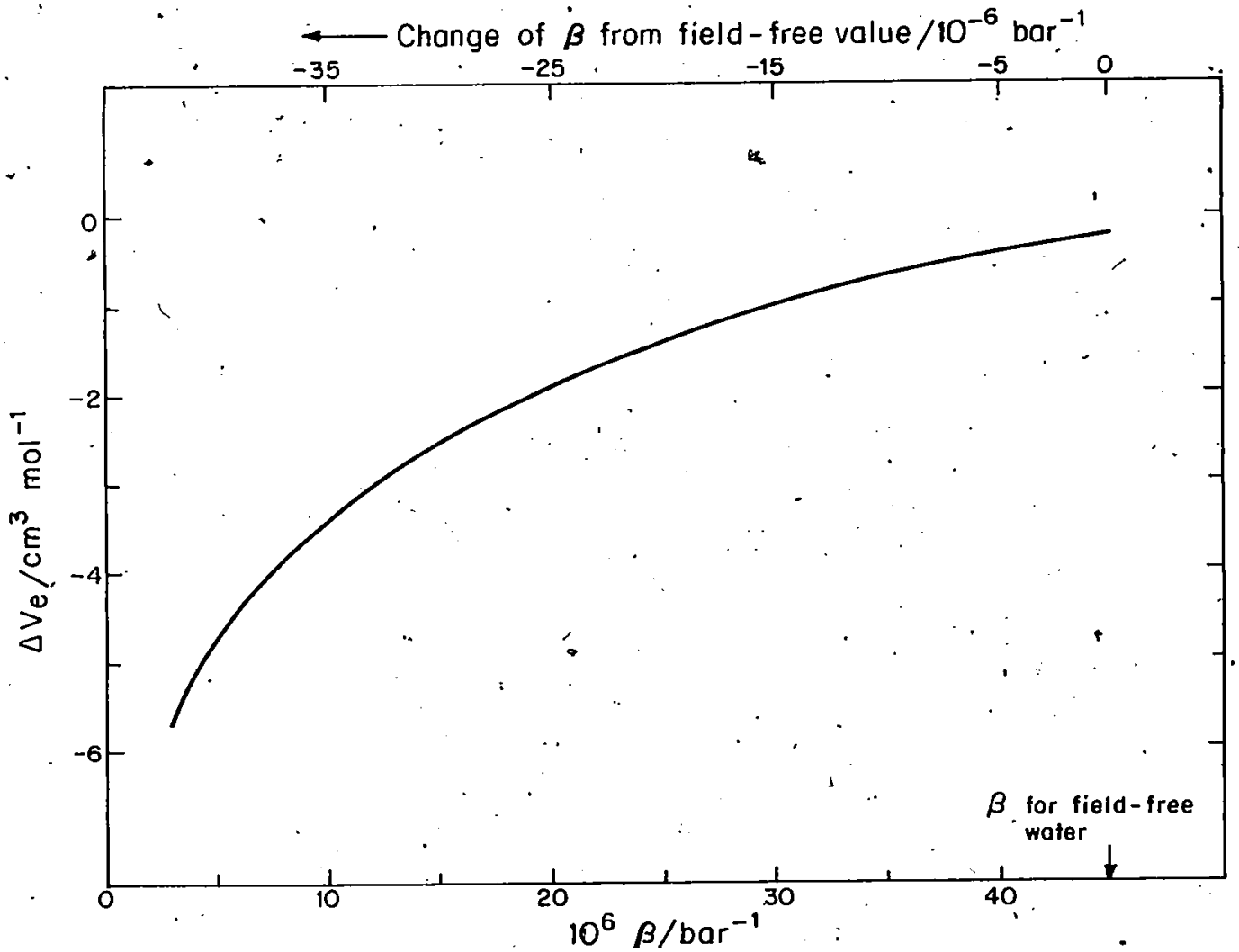

Figure 41 - The electrostriction volume change, ΔV_e per mole of water, against the specific compressibility β for water each as a function of field from the calculation of Desnoyers, Verrall and Conway[14].

to "high-field" conditions[14] in the general equation for calculation of electrostriction of water.

6. The Relation of $\bar{V}_i^o$ and $\bar{K}_{S,i}^o$ to Entropy Data for Oxyanions

Entropies of hydration and volumes of ions in solution are expected to be related through the electrostriction effect, as treated in various papers[13,19,20,94] (see also Section I.6). A corresponding relation to compressibilities would be expected. For the present series of oxyanions, data on entropies of hydration are not available, but a compilation of standard ionic entropies of solution, ΔS_s^o, by Cox and Parker[106] is useful. These data are referred to a state of the ions in their crystalline, e.g., Na^+, salts and the individual ionic contributions were evaluated on the assumption of equality of the entropies of tetraphenylarsonium and tetraphenylboride ions in solution. Figure 42 shows plots of both $\bar{V}_i^o$ and $\bar{K}_{S,i}^o$ against ΔS_s^o for the two oxyanion series together with the halide ion series. Good linear plots evidently arise, illustrating the common general relation between $\bar{V}_i^o$, $\bar{K}_{S,i}^o$ and ΔS_s^o. Plots against the entropy of hydration from the gas phase would have been preferable but, as argued by Cox and Parker[106], the entropies of the anions in comparable crystalline states provide a good reference basis for comparing entropies of ions in solution through ΔS_s^o.

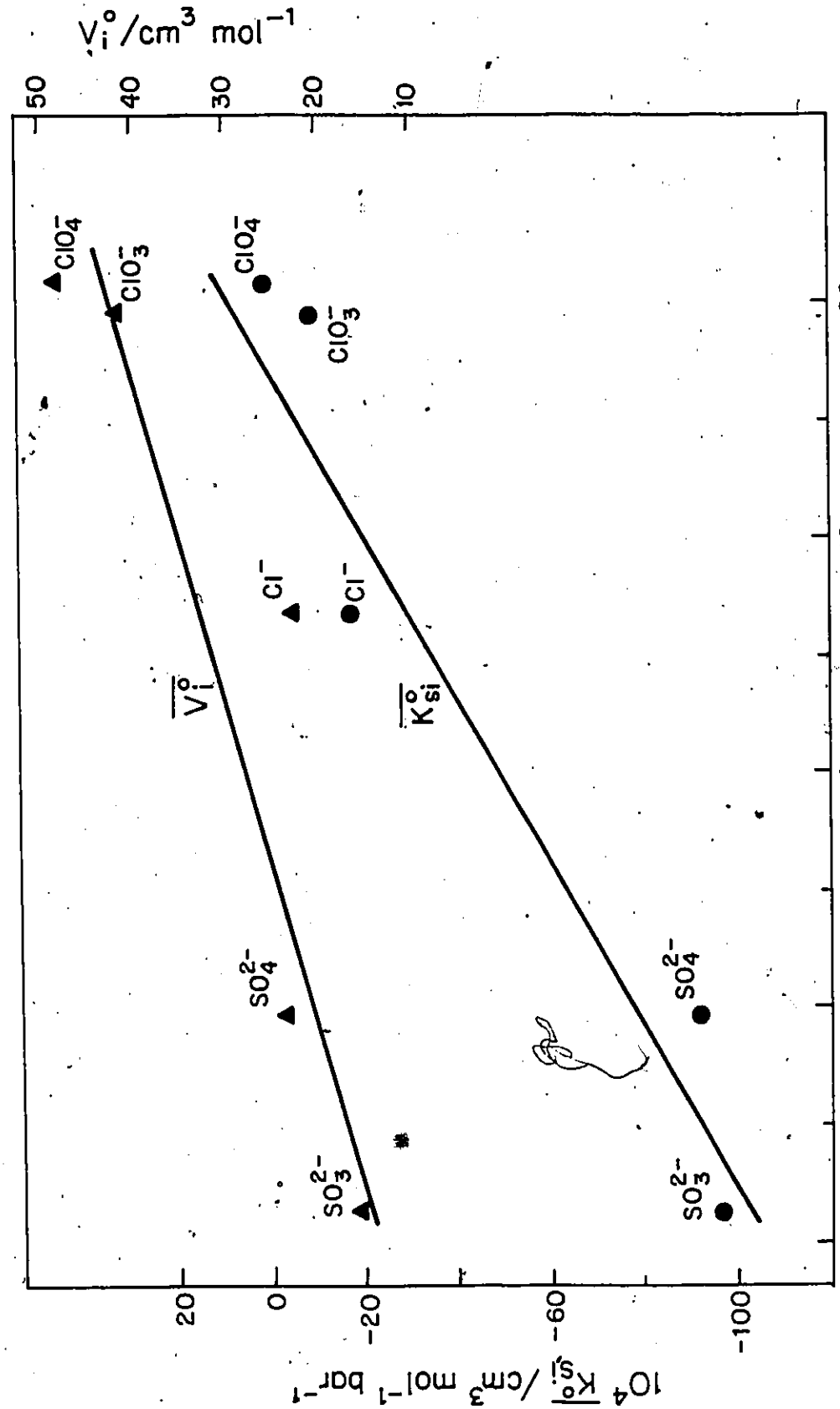

Figure 42 - Plots of $\overline{V}_i^\circ$ and $\overline{K}_{S,i}^\circ$ against entropy of solution, ΔS_s°, for oxyanions; ▲: $\overline{V}_i^\circ$ and ●: $\overline{K}_{S,i}^\circ$.

7. The Treatment of Concentration-Dependence of Apparent Molal Volume Data According to Redlich and Meyer's Equation and Masson's Equation

In Sections V.B.1 to V.B.6 the discussion was based on the infinite dilution values of apparent molal volumes and compressibilities for the oxyanion salts. However, concentration-dependences of these quantities are also important and give useful information on ion-ion and certain aspects of ion-solvent interactions. Therefore, in this and the next few sections, the concentration-dependence of apparent molal volumes and compressibilities for the salts of oxyanions will be treated.

Figures 4, 7 and 8 show the concentration-dependence of apparent molal volume of salts of oxyanions according to the Redlich-Meyer equation (Equation II.13). Comparative plots according to Masson's equation[111]

$$\phi_V = \phi_V^o + S_V^* \sqrt{c} \qquad V.9$$

are shown in Figure 43. The Redlich-Meyer plots were used to find ϕ_V^o values which were discussed in Sections V.B.1 to V.B.6.

Figures 4, 7 and 8 show clear examples of the distinct change of slope which the $\phi_V - S_V\sqrt{c}$ against c plots exhibit at some critical concentration dependent on the identity of the anion of the salt (Figures 4, 7 and 8) and its charge number (Figure 4 in relation to Figures 7 and 8).

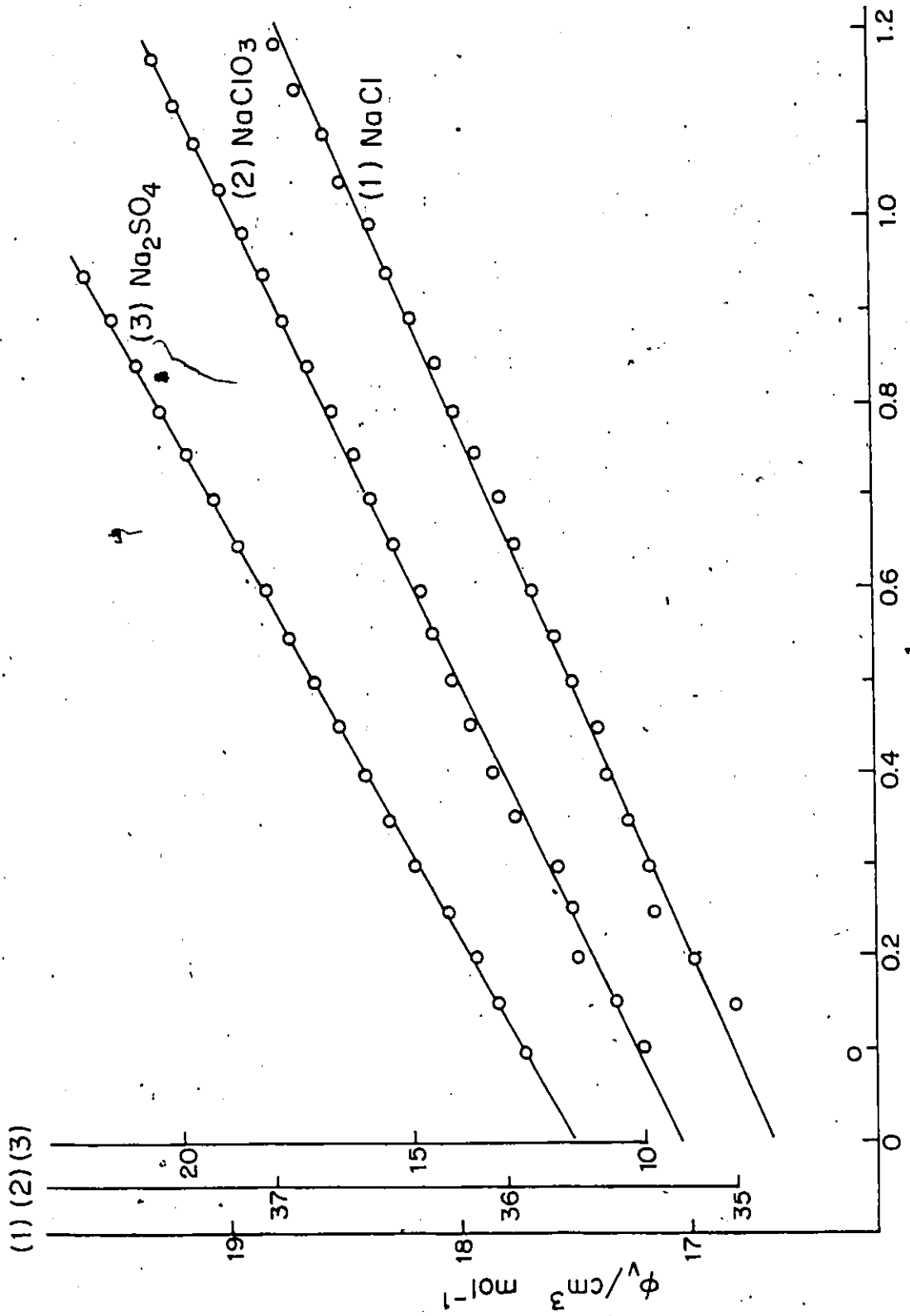

Figure 43 - Plots of ϕ_v against $c^{1/2}$ according to Masson's equation for (1) NaCl; (2) $NaClO_3$ and (3) Na_2SO_4.

The change of slope of these lines takes place over a concentration range as narrow as 0.1 mol L^{-1} for the 1:1 salts (Figure 4) and 0.05 mol L^{-1} for the 1:2 salts (Figures 7 and 8). This is surprisingly sharp.

The compressibility behaviour, calculated from ultrasonic velocity measurements together with the density data arising in the ϕ_v measurements, was plotted empirically as ϕ_{KS} vs $\sqrt{m}$ (Equation II.25) in Figures 5, 6, 9 and 10. A relation corresponding to Redlich and Meyer's equation (II.13) is not available for plotting the ϕ_{KS} data since the Debye-Hückel limiting slope, S_{KS}, for adiabatic compressibilities of salts in aqueous solution is not reliably known. For example, recently three different values for the slope S_{KS} were estimated[64] using three values for S_K, the corresponding isothermal compressibility slope[64,112,113].

The data on ϕ_v^o, b_v, ϕ_{KS}^o and S_{KS}^* for the sodium salts of oxyanions were given earlier (see Tables 1, 2, 3 and 4). S_v^* parameters in Masson's equation (V.9) for oxyanion salts are given below:

	$NaCl$	$NaClO_2$	$NaClO_3$	$NaClO_4$
$S_v^* \pm 0.08$	1.7_6	1.5_3	1.8_7	1.7_8
(cm^3 $mol^{-3/2}$ $L^{1/2}$)	Na_2SO_3	Na_2SO_4	$Na_2S_2O_3$	$Na_2S_2O_6$
	11.5_7	11.1_4	11.5_6	9.3_3

Millero[18] has referred to a possible relation between the difference of slopes, $S_v^*-S_v$, and b_v which is suggested by data for a variety of salts. The slope parameters obtained in the present work by plotting ϕ_v data as a function of concentration according to Equation II.13 or Equation V.9 are represented in Figure 44 as a relation between $S_v^*-S_v$ vs b_v which is evidently linear passing through the origin. The data for the Cl-oxyanions and the S-oxyanions actually fall into two different groups, each represented by lines passing through the origin. The $S_2O_6^{2-}$ ion datum falls on this graph as a point at the end of the family of data for the Cl- rather than the S-oxyanions. This is understandable since this ion can be understood as behaving as a dimeric SO_3^- ion with one charge at each end of a cylindrical molecule ion.

An attempt to rationalize the relation between $S_v^*-S_v$ and b_v could be made by subtracting Equation II.13 from V.9 which leads to

$$(S_v^* - S_v) = b_v \sqrt{c} \qquad \text{V.10}$$

However, this relation has no proportionality constant between the $S_v^*-S_v$ and b_v parameters such as is observed in Figure 44 since c is itself a concentration variable of indeterminate significance in Equation V.10. This suggests that relations between $S_v^*-S_v$ vs b_v, although they are apparently linear, have no physical significance.

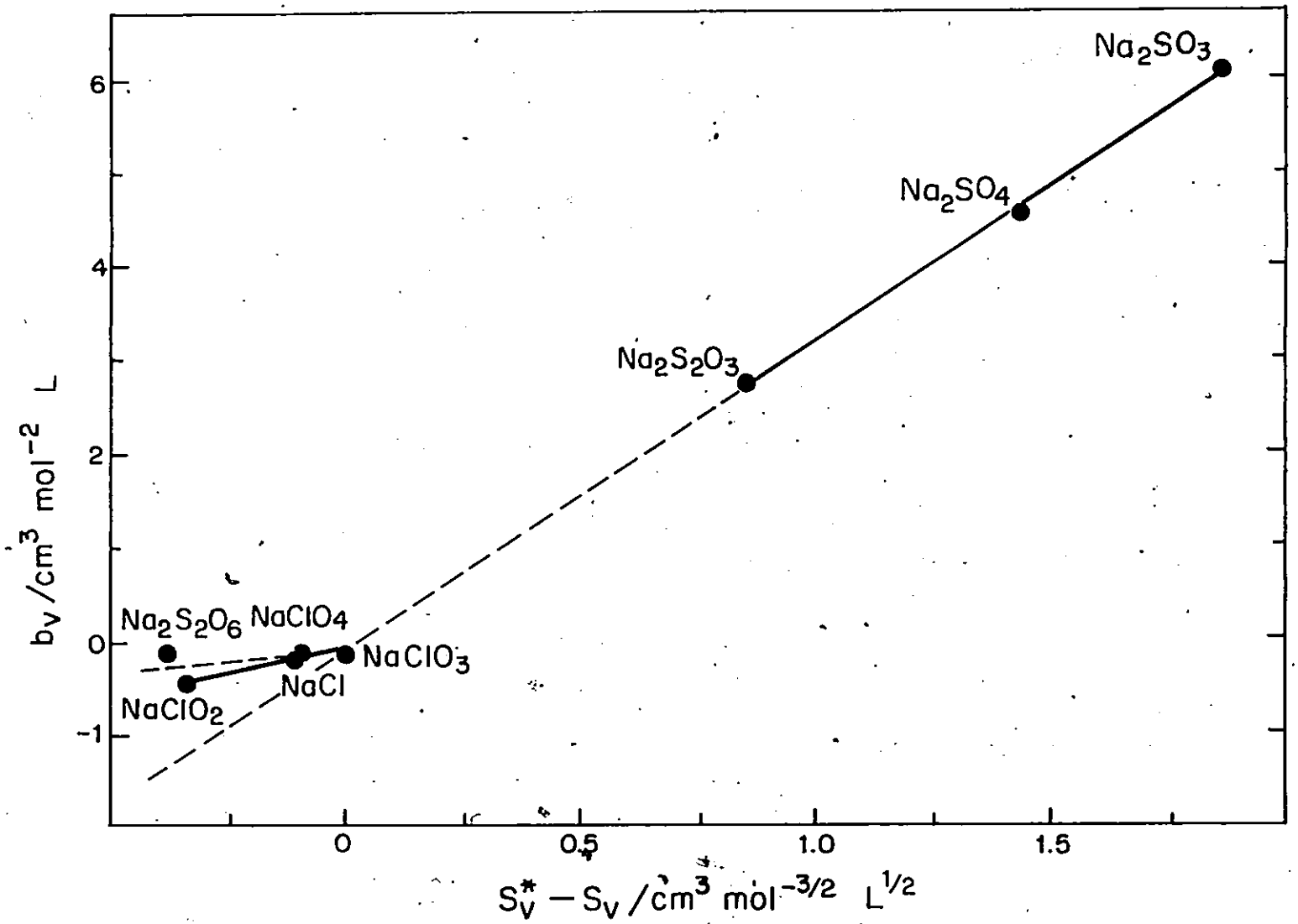

Figure 44 - A plot of b_v parameter in Redlich and Meyer's equation against $S_v^*-S_v$ in Masson's, and Redlich and Meyer's equations for the salts of Cl- and S-oxyanions.

The relation must arise fortuitously when Masson's equation fits the same data as Redlich and Meyer's equation. This is presumably because Masson's equation with slope S_V^* cannot be a correct representation of the $\sqrt{c}$ dependence of ϕ_V since, at sufficiently high dilutions, ϕ_V varies as $\sqrt{c}$ with the limiting law slope S_V, where $S_V \neq S_V^*$. This conclusion obviously follows when the full dependence of ϕ_V on c is considered in terms of the various pressure-dependent contributions in the Debye-Hückel equation for activity coefficients that determine[114,115] how ϕ_V varies with concentration. When all of these contributions, including the one leading to a linear term for variation of ϕ_V with c, are lumped empirically into a single slope term S_V^* for $\sqrt{c}$, as in Masson's equation, it can be seen qualitatively how S_V^* may be different than S_V and then how the difference $S_V^*-S_V$ may be related to how large is the b_V term in the Redlich-Meyer equation that allows for a proper Debye-Hückel term in $\sqrt{c}$. S_V^* in Masson's equation is, in effect, a "catch-all" slope factor for all concentration-dependent components in ϕ_V for $c > 0$.

This is illustrated by referring to Figure 43 where the same data as are plotted in Figures 4a, c and 8a according to the Redlich-Meyer procedure are shown as Masson plots. Figures 4, 7 and 8 show the clear inflections referred to earlier, in Sections IV.3a and IV.4a, while the

Masson plots completely obscure this effect, giving virtually straight-line graphs in the $\sqrt{c}$ plots.

Comparison of Equations II.13 and V.9 in another way can be made by rearranging Equation V.10 as $S_v^* = S_v + b_v\sqrt{c}$. It is seen that Masson slope S_v^* should, in fact, be a function of $\sqrt{c}$. Unless ϕ_v data are available over a wide range of c or $\sqrt{c}$, this effect is evidently obscured since the surprising feature of most Masson plots is their apparent linearity in $\sqrt{c}$.

The general conclusion to be reached is that Masson plots are inconsistent with the Debye-Hückel dependence of ϕ_v on concentration or with Redlich and Meyer's approximate representation of that dependence. The use of Masson plots is not to be recommended as (a) they evidently obscure interesting features of the dependence of ϕ_v on concentration (cf. Figures 4, 7 and 8) and (b) they are likely to lead to errors in extrapolation to c=0 when ϕ_v^o is to be evaluated[18].

8. Significance of Inflections in the Redlich-Meyer Plots

The inflections in Figures 4, 7 and 8 are sufficiently striking to justify special consideration of their significance. Reference to data for activity coefficients ($\gamma_\pm$) of 1:1 and 1:2 electrolytes shows that the first deviations from limiting law behaviour for $-\ln \gamma_\pm$ in $\sqrt{c}$ commence already below 0.01 mol L^{-1}, as is well known. Similarly,

in terms involving 1 + κa (the term 1+κa is encountered in the derivation of Debye-Hückel law for finite-sized ions[114]. 1/κ is an approximate measure of the thickness of the ionic atmosphere and has the units of length. 'a' is the closest approach parameter), κa can be neglected in comparison with unity only at concentrations $\lesssim 10^{-3}$ or $10^{-2.5}$ mol L^{-1} for 1:2 or 1:1 electrolytes, respectively. Both these limits are well below the concentrations at which the inflections in Figures 4, 7 and 8 appear, viz. c ≈ 0.5 ~ 0.7 for 1:1 and c ≈ 0.12 mol L^{-1} for the 1:2 salts. Hence it seems unlikely that the observed inflections can be accounted for by such factors. Moreover, it is difficult to see how such effects could set in as suddenly, at some apparently critical concentration, as the experimental data indicate.

From the above inflection concentrations, it therefore seems logical to suggest that the remarkably distinct changes of slope correspond to a rather sudden appearance in solution of pairs of ions, probably cation anion pairs, in a situation in which their Gurney hydration co-spheres are just beginning to overlap and thus cause an extra contribution in the excess volume function through the GUR term[8h,107,108].

Similar inflections have been observed in earlier work from this laboratory[24] on ϕ_v for organic ions and in work

of Vaslow[75,85] on simple salts such as alkali chlorides. He concluded that the inflections indicated some kind of change of property of the solution which he called "physical transition" of the solutions. It was suggested[75] that a "cooperative interaction among the co-spheres of a moderate number of ions" can be responsible for these abrupt changes.

In order to test the reality of the co-sphere overlap effect as an explanation of the inflections, it is useful to calculate the approximate concentrations at which hydration co-spheres just, on the average, overlap, for assumed co-sphere diameters related to the intrinsic radii of the ions plus one or two shells of hydration water molecules.

If the radius of the co-spheres of the anion and the cation are assumed to be equal (in most cases, the cationic co-sphere radius will actually be greater than that of the anion) and are designated by $r_{c\pm}$, then the diameter or the contact distance will be $2r_{c\pm}$. The number of ions per linear cm is then $1/2r_{c\pm}$. There are $1000/(2r_{c\pm})^3$ ions per dm^3. Overlap of co-spheres in an hexagonal, rather than cubic geometry, introduces the factor $(2/\sqrt{3})^3$ into the above calculation.

For NaCl, for example, $2r_{c\pm}$ is the sum of radii of Na^+ and Cl^- and of the diameter of an H_2O molecule for each

hydration co-sphere, i.e., $(0.95 + 1.81 + 2 \times 2.76) \times 10^{-8}$ $= 8.28 \times 10^{-8}$ cm when primary hydration shells are just in contact or 2.76×10^{-8} cm more for each additional shared spherical co-sphere water shell.

When the contact distance is 12×10^{-8} cm, which is approximately the case for NaCl when an extra spherical co-sphere shell is shared by the two ions beyond the primary hydration shell, there will be $1000/(12 \times 10^{-8})^3$ ions per dm^3 or 0.90 moles per dm^3. This corresponds to a concentration of 0.45 M for a 1:1 salt or 0.3 M for a 1:2 salt.

Master curves can be calculated relating the critical contact distance $2r_{c\pm}$ to the critical co-sphere overlap concentration. Figure 45 shows such curves for 1:1 and 1:2 or 2:1 electrolytes. It should be noted that owing to attractive interaction between positive and negative ions, the overlap effects may start to be significant at concentrations lower than the above critical values or at contact distances correspondingly shorter than 12×10^{-8} cm. This would introduce a cation-anion specificity into the critical co-sphere overlap effect of the type that is observed in the changes of slope of the ϕ_v lines. Anion-anion and cation-cation co-sphere overlaps are weighted with low probabilities owing to an unfavourable Boltzmann electrostatic factor for such pairwise interaction between like-charged ions (cf. the

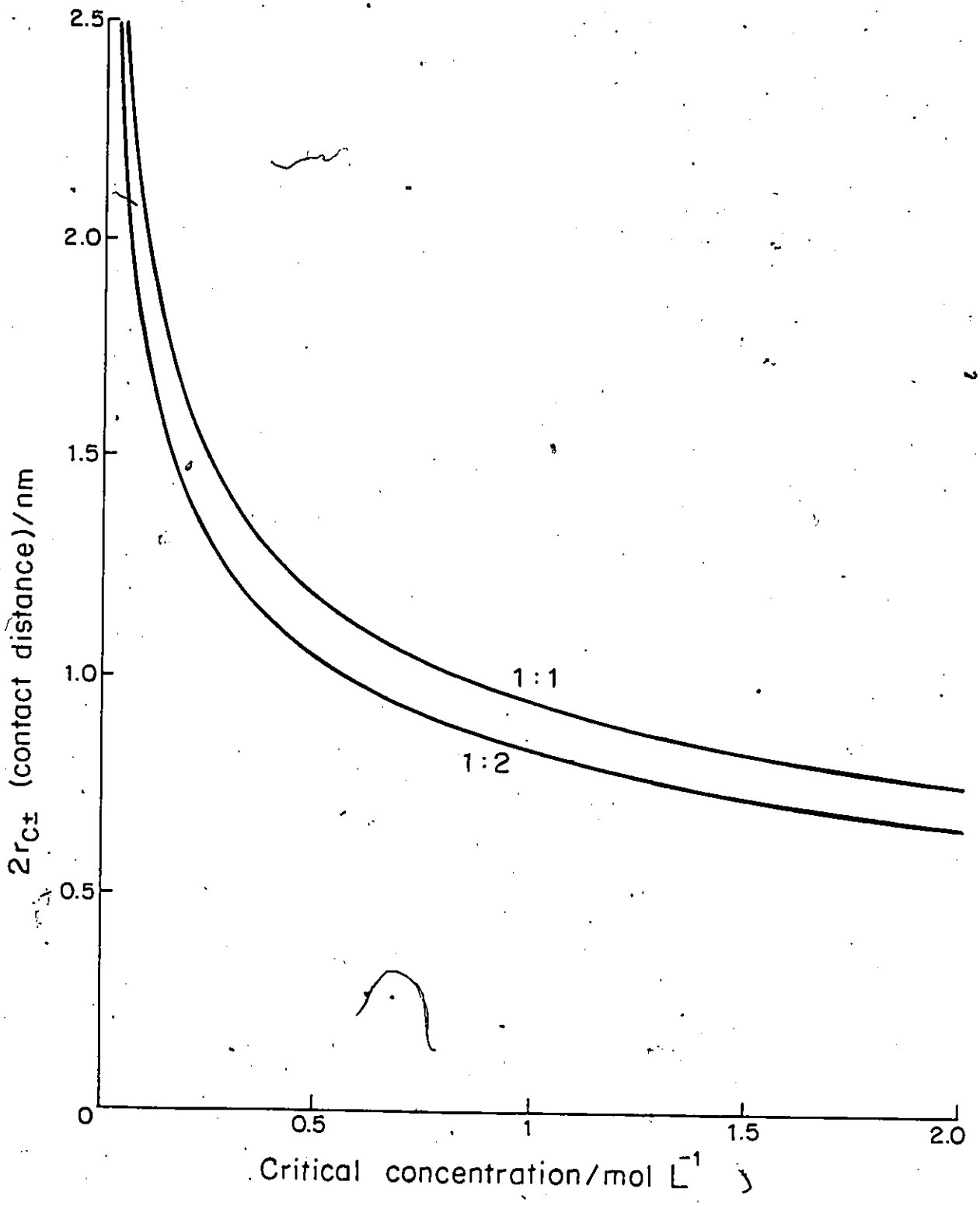

Figure 45 - Master curves relating the critical contact distance $2r_{c\pm}$ to the critical co-sphere overlap concentration.

g_{++} and g_{--} distribution functions treated by Friedman et al[108]).

On the basis of the model calculations given above, it is to be expected that the critical co-sphere overlap concentration will be lower for 1:2 salts than for 1:1 salts owing to (a) the greater hydration co-sphere radii of divalent anions and (b) the greater Boltzmann weighting of +, 2- interactions. Figures 7a, b and 8a show that this is indeed the case.

If co-sphere overlap causes return of some structure-broken water to its normal state[108], the compressibility will tend to increase. Similarly, the volume will tend to increase if water is returned to its normal state due to the co-sphere overlap effect at appreciable ionic concentrations.

Figures 4a-d, 5 and 6b confirm the direction of these changes for 1:1 type salts but for 1:2 type salts (Figures 7a-b and 8a) the opposite direction is observed. The complexity of the situation with the 1:2 salts is increased when it is noted that the direction of change of slope in compressibility is opposite to that in volume which is difficult to explain. Also the change in slope of the lines representing ϕ_{KS} as a function of $\sqrt{c}$ occurs at somewhat lower concentrations than those for the ϕ_v plots; this may indicate a greater sensitivity of the ϕ_{KS} quantity than the ϕ_v to structural changes in water in the vicinity of neighbouring cations and anions.

9. Relations of b_v and S^*_{KS} to the Infinite Dilution Volumes, ϕ^o_v

The possible origin of the inflections in Figures 4, 7 and 8 discussed above suggests that b_v may be related to ϕ^o_v. Such relations are shown in Figure 46a for the 1:1 (with Cl^-) and 1:2 oxyanion salts. For the divalent anion salts, the dependence of b_v on ϕ^o_v is much steeper than for the monovalent salts, a result that is expected on account of the larger volumes of solvent that are found (see Sections V.3 and 4) to be influenced by divalent than monovalent ions. The datum for $S_2O_6^{2-}$ falls as a common point on the lines for the Cl- and S- oxyanions presumably because it behaves, as mentioned earlier, as a dimeric monovalent ion, with charges at each end, rather than a single-centered, doubly charged molecule.

In Figure 46b, the empirical slope, S^*_{KS} for the compressibility data, ϕ_{KS}, is shown related to ϕ^o_v; again a more sensitive dependence on ϕ^o_v is seen for the di- in comparison with the monovalent ions.

While no attempt will be made here to interpret the S^*_{KS} parameter, the following points in relation to Figure 46b are useful to note: (i) the S^*_{KS} values are all positive; (ii) they are 5 to 20 times larger for the 1:2 type than for the 1:1 type salts, so that they contain other concentration-dependence factors beside the limiting law one;

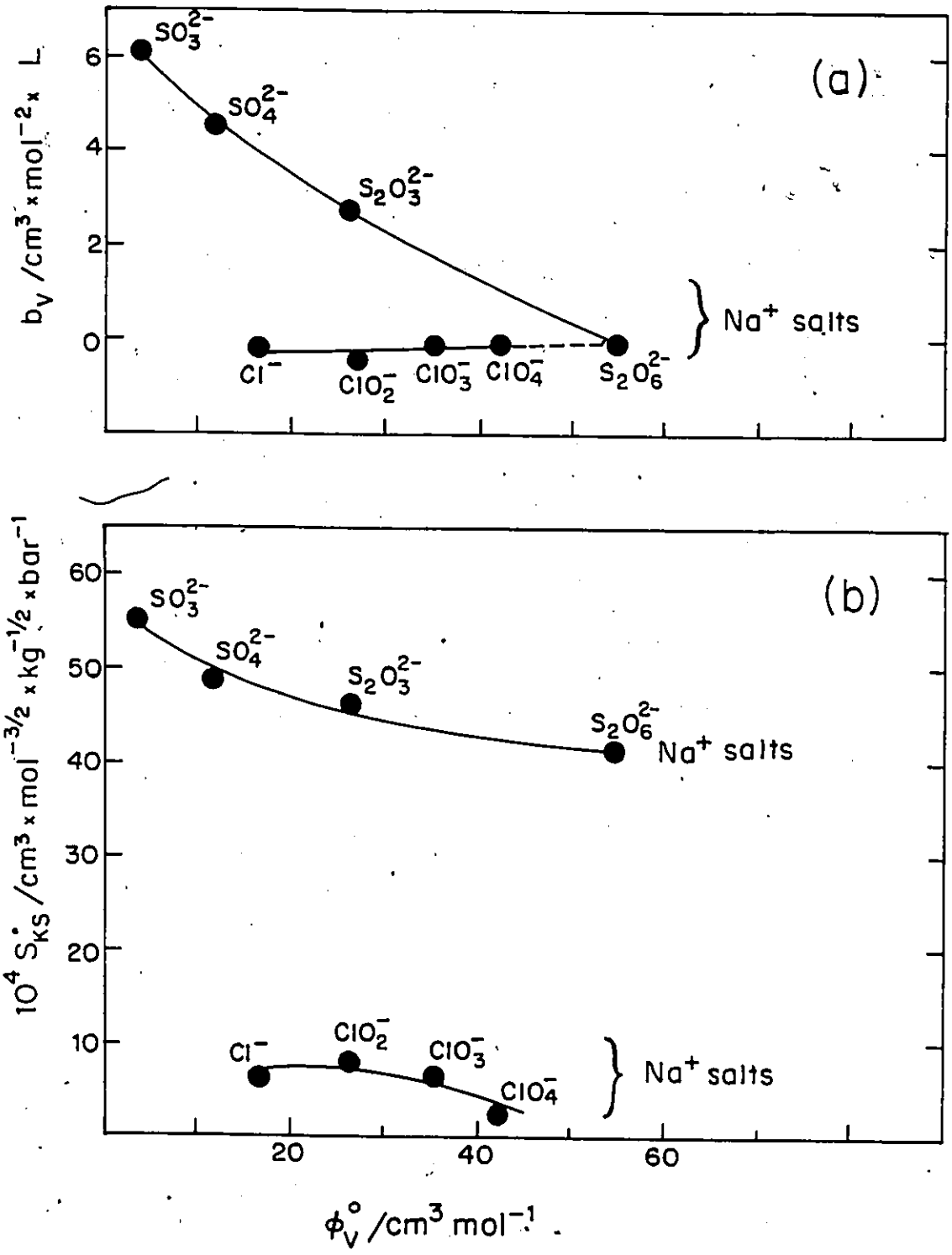

Figure 46 - Plots of (a) b_v and (b) S^*_{KS} against ϕ°_v for the sodium salts of oxyanions.

(iii) they decrease with increasing anion size for both 1:1 and 1:2 type salts, with the exception of NaCl; and (iv) the trend of the data for the salts of the various oxyanions (Figure 46b) in the plot of S^*_{KS} vs ϕ^o_v is similar to that in the plot of b_v vs ϕ^o_v (Figure 46a).

C. Organic Bases and their Ions

1. Structural Effects in the Volume and Compressibility Behaviour of Organic Bases in Aqueous Solution

Although the papers of Hepler et al.[57] and Cabani et al.[22,58] (published during the course of the present work) on volumetric behaviour of organic bases include some of the molecules also studied in the work being reported here, the compounds selected in a systematic way for this work cover a wider range of structures. This enables the following factors which influence hydration and ionization behaviour to be investigated for several series of structurally related organic bases: (i) the number of cyclic ring systems; (ii) replacement of -NH- by -O- in a ring; (iii) replacement of $-CH_2-$ by -O- in a ring; (iv) the number of 'N' centers in a ring (-CH-, N or $-CH_2-$, -NH- replacement in a ring); (v) aromaticity in a ring structure; (vi) position of 'N's in the ring; and (vii) the number of $-CH_2-$ groups in a ring. Additionally, complementary studies by means of adiabatic compressibility measurements were carried out in the present work.

In the light of the results obtained from complementary volume and compressibility measurements, the effects that the structural factors listed above have on the hydration behaviour of organic bases will now be discussed.

(i) The Number of Cyclic Ring Systems in the Molecule

A comparison between the $\overline{V}^{o}$ values in Table 6 and the $\overline{K}_{S}^{o}$ values in Table 7 for triethylenediamine, piperazine, ethylenediamine, piperidine and quinuclidine provides information on the effects of the number of cyclic ring systems on the hydration of these bases. For convenience, the changes δ in $\overline{V}^{o}$ and $\overline{K}_{S}^{o}$ values with increase in ring system complexity by bridging are given below:

Structure Change	$\delta\overline{V}^{o}/cm^{3}\ mol^{-1}$	$10^{4}\delta\overline{K}_{S}^{o}/cm^{3}\ mol^{-1}\ bar^{-1}$
(1) $H_2NCH_2CH_2NH_2$ ⟶ 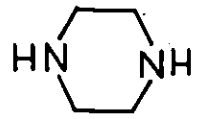	20.0_7	-1.2
(2) 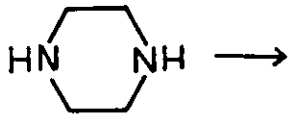 ⟶ 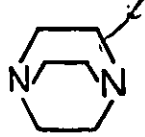	23.1_4	0.5
(3) 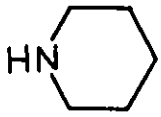 ⟶ 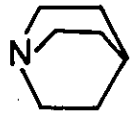	20.9_0	7.7

The change in structural grouping from ethylenediamine to piperazine and from piperazine to triethylenediamine is the same, i.e., there is an addition of a $-CH_2-CH_2-$ bridge between the two 'N's and removal of -H's, one from each N. The approximately 3 $cm^{3}\ mol^{-1}$ of extra volume change in structure change (2) compared to (1) above is probably due to the void space produced by the introduction of the third

$-CH_2-CH_2-$ group between the N's, inaccessible to water. Similarly, due to the introduction of the $-CH_2-CH_2-$ bridge, the $\overline{V}^o$ increases by 20.9$_0$ cm^3 mol^{-1} from piperidine to quinuclidine [(3) above] which is again larger by about 1 cm^3 mol^{-1} than the increase in $\overline{V}^o$ for (1)

The two other factors which might be involved in determining these changes in $\overline{V}^o$ are: (a) the increasing hydrophobicity introduced by the addition of $-CH_2-CH_2-$ groups, (the hydration around the hydrophobic groups is called "hydrophobic hydration" and it usually results in increasing the extent of local structure of water) and (b) changes in the character of H-bonding to water at the N centers. It is expected that both factors give positive contributions to $\delta\overline{V}^o$.

Recently two papers[116,117] have appeared in which proposals have been made of schemes of "group contributions" for volumes and heat capacities of organic molecules in aqueous and in methanolic solutions. The results discussed above show that consideration of only the group contributions to $\overline{V}^o$ of organic molecules is unlikely to be correct. Structural relationships also play an important role in determining the volumes of organic molecules in aqueous solutions. This point was recognized by Cabani et al.[116]. After an analysis of thermodynamic data for non-ionic organic molecules in aqueous solution, they arrived at the following

conclusion. Water reacts (physically) in a very specific way with respect to organic solutes; as a consequence, the thermodynamic properties in water of molecules showing many different structural features differ appreciably from those calculated as the sum of the contributions of each of the features separately.

The compressibility changes for the above structure changes, (1), (2) and (3), are more difficult to explain compared to the volume changes because the factors effecting the volumes do not always operate in the same direction for compressibilities. The following points should be noted in this connection: (a) addition of a group to the structure increases the intrinsic volume but may not necessarily change the intrinsic compressibility since the latter is a differential quantity, normalized with respect to volume, viz -dV/VdP; (b) hydrophobic hydration effects tend to increase the volume but decrease the compressibility due to more rigid water structure around the hydrophobic group. As was mentioned in Section V.A.2, this effect was first discovered by Verrall and Conway[21] who found a <u>decrease</u> in ϕ_{KS}^{o} values in the series tetramethyl-, tetraethyl-, tetrapropyl-, and tetrabutyl-ammonium ions. Water itself probably provides a simpler example for the changes of volume and compressibility in opposite directions: as liquid water at 273 K becomes frozen to ice its volume

increases but at the same time it becomes less compressible*; (c) H-bonding increases the volume but decreases the compressibility, depending on the strength of the bond and structures resulting from the H-bonding.

The negative $\delta\overline{K}_S^o$ for structure change (1) is, as expected, due to increase in hydrophobicity in piperazine compared to ethylenediamine. Also piperazine has a more rigid structure than ethylenediamine. The positive $\delta\overline{K}_S^o$ values for (2) and (3) are rather unexpected. The only positive contribution to $\delta\overline{K}_S^o$ may come from a decrease in H-bond strength upon hydration of these molecules. Thus the H-bond, $\rangle O \cdots H\text{-}N\langle$ is expected to be stronger than the H-bond, $\rangle O - H \cdots N\langle$, due to the larger electronegativity of O than N.

(ii) The Replacement of -O- by -NH- and -O- by $-CH_2-$ in the Ring

The effect of replacement of -O- by -NH- and -O- by $-CH_2-$ can be seen in the change of $\overline{V}^o$ and $\overline{K}_S^o$ for the structure changes given in the following table.

* Data illustrating this effect were shown in Table 12, p. 150.

Structure Change	$\delta\bar{V}^o$/cm^{3}mol^{-1}	$10^4\delta\bar{K}_S^o$/cm^{3}mol^{-1}bar^{-1}
(4) 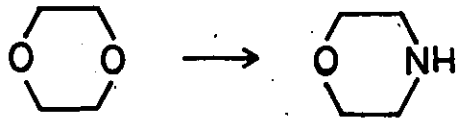	2.2_9	-2.0
(5) 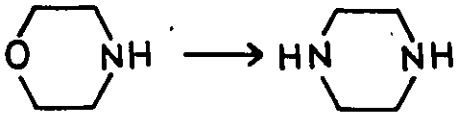	0.4_3	-3.4
(6) 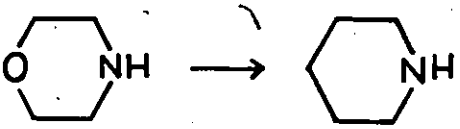	8.5_6	-4.2

It seems likely that the positive $\delta\bar{V}^o$ for the changes (4) and (5) above are due, apart from the volume contribution of the H atom, to stronger H-bonding to water at the >O center than at >NH. This is consistent with the electronegativity difference. On the other hand for the structure change -O- being replaced by $-CH_2-$, a much larger positive $\delta\bar{V}^o$ is observed corresponding to an increase in hydrophobic character which also tends to make the water solvent locally less compressible, corresponding to the negative $\delta\bar{K}_S^o$ value for structure change (6) above. The negative $\delta\bar{K}_S^o$ values for (4) and (5) are, however, again rather unexpected.

Conformational factors may also play an important role in determining $\bar{V}^o$ and $\bar{K}^o$ of the above 1,4 bifunctional

compounds; this aspect will be discussed separately in Section V.C.2.

(iii) The Replacement of -N- by -CH- or -NH- by $-CH_2-$ in the Ring

The magnitude of change in $\overline{V}^o$ by -N-, -CH- or by -NH-, $-CH_2-$ replacement is expected to be comparable to that by -O-, $-CH_2-$ replacement discussed in (ii) since, in both cases, a hydrophilic group is replaced by a hydrophobic one. The $\delta\overline{V}^o$ and $\delta\overline{K}_S^o$ values are listed below for some examples of -N-, -CH- and -NH-, CH_2 replacements.

Structure Change		$\delta\overline{V}^o/cm^3mol^{-1}$	$10^4\delta\overline{K}_S^o/cm^3mol^{-1}bar^{-1}$
(7)	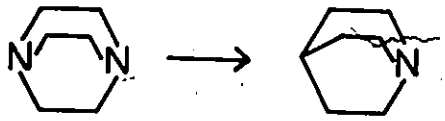	5.8_9	6.4
(8)	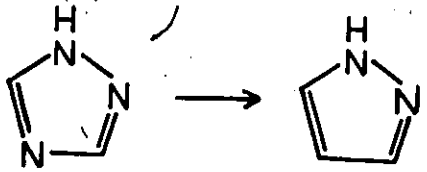	7.3_9	-0.9
(9)	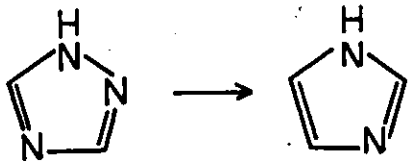	6.1_5	-1.3
(10)	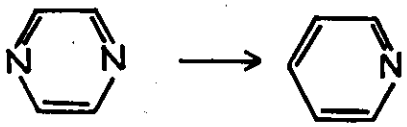	6.7_7	-4.7
(11)	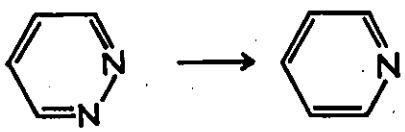	7.5_6	0.2

The positive $\delta\overline{V}^{o}$ and negative $\delta\overline{K}_{S}^{o}$ values for the above five structure changes [except $\delta\overline{K}_{S}^{o}$ for (7) and (11)] are probably due to the fact that hydrophobic groups in general tend to increase the volume but decrease the compressibility[21].

(iv) Aromaticity in the Ring Structure

The effect of aromaticity on hydration behaviour of organic compounds can be examined by comparing the $\overline{V}^{o}$ and $\overline{K}_{S}^{o}$ values for piperazine and pyrazine, and piperidine and pyridine, as shown in the following table.

Structure Change		$\delta\overline{V}^{o}/cm^{3}mol^{-1}$	$10^{4}\delta\overline{K}_{S}^{o}/cm^{3}mol^{-1}bar^{-1}$
(12)	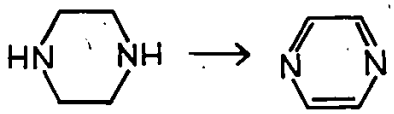	-12.0_{4}	6.5
(13)	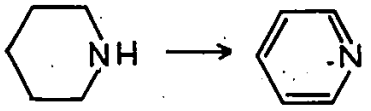	-13.4_{0}	2.6

$\overline{V}^{o}$ values decrease by 12.0_{4} and 13.4_{0} cm^{3} mol^{-1} from piperazine to pyrazine (12) and from piperidine to pyridine (13), respectively. Besides the removal of 6 H atoms in going from non-aromatic to corresponding aromatic heterocyclics, the following factors are also expected to be involved in determining the volume changes: (a) the aromatic molecule is both more planar and more rigid than the non-aromatic one; (b) the bonds between the atoms in the ring are shorter in the aromatic molecule than in the corresponding non-aromatic molecule;

(c) hydrophobic hydration is probably more important in the non-aromatic molecule than in the corresponding aromatic molecule; (d) H-bonding tends to occur more strongly at a non-aromatic N center than at an aromatic one. At a non-aromatic molecule, the H-bond has the form 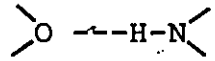 , whereas at an aromatic molecule it has the form 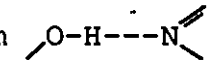 . Thus the H-bond is formed between H and O in the non-aromatic and between H and N in the aromatic molecule. Since O is more electronegative than N, the H-bond with water in the case of the non-aromatic molecule is expected to be stronger; and (e) aromatic molecules are known to be involved in H-bonding with water through the π-orbitals.

Factors (a), (b) and (c) give negative contributions to $\delta\overline{V}^{o}$ whereas factors (d) and (e) probably give small positive contributions. In the case of δK_S^o, factors (a) and (b) are not expected to affect the compressibility in any considerable way but (c) and (d) [especially (c)] make positive contributions as indicated by observation of positive $\delta\overline{K}_S^o$ values in the structure changes (12) and (13) shown above. Factor (e) might give rise to a small negative contribution to $\delta\overline{K}_S^o$.

(v) The Position of 'N's in the Heterocyclic Ring Systems

Pyrazine and pyridazine are structural isomers (see Table 5, page 108) having the same chemical formula: $C_4H_4N_2$;

'N's are in the 1,4 relation in pyrazine while they are in the 1,2 relation in pyridazine. Similarly, both imidazole and pyrazole have the same chemical formula: $C_3H_4N_2$; the 'N's are in the 1,2 relation in pyrazole while they are in the 1,3 relation in imidazole.

The differences in volume and compressibility behaviour of these isomers, as seen in the following table,

Structure Change	$\delta\bar{V}^o$/cm^{3}mol^{-1}	$10^4\delta\bar{K}_S^o$/cm^{3}mol^{-1}bar^{-1}
(14) 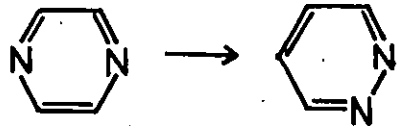	-0.7_9	-4.9
(15) 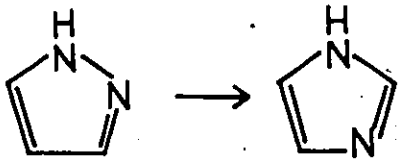	-1.2_4	-0.4

δ(dipole moment)/D
3.95
2.27

demonstrate very clearly the importance of structural effects in hydration of organic molecules.

If the concept of "group contributions"[116,117] to $\bar{V}^o$ is a correct viewpoint, then there would not be any difference in $\bar{V}^o$'s of the above isomers. However, the above figures for $\delta\bar{V}^o$ are 15 to 25 times larger than the limits of uncertainties in the $\bar{V}^o$ values themselves.

The negative $\delta\overline{V}^{o}$ and $\delta\overline{K}_{S}^{o}$ values for the above changes [(14) and (15)] can be explained by the differences in dipole moments of the isomers as shown in the last column of the above table. While pyrazine has no net dipole moment, pyridazine has a finite dipole moment[118] of 3.95 D. On the other hand, the dipole moments for pyrazole and imidazole are 1.57 and 3.84 D, respectively[119]. Normally it is found that the larger is the dipole moment of a solute the stronger is the interaction of the solute molecule with water.

When the interactions between the solute and water are stronger, then both the volume and the compressibility tend to be smaller. This behaviour is confirmed by the $\overline{V}^{o}$ and $\overline{K}_{S}^{o}$ data obtained for pyrazine, pyridazine, pyrazole and imidazole in the present work as seen in the above table[structure changes (14) and (15)].

The following structural differences between the isomers are also expected to have small effects in the observed behaviour: (a) the bond distances are not the same in the two isomers; and (b) the isomers have different resonance forms, e.g., pyrazine has two equivalent Kekulé structures whereas, in pyridazine, the two Kekulé structures are not equivalent: the canonical form 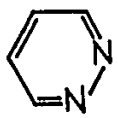 is preferred[118] where the N-N distance is larger than in the form 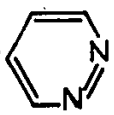 .

(vi) The Number of $-CH_2-$ Groups in the Ring

There is only one example that we can examine here which illustrates the effect of the number of $-CH_2-$ groups on the hydration behaviour of cyclic organic molecules:

Structure Change	$\delta\overline{V}^o/cm^3mol^{-1}$	$10^4\delta\overline{K}_S^o/cm^3mol^{-1}bar^{-1}$
(16) 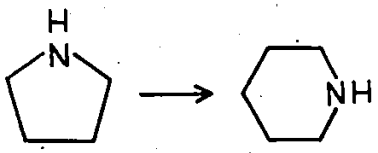	12.9_2	-3.6

From pyrrolidine to piperidine (16) the ring size is increased by one $-CH_2-$ group and the observed $\overline{V}^o$ value is increased by 12.9_2 cm^3 mol^{-1}, as seen above. This increase in $\overline{V}^o$ is not only due to the intrinsic volume of the $-CH_2-$ group but also to the increased hydrophobicity of the system. This last effect also explains the negative $\delta\overline{K}_S^o$ value for the structure change (16). The $\overline{V}^o$ value of 12.9_2 cm^3 mol^{-1} for a $-CH_2-$ group in a heterocyclic amine ring is much lower than the $\overline{V}^o$ value of 16.0 cm^3 mol^{-1}* for a $-CH_2-$ group in a straight chain amine and slightly lower (by about 1 cm^3 mol^{-1}) than the value of 14.09 cm^3 mol^{-1} found by Cabani et al.[116] for the $-CH_2-$ group contribution in a cyclic structure.

* This figure is based on a calculation according to the equation; $\{\overline{V}^o[(n\text{-}C_3H_7)_2NH_2Cl] - \overline{V}^o[(C_2H_5)_2NH_2Cl]\}/2$. The data for $\overline{V}^o$ values are taken from the work of Laliberté and Conway[23].

2. Conformational Effects

As was mentioned in Section I.7, it is probable, if not almost certain, that conformational effects will be important in hydration behaviour of flexible organic molecules. A well-known[8d] example of this effect can be seen by considering chair and boat forms of six-membered saturated cyclic ring systems. The molecules of this type studied in the present work are piperazine, 1,4 dioxane and morpholine. Interactions of these molecules and their ions with water are expected to be somewhat different when they are in the boat or the chair forms.

In order to investigate these effects, volume and compressibility measurements were made on 1,4 dioxane both in water and in 1M $MgCl_2$. It is to be expected that the boat form would tend to be preferred in the ionic environment due to the interactions of the lone pairs of electrons on 'O's with the positive charges on Mg^{2+} (cf. complexation of monatomic cations by crown-ether structures[49]).

As can be seen from Table 6, ϕ_v^o decreases by 1.0_7 cm^3 mol^{-1} and from Table 7, ϕ_{KS}^o increases by 5.9×10^{-4} cm^3 mol^{-1} bar^{-1} in going from the pure water medium to 1M aq. $MgCl_2$. Normally, when the volume decreases, the compressibility is also expected to decrease if specific structural (non-electrostatic) effects are not considered. From this

point of view, ϕ_V^o and ϕ_{KS}^o values do not seem to be conclusive at first glance. Therefore these particular conformational effects were further investigated by taking the C^{13} nmr spectra of 1,4 dioxane in H_2O, in 1M $MgCl_2$ and in 1M LiCl, and also of piperazine in H_2O and in 1M LiCl. One single major peak was observed in all the spectra and there was no change in chemical shift for each compound in the different ionic media. These C^{13} nmr results show that a change in conformation of 1,4 dioxane and piperazine by introduction of ions at appreciable concentration into their aqueous solutions cannot be detected in these experiments. Since, in the ionic medium, the boat conformation is expected to be favoured, the conformation of these compounds in water should also be boat according to the C^{13} nmr results. Morpholine is also expected to have the same conformation since its structure is in between that of 1,4 dioxane and piperazine.

The volume and compressibility behaviour of 1,4 dioxane in water and in 1M $MgCl_2$ can be explained as follows, according to the above findings. In water the boat form will already be favoured by formation of H-bonds between the hydrogens of a water molecule and the oxygens of a 1,4 dioxane molecule. In the case of 1M $MgCl_2$, the stronger interactions between Mg^{2+} and the oxygens of 1,4 dioxane would make the boat form again the preferred conformation. Owing to the structure and size of the water molecule, 1,4

dioxane, H-bonded to water (structure I below), has a larger volume than dioxane interacting with an Mg^{2+} ion (structure II below).

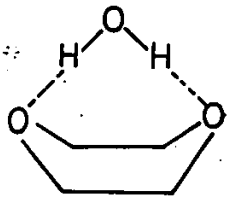

structure I

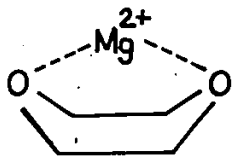

structure II

It should also be noted that when Mg^{2+} interacts with 1,4 dioxane, it should release probably two of its primary coordination shell hydration water molecules to the bulk water. This, of course, increases the volume but not as much as to compensate the larger volume caused by H-bonding between water and 1,4 dioxane as shown in structure I.

The larger $\overline{K}_S^o$ value for 1,4 dioxane in 1M $MgCl_2$ compared to that in H_2O would be attributed, on this model, to the release of two electrostricted (less compressible) water molecules per Mg^{2+} ion into the bulk water where it is more compressible.

3. Concentration-Dependence of ϕ_V and ϕ_{KS} for Organic Bases

Although the b_V' (in Equation II.12) values are reported in almost every work[22,56-58] on volumetric behaviour of

organic molecules, they mostly remain as empirical quantities in the tables of data. This is probably because the volume and compressibility behaviour of organic molecules is complex enough even at infinite dilution owing to the structural effects discussed above; the concentration-dependences of ϕ_v and ϕ_{KS} are expected to be even more complex. However, in the present work, there seems to be an interesting relation between b_v' and ϕ_v^o for the organic bases.

Normally, if there are neither hydration effects nor solute-solute interactions, ϕ_v and ϕ_{KS} are expected to be independent of concentration (i.e., b_v' and b_{KS} are zero in the equations $\phi_v = \phi_v^o + b_v' m$ and $\phi_{KS} = \phi_{KS}^o + b_{KS} m$). However, owing to the presence of functional groups, e.g., -NH-, $-NH_2-$, -O-, etc., hydrocarbon groups, and to the large sizes of organic molecules relative to H_2O, both hydration effects (due to H-bonding and hydrophobic hydration) and interactions between solute molecules through their hydration shells ("hydration co-sphere" interaction effects) are to be expected as the concentration increases.

Since these hydration effects are also expected to be reflected in the ϕ_v^o values, b_v' values were plotted against ϕ_v^o in Figure 47, for the organic compounds studied. The data points seem to fit on an agreeably smooth curve which shows that the larger is the infinite dilution

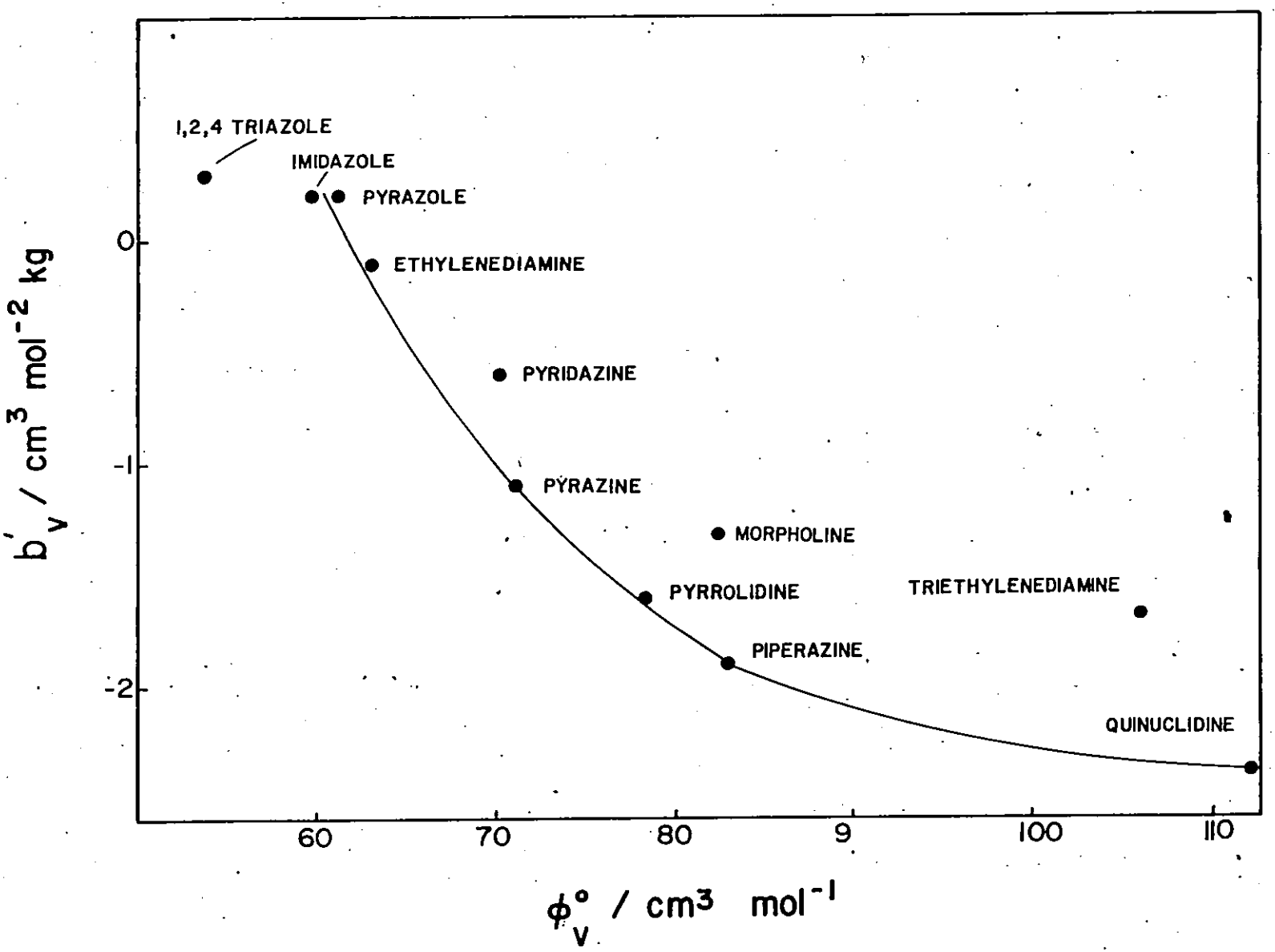

Figure 47 - A plot of b'_v parameter in Equation II.12 against ϕ^o_v for organic bases.

volume the greater is the deviation of b_V' from zero. The deviation is towards the negative side. This can be explained qualitatively as follows. At infinite dilution, both hydrophobic hydration and hydrogen bonding give positive contributions to the volume. Interaction (overlap) of the hydration shells of these molecules[129] would therefore result in a volume decrease, thus giving negative b_V' values. Also, the larger is the ϕ_V the more negative is the b_V'.

However, in the case of the compressibilities, the relation between b_{KS} and ϕ_V^o or ϕ_{KS}^o data was found to be more complex, as has been noted in other respects in this work when the compressibility property was related to other quantities.

4. The Volume and Compressibility Changes for Ionization of Organic Bases

The effects of ionization on hydration of organic molecules were investigated by studying the volume and compressibility behaviour of hydrochloride salts of the series of structurally related organic bases referred to in the previous sections. Since the structural effects associated with the volume and compressibility behaviour of the bases themselves were discussed in detail (Sections V.C.1 to 3), here the changes in volumes and compressibility resulting from ionization will be considered, mostly from the electrostatic point of view.

The partial molal volumes and compressibilities at infinite dilution of hydrochloride salts of the selected organic bases were given in Tables 8 and 9, respectively. Since both the individual ionic volume and compressibility of Cl^- are known (from Table 13: $\overline{V}^o$ (Cl^-) = 22.5

$cm^3\ mol^{-1}$ and $\overline{K}_S^o\ (Cl^-) = -17.0 \times 10^{-4}\ cm^3\ mol^{-1}\ bar^{-1}$), the individual ionic volumes and compressibilities of the organic ions can be obtained and are shown in Table 15.

However, the quantities $\Delta\overline{V}_i^o$ and $\Delta\overline{K}_{S,i}^o$, which are the changes in volume and compressibility upon ionization, respectively, are of more interest than the individual ionic quantities, $\overline{V}_i^o$ and $\overline{K}_{S,i}^o$.

The volume and compressibility change associated with the ionization process $B + H^+ \rightarrow BH^+$ where B is the organic base and BH^+ its conjugate acid, can be expressed as

$$\Delta\overline{V}_i^o = \overline{V}^o(BH^+) - \overline{V}^o(B) - \overline{V}^o(H^+) \qquad V.11$$

and

$$\Delta\overline{K}_{S,i}^o = \overline{K}_S^o(BH^+) - \overline{K}_S^o(B) - \overline{K}_S^o(H^+) \qquad V.12$$

However, these quantities can also be expressed as

$$\Delta\overline{V}_i^o = \overline{V}^o(BHCl) - \overline{V}^o(B) - \overline{V}^o(HCl) \qquad V.13$$

and

$$\Delta\overline{K}_{S,i}^o = \overline{K}_S^o(BHCl) - \overline{K}_S^o(B) - \overline{K}_S^o(HCl) \qquad V.14$$

and therefore can be evaluated without any thermodynamic ambiguity since evaluation of individual ionic properties is avoided here.

Table 15

$\bar{V}_i^o$ AND $\bar{K}_{S,i}^o$ VALUES FOR IONS OF THE ORGANIC BASES

Ion[a]	$\bar{V}_i^o$/cm^3 mol^{-1}	$10^4\bar{K}_{S,i}^o$/cm^3 mol^{-1} bar^{-1}
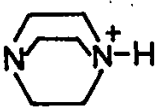	94.3	- 0.7
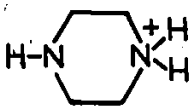	72.7	- 4.1
$H_2NCH_2CH_2N^+H_3$	61.6	- 9.9
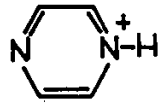	59.9	+11.3
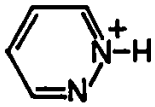	61.1	- 3.1
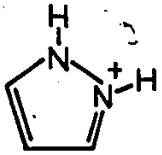	54.1	- 1.8
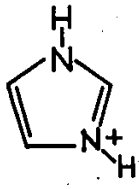	53.5	- 0.1
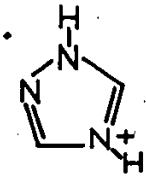	45.2	- 2.6

Table 15 cont'd

Ion	$\bar{V}_i^o$/cm^3 mol^{-1}	$10^4\bar{K}_{S,i}^o$/cm^3 mol^{-1} bar^{-1}
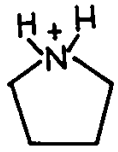	69.2	+ 1.4
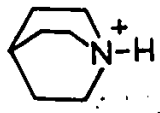	103.8	- 4.0
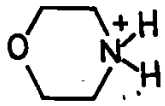	70.5	- 6.0
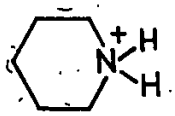	84.2	- 5.0
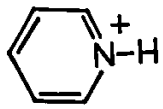	68.5	- 1.6

(a) When there is more than one ionizable N center in the structure of the base, the ionized centers shown in this table are the most likely ones due to the resonance stabilization.

$\Delta\overline{V}^{o}_{i,1}$ and $\Delta\overline{K}^{o}_{S,i,1}$ values were calculated for the first ionization of the organic molecules studied in the present work, using the data in Tables 8 and 9 for $\overline{V}^{o}$(BHCl) and $\overline{K}^{o}_{S}$(BHCl), respectively and those in Tables 6 and 7 for $\overline{V}^{o}$(B) and $\overline{K}^{o}_{S}$(B), respectively. $\overline{K}^{o}_{S}$(HCl) was taken from Reference 39 and $\overline{V}^{o}$(HCl) from Reference 7. The results are given in Table 16 where $\Delta\overline{V}^{o}_{i,1}$ and $\Delta\overline{K}^{o}_{S,i,1}$ values for a series of amines from previous work[21] in this lab have also been included for comparison.

The negative $\Delta\overline{V}^{o}_{i,1}$ and $\Delta\overline{K}^{o}_{S,i,1}$ values in all cases are due to electrostatic effects. The charged 'N' center electrostricts the water causing a smaller $\overline{V}^{o}$ for the ion than for the corresponding base. Since the electrostricted water is less compressible, the ion has a smaller $\overline{K}^{o}_{S,i}$ than has the corresponding base. The second ionization evaluated for several diacidic bases gives, as expected, more negative values (see Table 18).

5. The Relation Between $\Delta\overline{V}^{o}_{i,1}$ and $\Delta\overline{K}^{o}_{S,i,1}$ for the Organic Bases

Both the $\Delta\overline{V}^{o}_{i,1}$ and $\Delta\overline{K}^{o}_{S,i,1}$ data, evaluated in the previous section, directly reflect the electrostriction volume and compressibility, respectively, for the organic ions. The relation between electrostriction volume and compressibility was discussed in detail for oxyanions in

Table 16

$\Delta\bar{V}^{o}_{i,l}$, $\Delta\bar{K}^{o}_{S,i,l}$ AND $\Delta\bar{S}^{o}_{i,l}$ VALUES FOR THE IONIZATION OF A SERIES OF ORGANIC BASES

Base	$\Delta\bar{V}^{o}_{i,l}$/cm^{3}mol^{-1}	$10^4\Delta\bar{K}^{o}_{S,i,l}$/cm^{3}mol^{-1}bar^{-1}	$\Delta\bar{S}^{o}_{i,l}$/cal K^{-1}mol^{-1}
Triethylenediamine	-7.1	-10.2	-16.2
Piperazine	-5.6	-13.1	-10.2
Ethylenediamine	-6.6	-20.1	- 5.4
Pyrazine	-6.3	- 4.2	-
Pyridazine	-4.4	-13.7	-
Pyrazole	-2.3	-16.4	-
Imidazole	-1.7	-14.3	- 2.5
1,2,4 Triazole	-3.9	-18.1	-
Pyrrolidine	-4.3	-10.4	- 8.0
Quinuclidine	-3.5	-19.9	-13.7
Morpholine	-7.3	-18.5	- 7.6
Piperidine	-2.2	-13.2	- 8.1
Pyridine	-4.5	-12.4	- 7.6
Methylamine[a]	-4.1	-17.7	- 4.5
Dimethylamine[a]	-4.0	-19.4	- 8.9
Trimethylamine[a]	-5.2	-11.8	-15.3

(a) From previous work in this lab[21].

Section V.B.5 and trends were demonstrated which were consistent with the results of the theoretical work of Desnoyers, Verrall and Conway[14] (see Figures 40 and 41). A similar relation was examined for the organic ions. Figure 48 shows a plot of $\Delta\overline{V}^{o}_{i,1}$ against $\Delta\overline{K}^{o}_{S,i,1}$ for the organic bases studied in the present work. There seem to exist two curves representing the data points. The shapes of the curves are very similar to the ones found for the oxyanions (Figure 40). The two separate curves probably arise because of the structural differences between the groups of compounds. However, the structural differences in this series of compounds are not of the kind that could obviously account for the fact that the data evidently fall on two more or less distinguishable curves, as Figure 48 shows. However the trends of the two curves are in the expected direction for the influence of electrostatic effects: more negative $\Delta\overline{V}^{o}_{i,1}$ with more negative $\Delta\overline{K}^{o}_{S,i,1}$. The spread of the data points may be due to superimposition of other structural effects in each of the quantities measured on the main electrostatic one. The lack of good correlation between the $\Delta\overline{V}^{o}_{i,1}$ and $\Delta\overline{K}^{o}_{S,i,1}$ data in Figure 48 is not, however, due to any substantial errors in the data. In fact, the error-bar lengths for the quantities plotted in Figure 48 are quite small on the scales of this diagram.

6. The Relation of $\Delta\overline{V}^{o}_{i,1}$ to $\Delta\overline{S}^{o}_{i,1}$

The significance of the relation between volume and entropy of ionization was discussed in Section I.6 according to "Hepler's Relation"[20]. A similar relation was examined

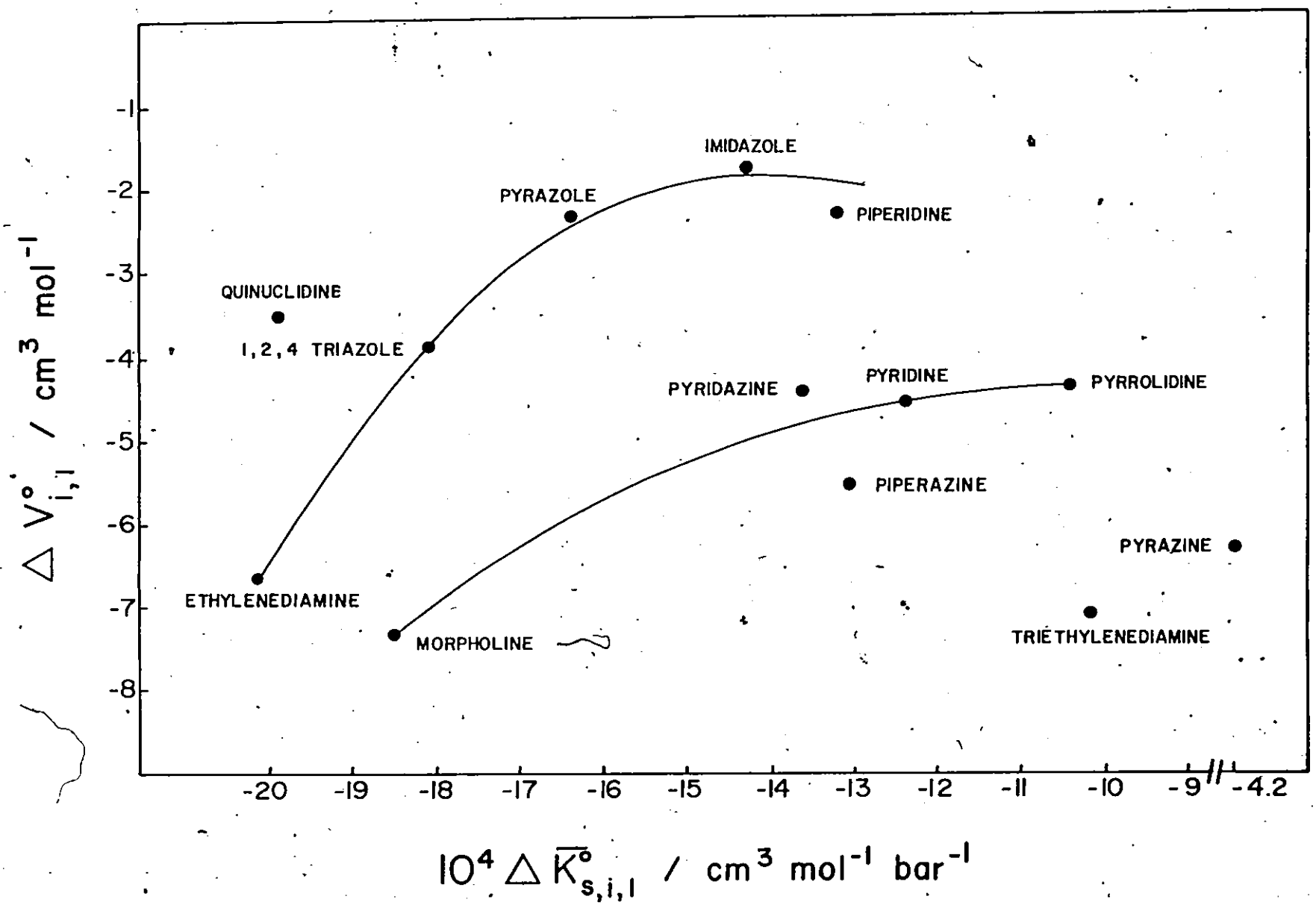

Figure 48 - The relation between $\Delta\overline{V}^{\circ}_{i,1}$ and $\Delta\overline{K}^{\circ}_{S,i,1}$ for the first ionization of organic bases.

for the organic bases studied in the present work. The data on entropy of ionization were obtained from References 22, 127 and 128, and are given in Table 16 together with the respective $\Delta\overline{V}^{o}_{i,1}$ and $\Delta\overline{K}^{o}_{S,i,1}$ values.

The available $\Delta\overline{S}^{o}_{i,1}$ data were plotted against $\Delta\overline{V}^{o}_{i,1}$ as shown in Figure 49. Hepler's relation is also shown by the dotted line in this figure. As can be seen, there is an appreciable scatter amongst the points. However, a least squares analysis including all the data points gives the relation drawn with the solid line in Figure 49; it has an intercept of -5.3 cal mol^{-1} K^{-1} and a slope of 0.7 cal cm^{-3} K^{-1} which can be compared with -7 cal mol^{-1} K^{-1} for the intercept and 1.05 cal cm^{-3} K^{-1} for the slope in "Hepler's relation".

It should be emphasized also here that the scatter amongst the various data points plotted in Figure 49 is not due to any appreciable errors in the data themselves but rather reflects a lack of systematic relationship between the quantities plotted, no doubt owing to the complexity of the structural and electrostatic effects associated with ionization of these "relatively complex" molecules.

7. The Volume and Compressibility Behaviour of Dihydrochloride Salts of Organic Bases

The study of dihydrochloride salts of organic bases was restricted to triethylenediamine, piperazine and

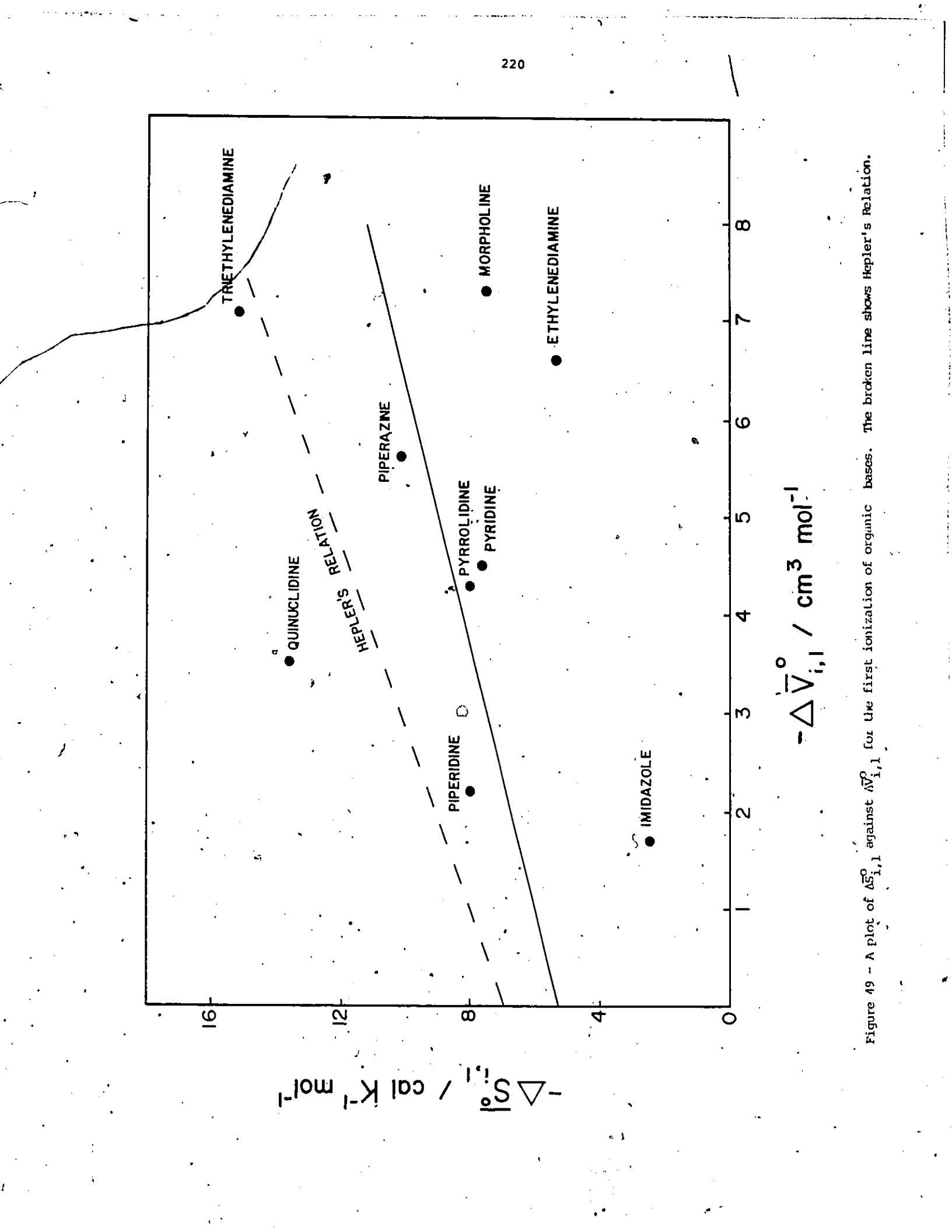

Figure 49 - A plot of $\Delta\overline{S}^{o}_{i,1}$ against $\Delta\overline{V}^{o}_{i,1}$ for the first ionization of organic bases. The broken line shows Hepler's Relation.

ethylenediamine because these were the only three compounds among the bases studied in the present work having sufficiently high $pK_a(2)$ values (see Table 5) that their dihydrochloride salts could be prepared without subsequent decomposition.

$\bar{V}^o$ and $\bar{K}_S^o$ values for these salts were given in Tables 10 and 11, respectively. Individual ionic volumes and compressibilities of the diprotonated bases can easily be calculated by subtracting twice the corresponding values for Cl^- ($\bar{V}^o(Cl^-) = 22.5$ cm^3 mol^{-1} and $\bar{K}_S^o(Cl^-) = -17.0 \times 10^{-4}$ cm^3 mol^{-1} bar^{-1}). These data are given in Table 17.

The changes in volume and compressibility for the second ionization process, BHCl + HCl → B.2HCl, can be calculated from

$$\Delta\bar{V}_{i,2}^o = \bar{V}^o(B.2HCl) - \bar{V}^o(B.HCl) - \bar{V}^o(HCl) \qquad V.15$$

and

$$\Delta\bar{K}_{S,i,2}^o = \bar{K}_S^o(B.2HCl) - \bar{K}_S^o(B.HCl) - \bar{K}_S^o(HCl) \qquad V.16$$

The data for the calculations were taken from Table 10 for $\bar{V}^o(B.2HCl)$, Table 11 for $\bar{K}_S^o(B.2HCl)$, Table 8 for $\bar{V}^o(B.HCl)$, Table 9 for $\bar{K}_S^o(B.HCl)$, Reference 7 for $\bar{V}^o(HCl)$ and Reference 39 for $\bar{K}_S^o(HCl)$. The calculated $\Delta\bar{V}_{i,2}^o$ and $\Delta\bar{K}_{S,i,2}^o$ values are given in Table 18.

Table 17

VALUES OF $\bar{V}_i^o$ AND $\bar{K}_{S,i}^o$ FOR DIPROTONATED BASES

Ion	$\bar{V}_i^o$/cm^3 mol^{-1}	$10^4\bar{K}_{S,i}^o$/cm^3 mol^{-1} bar^{-1}
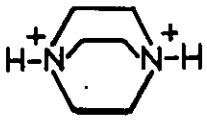	73.7	-19.4
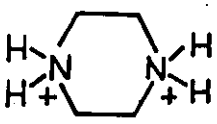	54.6	-28.9
$H_3NCH_2CH_2NH_3^{+\ +}$	35.1	-28.2

Table 18

VALUES OF $\Delta\bar{V}_{i,2}^o$ AND $\Delta\bar{K}_{S,i,2}^o$ FOR THE SECOND IONIZATION OF THREE DIACIDIC ORGANIC BASES

Base	$\Delta\bar{V}_{i,2}^o$/cm^3 mol^{-1}	$10^4\Delta\bar{K}_{S,i,2}^o$/cm^3 mol^{-1} bar^{-1}
Triethylenediamine	-15.9	-27.4
Piperazine	-13.4	-33.4
Ethylenediamine	-11.8	-26.9

It is difficult to make any generalization or examine any structural effects in detail with these compounds since only 3 data are available. However, it can be noted that $\Delta\bar{V}^{\circ}_{i,2}$ values become less negative in going from bicyclic to monocyclic and then to a non-cyclic, linear molecule. $\Delta\bar{K}^{\circ}_{S,i,2}$ values do not, however, show a similar systematic change. When compared with the corresponding values for the first ionization, $\Delta\bar{V}^{\circ}_{i,2}$ and $\Delta\bar{K}^{\circ}_{S,i,2}$ values are numerically about twice as large. This is obviously due to the greater electrostriction caused by the second ionized 'N' center.

APPENDIX I

EXPERIMENTAL RESULTS FOR THE APPARENT MOLAL VOLUMES AND DENSITIES OF SOLUTIONS STUDIED IN H_2O AT 298K ARE PRESENTED IN TABULAR FORM IN THIS SECTION

APPARENT MOLAL VOLUMES AND DENSITIES FOR AQUEOUS SOLUTIONS OF NaCl, $NaClO_2$, $NaClO_3$, $NaClO_4$ AT 298K

Sodium Chloride, NaCl

c/mol L^{-1}	ϕ_v/cm^3 mol^{-1}	d/g cm^{-3}
0.00951	16.32	0.997475
0.02241	16.81	0.998008
0.03988	16.99	0.998729
0.06213	17.16	0.999642
0.08935	17.17	1.000766
0.12150	17.26	1.002083
0.15899	17.36	1.003614
0.20133	17.40	1.005348
0.24842	17.51	1.007255
0.30025	17.58	1.009357
0.35712	17.67	1.011652
0.41800	17.75	1.014103
0.48549	17.82	1.016818
0.55723	17.91	1.019686
0.62816	18.01	1.022503
0.71160	18.09	1.025822
0.79766	18.20	1.029218
0.88800	18.29	1.032773
0.98388	18.37	1.036548
1.08119	18.48	1.040335
1.18442	18.57	1.044357
1.29317	18.68	1.048568
1.40624	18.78	1.052927

Sodium Chlorite, $NaClO_2$

c/mol L^{-1}	$\phi_v/cm^3\ mol^{-1}$	d/g cm^{-3}
0.00981	25.98	0.997707
0.02223	26.76	0.998491
0.03918	26.81	0.999570
0.06189	27.01	1.001004
0.08806	27.24	1.002646
0.11944	27.25	1.004631
0.15730	27.36	1.007009
0.19934	27.43	1.009651
0.24636	27.52	1.012595
0.29616	27.58	1.015714
0.35296	27.65	1.019266
0.41229	27.72	1.022966
0.47774	27.80	1.027038
0.54615	27.89	1.031283
0.62163	27.95	1.035971
0.69965	28.03	1.040797
0.78295	28.10	1.045947
0.86901	28.19	1.051241
0.96021	28.26	1.056857

Sodium Chlorate, $NaClO_3$

c/mol L^{-1}	ϕ_v/cm^3 mol^{-1}	d/g cm^{-3}
0.01060	35.39	0.997828
0.02347	35.53	0.998741
0.04172	35.68	1.000030
0.06344	35.71	1.001568
0.09011	35.78	1.003451
0.12319	35.96	1.005770
0.16014	36.04	1.008364
0.20242	36.15	1.011323
0.25014	36.22	1.014665
0.30287	36.30	1.018349
0.35814	36.36	1.022209
0.41838	36.47	1.026393
0.48409	36.57	1.030949
0.55356	36.65	1.035768
0.62672	36.74	1.040822
0.70456	36.84	1.046187
0.78713	36.94	1.051866
0.87493	37.04	1.057893
0.96673	37.13	1.064186
1.06192	37.23	1.070690
1.15973	37.33	1.077351
1.26082	37.42	1.084233
1.36791	37.52	1.091503

Sodium Perchlorate, $NaClO_4$

c/mol L^{-1}	ϕ_v/cm^3 mol^{-1}	d/g cm^{-3}
0.01006	41.90	0.997885
0.02281	42.34	0.998904
0.04048	42.82	1.000302
0.06214	42.84	1.002028
0.09070	42.93	1.004297
0.12283	43.05	1.006841
0.15907	43.15	1.009706
0.20026	43.25	1.012957
0.24619	43.34	1.016580
0.29809	43.43	1.020664
0.35462	43.49	1.025116
0.41522	43.60	1.029864
0.48114	43.67	1.035034
0.55022	43.75	1.040439
0.62427	43.84	1.046219
0.70204	43.91	1.052292
0.78569	44.03	1.058779
0.87082	44.10	1.065409
0.95804	44.19	1.072169
1.05116	44.30	1.079348
1.14780	44.39	1.086814
1.24800	44.47	1.094543
1.35638	44.57	1.102868
1.46897	44.66	1.111523

APPARENT MOLAL VOLUMES AND DENSITIES FOR AQUEOUS SOLUTIONS OF Na_2SO_3, Na_2SO_4, $Na_2S_2O_3$ AND $Na_2S_2O_6$ AT 298K

Sodium Sulphite, Na_2SO_3

c/mol L^{-1}	$\phi_v/cm^3\ mol^{-1}$	d/g cm^{-3}
0.01053	4.51	0.998354
0.02289	4.94	0.999846
0.03930	5.69	1.001805
0.06241	6.33	1.004547
0.09006	6.98	1.007799
0.12338	7.62	1.011689
0.16089	8.15	1.016048
0.20244	8.73	1.020830
0.24829	9.28	1.026073
0.30052	9.80	1.032019
0.35633	10.36	1.038308
0.41787	10.90	1.045207
0.48543	11.50	1.052698
0.55828	12.08	1.060721
0.63398	12.66	1.068985
0.71512	13.23	1.077779
0.80118	13.81	1.087029
0.89014	14.37	1.096524

Sodium Sulphate, Na_2SO_4

c/mol L^{-1}	$\phi_v/cm^3\ mol^{-1}$	d/g cm^{-3}
0.00989	12.55	0.998355
0.02236	13.11	0.999957
0.03988	13.61	1.002197
0.06195	14.23	1.004994
0.08970	14.90	1.008483
0.12209	15.46	1.012533
0.15859	15.98	1.017073
0.20161	16.53	1.022387
0.24752	17.07	1.028020
0.29953	17.62	1.034357
0.35591	18.15	1.041185
0.41719	18.71	1.048548
0.48397	19.25	1.056526
0.55440	19.83	1.064861
0.62967	20.37	1.073722
0.70917	20.92	1.083010
0.79288	21.46	1.092728
0.88069	22.00	1.102851

Sodium Thiosulphate, $Na_2S_2O_3$

$c/mol\ L^{-1}$	$\phi_v/cm^3\ mol^{-1}$	$d/g\ cm^{-3}$
0.01027	26.42	0.998427
0.02244	27.57	1.000005
0.03973	28.37	1.002232
0.06190	28.88	1.005079
0.08916	29.50	1.008548
0.12106	30.02	1.012592
0.15831	30.58	1.017277
0.20104	31.06	1.022634
0.24790	31.60	1.028460
0.30040	32.15	1.034941
0.35508	32.64	1.041660
0.41621	33.16	1.049121
0.48121	33.72	1.056982
0.55039	34.25	1.065303
0.62467	34.79	1.074171
0.70329	35.34	1.083487
0.78520	35.87	1.093142
0.87147	36.39	1.103238

Sodium Dithionate, $Na_2S_2O_6$

$c/mol\ L^{-1}$	$\phi_v/cm^3\ mol^{-1}$	$d/g\ cm^{-3}$
0.01064	55.95	0.998674
0.02360	56.08	1.000618
0.04122	56.52	1.003246
0.06410	57.15	1.006633
0.09207	57.59	1.010762
0.12437	58.12	1.015499
0.16172	58.60	1.020956
0.20383	59.04	1.027084
0.30184	59.92	1.041252
0.41720	60.86	1.057743
0.55184	61.78	1.076815
0.70041	62.69	1.097652

APPARENT MOLAL VOLUMES AND DENSITIES FOR AQUEOUS SOLUTIONS OF TRIETHYLENEDIAMINE, ETHYLENEDIAMINE, PIPERAZINE, MORPHOLINE, PYRAZINE, PYRIDAZINE, PYRAZOLE, IMIDAZOLE, 1,2,4 TRIAZOLE, PYRROLIDINE, 1,4 DIOXANE AND QUINUCLIDINE AT 298K

Triethylenediamine in 0.01N NaOH

$m/mol\ kg^{-1}$	$\phi_V/cm^3\ mol^{-1}$	$d/g\ cm^{-3}$
0.0		0.997097
0.01004	105.96	0.997662
0.02129	105.98	0.997734
0.04096	106.12	0.997854
0.06144	106.10	0.997983
0.08099	106.09	0.998106
0.10132	105.94	0.998247
0.14220	105.88	0.998513
0.18266	105.82	0.998780
0.22242	105.75	0.999047
0.26093	105.68	0.999308
0.30155	105.61	0.999588
0.34843	105.54	0.999910
0.39755	105.46	1.000252

Ethylenediamine in 0.01N NaOH

$m/mol\ kg^{-1}$	$\phi_v/cm^3\ mol^{-1}$	$d/g\ cm^{-3}$
0.0		0.997516
0.01079	62.82	0.997488
0.02061	62.75	0.997465
0.04157	62.76	0.997412
0.06120	62.82	0.997360
0.08191	62.96	0.997296
0.10267	62.88	0.997249
0.14295	62.90	0.997142
0.18291	62.92	0.997036
0.22301	62.83	0.996951
0.26323	62.87	0.996842
0.30313	62.86	0.996744
0.35346	62.86	0.996617
0.40299	62.86	0.996496

Piperazine in 0.01N NaOH

$m/mol\ kg^{-1}$	$\phi_v/cm^3\ mol^{-1}$	$d/g\ cm^{-3}$
0.0		0.997516
0.01066	83.07	0.997551
0.02101	82.93	0.997587
0.04052	82.92	0.997654
0.06056	82.86	0.997726
0.08018	82.80	0.997798
0.10508	82.72	0.997893
0.14642	82.70	0.998042
0.18772	82.49	0.998226
0.22519	82.55	0.998354
0.26455	82.47	0.998516
0.31178	82.31	0.998738
0.35718	82.28	0.998922
0.40784	82.23	0.999134

Morpholine in 0.01N NaOH

$m/mol\ kg^{-1}$	$\phi_v/cm^3\ mol^{-1}$	$d/g\ cm^{-3}$
0.0		0.997516
0.01010	83.94	0.997550
0.02030	82.65	0.997610
0.04005	82.64	0.997703
0.06041	82.44	0.997809
0.08040	82.32	0.997915
0.10051	82.43	0.998003
0.14079	82.39	0.998201
0.18088	82.33	0.998405
0.22146	82.23	0.998622
0.26142	82.23	0.998817
0.30191	82.18	0.999028
0.35165	82.07	0.999307
0.40223	82.04	0.999570

Pyrazine in H_2O

$m/mol\ kg^{-1}$	$\phi_v/cm^3\ mol^{-1}$	$d/g\ cm^{-3}$
0.01671	70.92	0.997230
0.04087	70.80	0.997460
0.08057	70.90	0.997825
0.13480	70.90	0.998325
0.16890	70.86	0.998644
0.21176	70.84	0.999041
0.26569	70.82	0.999539
0.33367	70.80	1.000162
0.41956	70.78	1.000943

Pyridazine in H_2O

$m/mol\ kg^{-1}$	$\phi_v/cm^3\ mol^{-1}$	$d/g\ cm^{-3}$
0.01063	70.39	0.997179
0.02042	70.21	0.997279
0.03998	70.13	0.997478
0.06039	70.05	0.997688
0.08080	70.14	0.997887
0.10048	70.08	0.998090
0.12084	70.07	0.998296
0.14114	70.02	0.998506
0.16079	70.07	0.998695
0.18117	70.02	0.998907
0.20090	70.01	0.999106
0.21975	70.04	0.999288
0.23936	69.98	0.999494
0.25983	69.98	0.999698
0.27962	70.01	0.999887
0.30003	69.96	1.000102
0.31981	69.95	1.000302

Imidazole in 0.01N NaOH

$m/mol\ kg^{-1}$	$\phi_v/cm^3\ mol^{-1}$	$d/g\ cm^{-3}$
0.0		0.997516
0.01106	59.41	0.997613
0.02275	59.85	0.997706
0.04296	59.82	0.997875
0.06318	59.93	0.998037
0.08454	59.89	0.998216
0.10469	60.01	0.998369
0.15374	59.99	0.998767
0.20324	59.95	0.999175
0.25424	59.97	0.999579
0.30329	59.99	0.999964
0.35188	59.99	1.000348
0.40625	59.98	1.000781

Pyrazole in H_2O

m/mol kg^{-1}	ϕ_v/cm^3 mol^{-1}	d/g cm^{-3}
0.00990	60.76	0.997148
0.02028	61.09	0.997219
0.04046	61.11	0.997362
0.06045	61.14	0.997501
0.08148	61.24	0.997642
0.10171	61.15	0.997791
0.14265	61.20	0.998069
0.18259	61.21	0.998343
0.22439	61.21	0.998630
0.26586	61.23	0.998909
0.30483	61.24	0.999169
0.35487	61.24	0.999506
0.40969	61.23	0.999875

1,2,4 Triazole in H_2O

m/mol kg^{-1}	ϕ_v/cm^3 mol^{-1}	d/g cm^{-3}
0.01099	54.57	0.997235
0.02010	53.75	0.997384
0.04130	53.74	0.997711
0.06151	53.83	0.998015
0.08279	53.76	0.998345
0.10293	53.79	0.998649
0.14288	53.84	0.999249
0.18284	53.86	0.999849
0.22373	53.83	1.000469
0.26422	53.87	1.001064
0.30533	53.88	1.001673
0.35477	53.88	1.002401
0.40459	53.91	1.003124

Pyrrolidine in 1N NaOH

$m/mol\ kg^{-1}$	$\phi_v/cm^3\ mol^{-1}$	$d/g\ cm^{-3}$
0.0		1.037929
0.01023	77.99	1.037825
0.02001	78.12	1.037722
0.03997	78.19	1.037514
0.06017	78.07	1.037313
0.08075	78.07	1.037104
0.10070	78.04	1.036905
0.14078	77.97	1.036512
0.18094	77.82	1.036143
0.22091	77.80	1.035759
0.26116	77.75	1.035386
0.30127	77.69	1.035024
0.35134	77.61	1.034582
0.40179	77.55	1.034143

1,4 Dioxane in H_2O

$m/mol\ kg^{-1}$	$\phi_v/cm^3\ mol^{-1}$	$d/g\ cm^{-3}$
0.01032	80.28	0.997157
0.02010	80.35	0.997234
0.04037	80.40	0.997393
0.06039	80.50	0.997544
0.08068	80.50	0.997701
0.10076	80.51	0.997855
0.14076	80.51	0.998162
0.18070	80.53	0.998462
0.22086	80.52	0.998768
0.26089	80.53	0.999065
0.30108	80.51	0.999370

1,4 Dioxane in 1M $MgCl_2$

m/mol kg^{-1}	$\phi_v/cm^3\ mol^{-1}$	d/g cm^{-3}
0.0		1.067817
0.00994	77.54	1.067873
0.02001	78.79	1.067902
0.04013	79.30	1.067963
0.06022	79.44	1.068027
0.08063	79.48	1.068094
0.10077	79.54	1.068156
0.14141	79.67	1.068270
0.18140	79.75	1.068379
0.22146	79.76	1.068499
0.26196	79.79	1.068615
0.30359	79.81	1.067731

Quinuclidine in 1N NaOH

m/mol kg^{-1}	$\phi_v/cm^3\ mol^{-1}$	d/g cm^{-3}
0.0		1.037929
0.01027	112.26	1.037872
0.02032	112.10	1.037821
0.03960	112.27	1.037711
0.06058	111.85	1.037623
0.07972	111.79	1.037533
0.10013	111.78	1.037433
0.13972	111.69	1.037253
0.17752	111.58	1.037094
0.21227	111.48	1.036957

APPARENT MOLAL VOLUMES AND DENSITIES FOR AQUEOUS SOLUTIONS OF MONOHYDROCHLORIDES OF TRIETHYLENEDIAMINE, PIPERAZINE, ETHYLENEDIAMINE, PYRAZINE, PYRIDAZINE, IMIDAZOLE, PYRAZOLE, 1,2,4 TRIAZOLE, PYRROLIDINE, QUINUCLIDINE AND MORPHOLINE AT 298K.

Triethylenediamine Monohydrochloride

$c/\text{mol L}^{-1}$	$d/\text{g cm}^{-3}$	$(\phi_v - 1.868\sqrt{c})/\text{cm}^3\ \text{mol}^{-1}$
0.00889	0.997363	116.35
0.02039	0.997724	116.85
0.03636	0.998234	116.73
0.05614	0.998851	116.89
0.08099	0.999638	116.79
0.10991	1.000555	116.69
0.14345	1.001595	116.76
0.181271	1.002779	116.72
0.22245	1.004049	116.75
0.26698	1.005424	116.75
0.31590	1.006928	116.74
0.36788	1.008535	116.70

Piperazine Monohydrochloride

c/mol L^{-1}	d/g cm^{-3}	$(\phi_V - 1.868\sqrt{c})$/cm^3 mol^{-1}
0.01065	0.997367	95.18
0.02187	0.997675	95.12
0.03893	0.998138	95.18
0.06180	0.998757	95.18
0.08754	0.999454	95.14
0.12081	1.000352	95.10
0.15664	1.001310	95.10
0.19741	1.002408	95.03
0.24318	1.003618	95.05
0.29214	1.004916	95.03
0.34711	1.006366	95.01
0.40534	1.007896	94.99

Ethylenediamine Monohydrochloride

c/mol L^{-1}	d/g cm^{-3}	$(\phi_V - 1.868\sqrt{c})$/cm^3 mol^{-1}
0.01202	0.997354	73.28
0.04040	0.997973	74.15
0.07238	0.998686	74.00
0.09994	0.999281	74.10
0.14509	1.000261	74.10
0.19011	1.001232	74.09
0.23854	1.002260	74.13
0.30014	1.003567	74.12
0.35987	1.004839	74.08
0.41802	1.006046	74.11

Pyrazine Hydrochloride, $pK_a = 0.65$

c/mol L^{-1}		d/g cm^{-3}	$(\phi_v - 1.868\sqrt{c})$/cm^3 mol^{-1}	
Uncorrected	Corrected		Uncorrected	Corrected
0.00993	0.00041	0.997363	87.53	59.41
0.02289	0.00196	0.997737	87.56	75.57
0.03965	0.00528	0.998216	87.64	81.27
0.06189	0.01139	0.998871	87.31	81.88
0.08870	0.02067	0.999658	87.12	82.79
0.11950	0.03324	1.000598	86.67	82.37
0.15495	0.04959	1.001677	86.36	82.44
0.19531	0.07007	1.002916	86.08	82.45
0.24224	0.09580	1.004366	85.78	82.46
0.29103	0.12425	1.005894	85.49	82.36

Pyridazine Hydrochloride, $pK_a = 2.24$

c/mol L^{-1}		d/g cm^{-3}	$(\phi_v - 1.868\sqrt{c})$/cm^3 mol^{-1}	
Uncorrected	Corrected		Uncorrected	Corrected
0.01005	0.00480	0.997381	86.06	84.09
0.02184	0.01314	0.997758	85.20	83.51
0.03933	0.02689	0.998321	84.72	83.36
0.06116	0.04506	0.999021	84.50	83.43
0.08815	0.06832	0.999884	84.37	83.49
0.11841	0.09503	1.000850	84.27	83.53
0.15601	0.12879	1.002053	84.15	83.51
0.19625	0.16540	1.003341	84.04	83.48
0.24193	0.20739	1.004803	83.93	83.44
0.29075	0.25262	1.006361	83.85	83.41
0.34297	0.30133	1.008019	83.79	83.40
0.39963	0.35447	1.009838	83.68	83.33

Pyrazole Hydrochloride, $pK_a = 2.48$

c/mol L^{-1}		d/g cm^{-3}	$(\phi_v - 1.868\sqrt{c})$/cm^3 mol^{-1}	
Uncorrected	Corrected		Uncorrected	Corrected
0.01346	0.00824	0.997440	77.36	76.44
0.05609	0.04402	0.998600	77.12	76.71
0.09670	0.08039	0.999702	77.01	76.73
0.13826	0.11846	1.000844	76.81	76.57
0.18228	0.15931	1.002033	76.76	76.57
0.22785	0.20199	1.003298	76.56	76.38
0.28482	0.25572	1.004801	76.64	76.50
0.35602	0.32330	1.006720	76.56	76.45
0.39716	0.36251	1.007812	76.55	76.46

Imidazole Hydrochloride

c/mol L^{-1}	d/g cm^{-3}	$(\phi_v - 1.868\sqrt{c})$/cm^3 mol^{-1}
0.01127	0.997407	75.02
0.01980	0.997638	76.01
0.02751	0.997861	75.84
0.04124	0.998248	75.92
0.05506	0.998631	76.05
0.08293	0.999415	76.00
0.11040	1.000187	75.95
0.13711	1.000927	75.97
0.20567	1.002728	76.43
0.27423	1.004716	75.92
0.34278	1.006617	75.83

1,2,4 Triazole Hydrochloride, $pK_a = 2.30$

c/mol L^{-1}		d/g cm^{-3}	$(\phi_v - 1.868\sqrt{c})/cm^3\ mol^{-1}$	
Uncorrected	Corrected		Uncorrected	Corrected
0.01017	0.00511	0.997440	69.56	67.66
0.02307	0.01454	0.997911	69.17	67.87
0.04012	0.02823	0.998541	68.79	67.74
0.06242	0.04706	0.999365	68.56	67.72
0.08951	0.07069	1.000367	68.39	67.68
0.12076	0.09854	1.001520	68.27	67.66
0.15797	0.13223	1.002899	68.12	67.59
0.20063	0.17133	1.004457	68.10	67.65
0.24595	0.21326	1.006127	68.00	67.60
0.29773	0.26153	1.008016	67.96	67.62
0.35251	0.31291	1.010028	67.88	67.57
0.40867	0.36585	1.012074	67.83	67.56
0.46909	0.42304	1.014285	67.76	67.51

Pyrrolidine Hydrochloride

c/mol L^{-1}	d/g cm^{-3}	$(\phi_v - 1.868\sqrt{c})/cm^3\ mol^{-1}$
0.01198	0.997266	91.61
0.05983	0.998016	91.65
0.11980	0.998953	91.52
0.17970	0.999887	91.40
0.28751	1.001532	91.34
0.35939	1.002631	91.27
0.41929	1.003539	91.22

Morpholine Hydrochloride

c/mol L^{-1}	d/g cm^{-3}	$(\phi_v - 1.868\sqrt{c})$ cm^3 mol^{-1}
0.00998	0.997378	93.20
0.02269	0.997771	92.85
0.03991	0.998292	92.96
0.06158	0.998948	92.96
0.08912	0.999776	92.98
0.12027	1.000714	92.94
0.15766	1.001835	92.91
0.19932	1.003087	92.85
0.24242	1.004365	92.86
0.29182	1.005831	92.84

Quinuclidine Hydrochloride

c/mol L^{-1}	d/g cm^{-3}	$(\phi_v - 1.868\sqrt{c})$ cm^3 mol^{-1}
0.00996	0.997289	126.25
0.02102	0.997525	126.29
0.03862	0.997901	126.24
0.06050	0.998364	126.24
0.08765	0.998941	126.17
0.11981	0.999619	126.13
0.15552	1.000373	126.07
0.19586	1.001233	125.96
0.24011	1.002177	125.85
0.28926	1.003233	125.72
0.33987	1.004320	125.61
0.39551	1.005521	125.49

APPARENT MOLAL VOLUMES AND DENSITIES FOR AQUEOUS SOLUTIONS OF DIHYDROCHLORIDE SALTS OF TRIETHYLENEDIAMINE, PIPERAZINE AND ETHYLENEDIAMINE AT 298K.

Triethylenediamine Dihydrochloride, $pK_a(2) = 2.95$

c/mol L^{-1}		d/g cm^{-3}	$(\phi_v - 9.706\sqrt{c})/cm^3\ mol^{-1}$	
Uncorrected	Corrected		Uncorrected	Corrected
0.01009	0.00724	0.997686	123.70	119.86
0.02169	0.01729	0.998426	121.44	118.53
0.04203	0.03570	0.999708	120.30	118.22
0.09181	0.08221	1.002829	118.78	117.38
0.15270	0.14016	1.006634	117.32	116.22
0.25502	0.23866	1.012943	115.47	114.59
0.30359	0.28569	1.015912	114.68	113.85
0.36142	0.34184	1.019423	113.80	113.01
0.42025	0.39909	1.022967	112.95	112.20

Piperazine Dihydrochloride, $pK_a(2) = 5.55$

c/mol L^{-1}		d/g cm^{-3}	$(\phi_v - 9.706\sqrt{c})/cm^3\ mol^{-1}$	
Uncorrected	Corrected		Uncorrected	Corrected
0.01008	0.00991	0.997670	99.27	99.07
0.02238	0.02213	0.998379	99.60	99.47
0.04013	0.03980	0.999398	99.50	99.41
0.06213	0.06171	1.000649	99.40	99.33
0.08901	0.08851	1.002169	99.22	99.17
0.12081	0.12023	1.003944	99.12	99.07
0.15726	0.15660	1.005968	98.95	98.92
0.19822	0.19747	1.008235	98.73	98.71
0.24401	0.24318	1.010741	98.56	98.53
0.29376	0.29285	1.013453	98.35	98.33
0.34654	0.34555	1.016285	98.21	98.20
0.40386	0.40280	1.019371	97.99	97.98

Ethylenediamine Dihydrochloride, $pK_a(2) = 6.85$

c/mol L^{-1}		d/g cm^{-3}	$(\phi_v - 9.706\sqrt{c})/cm^3\ mol^{-1}$	
Uncorrected	Corrected		Uncorrected	Corrected
0.01016	0.01012	0.997604	80.10	80.06
0.02250	0.02244	0.998239	80.02	80.00
0.03968	0.03961	0.999116	79.87	79.85
0.06183	0.06174	1.000232	79.77	79.76
0.08933	0.08922	1.001603	79.66	79.65
0.12134	0.12121	1.003194	79.44	79.43
0.15746	0.15731	1.004976	79.23	79.22
0.19873	0.19856	1.006980	79.09	79.08
0.24434	0.24415	1.009199	78.84	78.84
0.29510	0.29490	1.011634	78.65	78.65
0.34898	0.34876	1.014200	78.46	78.45
0.40762	0.40738	1.016976	78.25	78.24

APPENDIX II

EXPERIMENTAL RESULTS FOR THE APPARENT MOLAL ADIABATIC COMPRESSIBILITIES FOR SOLUTIONS AT 298K AND THE ASSOCIATED DATA USED IN THEIR CALCULATION ARE PRESENTED IN TABULAR FORM IN THIS SECTION

APPARENT MOLAL ADIABATIC COMPRESSIBILITIES, DENSITIES AND SOUND VELOCITIES FOR AQUEOUS SOLUTIONS OF NaCl, $NaClO_2$, $NaClO_3$ AND $NaClO_4$ AT 298K

Sodium Chloride, NaCl

$m/mol\ kg^{-1}$	$d/g\ cm^{-3}$	$u/m\ s^{-1}$	$10^4\phi_{KS}/cm^3\ mol^{-1}\ bar^{-1}$
0.00316	0.997207	1493.95	-51.24
0.01053	0.997516	1494.42	-51.09
0.02309	0.998033	1495.22	-49.83
0.04139	0.998785	1496.38	-49.33
0.06461	0.999733	1497.84	-48.94
0.09142	1.000834	1499.51	-48.66
0.12352	1.002140	1501.52	-48.32
0.16123	1.003668	1503.88	-48.06
0.20359	1.005386	1506.50	-47.72
0.25193	1.007323	1509.47	-47.31
0.30497	1.009446	1512.71	-46.90
0.36408	1.011796	1516.31	-46.47
0.42689	1.014282	1520.08	-46.01
0.49545	1.016986	1524.22	-45.59
0.57041	1.019915	1528.68	-45.10
0.64988	1.022993	1533.39	-44.59
0.73682	1.026313	1538.44	-44.08
0.82481	1.029713	1543.65	-43.57
0.92004	1.033331	1549.17	-43.04
1.01768	1.037023	1554.80	-42.53

Sodium Chlorite, $NaClO_2$

$m/mol\ kg^{-1}$	$d/g\ cm^{-3}$	$u/m\ s^{-1}$	$10^4\phi_{KS}/cm^3\ mol^{-1}\ bar^{-1}$
0.00302	0.997268	1493.74	-52.55
0.01034	0.997738	1494.11	-49.52
0.02275	0.998519	1494.75	-48.17
0.04028	0.999629	1495.64	-47.70
0.06262	1.001032	1496.77	-47.17
0.09003	1.002740	1498.15	-46.66
0.12241	1.004770	1499.77	-46.36
0.16014	1.007114	1501.65	-45.97
0.20258	1.009747	1503.74	-45.59
0.24963	1.012648	1506.07	-45.22
0.30406	1.015995	1508.73	-44.82
0.36058	1.019454	1511.49	-44.43
0.42181	1.023180	1514.46	-44.02
0.48670	1.027105	1517.60	-43.60
0.55787	1.031382	1521.03	-43.17
0.63202	1.035824	1524.58	-42.75

Sodium Chlorate, $NaClO_3$

$m/mol\ kg^{-1}$	$d/g\ cm^{-3}$	$u/m\ s^{-1}$	$10^4\phi_{KS}/cm^3\ mol^{-1}\ bar^{-1}$
0.00385	0.997347	1493.57	-38.86
0.01072	0.997834	1493.88	-41.42
0.02365	0.998747	1494.41	-41.03
0.04041	0.999925	1495.09	-40.60
0.06292	1.001508	1496.01	-40.35
0.08951	1.003370	1497.10	-40.20
0.12113	1.005563	1498.36	-39.75
0.15859	1.008160	1499.86	-39.43
0.19980	1.010998	1501.51	-39.13
0.24679	1.014227	1503.38	-38.81
0.30046	1.017893	1505.49	-38.43
0.35783	1.021794	1507.74	-38.08
0.42030	1.026002	1510.18	-37.68
0.48792	1.030525	1512.81	-37.27
0.56002	1.035325	1515.64	-36.91
0.63815	1.040477	1518.67	-36.49
0.72087	1.045887	1521.83	-36.05
0.80799	1.051536	1525.20	-35.63

Sodium Perchlorate, $NaClO_4$

$m/mol\ kg^{-1}$	$d/g\ cm^{-3}$	$u/m\ s^{-1}$	$10^4\phi_{KS}/cm^3\ mol^{-1}\ bar^{-1}$
0.00299	0.997314	1493.85	-30.35
0.01042	0.997912	1494.03	-31.95
0.02267	0.998886	1494.33	-31.90
0.04094	1.000323	1494.77	-31.18
0.06389	1.002138	1495.35	-31.27
0.09335	1.004456	1496.07	-31.10
0.12616	1.007022	1496.89	-30.94
0.16469	1.010020	1497.86	-30.76
0.20695	1.013292	1498.95	-30.63
0.25362	1.016890	1500.17	-30.51
0.30549	1.020863	1501.54	-30.39
0.36361	1.025295	1503.12	-30.28
0.42727	1.030102	1504.87	-30.14
0.49754	1.035379	1506.85	-30.01
0.57025	1.040794	1508.94	-29.88
0.64827	1.046553	1511.23	-29.74

APPARENT MOLAL ADIABATIC COMPRESSIBILITIES, DENSITIES AND SOUND VELOCITIES FOR AQUEOUS SOLUTIONS OF Na_2SO_3, Na_2SO_4, $Na_2S_2O_3$ AND $Na_2S_2O_6$ AT 298K

Sodium Sulphite, Na_2SO_3

m/mol kg^{-1}	d/g cm^{-3}	u/m s^{-1}	$10^4\phi_{KS}/cm^3\ mol^{-1}\ bar^{-1}$
0.00323	0.997465	1494.13	-160.36
0.01217	0.998548	1495.67	-157.34
0.02415	0.999989	1497.71	-155.29
0.04147	1.002047	1500.58	-152.53
0.06369	1.004672	1504.17	-149.59
0.09074	1.007841	1508.46	-146.76
0.12466	1.011782	1513.77	-143.85
0.16310	1.016222	1519.70	-141.17
0.20598	1.021123	1526.25	-138.49
0.25515	1.026699	1533.68	-135.77
0.30905	1.032772	1541.67	-132.96
0.36762	1.039295	1550.44	-130.42
0.43173	1.046378	1559.88	-127.73
0.50028	1.053855	1569.90	-125.03
0.57333	1.061749	1580.52	-122.37
0.65545	1.070516	1592.38	-119.56
0.74270	1.079727	1604.96	-116.80
0.83051	1.088889	1617.58	-114.21

Sodium Sulphate, Na_2SO_4

m/mol kg^{-1}	d/g cm^{-3}	u/m s^{-1}	$10^4\phi_{KS}$/cm^3 mol^{-1} bar^{-1}
0.00335	0.997506	1494.11	-155.93
0.01057	0.998438	1495.32	-153.86
0.02294	1.000022	1497.24	-148.83
0.04077	1.002293	1500.23	-149.47
0.06222	1.004999	1503.63	-147.01
0.08889	1.008333	1507.78	-144.44
0.12125	1.012356	1512.51	-140.75
0.15906	1.017023	1518.50	-139.42
0.20211	1.022294	1524.95	-136.80
0.25049	1.028163	1531.91	-133.71
0.30209	1.034367	1539.57	-131.39
0.35927	1.041185	1547.51	-128.26
0.42283	1.048679	1556.81	-125.86
0.48795	1.056291	1566.11	-123.35
0.56141	1.064769	1576.35	-120.52
0.63762	1.073481	1586.88	-117.80

Sodium Thiosulphate, $Na_2S_2O_3$

$m/mol\ kg^{-1}$	$d/g\ cm^{-3}$	$u/m\ s^{-1}$	$10^4\phi_{KS}/cm^3\ mol^{-1}\ bar^{-1}$
0.00303	0.997471	1494.02	-145.97
0.01000	0.998387	1495.14	-144.61
0.02256	1.000010	1497.12	-141.92
0.03995	1.002239	1499.81	-139.51
0.06277	1.005151	1503.30	-137.29
0.09065	1.008673	1507.48	-134.91
0.12445	1.012914	1512.50	-132.57
0.16198	1.017578	1518.01	-130.33
0.20491	1.022880	1524.25	-128.04
0.25289	1.028738	1531.17	-125.69
0.30679	1.035250	1538.86	-123.25
0.36384	1.042079	1546.93	-120.88
0.42518	1.049345	1555.52	-118.49
0.49286	1.057245	1564.93	-115.99
0.56600	1.065689	1575.07	-113.52
0.64124	1.074263	1585.40	-111.10
0.71118	1.082122	1594.95	-108.96
0.78725	1.090580	1605.29	-106.78

Sodium Dithionate, $Na_2S_2O_6$

m/mol kg^{-1}	d/g cm^{-3}	u/m s^{-1}	$10^4\phi_{KS}$/cm^3 mol^{-1} bar^{-1}
0.01127	0.998761	1495.15	-117.16
0.02344	1.000579	1496.58	-114.68
0.03948	1.002957	1498.45	-112.95
0.06048	1.006040	1500.88	-111.26
0.08677	1.009878	1503.80	-109.01
0.11957	1.014622	1507.38	-106.74
0.15907	1.020286	1511.66	-104.61
0.20652	1.027027	1516.74	-102.42
0.31456	1.042104	1528.07	- 98.17
0.43424	1.058396	1540.23	- 94.08
0.56661	1.075968	1553.53	- 90.20
0.71741	1.095421	1568.11	- 86.13

APPARENT MOLAL ADIABATIC COMPRESSIBILITIES, DENSITIES AND SOUND VELOCITIES FOR AQUEOUS SOLUTIONS OF TRIETHYLENEDIAMINE, ETHYLENEDIAMINE, PIPERAZINE, MORPHOLINE, PYRAZINE, PYRIDAZINE, PYRAZOLE, IMIDAZOLE, 1,2,4 TRIAZOLE, PYRROLIDINE, 1,4 DIOXANE AND QUINUCLIDINE AT 298K

Triethylenediamine in 0.01N NaOH

$m/mol\ kg^{-1}$	$d/g\ cm^{-3}$	$u/m\ s^{-1}$	$10^4\phi_{KS}/cm^3\ mol^{-1}\ bar^{-1}$
0.0	0.997597	1494.92	
0.00968	0.997657	1495.62	0.88
0.03959	0.997847	1497.81	0.79
0.06030	0.997980	1499.30	0.93
0.08132	0.998115	1500.82	0.86
0.10129	0.998245	1502.27	0.83
0.14087	0.998504	1505.13	0.81
0.18021	0.998764	1507.95	0.80
0.21879	0.999022	1510.69	0.82
0.26004	0.999301	1513.62	0.81
0.29961	0.999572	1516.37	0.91

Piperazine in 0.01N NaOH

$m/mol\ kg^{-1}$	$d/g\ cm^{-3}$	$u/m\ s^{-1}$	$10^4\phi_{KS}/cm^3\ mol^{-1}\ bar^{-1}$
0.0	0.997516	1494.75	
0.01027	0.997550	1495.35	0.33
0.02193	0.997591	1496.07	-0.53
0.04212	0.997662	1497.23	0.16
0.06509	0.997744	1498.55	0.39
0.08675	0.997823	1499.82	0.31
0.11303	0.997921	1501.35	0.28
0.15746	0.998091	1503.94	0.18
0.19758	0.998249	1506.36	-0.16
0.23878	0.998417	1508.93	-0.63
0.28080	0.998593	1511.54	-0.97
0.32314	0.998776	1514.19	-1.28

Morpholine in 0.01N NaOH

$m/mol\ kg^{-1}$	$d/g\ cm^{-3}$	$u/m\ s^{-1}$	$10^4\phi_{KS}/cm^3\ mol^{-1}\ bar^{-1}$
0.0	0.997516	1494.83	
0.01027	0.997559	1495.33	6.00
0.02055	0.997611	1495.86	4.78
0.04135	0.997714	1496.97	3.70
0.06160	0.997813	1497.99	3.83
0.08286	0.997918	1499.09	3.78
0.10311	0.998018	1500.11	3.84
0.14312	0.998217	1502.18	3.70
0.18264	0.998415	1504.23	3.56
0.22267	0.998620	1506.24	3.61
0.26278	0.998828	1508.21	3.74

Quinuclidine in 1N NaOH

m/mol kg^{-1}	d/g cm^{-3}	u/m s^{-1}	$10^4\phi_{KS}$/cm^3 mol^{-1} bar^{-1}
0.0	1.037929	1585.59	
0.01077	1.037869	1586.47	7.03
0.02159	1.037813	1587.36	6.79
0.04231	1.037709	1589.10	6.07
0.06158	1.037614	1590.73	5.75
0.08054	1.037523	1592.30	5.74
0.10029	1.037431	1593.90	5.89
0.13893	1.037259	1597.00	6.07
0.18285	1.037074	1600.46	6.29
0.22188	1.036918	1603.37	6.72

Ethylenediamine in 0.01N NaOH

m/mol kg^{-1}	d/g cm^{-3}	u/m s^{-1}	$10^4\phi_{KS}$/cm^3 mol^{-1} bar^{-1}
0.0	0.997516	1494.85	
0.01058	0.997490	1495.33	2.11
0.02166	0.997461	1495.87	1.13
0.04218	0.997406	1496.83	1.09
0.06241	0.997352	1497.84	0.55
0.08283	0.997299	1498.88	0.07
0.10322	0.997246	1499.90	-0.08
0.14288	0.997145	1501.88	-0.27
0.18320	0.997043	1503.86	-0.28
0.22402	0.996940	1505.91	-0.44
0.25781	0.996856	1507.63	-0.56

Pyrrolidine in 1N NaOH

$m/mol\ kg^{-1}$	$d/g\ cm^{-3}$	$u/m\ s^{-1}$	$10^4\phi_{KS}/cm^3\ mol^{-1}\ bar^{-1}$
0.0	1.037929	1585.68	
0.01033	1.037820	1586.35	3.40
0.02043	1.037716	1587.00	3.48
0.04060	1.037511	1588.26	3.93
0.06121	1.037303	1589.54	4.19
0.08156	1.037099	1590.75	4.51
0.10126	1.036904	1591.94	4.64
0.14198	1.036507	1594.34	4.92
0.18203	1.036123	1596.71	5.04
0.22181	1.035748	1599.08	5.06

Pyrazine in H_2O

$m/mol\ kg^{-1}$	$d/g\ cm^{-3}$	$u/m\ s^{-1}$	$10^4\phi_{KS}/cm^3\ mol^{-1}\ bar^{-1}$
0.01671	0.997230	1494.24	3.05
0.04087	0.997460	1494.98	6.63
0.08057	0.997825	1496.28	7.24
0.13480	0.998324	1498.06	7.42
0.16890	0.998644	1499.14	7.59
0.21176	0.999041	1500.49	7.72
0.26569	0.999539	1502.19	7.82
0.33367	1.000162	1504.09	8.32
0.41956	1.000943	1506.53	8.65

Pyridazine in H_2O

m/mol kg^{-1}	d/g cm^{-3}	u/m s^{-1}	$10^4\phi_{KS}$/cm^3 mol^{-1} bar^{-1}
0.01120	0.997187	1494.29	2.34
0.02112	0.997287	1494.70	2.16
0.04002	0.997479	1495.47	2.18
0.06010	0.997682	1496.27	2.39
0.08094	0.997893	1497.12	2.34
0.10203	0.998106	1497.96	2.42
0.14153	0.998505	1499.52	2.55
0.18191	0.998912	1501.03	2.87
0.22224	0.999319	1502.54	3.07
0.26231	0.999722	1504.00	3.30
0.30184	1.000119	1505.42	3.49
0.35153	1.000617	1507.25	3.57
0.40319	1.001135	1508.95	3.93

Pyrazole in H_2O

m/mol kg^{-1}	d/g cm^{-3}	u/m s^{-1}	$10^4\phi_{KS}$/cm^3 mol^{-1} bar^{-1}
0.01019	0.997149	1494.21	5.90
0.02051	0.997221	1494.53	5.68
0.04151	0.997368	1495.15	6.11
0.06285	0.997516	1495.79	6.20
0.08275	0.997655	1496.38	6.24
0.10269	0.997793	1496.97	6.28
0.14312	0.998072	1498.12	6.51
0.18371	0.998350	1499.28	6.62
0.22278	0.998617	1500.37	6.73
0.26290	0.998889	1501.50	6.80
0.30464	0.999171	1502.66	6.89
0.35496	0.999508	1503.99	7.07

Imidazole in 0.01N NaOH

m/mol kg^{-1}	d/g cm^{-3}	u/m s^{-1}	$10^4\phi_{KS}$/cm^3 mol^{-1} bar^{-1}
0.0	0.997516	1494.77	
0.01022	0.997604	1495.05	6.56
0.02131	0.997694	1495.38	6.01
0.04089	0.997855	1495.93	6.03
0.06086	0.998018	1496.54	5.67
0.08158	0.998187	1497.12	5.79
0.10111	0.998345	1497.69	5.75
0.14097	0.998668	1498.83	5.82
0.18080	0.998989	1499.97	5.84
0.22162	0.999317	1501.10	5.92
0.26173	0.999637	1502.21	6.00
0.30249	0.999961	1503.29	6.14
0.35345	1.000364	1504.65	6.26
0.40496	1.000768	1505.99	6.38

1,2,4 Triazole in H_2O

m/mol kg^{-1}	d/g cm^{-3}	u/m s^{-1}	$10^4\phi_{KS}$/cm^3 mol^{-1} bar^{-1}
0.01073	0.997238	1494.00	7.91
0.02099	0.997396	1494.18	7.39
0.04068	0.997698	1494.51	7.28
0.06068	0.998004	1494.85	7.11
0.08189	0.998327	1495.21	7.09
0.10165	0.998628	1495.53	7.15
0.14232	0.999244	1496.18	7.31
0.18525	0.999890	1496.86	7.39
0.22557	1.000492	1497.47	7.52
0.26690	1.001106	1498.05	7.72
0.30929	1.001732	1498.65	7.87
0.35980	1.002473	1499.37	7.98

1,4 Dioxane in H_2O

$m/mol\ kg^{-1}$	$d/g\ cm^{-3}$	$u/m\ s^{-1}$	$10^4\phi_{KS}/cm^3\ mol^{-1}\ bar^{-1}$
0.01000	0.997155	1494.25	4.79
0.01979	0.997231	1494.67	5.76
0.03948	0.997383	1495.55	5.74
0.05995	0.997541	1496.41	6.28
0.08010	0.997697	1497.28	6.37
0.10025	0.997851	1498.14	6.42
0.14943	0.998227	1500.16	6.83
0.19000	0.998535	1501.79	7.13
0.22290	0.998783	1503.03	7.49
0.26278	0.999082	1504.59	7.67
0.30296	0.999382	1506.13	7.88
0.35325	0.999754	1507.98	8.17

1,4 Dioxane in 1M $MgCl_2$

$m/mol\ kg^{-1}$	$d/g\ cm^{-3}$	$u/m\ s^{-1}$	$10^4\phi_{KS}/cm^3\ mol^{-1}\ bar^{-1}$
0.0	1.067817	1594.34	
0.01072	1.067866	1594.73	11.86
0.02075	1.067902	1595.10	12.01
0.04147	1.067972	1595.87	12.01
0.06134	1.068035	1596.67	11.65
0.08120	1.068096	1597.38	11.92
0.10116	1.068154	1598.10	12.07
0.14140	1.068269	1599.54	12.29
0.18171	1.068383	1600.94	12.51
0.22287	1.068502	1602.35	12.66
0.26271	1.068617	1603.69	12.80
0.30265	1.068729	1605.01	12.93
0.35278	1.068851	1606.63	13.12
0.40330	1.068935	1608.23	13.35

APPARENT MOLAL ADIABATIC COMPRESSIBILITIES, DENSITIES AND SOUND VELOCITIES FOR AQUEOUS SOLUTIONS OF MONOHYDROCHLORIDE SALTS OF TRIETHYLENEDIAMINE, PIPERAZINE, ETHYLENEDIAMINE, PYRAZINE, PYRIDAZINE, PYRAZOLE, IMIDAZOLE, 1,2,4 TRIAZOLE, PYRROLIDINE, QUINUCLIDINE AND MORPHOLINE AT 298K

Triethylenediamine Monohydrochloride

$m/mol\ kg^{-1}$	$d/g\ cm^{-3}$	$u/m\ s^{-1}$	$10^4\phi_{KS}/cm^3\ mol^{-1}\ bar^{-1}$
0.00895	0.997364	1494.71	-17.79
0.02022	0.997715	1495.76	-17.63
0.03629	0.998224	1497.26	-17.83
0.05660	0.998849	1499.17	-17.82
0.08168	0.999628	1501.46	-17.44
0.11135	1.000545	1504.16	-17.16
0.14522	1.001561	1507.22	-16.72
0.18388	1.002723	1510.72	-16.47
0.22731	1.003997	1514.59	-16.07
0.27411	1.005356	1518.70	-15.64

Piperazine Monohydrochloride

m/mol kg^{-1}	d/g cm^{-3}	u/m s^{-1}	$10^4\phi_{KS}$/cm^3 mol^{-1} bar^{-1}
0.00997	0.997349	1494.69	-21.97
0.02256	0.997689	1495.75	-20.89
0.03998	0.998158	1497.26	-21.02
0.06241	0.998758	1499.18	-20.94
0.09023	0.999497	1501.55	-20.77
0.12314	1.000364	1504.33	-20.47
0.16128	1.001358	1507.53	-20.19
0.20384	1.002455	1511.04	-19.80
0.25095	1.003654	1514.90	-19.41
0.30318	1.004964	1519.12	-18.97
0.36093	1.006388	1523.75	-18.54
0.42510	1.007942	1528.87	-18.14

Ethylenediamine Monohydrochloride

m/mol kg^{-1}	d/g cm^{-3}	u/m s^{-1}	$10^4\phi_{KS}$/cm^3 mol^{-1} bar^{-1}
0.01207	0.997354	1494.69	-28.91
0.04064	0.997973	1496.91	-24.71
0.07298	0.998686	1499.42	-24.07
0.10098	0.999281	1501.56	-23.46
0.14712	1.000261	1505.00	-22.58
0.19342	1.001232	1508.47	-22.14
0.24360	1.002260	1512.11	-21.47
0.30797	1.003567	1516.79	-20.94
0.37097	1.004839	1521.37	-20.59
0.43287	1.006046	1525.80	-20.16

Pyrazine Hydrochloride, $pK_a = 0.65$

m/mol kg^{-1}		d/g cm^{-3}	u/m s^{-1}	$10^4\phi_{KS}$/cm^3 mol^{-1} bar^{-1}	
Uncorrected	Corrected			Uncorrected	Corrected
0.00860	0.00031	0.997315	1493.99	- 1.23	+ 0.58
0.01997	0.00152	0.997644	1494.52	- 1.51	- 5.94
0.03682	0.00463	0.998132	1495.31	- 1.72	- 6.83
0.05766	0.01010	0.998737	1496.28	- 1.85	- 6.60
0.08432	0.01304	0.999513	1497.54	- 2.10	- 7.01
0.11723	0.03225	1.000475	1499.09	- 2.30	- 7.01
0.15452	0.04938	1.001571	1500.87	- 2.56	- 7.27
0.19630	0.07059	1.002805	1502.89	- 2.90	- 7.72
0.24068	0.09491	1.004214	1505.15	- 3.23	- 8.13
0.24152	0.09539	1.004149	1505.09	- 3.22	- 8.10
0.29370	0.12585	1.005711	1507.65	- 3.57	- 8.49

Pyridazine Hydrochloride, $pK_a = 2.24$

m/mol kg^{-1}		d/g cm^{-3}	u/m s^{-1}	$10^4\phi_{KS}$/cm^3 mol^{-1} bar^{-1}	
Uncorrected	Corrected			Uncorrected	Corrected
0.00992	0.00471	0.997381	1494.36	-12.44	-19.28
0.02258	0.01370	0.997783	1495.19	-14.55	-19.97
0.04013	0.02754	0.998340	1496.38	-15.57	-19.89
0.06260	0.04628	0.999051	1497.92	-16.33	-19.94
0.09020	0.07011	0.999919	1499.83	-16.83	-19.93
0.12244	0.09862	1.000929	1502.05	-17.01	-19.68
0.15957	0.13201	1.002085	1504.62	-17.19	-19.54
0.20223	0.17087	1.003404	1507.53	-17.17	-19.24
0.25021	0.21503	1.004876	1510.78	-17.07	-18.91
0.30366	0.26464	1.006501	1514.38	-16.94	-18.58
0.36215	0.31929	1.008262	1518.26	-16.73	-18.21
0.42680	0.38004	1.010187	1522.51	-16.49	-17.82

Pyrazole Hydrochloride, $pK_a = 2.48$

m/mol kg^{-1}		d/g cm^{-3}	u/m s^{-1}	$10^4\phi_{KS}$/cm^3 mol^{-1} bar^{-1}	
Uncorrected	Corrected			Uncorrected	Corrected
0.01352	0.00828	0.997440	1494.62	-14.79	-22.75
0.05650	0.04438	0.998600	1497.17	-13.54	-16.67
0.09772	0.081311	0.999702	1499.54	-12.83	-15.00
0.14017	0.12022	1.000844	1502.12	-13.24	-15.10
0.18544	0.16226	1.002033	1504.76	-12.99	-14.57
0.23263	0.20648	1.003298	1507.47	-12.84	-14.23
0.29211	0.26226	1.004801	1510.76	-12.24	-13.40
0.31127	0.28078	1.005287	1511.74	-11.90	-12.99
0.36722	0.33397	1.006720	1514.93	-11.84	-12.83
0.41102	0.37575	1.007812	1517.25	-11.49	-12.39

Imidazole Hydrochloride

m/mol kg^{-1}	d/g cm^{-3}	u/m s^{-1}	$10^4\phi_{KS}$/cm^3 mol^{-1} bar^{-1}
0.01131	0.997407	1494.24	-14.14
0.01989	0.997638	1494.76	-13.90
0.02764	0.997861	1495.29	-15.71
0.04150	0.998248	1496.17	-16.04
0.05546	0.998631	1497.02	-15.62
0.08370	0.999415	1498.73	-15.32
0.11167	1.000187	1500.40	-15.01
0.13898	1.000927	1502.09	-15.01
0.20960	1.002728	1506.41	-14.42
0.28095	1.004716	1510.26	-13.60
0.35310	1.006617	1514.34	-13.21

1,2,4 Triazole Hydrochloride, $pK_a = 2.30$

m/mol kg^{-1}		d/g cm^{-3}	u/m s^{-1}	$10^4\phi_{KS}$/cm^3 mol^{-1} bar^{-1}	
Uncorrected	Corrected			Uncorrected	Corrected
0.01110	0.00574	0.997474	1494.27	-11.30	-20.59
0.02360	0.01496	0.997933	1494.87	-13.11	-19.95
0.04207	0.02984	0.998609	1495.78	-14.13	-19.40
0.06408	0.04849	0.999413	1496.92	-15.02	-19.46
0.09141	0.07237	1.000408	1498.35	-15.62	-19.42
0.12365	0.10114	1.001575	1500.04	-16.03	-19.34
0.16192	0.13583	1.002952	1502.07	-16.29	-19.21
0.20408	0.17451	1.004460	1504.23	-16.27	-18.85
0.25185	0.21871	1.006156	1506.69	-16.24	-18.54
0.30407	0.26746	1.007994	1509.32	-16.07	-18.13
0.36101	0.32091	1.009981	1512.15	-15.84	-17.70
0.42742	0.38358	1.012273	1515.40	-15.57	-17.25

Pyrrolidine Hydrochloride

m/mol kg^{-1}	d/g cm^{-3}	u/m s^{-1}	$10^4\phi_{KS}$/cm^3 mol^{-1} bar^{-1}
0.01203	0.997266	1495.04	-21.60
0.06034	0.998016	1499.26	-13.36
0.12149	0.998953	1504.52	-11.91
0.18326	0.999887	1509.82	-11.39
0.29622	1.001532	1519.25	-10.46
0.37283	1.002631	1525.36	- 9.71
0.43748	1.003539	1530.25	- 8.93

Morpholine Hydrochloride

m/mol kg^{-1}	d/g cm^{-3}	u/m s^{-1}	$10^4\phi_{KS}$/cm^3 mol^{-1} bar^{-1}
0.00993	0.997378	1494.51	-22.14
0.02107	0.997714	1495.36	-19.98
0.03769	0.998214	1496.74	-20.60
0.05995	0.998880	1498.59	-20.98
0.08611	0.999658	1500.69	-20.65
0.11820	1.000604	1503.24	-20.23
0.15620	1.001713	1506.17	-19.62
0.19965	1.002967	1509.51	-19.09
0.24889	1.004369	1513.31	-18.72

Quinuclidine Hydrochloride

m/mol kg^{-1}	d/g cm^{-3}	u/m s^{-1}	$10^4\phi_{KS}$/cm^3 mol^{-1} bar^{-1}
0.01010	0.997294	1495.02	-20.89
0.02290	0.997562	1496.42	-19.72
0.04052	0.997930	1498.36	-19.35
0.06321	0.998403	1500.82	-18.79
0.09114	0.998981	1503.87	-18.64
0.12414	0.999661	1507.40	-18.23
0.16082	1.000411	1511.25	-17.70
0.20496	1.001307	1515.91	-17.38
0.25146	1.002243	1520.77	-17.06
0.30519	1.003314	1526.25	-16.55
0.36208	1.004436	1531.98	-16.08
0.42481	1.005659	1538.25	-15.64

APPARENT MOLAL ADIABATIC COMPRESSIBILITIES, DENSITIES AND SOUND VELOCITIES FOR AQUEOUS SOLUTIONS OF DIHYDROCHLORIDE SALTS OF TRIETHYLENEDIAMINE, PIPERAZINE AND ETHYLENEDIAMINE AT 298K

Triethylenediamine Dihydrochloride, $pK_a(2) = 2.95$

m/mol kg^{-1}		d/g cm^{-3}	u/m s^{-1}	$10^4\phi_{KS}$/cm^3 mol^{-1} bar^{-1}	
Uncorrected	Corrected			Uncorrected	Corrected
0.01011	0.00725	0.997686	1495.08	-45.51	-53.21
0.02172	0.01731	0.998426	1496.55	-47.99	-53.62
0.04204	0.03571	0.999708	1499.12	-49.00	-53.11
0.09156	0.08197	1.002829	1505.49	-50.14	-52.99
0.15172	0.13922	1.006634	1513.22	-50.57	-52.80
0.25182	0.23556	1.012943	1526.27	-51.12	-52.87
0.29893	0.28117	1.015912	1532.43	-51.26	-52.88
0.35466	0.33527	1.019423	1539.75	-51.42	-52.91
0.41099	0.39007	1.022967	1547.19	-51.54	-52.93

Piperazine Dihydrochloride, $pK_a(2) = 5.55$

m/mol kg^{-1}		d/g cm^{-3}	u/m s^{-1}	$10^4\phi_{KS}$/cm^3 mol^{-1} bar^{-1}	
Uncorrected	Corrected			Uncorrected	Corrected
0.01018	0.01001	0.997681	1495.18	-61.89	-62.43
0.02265	0.02240	0.998387	1496.77	-58.64	-58.97
0.04010	0.03977	0.999370	1498.97	-57.18	-57.41
0.06349	0.06307	1.000677	1501.88	-55.91	-56.09
0.09103	0.09053	1.002202	1505.24	-54.64	-54.78
0.12363	0.12304	1.003987	1509.15	-53.37	-53.49
0.16142	0.16075	1.006029	1513.60	-52.05	-52.15
0.20444	0.20368	1.008317	1518.60	-50.79	-50.87
0.25136	0.25049	1.010769	1523.94	-49.49	-49.56
0.30389	0.30297	1.013463	1529.78	-48.08	-48.14
0.36182	0.36081	1.016367	1536.13	-46.70	-46.75
0.42487	0.42378	1.019449	1542.88	-45.25	-45.29

Ethylenediamine·Dihydrochloride, $pK_a(2) = 6.85$

$m/mol\ kg^{-1}$		$d/g\ cm^{-3}$	$u/m\ s^{-1}$	$10^4\phi_{KS}/cm^3\ mol^{-1}\ bar^{-1}$	
Uncorrected	Corrected			Uncorrected	Corrected
0.01044	0.01040	0.997626	1495.25	-59.48	-59.57
0.02354	0.02348	0.998284	1496.82	-58.33	-58.39
0.04189	0.04181	0.999202	1498.98	-57.37	-57.41
0.06447	0.06438	1.000323	1501.56	-56.02	-56.05
0.09227	0.09217	1.001691	1504.70	-54.85	-54.87
0.12557	0.12544	1.003312	1508.40	-53.71	-53.73
0.16328	0.16313	1.005124	1512.53	-52.48	-52.60
0.20914	0.20897	1.007296	1517.44	-51.26	-51.27
0.25651	0.25632	1.009501	1522.41	-50.01	-50.02
0.30993	0.30972	1.011941	1527.93	-48.74	-48.75
0.36704	0.36681	1.014495	1533.74	-47.50	-47.51
0.43129	0.43104	1.017301	1540.14	-46.18	-46.19

CLAIMS TO ORIGINAL RESEARCH

1) The apparent molal volumes of (a) the salts of a series of Cl- and S-oxyanions; (b) a series of structurally related N and/or O containing heterocyclic bases and (c) the hydrochloride salts of these bases have been measured at low concentrations using a differential buoyancy technique.

2) The apparent molal adiabatic compressibilities of the salts and neutral bases mentioned in (1) have been precisely measured down to low concentrations using the "sing-around" method.

3) Methods for evaluation of intrinsic volumes of ions have been comparatively and critically examined. It has been found that the method using molecular models, proposed in the present work, is to be preferred for the evaluation of the sizes of polyatomic ions.

4) It has been found that the electrostrictive effects in the series of oxyanions are dependent on the size and geometry of the ions, as well as their charges.

5) The electrostriction volumes derived from the molecular model method have been found to be interestingly related to the $\overline{K}^{o}_{S,i}$ values for the oxyanions in a manner that can be

rationalized in terms of a priori calculation of electrostriction and local solvent compressibility in an ionic field.

6) The dithionate ion, $S_2O_6^{2-}$ has been found to behave more like a dimerized univalent ion than a divalent ion for reasons understandable in terms of its charge distribution.

7) Clear relations have been demonstrated between $\overline{V}_i^o$ and $\overline{K}_{S,i}^o$ as well as between $\overline{V}_i^o$ and $\overline{K}_{S,i}^o/\overline{V}_i^o$ for both Cl- and S-oxyanions.

8) The treatment of concentration dependence of apparent molal volume data according to Redlich and Meyer's and Masson's equations has been critically examined. It was found that for the series of oxyanion salts, use of Masson's equation obscures some interesting inflections which are otherwise seen if ϕ_v is plotted according to Redlich and Meyer's equation which takes into account the Debye-Hückel limiting-law dependence of ϕ_v on $\sqrt{c}$.

9) It has been suggested that the inflections observed when ϕ_v data are treated according to Redlich and Meyer's equation, for the oxyanion salts, are due to Gurney co-sphere overlap effects. This proposal was supported by some elementary calculations.

10) It is concluded that the concept of "group contributions" for representing partial molal volumes of organic molecules at infinite dilution is not a correct viewpoint. Structural factors play an important role in determining both ϕ_v^o and ϕ_{KS}^o values.

11) Experiments were conducted to examine if the boat form is the preferred conformation in water and in ionic media for piperazine, morpholine and 1,4 dioxane. The result from nmr experiments were inconclusive.

12) The volume and adiabatic compressibility changes upon ionization of some N and O containing heterocyclic bases have been determined.

13) It has been found that the changes of volumes and adiabatic compressibilities associated with ionization of the organic bases are related to each other in a manner similar to that between V_e and $\overline{K}_{S,i}^o$ demonstrated for oxyanions.

14) The relations of $\overline{V}_i^o$ and $\overline{K}_{S,i}^o$ to entropies of solution for oxyanions, as well as the relation of $\Delta\overline{V}_{i,1}^o$ to $\Delta\overline{S}_{i,1}^o$ (Hepler's relation) for the first ionization of organic bases, have been examined in terms of electrostrictive and solvent structure effects.

REFERENCES

1. B.E. Conway, Ann. Rev. Phys. Chem., 17, 481 (1966).

2. G.S. Kell, in Structure and Transport Process in Water and Aqueous Solutions, Ed. R.A. Horne, Chapter 9, John Wiley, N.Y. (1972).

3. C.M. Davis, in Structure and Transport Process in Water and Aqueous Solutions, Ed. R.A. Horne, Chapter 10, John Wiley, N.Y. (1972).

4. D. Eisenberg and W. Kauzman, The Structure and Properties of Water, p. 266, Oxford Univ. Press, N.Y. (1969).

5. F.H. Stillinger and A. Rahman, J. Chem. Phys., 61, 4973 (1974), see also J. Chem. Phys., 60, 1545 (1974).

6. P. Kebarlé, in Modern Aspects of Electrochemistry, Vol. 11, Eds. B.E. Conway and J.O'M. Bockris, Chapter 1, Plenum, N.Y. (1974).

7. F.J. Millero, in Structure and Transport Process in Water and Aqueous Solutions, Ed. R.A. Horne, Chapter 12, John Wiley, N.Y. (1972).

8. B.E. Conway, Ionic Hydration in Chemistry and Biophysics, Elsevier, Amsterdam (1981): a) p. 531; b) p. 371; c) p. 549; d) p. 473; e) p. 101; f) Chapter 16; g) p. 58; h) Chapter 18.

9. B.E. Conway, J.E. Desnoyers and C. Smith. Phil. Trans. Roy. Soc., London, A256, 389 (1964).

10. B.S. Krumgalz, J. Chem. Soc., Faraday Trans. I, 76, 1887 (1980).

11. L.G. Hepler, J. Phys. Chem., 61, 1426 (1957).

12. P. Drude and W. Nernst, Z. Phys. Chem., 15, 79 (1894).

13. H.S. Frank, J. Chem. Phys., 23, 2033 (1955).

14. J.E. Desnoyers, R.E. Verrall, and B.E. Conway, J. Chem. Phys., 43, 243 (1965).

15. R. Zana and E.B. Yeager, in L'eau et le système biologique, C.N.R.S. No. 246, p. 155, Paris (1976).

16. S.D. Hamann and S.C. Lim, Aust. J. Chem., 7, 329 (1954).

17. B.E. Conway and J. O'M. Bockris, in Modern Aspects of Electrochemistry, Vol. 1, Ed. J. O'M. Bockris, Chapter 2, Butterworths Scien. Pub., London (1954).

18. F.J. Millero, Chem. Rev., 71, 147 (1971).

19. B.E. Conway, R.E. Verrall and J.E. Desnoyers, Z. Phys. Chem., 230, 157 (1965).

20. L.G. Hepler, J. Phys. Chem., 69, 965 (1965).

21. R.E. Verrall and B.E. Conway, J. Phys. Chem., 70, 3961 (1966).

22. S. Cabani, V. Mollica, L. Lepori and S.T. Lobo, J. Phys. Chem., 81, 982 and 987 (1977).

23. L.H. Laliberté and B.E. Conway, J. Phys. Chem., 74, 4116 (1970).

24. B.E. Conway and L.H. Laliberté, in Hydrogen Bonded Solvent Systems, Eds. A. Covington and P. Jones, p. 139, Taylor and Francis, London (1968).

25. A.M. Couture and K.J. Laidler, Can. J. Chem., 35, 207 (1957).

26. A.M. Couture and K.J. Laidler, Can. J. Chem., 34, 1209 (1956).

27. J. Mukerjee, J. Phys. Chem., 65, 740 (1961).

28. J.W. Akitt, J. Chem. Soc., Faraday Trans. I, 76 2259 (1980).

29. D.H. Everett, W.F.K. Wynne-Jones, Trans. Faraday Soc., 35, 1380 (1939).

30. D.A. Lown, H.R. Thirsk and Lord Wynne-Jones, Trans. Faraday Soc., 64, 2073 (1968).

31. C.H. Rochester and B. Rossal, Trans. Faraday Soc., 65, 992 (1969).

32. S. Cabani, G. Conti, E. Matteoli and M.R. Tiné, J. Chem. Soc., Faraday Trans. I, 77, 2377 (1981).

33. K.J. Laidler, Chemical Kinetics, Second Edn., pp. 232-238, McGraw-Hill, N.Y. (1965).

34. E. Whalley, Trans. Faraday Soc., 55, 798 (1959).

35. J.E. Desnoyers and P.R. Philip, Can. J. Chem., 50, 1094 (1972).

36. F.J. Millero, in Activity Coefficient of Electrolyte Solutions, Ed. J. Pytkowicz, Vol. 2, Chapter 2, CRC Press, Miami (1979).

37. J.G. Mathieson and B.E. Conway. J. Chem. Soc., Faraday Trans. I, 70, 752 (1974).

38. F.J. Millero, G.K. Ward, F.K. Lepple and E.V. Hoff., J. Phys. Chem., 78, 1636 (1974).

39. J.G. Mathieson and B.E. Conway, J. Solution Chem., 3, 455 (1974).

40. B.B. Owen and S.R. Brinkley, Chem. Rev., 29, 461 (1941).

41. J. Padova, J. Chem. Phys., 40, 691 (1964).

42. J.E. Desnoyers and C. Jolicoeur, in Modern Aspects of Electrochemistry, Vol. 5, Eds. J. O'M. Bockris and B.E. Conway, Chapter 1, Plenum Press, N.Y. (1969).

43. B.E. Conway, J. Solution Chem., 7, 721 (1978).

44. J.D. Bernal and R.H. Fowler, J. Chem. Phys., 1, 515 (1933).

45. R.M. Noyes, J. Amer. Chem. Soc., 86, 971 (1964).

46. E. Glueckauf, Trans. Faraday Soc., 61, 914 (1965).

47. B.E. Conway, R.E. Verrall and J.E. Desnoyers, Trans. Faraday Soc., 62, 2738 (1966).

48. R.L. Kay, Faraday Discussions Chem. Soc., 64, 252 (1978).

49. C.J. Pedersen, J. Amer. Chem. Soc., 89, 2495 (1967).

50. J.M. Lehn, Accounts of Chem. Res., 11, 49 (1978).

51. R. Zana and E.B. Yeager, J. Phys. Chem., 71, 521 (1967).

52. E. Glueckauf, Trans. Faraday Soc., 64, 2425 (1968).

53. A. Roux, G.M. Musbally, G. Perroni and J.E. Desnoyers, and P.P. Singh, E.M. Wooley and L.G. Hepler, Can. J. Chem., 56, 24 (1978).

54. I.V. Olofsson, J.J. Spitzer and L.G. Hepler, Can. J. Chem., 56, 1871 (1978).

55. W.Y. Wen, N. Takeguchi and D.P. Wilson, J. Solution Chem., 3, 103 (1974).

56. O. Kiyohara, G. Perron and J.E. Desnoyers, Can. J. Chem., 53, 2591 (1975).

57. O. Enea, C. Jolicoeur and L.G. Hepler, Can. J. Chem., 58, 704 (1980).

58. S. Cabani, G. Conti and L. Lepori, J. Phys. Chem., 76, 1338 and 1343 (1972).

59. J.G. Mathieson and B.E. Conway, Anal. Chem., 44, 1517 (1972).

60. R. Garnsey, R.J. Boe, R. Mahoney and T.A. Litovitz, J. Chem. Phys., 50, 5222 (1969).

61. B.B. Owen and H.L. Simon, J. Phys. Chem., 61, 479 (1957).

62. B.B. Owen and P.L. Kronick, J. Phys. Chem., 65, 84 (1961).

63. F.J. Millero, G.K. Ward and P.V. Chetirkin, J. Acoust. Soc. Amer., 61, 1492 (1977).

64. M. Sakurai, T. Komatsu and T. Nakagawa, Bull. Chem. Soc. Japan, 54, 643 (1981).

65. B.E. Conway, J.G. Mathieson and H.P. Dhar, J. Phys. Chem., 78, 1226 (1974).

66. M.V. Kaulgud and K.J. Patil, J. Phys. Chem., 78, 714 (1974); 80, 138 (1976).

67. J. Lawrence and B.E. Conway, J. Phys. Chem., 75, 2362 (1971).

68. R.E. Verrall, Ph.D. Thesis, Univ. of Ottawa (1966).

69. L.H. Laliberté, Ph.D. Thesis, Univ. of Ottawa (1969).

70. C. Marignac, Ann. Chim. (Paris), 22, 415 (1871).

71. O. Redlich and D.M. Meyer, Chem. Rev., 64, 221 (1964).

72. F. Kohlrausch and W. Hallwachs, Weid. Ann. d. Phys., 50, 118 (1893).

73. H.E. Wirth, J. Amer. Chem. Soc., 59, 2549 (1937).

74. J.G. Mathieson and B.E. Conway, J. Solution Chem., 4, 17 (1974).

75. F. Vaslow, J. Phys. Chem., 70, 2286 (1966).

76. G.S. Kell, J. Chem. Eng. Data, 12, 66 (1967).

77. A. Passynski, Acta Physicochim., U.R.S.S., 8, 385 (1938).

78. E. Carstenson, J. Acoust. Soc. Amer., 26, 858 (1954).

79. Model 6105, NUS Corporation (Velocimeter), Underwater System Division, Paramus, N.J.

80. Instruction Manual for Laboratory Velocimeter, Model 6105, NUS Corporation, Underwater System Division, Paramus, N.J.

81. Handbook of Chemistry and Physics, 56th edn., p. E-47, CRC, Cleveland, Ohio (1975).

82. Kirk-Othmer Encyclopedia of Chemical Technology, 2nd edn., pp. 31-35, Vol. 5, John Wiley, N.Y. (1964).

83. D.A. Skoog and D.M. West, Fundamentals of Analytical Chemistry, 2nd edn., pp. 233-234, Holt, Rinehart and Winston, N.Y. (1969).

84. D.D. Perrin, Dissociation Constants of Organic Bases in Aqueous Solutions, Butterworths, London (1965) and the Supplementary (1972).

85. F. Vaslow, J. Phys. Chem., 71, 4585 (1967).

86. W. Geffcken and D. Price, Z. Phys. Chem., B26, 81 (1934).

87. L.A. Dunn, Trans. Faraday Soc., 62, 2348 (1966).

88. J. Lawrence and B.E. Conway, J. Phys. Chem., 75, 2353 (1971).

89. F. Franks, J.R. Ravenhill and D.S. Reid, J. Solution Chem., 1, 3 (1972).

90. M. Sakurai, Bull. Chem. Soc. Japan, 46, 1596 (1973).

91. A.F. Scott, J. Phys. Chem., 35, 3379 (1931).

92. J.S. Rosen, J. Phys. Chem., 60, 7 (1956).

93. E. Darmois, J. Phys. Rad., 2, 2 (1941).

94. W.M. Latimer and C. Kasper, J. Amer. Chem. Soc., 51, 2293 (1929).

95. H.S. Frank and M.W. Evans, J. Chem. Phys., 13, 507 (1945).

96. A. Holtzer and M.F. Emerson, J. Phys. Chem., 73, 26 (1969).

97. H. Høiland, J.A. Ringseth and E. Vikingstad, J. Solution Chem., 7, 515 (1978).

98. G. Nemethy and H.A. Scheraga, J. Chem. Phys., 36, 3382 (1962).

99. B.E. Conway and L.H. Laliberté, Trans. Faraday Soc., 66, 3032 (1970).

100. E. Glueckauf, Trans. Faraday Soc., 60, 572 (1964).

101. B.S. Gourary and F.J. Adrian, Solid State Physics, 10, 217 (1960).

102. A.F. Kapustinskii, Dokl. Akad. Nauk., U.S.S.R., 32; 59 (1941).

103. A.M. Couture and K.J. Laidler, Can. J. Chem., 35, 202 (1957).

104. R.H. Stokes, J. Amer. Chem. Soc., 86, 979 (1964).

105. G. Brink and M. Falk, Can. J. Chem., 48, 3019 (1970).

106. B.G. Cox and A.J. Parker, J. Amer. Chem. Soc., 95, 6879 (1973).

107. R.W. Gurney, Ionic Processes in Solutions, Dover Publications Reprint, N.Y. (1960).

108. P.S. Ramanathan, C.V. Krishnan and H.L. Friedman, J. Solution Chem., 1, 237 (1972).

109. Mellor's Modern Inorganic Chemistry, Chapters 21 and 22, Revised and Edited by G.D. Parkes, Longmans, Green and Co., London (1956).

110. F. Ephraim, Inorganic Chemistry, 6th edition, Chapters 20, 21 and 26, Oliver and Boyd, London (1954).

111. D.O. Masson, Phil. Mag., 8, 218 (1929).

112. F.J. Millero, J. Solution Chem., 2, 1 (1973).

113. D.J. Bradley and K.S. Pitzer, J. Phys. Chem., 83, 1599 (1979).

114. B.B. Owen and S.R. Brinkley, Ann. N.Y. Acad. Sci., 51, 753 (1949).

115. G. Scatchard and L.F. Epstein, Chem. Rev., 30, 211 (1942).

116. S. Cabani, P. Gianni, V. Mollica and L. Lepori, J. Solution Chem., 10, 563 (1981).

117. R.N. French and C.M. Criss, J. Solution Chem., 10, 699 (1981).

118. A.G. Lenhert and R.N. Castle, in Pyridazines, Chapter 1, Ed. R.N. Castle, John Wiley, N.Y. (1973).

119. K. Hofmann, Imidazole and its Derivatives, Chapter 1, Interscience, N.Y. (1953).

120. P.W. Bridgman, The Physics of High Pressure, pp. 116-148, Bell, London (1952).

121. T.W. Richards and C.L. Speyers, J. Amer. Chem. Soc., 36, 491 (1914).

122. P.W. Bridgman, Proc. Am. Acad. Arts and Sciences, 47, 473 (1912).

123. E.A. Moelwyn-Hughes, Physical Chemistry, pp. 596-599, Cambridge Univ. Press, Cambridge (1947).

124. J.A. Pople, Proc. Roy. Soc. London, A205, 163 (1951).

125. B.E. Conway, Can. J. Chem., 37, 613 (1959).

126. J. Paquette and C. Jolicoeur, J. Solution Chem., 6, 403 (1977).

127. F.M. Jones and E.M. Arnett, Prog. Phys. Org. Chem., 11, 263 (1974).

128. J.W. Larson and L.G. Hepler, in Solute-Solvent Interactions, Eds. J.F. Coetzee and C.D. Ritchie, p. 1, Marcel Dekker, N.Y. (1969).

129. J.E. Desnoyers, M. Arel, G. Perron and C. Jolicoeur, J. Phys. Chem., 73, 3346 (1969).